NASA Tech Briefs

National Aeronautics and Space Administration

"Prepregs" — glass, quartz, and graphite fibers impregnated with polyimides — are the raw materials for lightweight structural composites. This sampling of commercial prepregs incorporates polyimides developed at NASA's Lewis Research Center. [*See the bottom of page A1.*]

Vol. 8, No. 3

Spring 1984

About the NASA Technology Utilization Program

The National Aeronautics and Space Act of 1958, which established NASA and the United States civilian space program, requires that "The Administration shall provide for the widest practicable and appropriate dissemination of information concerning its activities and the results thereof."

To help carry out this objective, NASA's Technology Utilization (TU) Program was established in 1962. Now, as an element of NASA's Technology Utilization and Industry Affairs Division, this program offers a variety of valuable services to help transfer aerospace technology to nonaerospace applications, thus assuring American taxpayers maximum return on their investment in space research; thousands of spinoffs of NASA research have already occurred in virtually every area of our economy.

The TU program has worked for engineers, scientists, technicians, and businessmen; and it can work for you.

NASA Tech Briefs

Tech Briefs is published quarterly and is free to engineers in U.S. industry and to other domestic technology transfer agents. It is both a current-awareness medium and a problem-solving tool. Potential products . . . industrial processes . .. basic and applied research . . . shop and lab techniques . . . computer software . . . new sources of technical data . . . concepts . . . can be found here. The short section on New Product Ideas highlights a few of the potential new products contained in this issue. The remainder of the volume is organized by technical category to help you quickly review new developments in your areas of interest. Finally, a subject index makes each issue a convenient reference file.

Further Information on Innovations

Although some new technology announcements are complete in themselves, most are backed up by Technical Support Packages (TSP's). TSP's are available without charge and may be ordered by simply completing a TSP Request Card found at the back of this volume. Further information on some innovations is available for a nominal fee from other sources, as indicated. In addition, Technology Utilization Officers at NASA Field Centers will often be able to lend necessary guidance and assistance.

Patent Licenses

Patents have been issued to NASA on some of the inventions described, and patent applications have been submitted on others. Each announcement indicates patent status and availability of patent licenses if applicable.

Other Technology Utilization Services

To assist engineers, industrial researchers, business executives, Government officials, and other potential users in applying space technology to their problems, NASA sponsors Industrial Applications Centers. Their services are described on page A7. In addition, an extensive library of computer programs is available through COSMIC, the Technology Utilization Program's outlet for NASA-developed software.

Applications Program

NASA conducts applications engineering projects to help solve public-sector problems in such areas as safety, health, transportation, and environmental protection. Two applications teams, staffed by professionals from a variety of disciplines, assist in this effort by working with Federal agencies and health organizations to identify critical problems amenable to solution by the application of existing NASA technology.

Reader Feedback

We hope you find the information in *NASA Tech Briefs* useful. A reader-feedback card has been included because we want your comments and suggestions on how we can further help you apply NASA innovations and technology to your needs. Please use it; or if you need more space, write to the Manager, Technology Transfer Division, P.O. Box 8757, Baltimore/ Washington International Airport, Maryland 21240.

NASA Tech Briefs

National Aeronautics and Space Administration

SPRING 1984
Volume 8, Number 3

COVERS: The photographs on the front and back covers illustrate developments by NASA and its contractors that have resulted in commercial and nonaerospace spinoffs. You can use the TSP Request Card at the back of this issue to learn more about the Composite Prepregs [Circle 167] and the Computerized Design Station [Circle 168].

About This NASA Publication

NASA Tech Briefs, a quarterly publication, is distributed free to qualified U.S. citizens to encourage commercial application of U.S. space technology. For information on publications and services available through the NASA Technology Utilization Program, write to the Manager, Technology Transfer Division, P.O. Box 8757, Baltimore/Washington International Airport, Maryland 21240.

"The Administrator of National Aeronautics and Space Administration has determined that the publication of this periodical is necessary in the transaction of the public business required by law of this Agency. Use of funds for printing this periodical has been approved by the Director of the Office of Management and Budget."

Change of Address

If you wish to have NASA Tech Briefs forwarded to your new address, use the Subscription Card enclosed at the back of this volume of NASA Tech Briefs. Be sure to check the appropriate box indicating change of address, and also fill in your identification number (T number) in the space indicated.

Communications Concerning Editorial Matter

For editorial comments or general communications about NASA Tech Briefs, you may use the Feedback card in the back of NASA Tech Briefs, or write to: The Publications Manager, Technology Utilization Office (LGT-1), NASA Headquarters, Washington, DC 20546. Technical questions concerning specific articles should be directed to the Technology Utilization Officer of the sponsoring NASA Center (addresses listed on page A4).

Expanded Format

To speed the publication of our backlog of Tech Brief items, we have increased our per-issue contents by adding short articles to the end of each subject section of NASA Tech Briefs. Titled "MiniBriefs," these short articles describe NASA innovations and reports in an abbreviated format. Most are backed up by Technical Support Packages (TSP's), which can be obtained by using the TSP Request Card at the back of this issue.

Acknowledgements

NASA Tech Briefs is published quarterly by the National Aeronautics and Space Administration, Technology Transfer Division, Washington, DC: Administrator: **James M. Beggs;** Director, Technology Utilization and Industry Affairs Division: **Ronald J. Philips;** Publications Manager: **Leonard A. Ault.** Prepared for the National Aeronautics and Space Administration by **Logical Technical Services Corp.:** Editor-in-Chief: **Jay Kirschenbaum;** Art Director: **Ernest Gillespie;** Managing Editor: **Jerome Rosen;** Chief Copy Editor: **Oden Browne;** Staff Editors: **James Boyd, Larry Grunberger, Paul Johnson, Jordan Randjelovich, Ted Selinsky, George Watson;** Graphics: **Andrew Abramoske, Ron Krause, Luis Martinez, Huburn Profitt;** Editorial & Production: **Camille McQueen, Richard Johnson, Tony Franchina, Sabrina Gibson, Stephanie Godino, Leslie Iwaskow, Henry Lai, Marion Larson, Linda Lucas, Frank Ponce, Joe Renzler, Melanie Tarka, Elizabeth Texeira, Ernestine Walker.**

NASA TU SERVICES

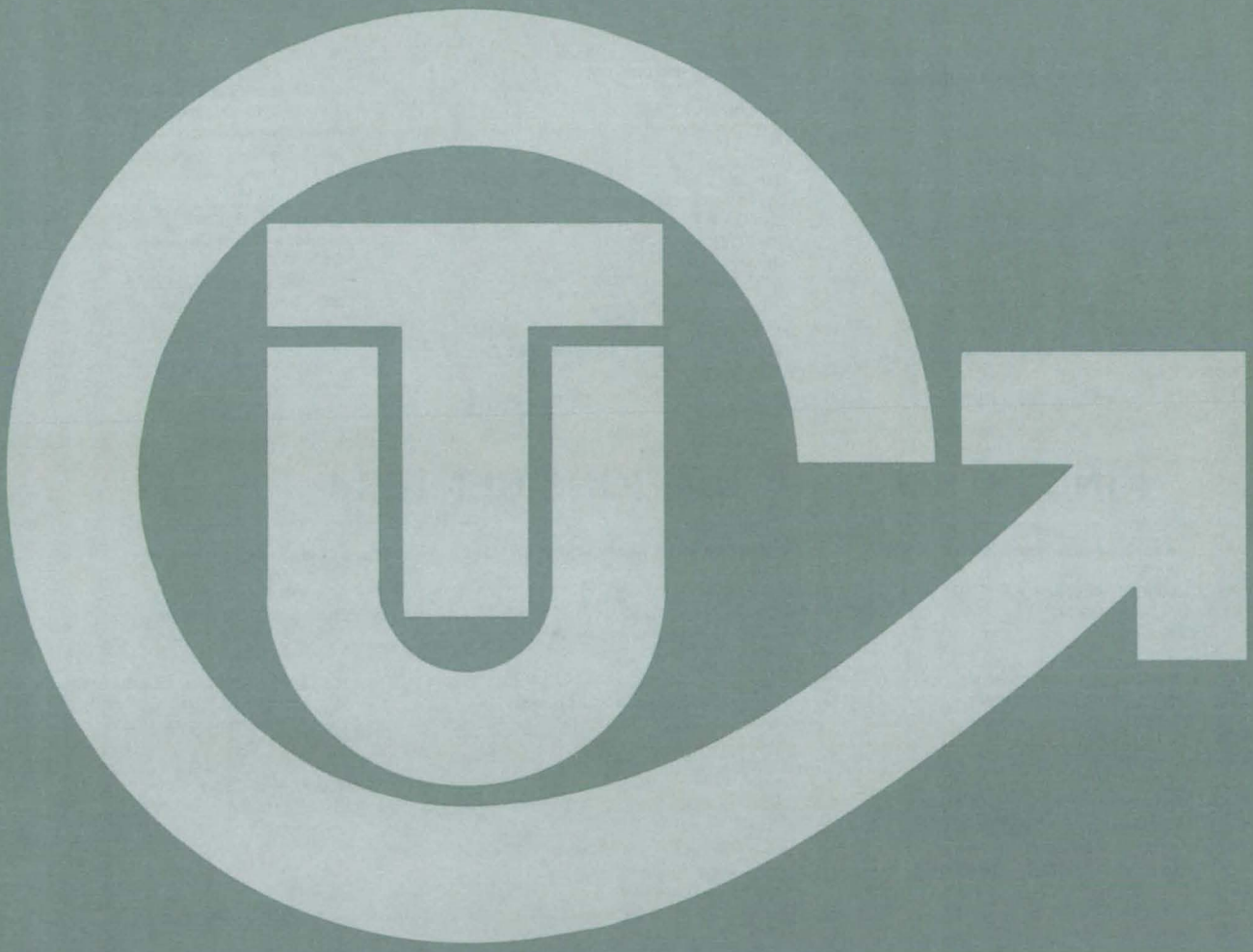

NASA TECHNOLOGY UTILIZATION NETWORK

★ TECHNOLOGY UTILIZATION OFFICERS

Stanley A. Miller
Ames Research Center
Code 240-10
Moffett Field, CA 94035
(415) 965-6471

Stanley A. Miller
Hugh L. Dryden Flight Research Center
Code 240-10
Moffett Field, CA 94035
(415) 965-6471

Donald S. Friedman
Goddard Space Flight Center
Code 702.1
Greenbelt, MD 20771
(301) 344-6242

William Chmylak
Lyndon B. Johnson Space Center
Code AL-32
Houston, TX 77058
(713) 483-3809

U. Reed Barnett
John F. Kennedy Space Center
Code PT-SPD
Kennedy Space Center, FL 32899
(305) 867-3017

John Samos
Langley Research Center
Mail Stop 139A
Hampton, VA 23665
(804) 865-3281

Harrison Allen, Jr.
Lewis Research Center
Mail Code 7-3
21000 Brookpark Road
Cleveland, OH 44135
(216) 433-4000, Ext. 6422

Ismail Akbay
George C. Marshall Space Flight Center
Code AT01
Marshall Space Flight Center, AL 35812
(205) 453-2224

Leonard A. Ault
NASA Headquarters
Code ETD-6
Washington, DC 20546
(202) 453-8424

Aubrey Smith
NASA Resident Office-JPL
4800 Oak Grove Drive
Pasadena, CA 91103
(818) 354-4849

Gilmore H. Trafford
Wallops Flight Center
Code OD
Wallops Island, VA 23337
(804) 824-3411, Ext. 201

● INDUSTRIAL APPLICATIONS CENTERS

Aerospace Research Applications Center
1201 East 38th Street
Indianapolis, IN 46205
John M. Ulrich, director
(317) 264-4644

Computer Software Management and Information Center (COSMIC)
Suite 112, Barrow Hall
University of Georgia
Athens, GA 30602
John A. Gibson, director
(404) 542-3265

Kerr Industrial Applications Center
Southeastern Oklahoma State University
Durant, OK 74701
James Harmon, director
(405) 924-0121, Ext. 413

NASA Industrial Applications Center
701 LIS Building
University of Pittsburgh
Pittsburgh, PA 15260
Paul A. McWilliams, executive director
(412) 624-5211

New England Research Applications Center
Mansfield Professional Park
Storrs, CT 06268
Daniel Wilde, director
(203) 486-4533

North Carolina Science and Technology Research Center
Post Office Box 12235
Research Triangle Park, NC 27709
James E. Vann, director
(919) 549-0671

Technology Applications Center
University of New Mexico
Albuquerque, NM 87131
Stanley Morain, director
(505) 277-3622

NASA Industrial Applications Center
University of Southern California
Denny Research Building
University Park
Los Angeles, CA 90007
Robert Mixer, acting director
(213) 743-6132

■ STATE TECHNOLOGY APPLICATIONS CENTERS

NASA/University of Florida
State Technology Applications Center
500 Weil Hall
University of Florida
Gainesville, FL 32611
J. Ronald Thornton, director

Gainesville:	(904) 392-6760
Boca Raton:	(305) 395-5100, Ext. 2292
Fort Lauderdale:	(305) 776-6645
Jacksonville:	(904) 646-2478
Orlando:	(305) 275-2706
Pensacola:	(904) 476-9500, Ext. 426
Tampa:	(813) 974-2499

NASA/University of Kentucky
State Technology Applications Program
109 Kinkead Hall
University of Kentucky
Lexington, KY 40508
William R. Strong, manager
(606) 258-4632

◆ PATENT COUNSELS

Robert F. Kempf
Asst. Gen. Counsel for patent matters
NASA Headquarters
Code GP-4
400 Maryland Avenue, SW.
Washington, DC 20546
(202) 755-3954

Darrell G. Brekke
Ames Research Center
Mail Code: 200-11A
Moffett Field, CA 94035
(415) 965-5104

Darrell G. Brekke
Hugh L. Dryden Flight Research Center
Mail Code: 201-11A
Moffett Field, CA 94035
(415) 965-5104

John O. Tresansky
Goddard Space Flight Center
Mail Code: 204
Greenbelt, MD 20771
(301) 344-7351

Marvin F. Matthews
Lyndon B. Johnson Space Center
Mail Code: AL-3
Houston, TX 77058
(713) 483-4871

James O. Harrell
John F. Kennedy Space Center
Mail Code: SA-PAT
Kennedy Space Center, FL 32899
(305) 867-2544

Howard J. Osborn
Langley Research Center
Mail Code: 279
Hampton, VA 23665
(804) 827-3725

Norman T. Musial
Lewis Research Center
Mail Code: 500-311
21000 Brookpark Road
Cleveland, OH 44135
(216) 433-4000, Ext. 346

Leon D. Wofford, Jr.
George C. Marshall Space Flight Center
Mail Code: CC01
Marshall Space Flight Center, AL 35812
(205) 453-0020

Paul F. McCaul
NASA Resident Office-JPL
Mail Code: 180-601
4800 Oak Grove Drive
Pasadena, CA 91103
(818) 354-2700

▲ APPLICATION TEAMS

Doris Rouse, director
Research Triangle Institute
Post Office Box 12194
Research Triangle Park, NC 27709
(919) 541-6980

James P. Wilhelm, director
SRI International
333 Ravenswood Avenue
Menlo Park, CA 94026
(415) 326-6200, Ext. 3520

TECHNOLOGY UTILIZATION OFFICERS

Technology transfer experts can help you apply the innovations in NASA Tech Briefs.

The Technology Utilization Officer at each NASA Field Center is an applications engineer who can help you make use of new technology developed at his center. He brings you NASA Tech Briefs and other special publications, sponsors conferences, and arranges for expert assistance in solving technical problems.

Technical assistance, in the form of further information about NASA innovations and technology, is one of the services available from the TUO. Together with NASA scientists and engineers, he can often help you find and implement NASA technology to meet your specific needs.

Technical Support Packages (TSP's) are prepared by the center TUO's. They provide further technical details for articles in NASA Tech Briefs. This additional material can help you evaluate and use NASA technology. You may receive most TSP's free of charge by using the TSP Request Card found at the back of this issue.

Technical questions about articles *in NASA Tech Briefs are answered in the TSP's. When no TSP is available, or you have further questions, contact the Technology Utilization Officer at the center that sponsored the research* [see page A4].

NASA INVENTIONS AVAILABLE FOR LICENSING

Over 3,500 NASA inventions are available for licensing in the United States — both exclusive and nonexclusive.

NASA grants patent licenses, both exclusive and nonexclusive, for the commercial use of U.S. and foreign patents and patent applications owned by NASA. All licenses require royalties and are granted by express written agreements in accordance with the NASA Patent-Licensing Regulations.

Additional Information about NASA inventions may be found in the *"NASA Patent Abstract Bibliography"* (PAB), containing abstracts of all NASA inventions, which can be purchased from the National Technical Information Service, Springfield, VA 22161. The PAB is updated semiannually.

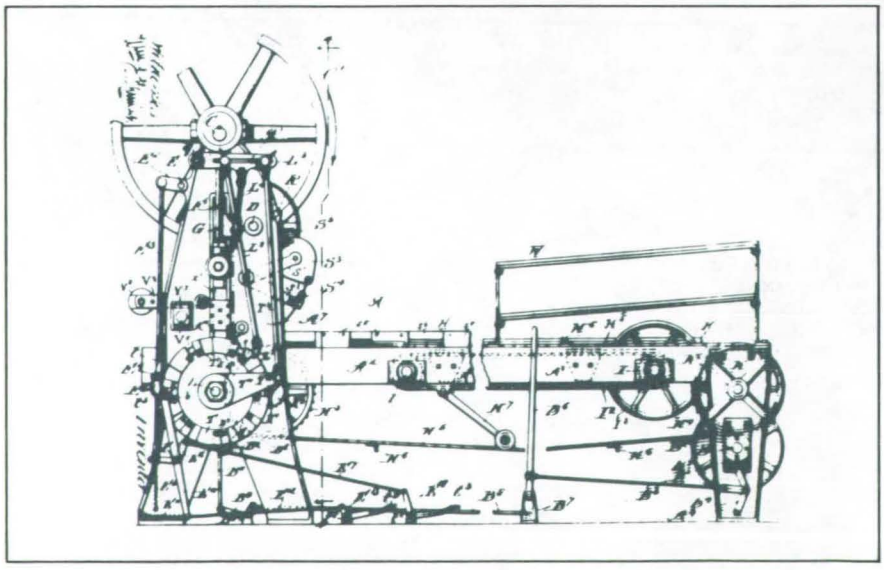

Patent licenses for inventions *described in NASA Tech Briefs are frequently available. Many of the inventions reported in NASA Tech Briefs are patented or are under consideration for a patent at the time they are published. The current patent status is described at the end of the article; if no patent action is contemplated by NASA, there is no statement about patents. If you want to know more about the patent program or are interested in licensing a particular invention, contact the Patent Counsel at the NASA Field Center that sponsored the research* [see page A5]. *Be sure to refer to the NASA reference number at the end of the Tech Brief.*

APPLICATION TEAMS

Technology-matching and problem-solving assistance to public-sector organizations

Application engineering projects are conducted by NASA to help solve public-sector problems in such areas as safety, health, transportation, and environmental protection. Some application teams specialize in biomedical disciplines; others, in engineering and scientific problems. Staffed by professionals from various disciplines, these teams work with other Federal agencies and health organizations to identify critical problems amenable to solution by the application of existing NASA technology.

Public-sector organization *representatives can learn more about application teams by contacting a nearby NASA Field Center Technology Utilization Office* [*see page A4*].

INDUSTRIAL APPLICATIONS CENTERS

Computerized access to over 10 million documents worldwide

Computerized information retrieval from one of the world's largest banks of technical data is available from NASA's network of Industrial Applications Centers (IAC's). The IAC's give you access to 1,800,000 technical reports in the NASA data base and to more than 10 times that many reports and articles found in nearly 200 other computerized data bases.

The major sources include:

- *750,000 NASA Technical Reports*
- *Selected Water Resources Abstracts*
- *NASA Scientific and Technical Aerospace Reports*
- *Air Pollution Technical Information Center*
- *NASA International Aerospace Abstracts*
- *Chem Abstracts Condensates*
- *Engineering Index*
- *Energy Research Abstracts*
- *NASA Tech Briefs*
- *Government Reports*
- *Announcements*

and many other specialized files on food technology, textile technology, metallurgy, medicine, business, economics, social sciences, and physical science.

The IAC services range from tailored literature searches through expert technical assistance:

- *Retrospective Searches:* Published or unpublished literature is screened, and documents are identified according to your interest profile. IAC engineers tailor results to your specific needs and furnish abstracts considered the most pertinent. Complete reports are available upon request.
- *Current-Awareness Searches:* IAC engineers will help design a program to suit your needs. You will receive selected monthly or quarterly abstracts on new developments in your area of interest.
- *Technical Assistance:* IAC engineers will help you evaluate the results of your literature searches. They can help find answers to your technical problems and put you in touch with scientists and engineers at appropriate NASA Field Centers.

Prospective clients *can obtain more information about these services by contacting the nearest IAC* [*see page A4*]. *User fees are charged for IAC information services.*

STATE TECHNOLOGY APPLICATIONS CENTERS

Technical information services for industry
and state and local government agencies

Government and private industry
in Florida and Kentucky can utilize the services of NASA's State Technology Applications Centers (STAC's). The STAC's differ from the Industrial Applications Centers described on page A7, primarily in that they are integrated into existing state technical assistance programs and serve only the host state, whereas the IAC's serve multistate regions.

Many data bases,
including the NASA base and several commercial bases, are available for automatic data retrieval through the STAC's. Other services such as document retrieval and special searches are also provided. (Like the IAC's, the STAC's normally charge a fee for their services.)

To obtain information
about the services offered, write or call the STAC in your state [*see page A4*].

COSMIC®

An economical source of computer programs
developed by NASA and other government agencies

A vast software library
is maintained by COSMIC — the Computer Software Management and Information Center. COSMIC gives you access to approximately 1,600 computer programs developed for NASA and the Department of Defense and selected programs for other government agencies. Programs and documentation are available at reasonable cost.

Available programs
range from management (PERT scheduling) to information science (retrieval systems) and computer operations (hardware and software). Hundreds of engineering programs perform such tasks as structural analysis, electronic circuit design, chemical analysis, and the design of fluid systems. Others determine building energy requirements and optimize mineral exploration.

COSMIC services
go beyond the collection and storage of software packages. Programs are checked for completeness; special announcements and an indexed software catalog are prepared; and programs are reproduced for distribution. Customers are helped to identify their software needs; and COSMIC follows up to determine the successes and problems and to provide updates and error corrections. In some cases, NASA engineers can offer guidance to users in installing or running a program.

Information about programs
described in NASA Tech Briefs articles can be obtained by completing the COSMIC Request Card at the back of this issue. Just circle the letters that correspond to the programs in which you are interested.

NEW PRODUCT IDEAS

NEW PRODUCT IDEAS are just a few of the many innovations described in this issue of NASA Tech Briefs and having promising commercial applications. Each is discussed further on the referenced page in the appropriate section in this issue. If you are interested in developing a product from these or other NASA innovations, you can receive further technical information by requesting the TSP referenced at the end of the full-length article or by writing the Technology Utilization Office of the sponsoring NASA center (see page A4). NASA's patent-licensing program to encourage commercial development is described on page A6.

Containerless Manufacture of Glass Optical Fibers

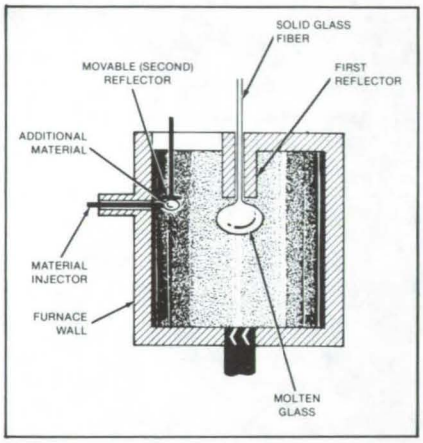

Glass optical fibers of high purity would be made in a proposed new containerless process. Since the molten glass would not make contact with any solid objects, there would be no opportunity for solid contaminants to dissolve in the melt. A solid optical fiber would be drawn from an acoustically levitated lump of molten glass. New material is added in solid form, melted, and then moved into the main body of molten glass.
(See page 354.)

Vacuum Seal Permits Limited Rotation

A flexible metal seal permits ±45° rotation of an object in a vacuum chamber. It was originally designed for the rotation of sample probes in electron spectroscopy for chemical analysis,

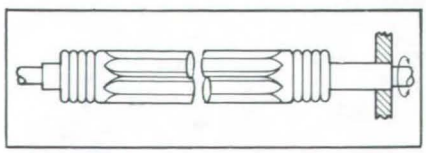

although other applications are likely. The seal is made from three bellows. Connecting tubes are installed at both ends of the seal. A sample on a rod extending through the bellows into the vacuum system can be rotated without the loss of vacuum.
(See page 398.)

Improved Ellipsoidal Radiation Furnace

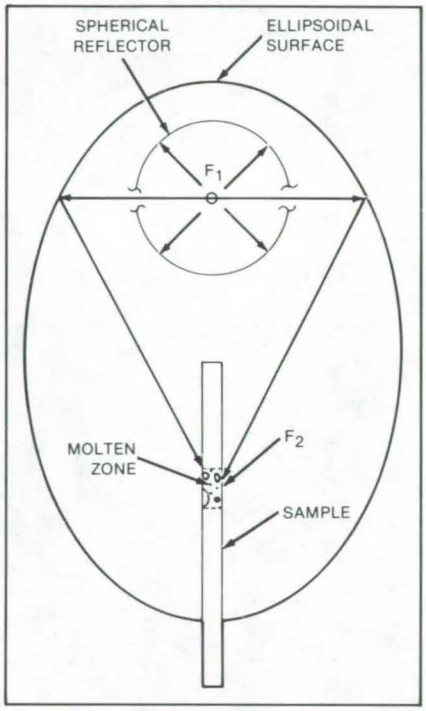

A proposed radiation furnace would heat a small zone of a cylindrical sample while reducing waste heat. The axisymmetric monoellipsoidal furnace has a spherical reflector around the "point" heat source. This arrangement uses the heat efficiently, reduces waste heat generation, and permits full view of the specimen. The heat reflected back to the source helps to maintain the equilibrium temperature with less power input than furnaces without the reflector.
(See page 370.)

Temperature-Gradient Furnace for Solidification Experiments

A cylindrical furnace provides axial temperature profiles for material-processing experiments. Temperature gradients inside the central ceramic furnace tube can be varied locally from isothermal (zero gradient) to 500° C/cm

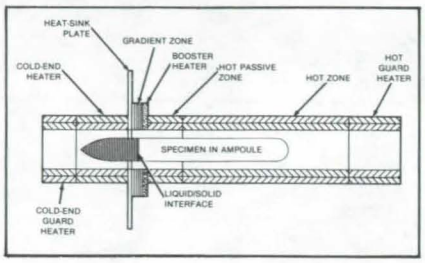

by controlling the electric power to five independent heating elements and a heat-removal plate. The furnace has eight temperature zones. A zone is heated, cooled, or passive, depending on the required temperature profile.
(See page 369.)

Rapid Adhesive Bonding for Metals and Composites

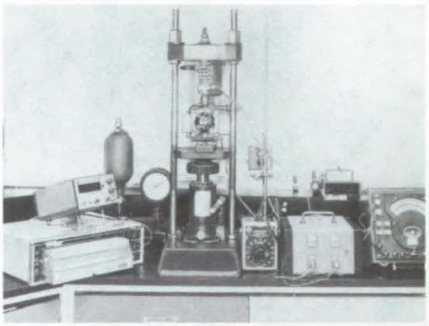

A technique similar to spot welding in metallic structures has been used for rapid bonding of graphite/polyimide and graphite/epoxy composites, titanium and aluminum alloys, and metallic and composite specimens with adherends of unlike materials. The process, which uses a toroidal induction heater, does not damage composites that cannot withstand high temperatures for long time intervals. The process can be scaled up for production.
(See page 410.)

Measuring Absolute Oxygen Pressure

A sensor determines the absolute pressure of oxygen without the need for a reference pressure source. A prototype was used to control the air/fuel ratio

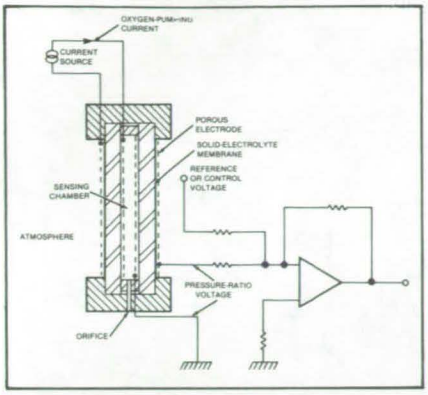

of an automobile. The device has a small sensing volume and one or two solid-electrolyte membranes through which oxygen enters the sensing volume. The oxygen flows back into the surrounding atmosphere through a narrow duct. Electrodes on both sides of the membranes sample the current through or voltage across each membrane.
(See page 379.)

Joint for Erectable and Collapsible Frames

A mechanism allows a truss structure to be folded and stowed in a small space. On command, the mechanism unfolds, erecting the structure and locking its members in place. The mechanism can also be collapsed so that the structure can be restowed. Developed for structures to be erected in space (for example,

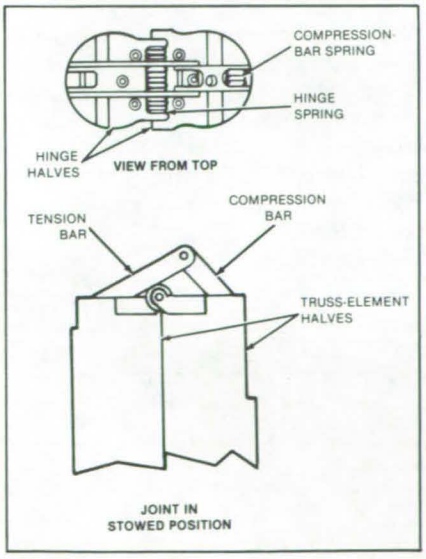

antennas, solar panels, solar sails, and masts), the joint mechanism can be readily adapted to window-opening struts, folding furniture, and television antennas.
(See page 383.)

Interferometer Measures Broadband Surface Acoustic Waves

A dual differential interferometer uses two pairs of orthogonally-polarized optical beams to measure the amplitude and orientation of broadband ultrasonic surface acoustic waves. Each of the two pairs of focused laser-probe beams is used in a separate wideband differential interferometer to detect independently the component of surface-wave motion along one direction. By combining the two signals,

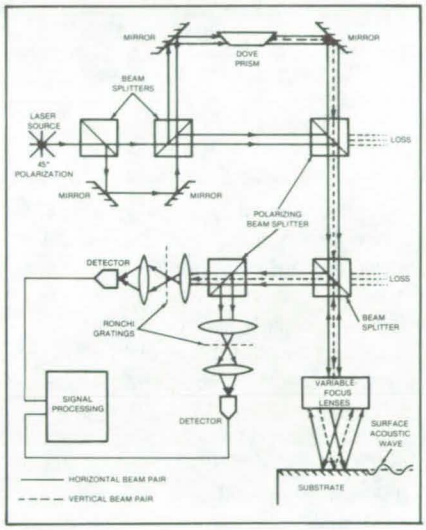

the interferometer determines a two-dimensional surface-wave profile and its variation as a function of time. The system has an optically-adjustable acoustic bandwidth from the kilohertz to megahertz range and can detect peak-to-peak displacements in the subangstrom range.
(See page 341.)

Zero-Net-Charge Air Ionizer

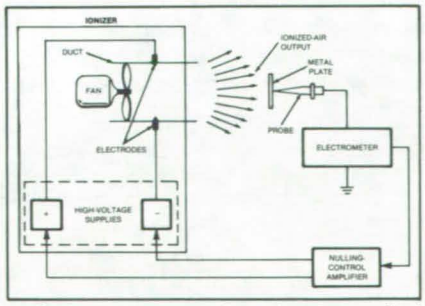

An instrument monitors the air supplied by an air ionizer to ensure that the net charge is neutral. It is useful where integrated-circuit chips are manufactured, inspected, tested, or assembled since it prevents a localized buildup of electric charge and thus protects against damage from electrostatic discharges. The instrument includes a probe, an electrometer, and an amplifier.
(See page 345.)

Beam Window for Pressure Chambers

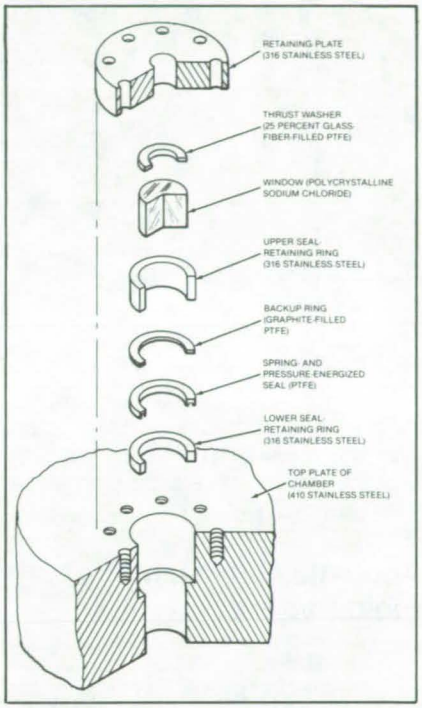

A sodium chloride window seals over chamber pressures from 0.1 to 13.8 MPa while absorbing minimal energy from a CO_2 laser beam that passes through it into the chamber. The window, which is inexpensive and easily replaceable, resists clouding by smoke particles produced in the chamber during combustion experiments in an oxygen atmosphere. It also resists damage by droplets of molten material ejected from the combustion zone.
(See page 374.)

Transducers for Heart Research

A series of transducers with seven different configurations enables the measurement of forces and displacements in the cardiac wall. The new transducers are small, cause minimal perturbation of the heart function, and can be attached and detached without causing excessive tissue damage. A myocardial force transducer measures the local force of contraction along a line between two tines embedded in the heart wall. The longitudinal groove in the beam serves as a protective recess for the strain gage. The transverse groove is shallow enough to

(continued on next page)

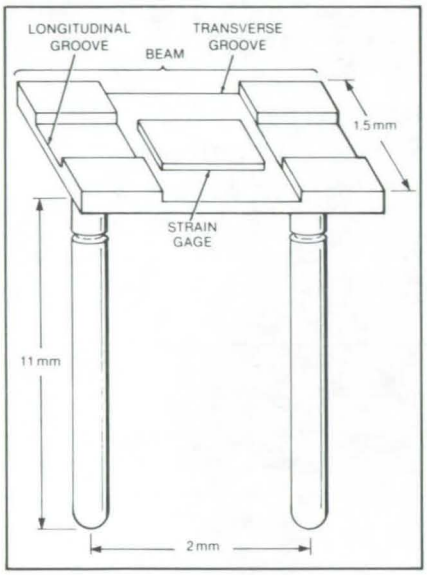

keep the beam compliance low, yet deep enough to allow the beam to bend slightly about the sensitive axis of the strain gage.
(See page 363.)

Acoustic Gaussian Far-Field Pattern

A new ultrasonic transducer with concentric electrode rings produces a far-field beam with a Gaussian spatial profile for materials evaluation applications. The transducer is constructed by depositing a circularly-symmetric metallic multielectrode array on a 12.7-mm-diameter X-cut quartz disk. Each electrode is independently connected to an impedance network optimized to produce the Gaussian distribution with less than 2 percent error.
(See page 342.)

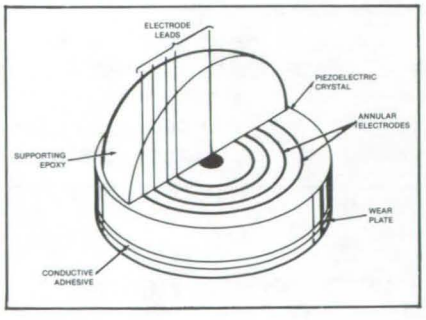

Eddy-Current Inspection of Ball Bearings

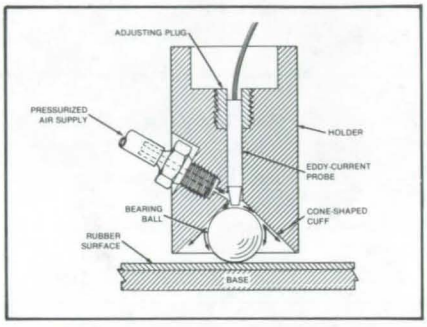

An eddy-current probe reliably detects surface and near-surface cracks, voids, and material anomalies in bearing balls or other spherical objects. The inspection apparatus includes a nonabrasive high-friction base and a holder with an eddy-current probe mounted on one side. A recess in the holder in the shape of an inverted cone accommodates different ball sizes. The low-friction air cushion within the cone allows the ball to roll easily.
(See page 371.)

Circularly-Polarized Microstrip Antenna

A circularly-polarized microstrip antenna is made of concentric cylindrical layers of conductive and dielectric materials. Coaxial-cable feedlines are connected to the horizontal and vertical subelements from the inside. In this configuration, the vertical subelement acts as the ground for the horizontal subelement. The antenna is compact enough for mobile use. Its radiation pattern is azimuthally omnidirectional; in elevation it covers a swath 50° wide.
(See page 320.)

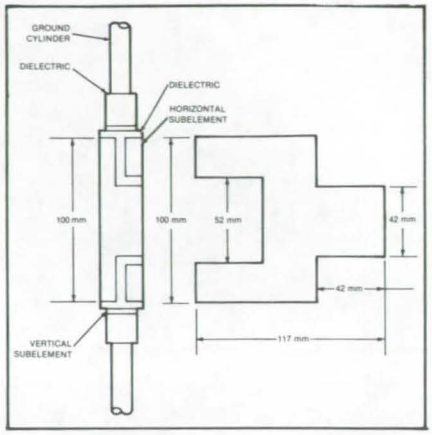

Improved RF Isolation Amplifier

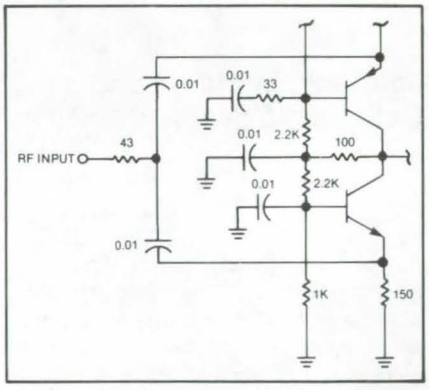

A radio-frequency isolation amplifier with a frequency response of 0.5 to 400 MHz ±0.5 dB does not require selected or matched components or a directional coupling device. The circuit can be used in applications requiring high reverse isolation, such as receiver intermediate-frequency strips and frequency distribution systems.
(See page 322.)

Electronic Components and Circuits

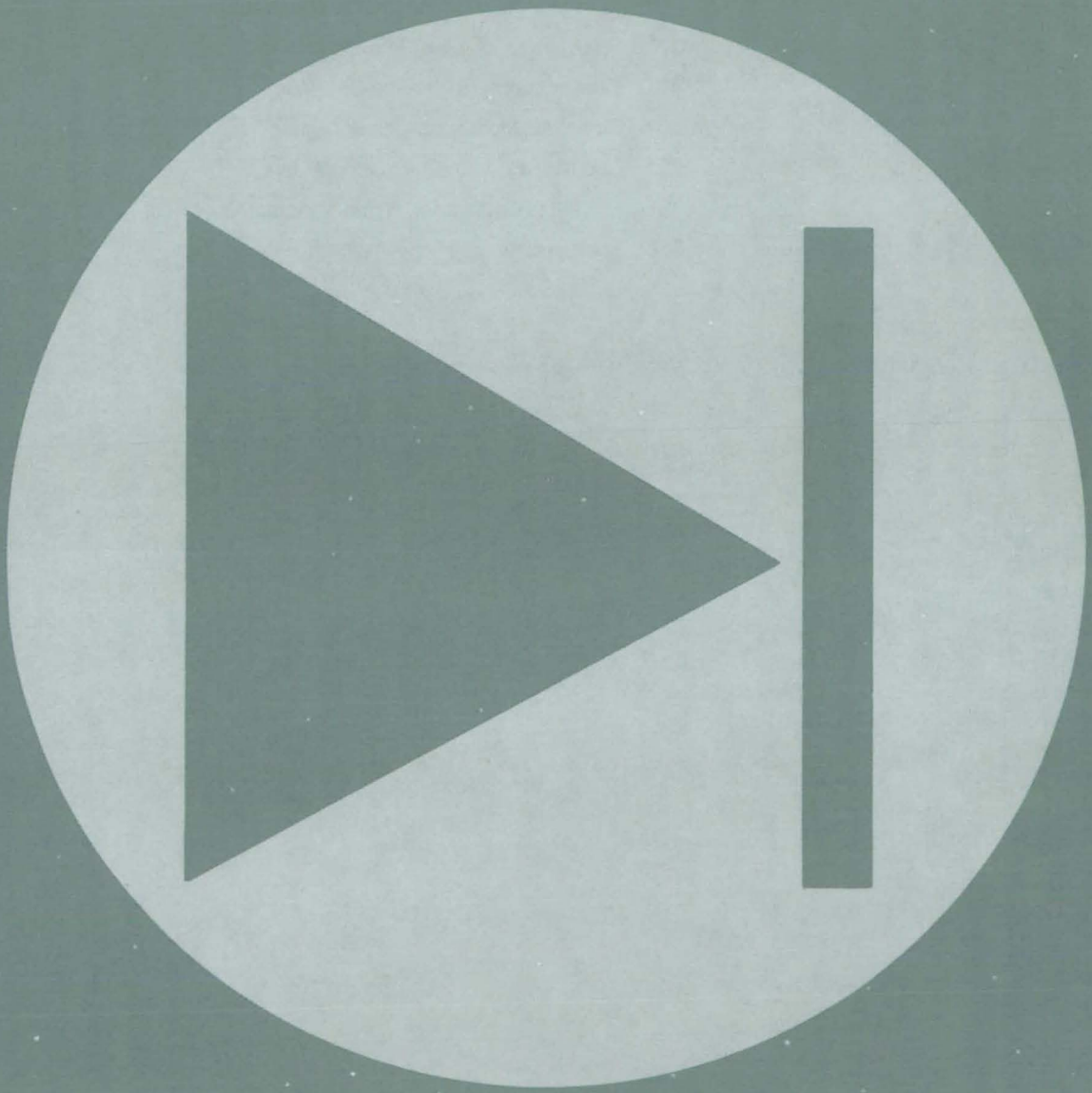

Hardware, Techniques, and Processes

Computer Programs

MiniBriefs

Battery-Operated High-Voltage Power Supply

Circuitry allows large multiplication of voltage.

Goddard Space Flight Center, Greenbelt, Maryland

A new battery-operated power supply has several high-voltage outputs. The circuitry provides independently adjustable voltages in the kilovolt range for X-ray tubes and other instruments.

For three output voltages, the power supply is formed by three circuits in parallel between the battery (or other dc source) terminals on the input side and with a common output terminal (see figure). Circuit 1 of the power supply provides a well-regulated voltage having an amplitude of several tens of kilovolts (for example, -80 kV) between terminals P_1 and P_2. Circuits 2 and 3 provide outputs that differ from that at P_1 by less than 1 kV.

Circuit 1 includes a switching regulator that drives a sine-wave oscillator. A variable resistance adjusts the duty cycle of the regulator. The oscillator output is applied to the primary winding of a step-up isolation transformer, the secondary voltage of which is about 10 kV. The secondary winding connects to a 10-stage capacitor/diode voltage multiplier, which full-wave-rectifies the transformer output and raises it to 80 kV between P_1 and P_2. The voltage multiplier provides an extremely large multiplication of the potential difference across the transformer with only a few components and a saving of power.

Circuit 2 also has a switching regulator and variable resistor. The regulator drives an oscillator, which is connected to the primary winding of an isolation transformer. The secondary winding of the transformer connects to output terminal P_3 and the common output terminal P_1.

Circuit 3 includes a linear regulator that provides power to an oscillator. The regulator functions as a linear resistance that senses and controls the amplitude of the output. The oscillator output is applied to the primary of an isolation transformer. The secondary winding of the transformer connects to the common output terminal P_1 and terminal P_4. The secondary winding develops an output that is rectified by diode D_1 and filtered by capacitor C_1, providing a low-amplitude direct voltage between terminals P_1 and P_4.

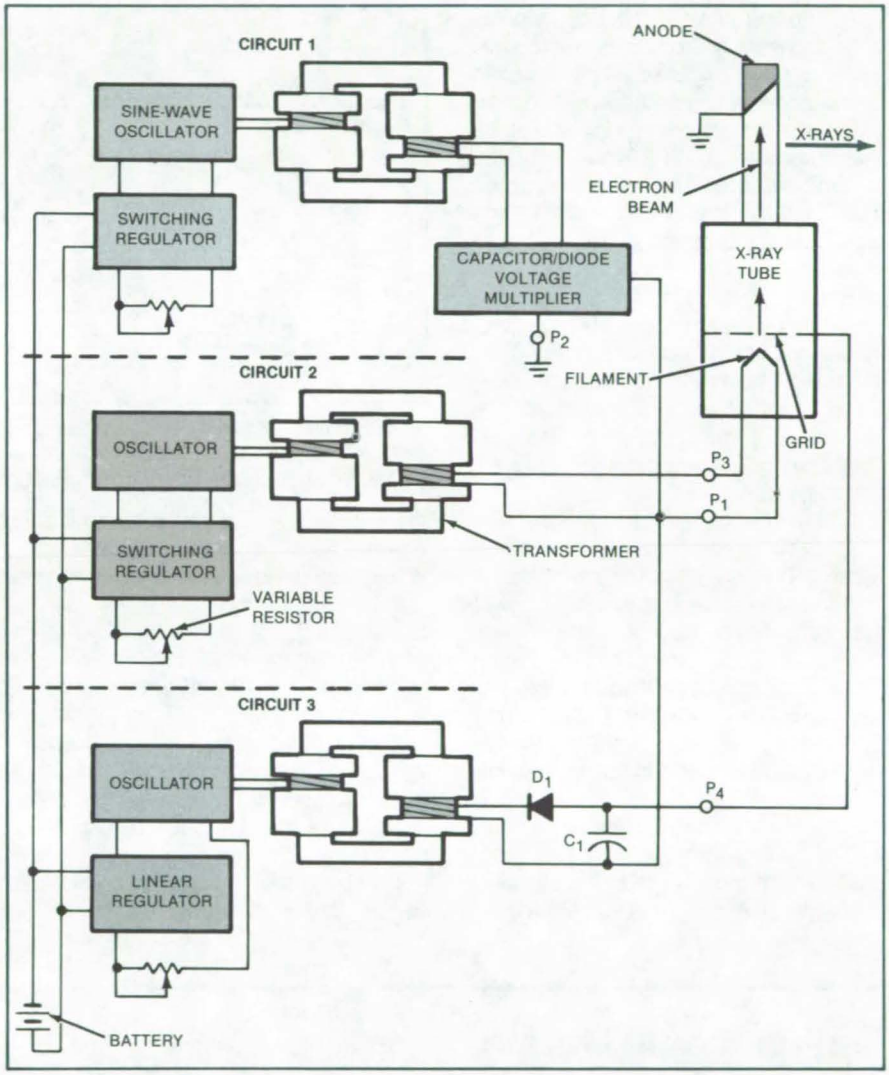

One Use of the Power Supply is to establish the operating potentials for a triode X-ray tube. The filament voltage is -80 kV. The potential difference between terminals P_3 and P_4 is adjusted to make the grid 80 to 150 volts more negative than the filament. This enables the grid to focus electrons from the filament into a stream that impinges on the anode, which then emits X-rays.

The power supply is compact, lightweight, and efficient. It can be housed in a container having a volume of about 128 cubic inches (2,098 cm^3). Since it draws only 8 watts, it can operate for several hours on a dry-cell battery. With the regulators switching at a frequency of 50 to 60 kHz and the oscillators resonating at 15 to 30 kHz, the harmonic frequencies generated by the regulators are attenuated by the oscillators, and extensive filtering is therefore not needed.

This work was done by Arthur P. Ruitberg and Kenneth M. Young of **Goddard Space Flight Center.** *For further information, Circle 1 on the TSP Request Card.*
GSC-12818

X-Band Strip-Line Power Divider/Combiner

Foil transmission line matches impedances.

NASA's Jet Propulsion Laboratory, Pasadena, California

A strip-line circuit for X-band signals both divides and combines microwave power for a distributed amplifier. Eight distributed input and output ports are located at half-wavelength points along the transmission-line segments of the pattern, and a quarter-wave stub at the main input or output port matches the distributed impedances to the main impedance.

The strip-line substrate and foil pattern is shown in the figure. Half-wave relationships among ports 1 through 8 are indicated. The main input/output port foil pattern has an expanded area for the quarter-wave matching stub. This port "sees" a half wavelength in either direction to point A or B.

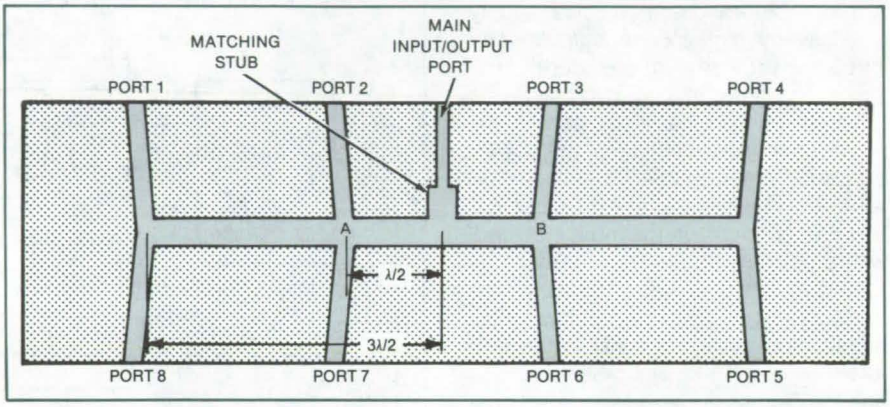

The Strip-line Pattern (foil pattern over an insulating layer over a ground plane) is laid out so that all eight distributed ports lie at electrical distances of odd integral multiples of a half wavelength from the main input/output port.

When the strip line is used as a power divider, the signal source is connected at the main input port, while each of the distributed loads is connected to one of the distributed output ports. When using the pattern as a power combiner, each of the distributed amplifiers or other signal sources is connected to one of the distributed input ports, and power is delivered to the load through the main output port.

The strip-line configuration is identical for the dividing and combining functions, except for the use of different connectors at the various ports, depending on the nature of signal sources and loads. Using this configuration, eight microwave amplifier outputs can be summed by placing a common load at the main input/output port. In the configuration shown, eight 2-watt signals are summed to produce the 12-watt equivalent of a traveling-wave tube.

The application for which the pattern was designed calls for both a dividing and a combining strip line. An 8.4-GHz input signal is sent through the eight-way divider into eight channels. Each channel is comprised of a combined circulator and phase shifter and a three-stage solid-state amplifier that puts out approximately 2 watts. The output of each channel is adjusted at the phase shifter so that the phases of all the channels at the input to the combiner are identical. The amplifier outputs are combined back in the eight-way combiner. The combiner output is fed to a load at the main output port.

This work was done by Bruce L. Conroy of Caltech for **NASA's Jet Propulsion Laboratory.** *For further information, Circle 2 on the TSP Request Card.*

NPO-16086

Optical Logic Gates

Photonic analogs mimic digital electronic logic.

NASA's Jet Propulsion Laboratory, Pasadena, California

Logic gates for light signals would be constructed from combinations of prisms, polarizing plates, and quarter-wave plates, according to a proposal. The signals would be transmitted to and from the gates along optical fibers.

A basic optical logic gate is shown in the figure. Unpolarized light from a remote monochromatic source arrives along two input paths of equal optical length. One or both paths may include an optical transducer or logic gate that turns the signal off (logic "0") or on (logic "1").

The input signals from both paths are transmitted through a sheet of linearly polarizing material. One of the linearly polarized beams is passed through a birefringent quarter-wave plate to convert it to circular polarization, while the other beam is passed through a three-quarter-wave plate to obtain the opposite circular polarization.

The two circularly polarized beams merge through a prism into a common fiber, along which they optically interfere with each other. When both beams are

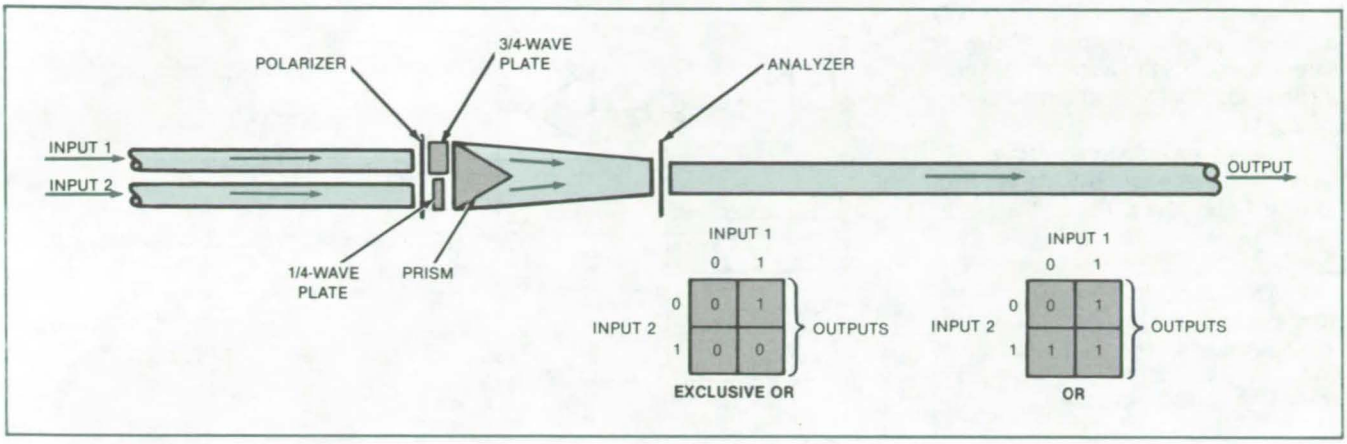

An **Optical Logic Gate** performs an elementary logic operation on light signals received along two optical fibers. Whether the gate performs the OR function or the exclusive-OR function depends on the orientation of the analyzer.

on, the interference sum is linearly polarized. An analyzer (a second linearly polarizing sheet) is placed at the output end of the interference channel.

When the polarization axis of the analyzer is perpendicular to that of the interference sum, no light will get through to the output fiber. If only one of the input beams is on, there will be an output beam because a circularly polarized beam passes through a linearly polarizing plate, emerging with half the incident intensity. If the attenuated output beam is considered to represent logic "1," then the gate as described acts as an exclusive-OR gate.

When the analyzer is rotated 30° from the extinction position, it passes half of either circularly polarized beam as before or one-fourth of the interference sum (which is equivalent in intensity to half of one of the beams). Thus, the gate implements the OR function. The exclusive-OR and OR functions are summarized in the truth tables in the figure. Nonbinary truth tables can also be obtained by rotating the polarizer or analyzer to other positions or inserting other quarter-wave plates.

The other basic logic gates (AND, NOR, NAND) and logic systems can be constructed with various series and parallel combinations of these two gates. Because of the attenuation in the polarizing sheets, large or complicated logic systems will require light amplification. Preferably, the primary light source and the in-line amplifiers would be lasers of the same wavelengths.

This work was done by Eugene R. du Fresne and Warren L. Dowler of Caltech for **NASA's Jet Propulsion Laboratory.** *For further information, Circle 3 on the TSP Request Card.*
NPO-15134

Tuning Concept for Resonant Cavities

Deviations from resonance are detected by sampling phases.

NASA's Jet Propulsion Laboratory, Pasadena, California

A resonant cavity would be adjusted in response to the phase difference between the signals in the E and H planes, according to a concept for hydrogen-maser tuning. The signals would be sampled by probes so as to disturb the maser operation as little as possible.

The concept relies on the principle that at resonance the E (electric) and H (magnetic) fields are in spatial and temporal quadrature, while at a slightly off-resonance frequency the phase difference between E and H varies roughly as the inverse cotangent of the frequency offset divided by the cavity bandwidth. Thus, by detecting the deviation in phase difference from 90°, the departure of the cavity from resonance at the sampling frequency can be detected and corrected. A tuning system based on this principle would automatically tune the cavity to resonance at the maser frequency, thereby compensating for gradual changes in cavity dimensions with age and preventing the frequency-pulling effect that would normally result from such changes.

In the proposed system (see figure), the E and H signals would be sensed by two weakly coupled probes — a dipole and a loop, for example — at the same location. The E and H signals would be passed through low-noise amplifiers to achieve the required signal-to-noise ratio in the sampled signals while minimizing the coupling to the maser cavity.

A portion of the maser output would be fed to the orthogonal E- and H-plane phase detectors. The deviation of the phase difference from 90° would be detected and used to generate an error signal. The error signal would be fed to a varactor or other control element to retune the cavity to resonance.

The proposed technique has been estimated to be sensitive to a fractional frequency deviation of about 5×10^{-16}. The

(continued on next page)

technique should be applicable not only to masers but also to other microwave elements, including klystrons, general-purpose oscillators, and frequency standards.

This work was done by Richard L. Sydnor of Caltech for **NASA's Jet Propulsion Laboratory.** *For further information, Circle 4 on the TSP Request Card.*

Inquiries concerning rights for the commercial use of this invention should be addressed to the Patent Counsel, NASA Resident Office-JPL [see page A5]. Refer to NPO-15890.

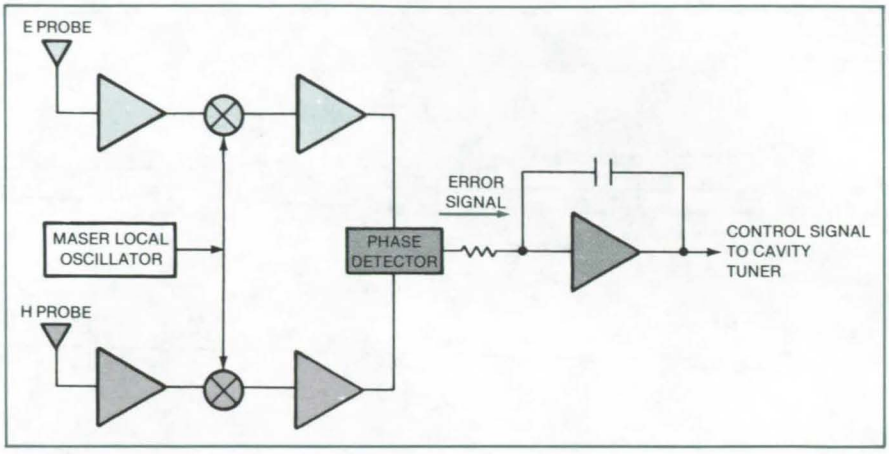

This **Automatic Tuner** is a feedback-control system that derives its error signal from the E-and H-plane probe signals. The control objective is to maintain the phase difference between E and H at 90°.

Isolation Mounting for Charge-Coupled Devices

CCD's are suspended by wires under tension.

NASA's Jet Propulsion Laboratory, Pasadena, California

A support for small imaging devices provides both cooling and vibration isolation. Developed for charge-coupled devices (CCD's) in infrared telescopes, the support is adaptable to sensors in a variety of environments — for example, sensors in nuclear reactors, engine exhausts, and plasma chambers.

The CCD image detector is mounted in a socket. Wires from the socket lead to connectors set in the walls of the CCD chamber (see figure). The socket is mounted on a copper post, to which a cable is attached. Heat from the assembly is conducted to the cold-plate side of a thermoelectric cooler through the flexible cable.

The copper post is mounted at the center of a three-legged bracket or spider. Each leg is suspended by three titanium wires that are held in tension by brackets on the chamber wall. The tension in each set of wires is adjusted by a setscrew to about one-third of the elastic limit. This tension not only holds the three-legged bracket securely but also resists shock- and vibration-induced motion.

This work was done by Willis C. Goss and Phil M. Salomon of Caltech for **NASA's Jet Propulsion Laboratory.** *For further information, Circle 5 on the TSP Request Card.*
NPO-15551

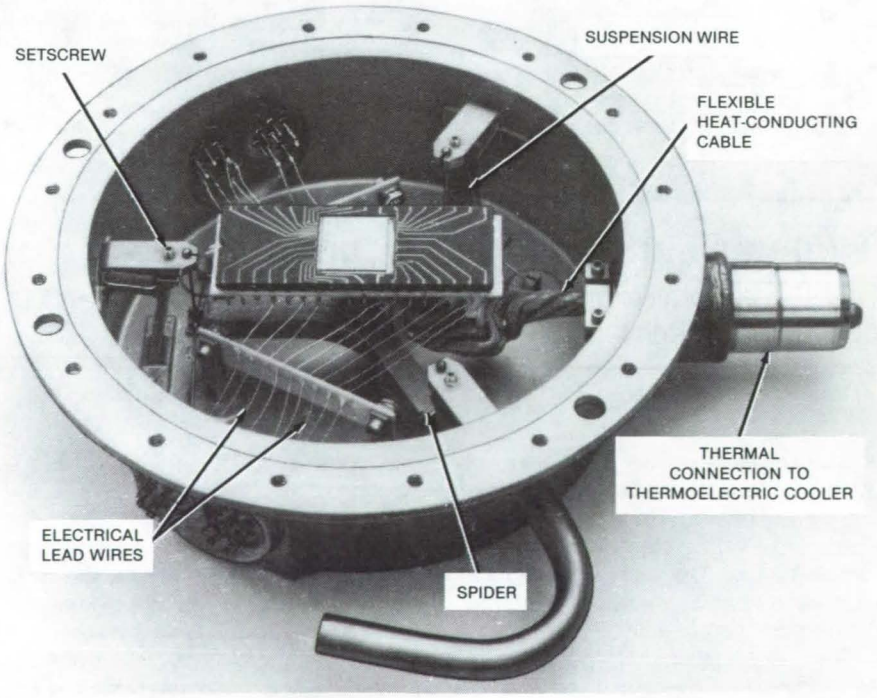

Remote Thermoelectric Cooling of a Charge-Coupled Device allows vibration-isolating mounting of the CCD assembly alone, without having to suspend the entire mass and bulk of a thermoelectric module. The mounting hardware is therefore simple and light.

Semiconductor Laser Phased Array

Oscillations are synchronized and modulated individually for beam steering.

NASA's Jet Propulsion Laboratory, Pasadena, California

A proposed phased array of GaAs infrared lasers would put out a powerful, electronically-steerable coherent beam. Fabricated as an integrated circuit on a GaAs chip, the new device would be particularly suited to optical communications, optical data processing, and optical detection and ranging systems. The concept evolved from a need to obtain a steerable beam of higher power than is available from a single semiconductor laser.

Monolithic integration will be exploited to provide the mutual coupling that is necessary to synchronize the oscillations of the individual lasers. This synchronization will make possible the higher output-power densities that can be achieved only by coherent addition of the individual output beams: The maximum power density varies roughly with the square of the number of elements instead of linearly with the number as in incoherent addition.

A possible integrated configuration is shown in the figure. Each laser has a separate power contact, and each is equipped with an electro-optic modulator for fine tuning of its oscillation frequency and maintenance of the phase lock with the other lasers in the array. An electro-optical phase shifter also operates in tandem with each laser to adjust the phase of the individual output beam without significantly disturbing the frequency. The output beam resulting from the combination of the individual beams is steered by controlling the individual phase shifts, in the manner of phased-array radio antennas.

The modulators and phase shifters rely on the linear electro-optic effect in which the tensor index of refraction of the medium varies linearly with the applied electric field. For a GaAs medium in the configuration shown here, a relative frequency change of 10^{-4} is possible, and a phase shifter 100 microns long can produce a shift of about 1 radian. The frequency and phase shifts are limited by the onset of avalanche breakdown at high applied electric fields.

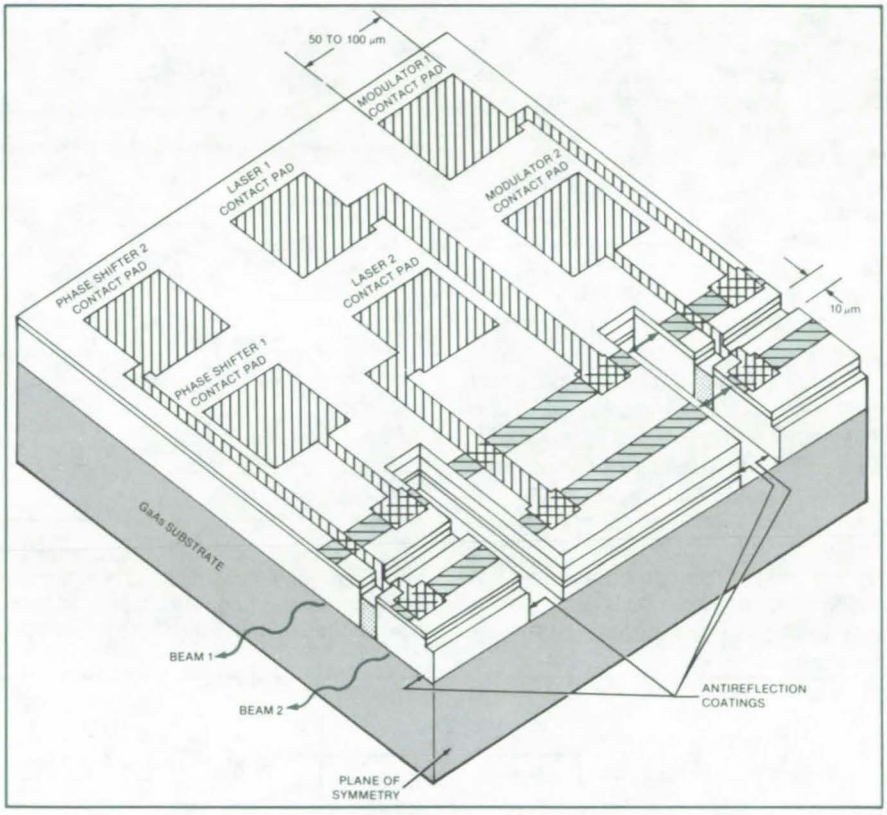

This **Two-Element Semiconductor Laser Array** is half of a symmetrical four-element array to be fabricated on a single GaAs substrate. The dimensions shown here are only typical. For clarity, the oxide insulating layer between the two metalization layers is not shown.

For close coupling between each laser and its modulator, an anti-reflection coating would be applied to the faces between these two parts. The modulator therefore functions as though it were in the laser cavity. The lateral distance between the elements of an array is typically 10 microns or less to assure close coupling. Two levels of metalization are needed to form the contact strips to the multiple elements of the array.

This work was done by Joseph Katz of Caltech for **NASA's Jet Propulsion Laboratory.** *For further information, Circle 6 on the TSP Request Card.*
NPO-15963

Direct-Current Unbalance Detector

Short circuits to ground are indicated by voltage changes.

NASA's Jet Propulsion Laboratory, Pasadena, California

A current transducer connected in a bridge circuit with a "floating" 30-Vdc power supply measures the voltage unbalance between the positive and negative powerlines and ground. The detection-circuit output swings higher or lower than the normal balanced-condition voltage to signify unbalance toward the positive or negative side, respectively. This circuit configuration can be adapted to monitor 4- to 20-mA current loops often found in industrial controls.

As shown in Figure 1, the current transducer (of input resistance much less than 2,000Ω) is wired in series with a pair of 2,000-Ω resistors. One side of the transducer input is connected to ground. The transducer normally develops 3 Vdc output at an input of 15 mA. During normal balanced operation, the positive and negative dc lines are each 15 V from ground, and resistors R_1 and

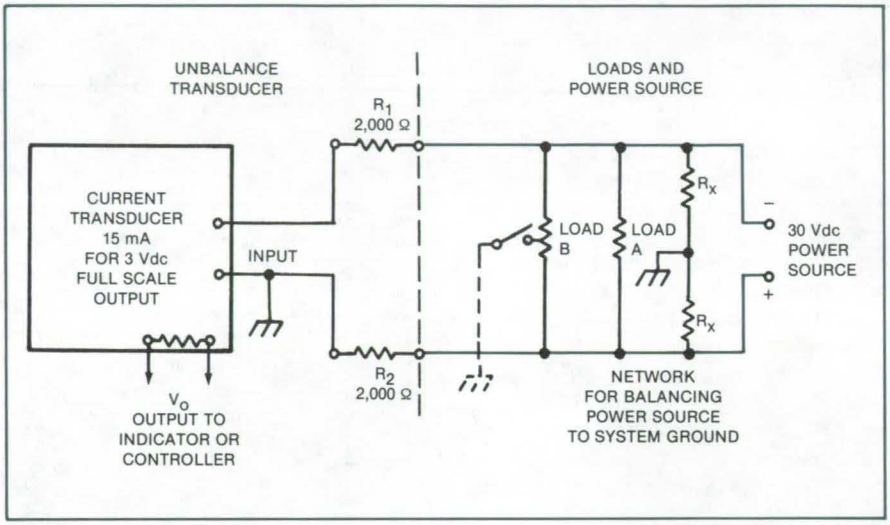

Figure 1. This **Direct-Current Unbalance Detection Circuit** signals full and partial short circuits to ground. Transducer output V_O swings above or below a normal balanced voltage level depending upon the degree of load unbalance. If load B sustains a partial short toward the positive side of the power bus, V_O swings higher.

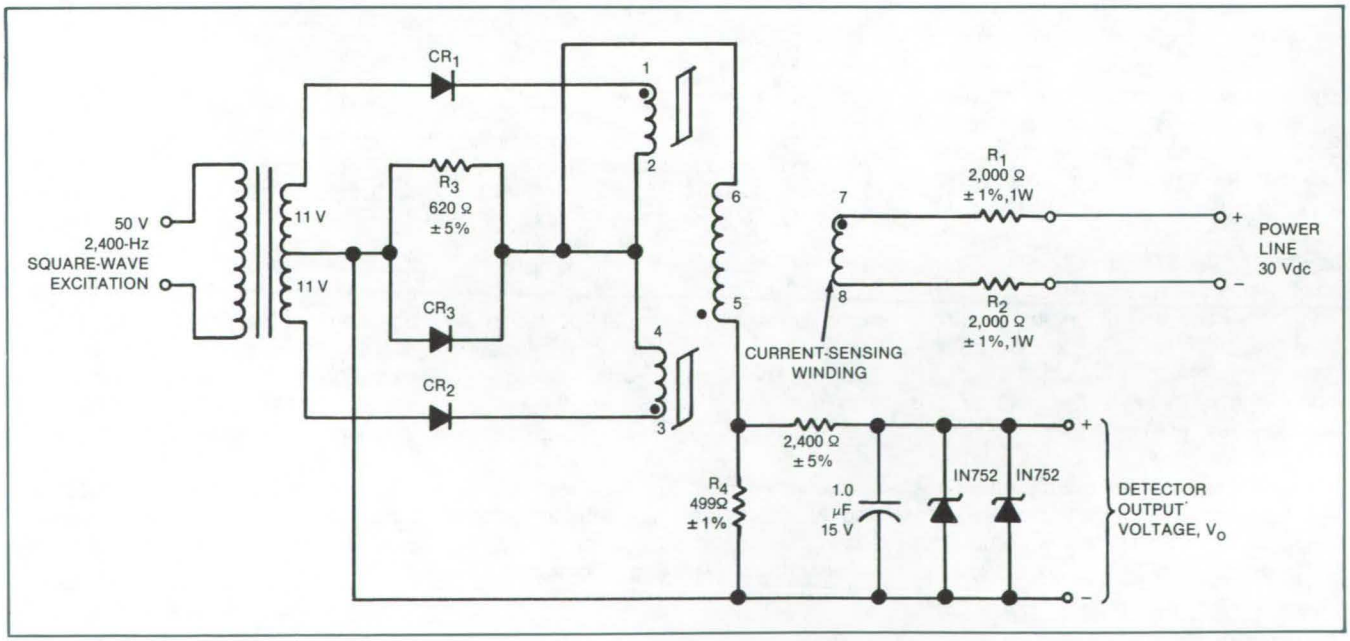

Figure 2. The **Current Transducer** uses magnetic-amplifier circuitry, which provides low input resistance and isolation of the output voltage from both ground and the dc power supply being monitored.

R_2 pass 7.5 mA to develop 1.5 V of transducer output. If the positive line shorts to ground, the full 30 V appear across R_1, causing a current of 15 mA in R_1 and through the transducer and a consequent transducer output of 3.0 Vdc. If the negative side of the line shorts to ground, there is no transducer input current and the transducer output falls to 0 V. A short elsewhere produces an intermediate output voltage.

Resistors R_X form a balancing network. They can be eliminated, however, since the detector circuit provides redundant balancing.

A typical isolating current transducer is shown in Figure 2. It includes a square-wave-chopped magnetic amplifier having four windings on a pair of saturable cores and a smoothing output filter.

This work was done by Albert P. Wagner of Caltech for **NASA's Jet Propulsion Laboratory.** *For further information, Circle 7 on the TSP Request Card.*
NPO-15978

Circuit for Monitoring Cell Voltages

It uses two multiplexers and a differential amplifier

Marshall Space Flight Center, Alabama

The circuit shown in the figure monitors the voltage of each cell in an electrical battery within a few millivolts. It includes two bipolar analog multiplexers that repeatedly sample the outputs of 12 1.5-volt cells. The terminals of multiplexer 1 are connected to the positive sides of the cells, and the terminals of multiplexer 2 are connected to the negative sides. The outputs of the multiplexers are connected to a differential operational amplifier, which provides signals for recording and display.

Both chips derive a common reference voltage from a battery center tap between cells 6 and 7. This common reference halves the voltage range faced by either chip, thereby allowing the chips to scan 12 cells without exceeding their rated positive and negative voltages (± 10 volts).

Each multiplexer chip has 16 input ports. Since only 12 ports are required for the cells, ports 13 and 14 are used to read the scaled voltage of the series strings of cells 1 through 6 and 7 through 12, respectively. These readings provide additional data for the verification of individual cell readings. For example, if one cell reads zero but the six-cell reading is normal, the zero reading is suspect.

Input port 15 monitors the reference voltage of the analog-to-digital converter that follows the operational amplifier, allowing calibration of the scaling amplifiers in the circuit between the multiplexers and the analog-to-digital converter. Input port 16 provides a zero reference for the calibration of any offset in the analog-to-digital converter.

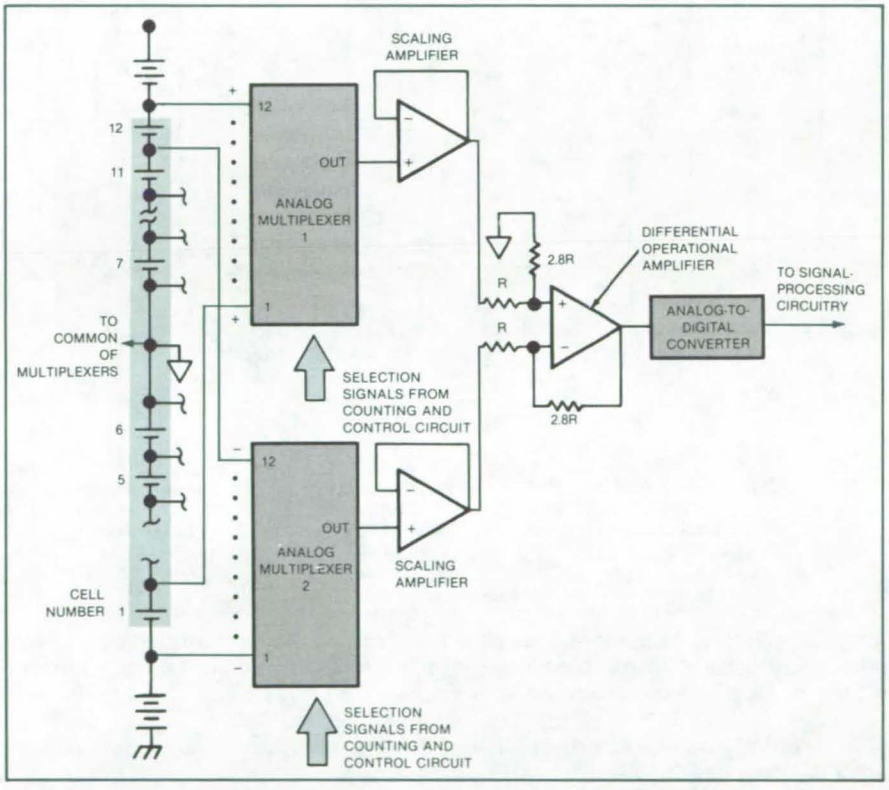

The Center Tap on the battery stack is connected to the common inputs of the two analog multiplexers. The maximum excursion of the analog inputs is thus less than the maximum multiplexer rating of ± 10 volts.

This work was done by Jack W. Lepisto of TRW, Inc., for **Marshall Space Flight Center.** *For further information, Circle 8 on the TSP Request Card.*

Inquiries concerning rights for the commercial use of this invention should be addressed to the Patent Counsel, Marshall Space Flight Center [see page A5]. *Refer to MFS-25924.*

Circularly-Polarized Microstrip Antenna

Microstrip construction is compact for mobile applications.

NASA's Jet Propulsion Laboratory, Pasadena, California

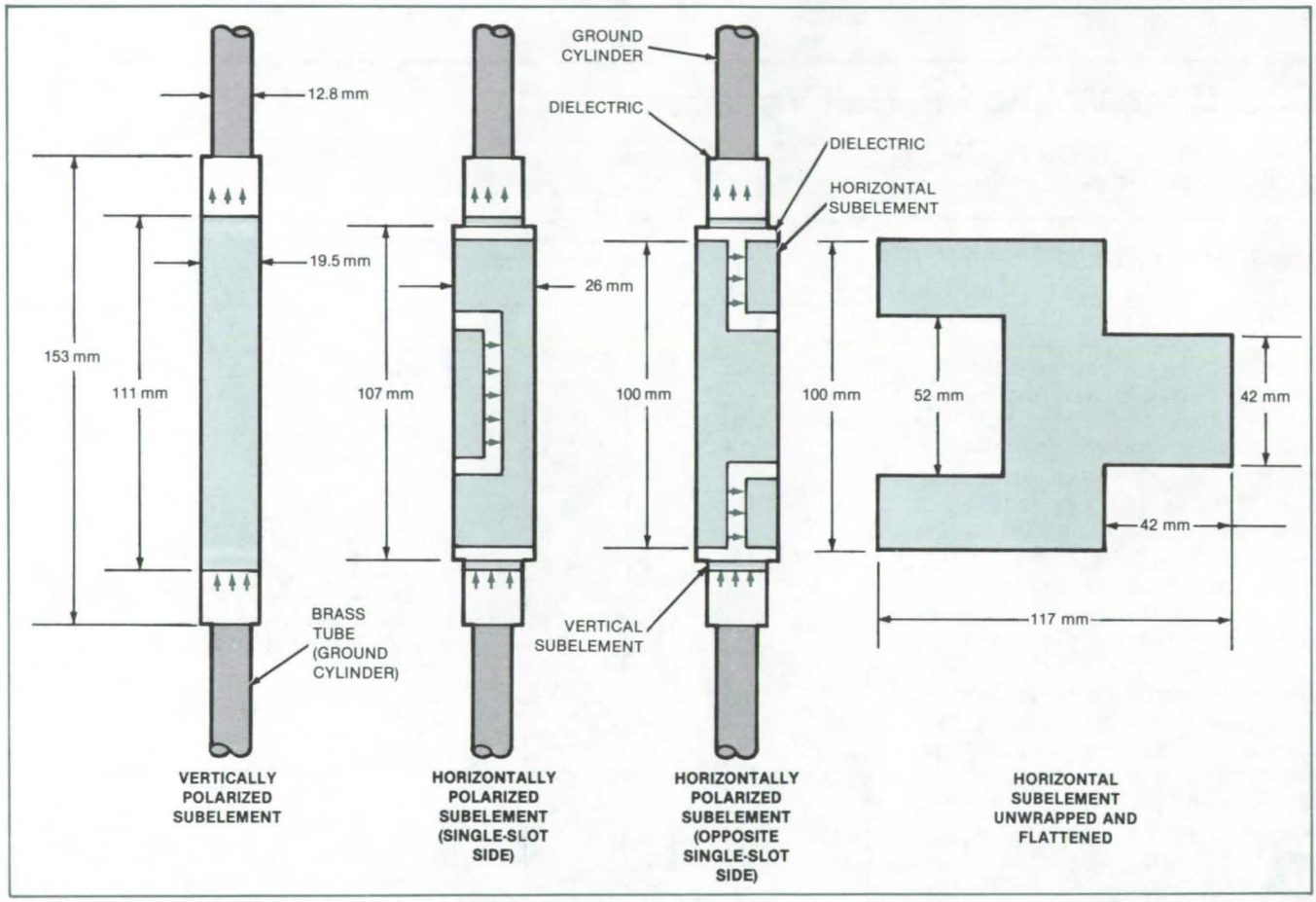

A **Circularly-Polarized Microstrip Antenna** is made of concentric cylindrical layers of conductive and dielectric materials. Coaxial-cable feedlines are connected to the horizontal and vertical subelements from the inside. In this configuration, the vertical subelement acts as the ground for the horizontal subelement.

A circularly-polarized microstrip antenna under development is compact enough for mobile use. Its radiation pattern is azimuthally omnidirectional; in elevation it covers a swath 50° wide. NASA's prototype operates at 953 MHz.

The antenna is assembled from cylindrical elements (see figure), one for the horizontal polarization and one for the vertical polarization. Each element is slightly less than one-half wavelength long and about one-twelfth wavelength in diameter. The structure is supported by a brass tube that serves as the ground cylinder. A polytetrafluoroethylene dielectric cylinder around the brass tube is the substrate for the cylindrical elements.

Coaxial feedlines are routed through the inside of the ground cylinder. The outer conductor of the vertical feed is connected to the ground cylinder and the inner conductor to the vertical subelement. The outer conductor of the horizontal feed is connected to the vertical subelement, while the inner conductor is connected to the horizontal subelement.

The positions of the feedline connections are chosen to give the optimum impedance match. The vertical and horizontal feeds are cut to the proper electrical lengths and interconnected through a power splitter/combiner to yield a 90° phase shift between the vertical and horizontal far fields; that is, to give a circularly-polarized radiation field.

This work was done by Philip H. Stanton of Caltech for **NASA's Jet Propulsion Laboratory.** *For further information, Circle 9 on the TSP Request Card.*

Inquiries concerning rights for the commercial use of this invention should be addressed to the Patent Counsel, NASA Resident Office-JPL [see page A5]. Refer to NPO-15875

Powerline Coupler for Windmill Motor/Generators

Efficiency at low windspeed is increased by firing-angle control.

Marshall Space Flight Center, Alabama

Power is coupled from a wind-driven induction motor/generator to an ac powerline with the help of the circuit shown in the figure. The circuit reduces the power consumed by the field windings, thereby improving efficiency at low windspeeds.

The control circuit includes a zero-crossing detector, ramp generator, and comparator similar to those used to set the firing angles for thyristors in power-factor motor controllers. The ramp and comparator reference voltage are adjusted so that the thyristor is switched on when the line voltage is about 150° into each half cycle. From that point, and until the 180° point (at which the line voltage passes through zero), the powerline supplies field current to the motor.

Because of the phase lag between the line voltage and the motor current, a positive current continues to flow during part of the following negative voltage half cycle. During that time, power is returned to the line. The thyristor turns off only when the current crosses zero, at which point the generator ceases to deliver power to the line. The coupling circuit thus reduces the portion of each half cycle in which current is drawn by the generator, thus substantially improving its efficiency by reducing the power consumption.

The late start of the conduction interval reduces the time during which the product of current and voltage (that is, the power consumed) is positive. The flow of power back into the line during the negative-product interval remains unimpaired, however, with the result that the average power consumed is decreased relative to the average power generated.

This work was done by Frank Nola of **Marshall Space Flight Center.** *For further information, Circle 10 on the TSP Request Card.*

Inquiries concerning rights for the commercial use of this invention should be addressed to the Patent Counsel, Marshall Space Flight Center [see page A5]. *Refer to MFS-25944.*

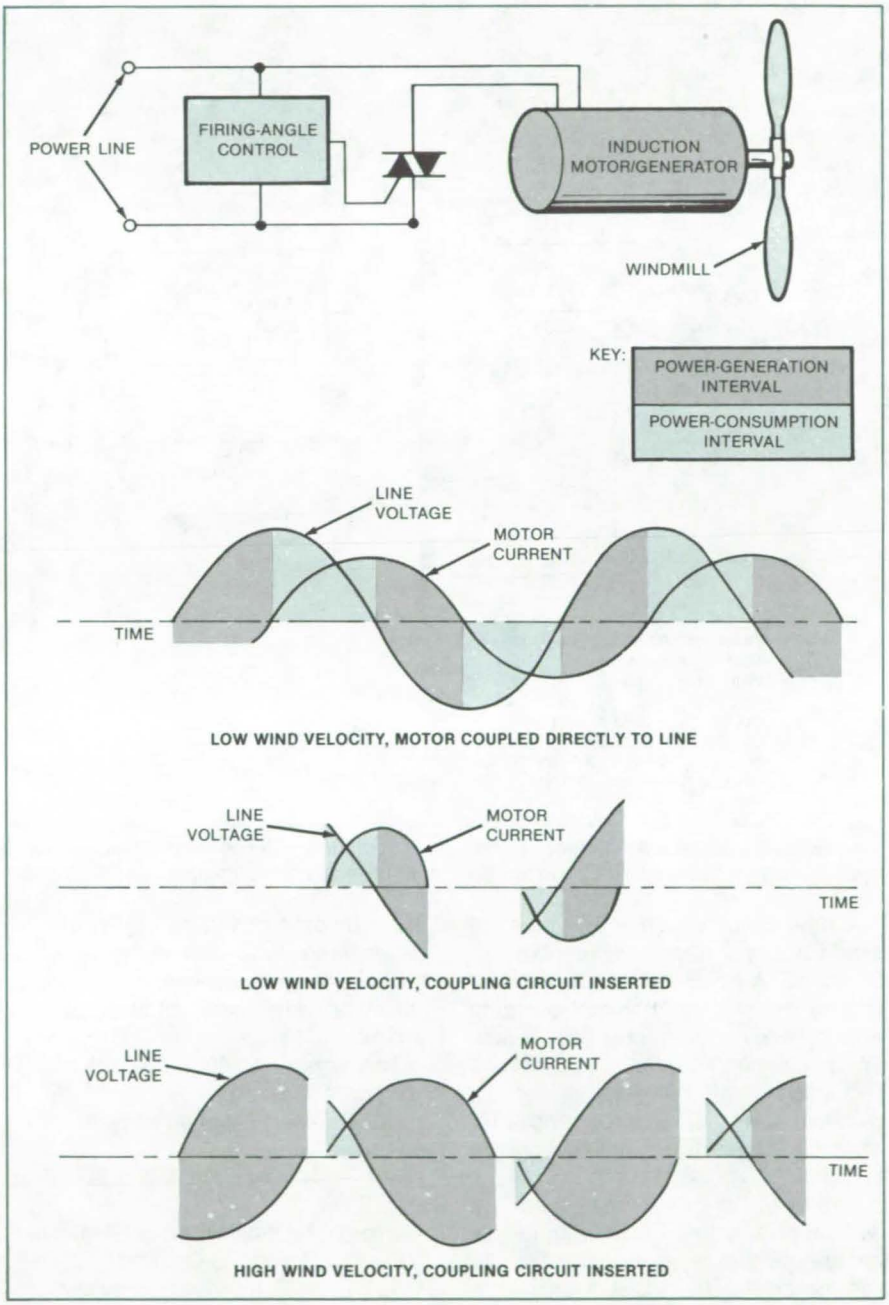

Firing-Angle Control Circuitry decreases the power consumption portion of the line-voltage cycle, increasing the efficiency of a windmill-driven induction motor/generator.

Improved RF Isolation Amplifier

Circuit has high reverse isolation and a wide bandwidth.

NASA's Jet Propulsion Laboratory, Pasadena, California

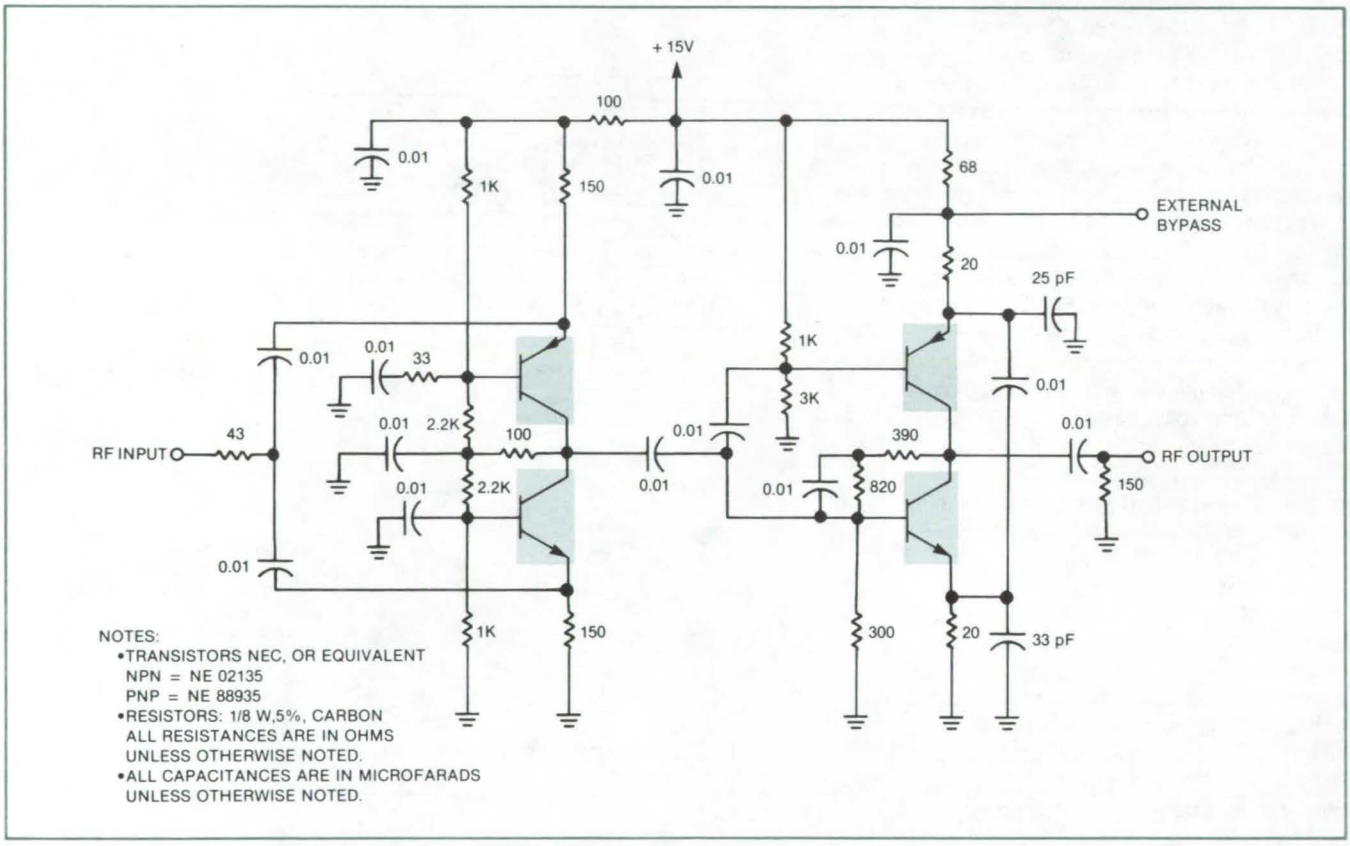

The Wideband Isolation Amplifier has a low intermodulation distortion and high reverse isolation. The circuit, which will be implemented in a hybrid package, is expected to find application in RF and video signaling.

A new radio-frequency (RF) isolation amplifier has a frequency response of 0.5 to 400 MHz ± 0.5 dB. It does not require selected or matched components or a directional coupling device. The circuit can be used in applications requiring high reverse isolation, such as receiver intermediate-frequency (IF) strips and frequency distribution systems.

The circuit shown in the figure is a two-stage amplifier. Both stages use complementary-symmetry transistor arrangements. The input stage is a common-base connection for the complementary circuit. The output stage, which supplies the positive gain, is a common-emitter circuit using emitter degeneration and collector-base feedback for impedance control. The input stage provides most of the reverse isolation.

The amplifier has the following characteristics:

- dc Supply, +15 V at 40 milliamperes;
- Gain, +7 dB;
- Frequency Response, 0.5 to 400 MHz +0.5 dB;
- Reverse Isolation, 80 dB at 20 MHz, 67 dB at 100 MHz, and 56 dB at 300 MHz;
- 1-dB Gain Compression Level, +16 dBm at 100 MHz;
- Input Standing-Wave Ratio, better than 1.1 between 0.5 and 400 MHz;
- Output Standing-Wave Ratio, better than 1.7 between 0.5 and 100 MHz; and
- Noise Figure, 12 dBm.

The intermodulation distortion using a two-tone test has a third-order intercept point at +26 dBm. The output impedance control is improved by resistive loading on the output port.

This work was done by Gary L. Stevens and John MacConnell of Caltech for **NASA's Jet Propulsion Laboratory.** *For further information, Circle 11 on the TSP Request Card.*
NPO-16026

Digital Sequence Controller

The length and timing of pulse sequences are user-controlled.

NASA's Jet Propulsion Laboratory, Pasadena, California

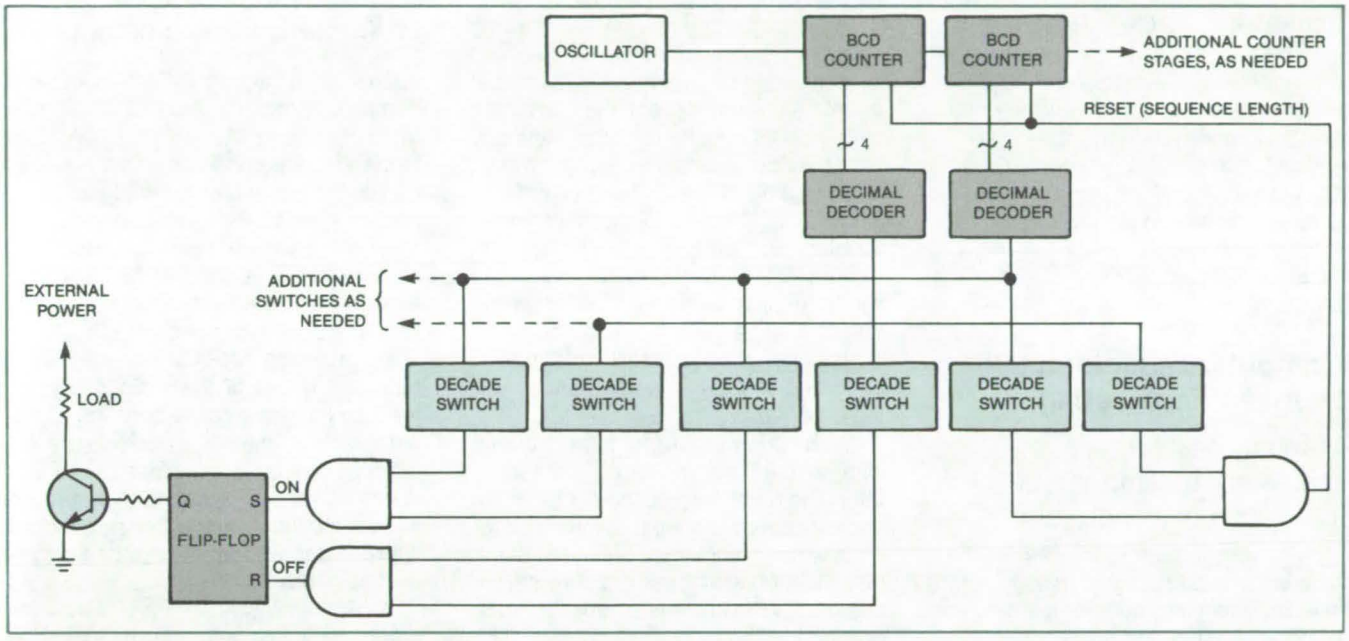

The **Digital Sequence Controller** in this simplified block diagram (only one load is shown) could drive several loads, such as solenoid pumps that must be synchronized.

A digital circuit generates several pulse streams to control loads that must be synchronized. It allows the duration and phasing of each stream to be varied independently. The original application of the circuit was to control a pump for biomedical applications.

In the digital controller shown in the figure, an astable circuit drives cascaded BCD counters. The astable period establishes the basic time resolution of the controller and, together with the counter length, sets the maximum sequence length or period.

The loads are controlled by solid-state switches, which are driven by flip-flops. These flip-flops are set and reset by decoded, switch-selected counter outputs. The loads are thus turned on and off at any chosen points in the sequence. If desired, the astable period could also be adjustable, allowing the entire sequence to be modified by a scale factor.

A prototype of the circuit was used to drive two pairs of solenoids. With the astable element operating at 100 Hz and using two BCD counter/decoder stages, its maximum period was 1 second and the basic resolution 0.01 second. Using a 555 timer as the astable element and CMOS logic and counting circuits, power consumption was low enough for battery operation.

This work was done by James O. Lonborg of Caltech for **NASA's Jet Propulsion Laboratory.** *For further information, Circle 12 on the TSP Request Card.*

NPO-15725

Computer Programs

These programs may be obtained at very reasonable cost from COSMIC, a facility sponsored by NASA to make new programs available to the public. For information on program price, size, and availability, circle the reference letter on the COSMIC Request Card in this issue.

Software for PROM Programing

Driver program allows for the programing, reading, and verification of various PROM's.

A driver program for the DATA I/O PROM Programmer has been developed on the Motorola M6800 EXORCISOR Development Workstation. The program allows for the programing, reading, and verification of various PROM's.

Manual entry of data to the DATA I/O PROM Programmer is time-consuming and error-prone. This driver program

(continued on next page)

combines the file management capability of the EXORCISOR with the flexibility of the DATA I/O system. It provides the user with a way of reading, programing, and verifying PROM's, storing data on disk, modifying files, and printing the data.

This program is written in Assembler for the Motorola EXORCISOR with EXORDISK and 16K of RAM operating under MDOS. The program acts as a driver for the DATA I/O System 19 PROM Programmer with the remote option. This program was developed in 1981.

This program was written by Charles W. Goolsby of Rockwell International Corp. for **Johnson Space Center.** *For further information, Circle A on the COSMIC Request Card.*
MSC-20641

Computerized Interactive Harness Engineering

Manual methods are emulated, making the user interface very "natural."

The computerized interactive harness engineering program is an inexpensive, interactive system for learning and using an engineering approach to interconnection systems. It is basically a data-base system that stores information as files of individual connectors and handles wiring information in circuit groups stored as records. This directly emulates the typical manual engineering methods of data handling. Data files are created, viewed, manipulated, or printed in real time. The printed output is in a form ready for use by fabrication and engineering personnel. The program also contains error-checking routines including connector contact checks during hardcopy generation.

The user may edit existing harness data files or create new files. In creating a new file the user can insert all the connector and harness boilerplate data that would be part of a normal connector wiring diagram. These data include the following: (1) connector reference designator, (2) connector part number, (3) backshell part number, (4) cable reference designator, (5) cable part number, (6) drawing revision, (7) relevant notes, (8) standard wire gage, and (9) maximum circuit count. Any item except the maximum circuit count may be left blank, and any item may be changed at a later time.

Once a file is created and organized, the user is directed to the main menu and has access to the file boilerplate, the circuit wiring records, and the wiring-records index list. The organization of a file is such that record "zero" contains the connector/cable boilerplate and all other records contain wiring data.

Each wiring record handles a circuit with as many as nine wires in the interface. The record stores the circuit name and wire count and the following data for each wire: (1) wire identifier, (2) contact, (3) splice, (4) wire gage if different from standard, (5) wire/group type, (6) wire destination, and (7) note number. The record structure allows for a wide variety of wiring forms using splices and shields, yet retains sufficient structure to maintain ease of use.

The computerized interactive harness engineering program is written in Pascal and has been implemented on an Apple II computer with a memory of 64K of 8-bit bytes, two 5 1/4-inch floppy disk drives, and an Epson MX-series printer. This program was developed in 1983.

This program was written by Joseph W. Billitti of Caltech for **NASA's Jet Propulsion Laboratory.** *For further information, Circle B on the COSMIC Request Card.*
NPO-16272

Antenna Radiation-Pattern Program

The effects of reflector deformations and feed characteristics are computed.

The JPL Antenna Radiation Pattern computer program, ANRAD, evaluates the performance of a radio-frequency antenna with a paraboloidal main reflector by solving the scalar far-field radiation-pattern integral. Reflector surface deformations, aperture blockage, and displacement of the primary feed from the focus are several factors that can diminish radio-frequency performance.

By providing ANRAD with the amplitude and phase of the radio-frequency feed and surface characteristics of the paraboloidal reflector, these detrimental factors can be represented, and the user may obtain the radiation pattern of the composite antenna (main reflector, subreflector, and feed) and the normalized gain loss.

ANRAD is written in FORTRAN V for batch execution and has been implemented on a UNIVAC 1100-series computer with a central memory requirement of approximately 65K of 36-bit words. The present configuration of ANRAD was developed in 1983.

This program was written by Robert D. Hughes, Cecilia N. Guiar, and Charles L. Lawson of Caltech for **NASA's Jet Propulsion Laboratory.** *For further information, Circle C on the COSMIC Request Card.*
NPO-16217

MiniBriefs describe NASA innovations and reports in an abbreviated format. Readers desiring additional information on these items should request the Technical Support Packages (TSP's), available in most cases, which can be obtained by using the TSP Request Card at the back of this issue.

Temperature-Stabilized Phase Detector

Precise phase detector is stable over large ambient-temperature ranges.

A precise temperature-stabilized phase detector for clock-signal distribution maintains a 100-MHz signal with stability of 5 parts in 10^{16} even for step changes of 20° C in ambient temperatures. Temperature stabilization is achieved by heating the unit to 45° C and maintaining the temperature through a bridge circuit.

A conventional thermistor bridge is set with the bridge resistance equal to the thermistor resistance at 45° C. As ambient temperatures rise, power input to the heaters is reduced. When ambient temperatures drift downward, the unbalance of the thermistor bridge is amplified and converted to current to drive the heater circuit. Stabilization of this sort is useful in phase-locked-loop receivers.

This work was done by Lo Yeeman of **NASA's Jet Propulsion Laboratory.** *For further information, Circle 25 on the TSP Request Card.*
NPO-15766

Negatively Coupled Inductors for Odd-Phase Choppers

A modification of the output inductor circuit is required.

Splitting the windings of the output inductors of a negatively-coupled "boost" chopper extends its applicability to an odd number of phases — including three phases, the number most frequently used. The new version concatenates the output inductors of each phase with those of neighboring phases, achieving a negative coupling effect that suppresses unwanted harmonics. For a three-phase chopper, three output transformers are required. Although this is one more than needed for a four-phase chopper of the previous configuration, each transformer is small and the net weight and volume should be no greater than the previous version.

This work was done by Robert S. Jamieson of Caltech for **NASA's Jet Propulsion Laboratory.** *For further information, Circle 26 on the TSP Request Card.*

Inquiries concerning rights for the commercial use of this invention should be addressed to the Patent Counsel, NASA Resident Office-JPL [see page A5]. *Refer to NPO-15380.*

Mathematical Storage-Battery Models

Eventual applications include electric-vehicle "fuel" gages and powerline load leveling.

An empirical formula represents the performance of electric storage batteries. The formula covers many battery types and includes numerous coefficients that can be adjusted to fit the peculiarities of each type. Battery and load parameters taken into account include power density in the battery, discharge time, discharge rate, and electrolyte temperature.

Representative lead/acid batteries were studied in laboratory tests and computer simulations with models that include elements of the generic formula. The most promising of the tested battery-in-vehicle models is the JPL/Purdue model that assumes an optimal battery capacity (different from the traditional cited ampere-hour capacity) and that the battery recovers some capacity during idle periods.

This work was done by C. Phil Chapman and Martha Aston of Caltech for **NASA's Jet Propulsion Laboratory.** *For further information, Circle 27 on the TSP Request Card.*
NPO-15615

Improved Spark-Ignitor Circuitry

Transformer reduces the flyback voltage to 350 V.

Several modifications have been made to an inductive-discharge spark-ignitor system for a rocket engine, which substantially reduce the complexity of the circuits and eliminate the difficulties associated with component matching. The primary feature of the new design is the utilization of a transformer that reduces the flyback voltage from 700 V to 350 V, resulting in less-stringent selection requirements for the high-voltage switching transistor. Other features include removal of the active feedback winding to prevent transistor overstress, and addition of a snubbing capacitor across the transistor to establish a safe voltage- or current-crossover point. Further reliability in the system was obtained by incorporating integrated circuits and reducing the overall number of components.

This work was done by David G. Olschansky of Rockwell International Corp. for **Marshall Space Flight Center.** *For further information, Circle 28 on the TSP Request Card.*

Inquiries concerning rights for the commercial use of this invention should be addressed to the Patent Counsel, Marshall Space Flight Center [see page A5]. *Refer to MFS-19751.*

Stowable Solar-Cell Array

Interconnected cells could be rolled up like a blanket.

A proposed solar-electric power source would be easily storable and transportable. The source would employ a blanket of photovoltaic cells that could be rolled up when not in use.

The cells would be placed between a flexible substrate containing electrical interconnections and a flexible transparent cover. This blanket could be rolled up on a reel in a storage canister. For use, the blanket would be unfurled and supported by collapsible legs. The power and voltage output could be varied according to the amount of extension of the blanket from the canister. The hollow core of the canister reel could be used as storage space for radio equipment, first-aid supplies, or the like.

This work was done by Paul M. Stella of Caltech for **NASA's Jet Propulsion Laboratory.** *For further information, Circle 29 on the TSP Request Card.*
NPO-15893

Burnwire Simulator

A fuse-containing device simulates pyrotechnic firing circuitry.

An easily-installable fuse, which simulates a bridgewire, has been shown to test pyrotechnic firing circuits effectively and economically. The simulator includes a housing, a receptacle connector at one end, and a fuse holder with an easily removable fuse at the opposite end. The electrical properties of the fuse are selected to match the electrical resistance of the bridgewire circuit. Following a firing test, the blown fuse can be replaced and the system easily readied for further testing. The fuse circuit is useful in any system having complex built-in wiring for current-pulse applications.

This work was done by Glenn L. Bummer of Caltech for **NASA's Jet Propulsion Laboratory.** *For further information, Circle 30 on the TSP Request Card.*
NPO-15883

A Sensitive Infrared Photodetector

This detector uses photodetachment of negative ions to measure infrared spectra.

A technique utilizing photodetachment of negative ions is incorporated into a sensitive photodetector. This photodetachment allows detection of low-energy infrared photons, without inherent noise sources and without resorting to cryogenic cooling. The process is easily accomplished by the incoming low-energy photons because the energy required to detach an electron from some negative ions is near zero. The detached electrons are then collected to form a current pulse. This pulse is shaped and measured as a signal that is proportional to the number of low-energy photons.

This work was done by Santosh K. Srivastava and Lutfollah Maleki of

(continued on next page)

Caltech for **NASA's Jet Propulsion Laboratory.** *For further information, Circle 31 on the TSP Request Card.*
NPO-15926

Precise Control of a Tunable IR Diode Laser

Accurate control of temperature and current yields 3-MHz stability over 1.5-hour period.

A tuning system applicable to lead-salt semiconductor tunable diode laser (TDL) and other solid-state lasers with temperature- and current-dependent emission wavelength has been developed for a balloon-borne, high-resolution spectrometer that measures trace atmospheric constituents in the stratosphere. The instrument measures absorption at approximately 20 points in a 100-MHz-wide spectral line.

A digital feedback loop controls junction current and bulk temperature of the TDL with a programable current source (CS) and temperature-set apparatus, each having 16-bit resolution. The CS range is 0 to 1.048 A; the CS stability, 20 ppm/°C; temperature-set resolution is 0.36 mK; temperature stability is 0.1 mK for a 1.5 h period.

This work was done by Robert T. Menzies and Charles W. Rutledge of Caltech for **NASA's Jet Propulsion Laboratory.** *For further information, Circle 32 on the TSP Request Card.*

Inquiries concerning rights for the commercial use of this invention should be addressed to the Patent Counsel, NASA Resident Office-JPL [see page A5]. *Refer to NPO-16000.*

Tube-Wall Thickness Detector

Eddy-current measurements detect wear in thin-wall tubing.

Eddy-current measurements can be used to detect wear of thin walls [0.01 in. (0.25 mm)] in small-diameter [0.19 in. (5 mm)] heat-exchanger tubing. Wall thinning caused by wear is detected by a small-diameter eddy-current coil placed inside the tube to measure the change in coil inductance and phase shift resulting from wall thinning. A flexible, durable thin rod inserts the eddy-current coil into the heat-exchanger tube.

This work was done by Roderic E. Kleint and Richard D. Baily of Rockwell International Corp. for **Marshall Space Flight Center.** *For further information, Circle 33 on the TSP Request Card.*

Inquiries concerning rights for the commercial use of this invention should be addressed to the Patent Counsel, Marshall Space Flight Center [see page A5]. *Refer to MFS-19741.*

Twist-Free Wire Stranding

Trouble-free device eliminates kinks and breaks in stranded-wire assemblies.

A device for wire-stranding operations provides uniform tension and twist-free conditions for 30-gage or smaller, high-strand-density flexible cable assemblies. Wire position is controlled by fixing the orientation and location of the wire spool relative to the wire-loading frame. This prevents rotation and eliminates twisting, breaking, and kinking of the wire. Equalized and precise wire tension is maintained by identical compression springs and multiple loops over spring-loaded rockers.

This work was done by Robert W. Hines of Honeywell, Inc., for **Marshall Space Flight Center.** *For further information, Circle 34 on the TSP Request Card.*
MFS-25914

Electronic Systems

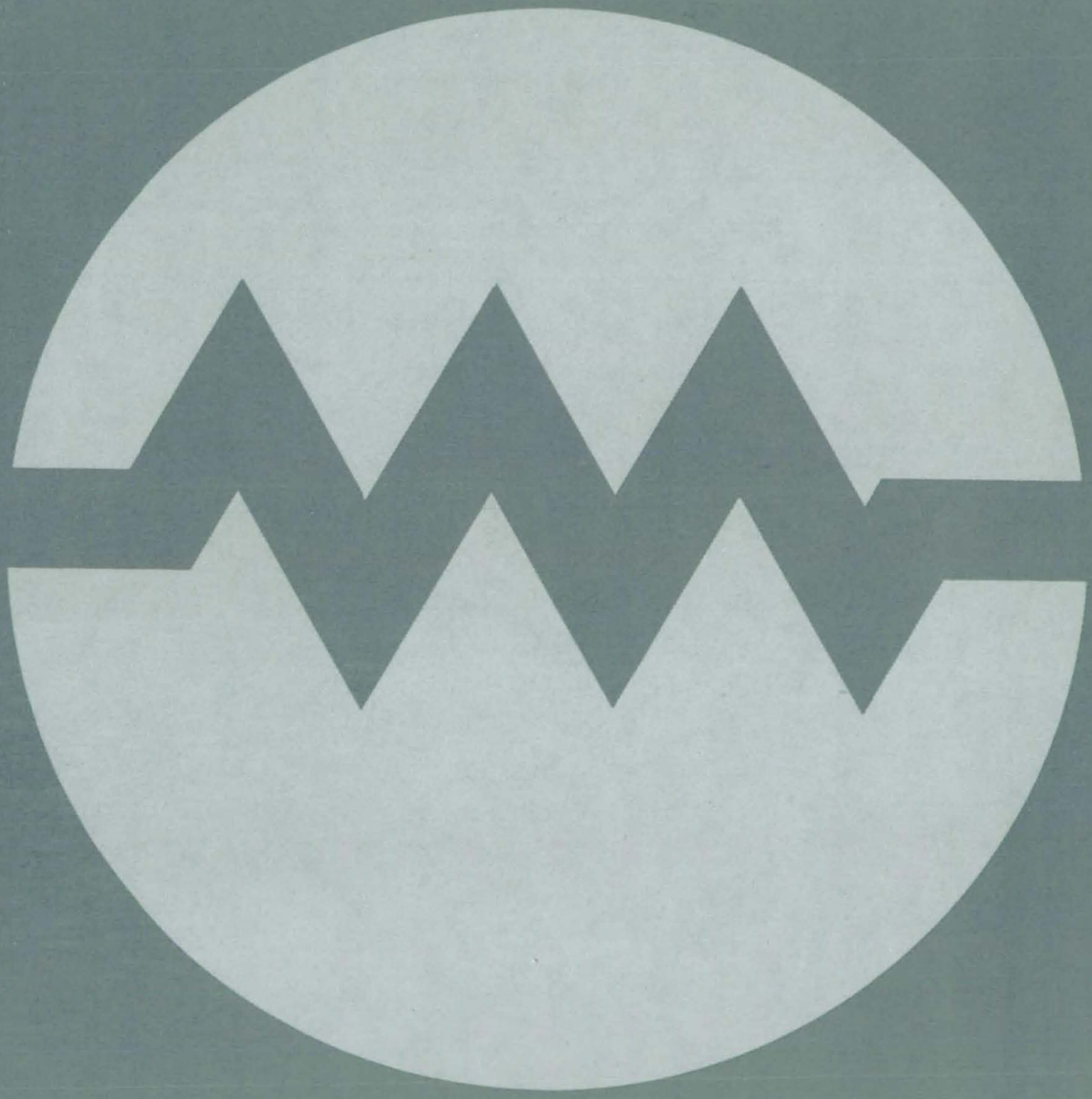

Fast Dual Analog-to-Digital Converter

Unit delivers blocks of quadrature data to computer memory.

NASA's Jet Propulsion Laboratory, Pasadena, California

A high-speed analog-to-digital converter automatically transfers blocks of data from its memory to specific memory locations in a computer. The unit contains 105 integrated-circuit packages in a 19- by 3½-inch (48.26- by 8.89-cm) rack-mounted drawer with internal forced-air blowers (see figure). Intended for synchronous sampling of quadrature pairs of data, it samples with minimal skew (about 10 nanoseconds) using video-type high-speed sampling technology. The unit is equipped for computer-controlled self-testing.

The converter was originally developed for a planetary radar data-acquisition system. Its first application was in the measurement of continuous-wave total reflected spectra from such celestial bodies as Venus, Ganymede, Callisto, and various asteroids. It fills a need in gathering measurements for the computation of high-resolution spectra (fast Fourier transforms of more than 512 points) in the bandwidth range of 5 to 350 kilohertz.

The equipment is essentially a computer-controlled dual analog-to-digital converter of 8-bit resolution. Sampling can be commanded directly by the computer program or can be controlled by an external clock. When the external clock is used, the converter samples automatically and transfers the samples automatically to blocks of memory locations specified by the program.

The data-transfer rate depends on whether the computer and other peripherals are competing for use of the data bus. With other peripheral equipment off and with the computer in its waiting state, the converter can transfer pairs of 16-bit numbers at the rate of 270,000 per second. This rate is for a computer having a relatively slow type of core memory. With a zero-delay memory, the theoretical maximum transfer rate is 1.2 million pairs of numbers per second. However, the converter is not designed to capture the data bus continously during an entire memory-block transfer, and it therefore cannot transmit at the theoretical maximum rate.

(continued on next page)

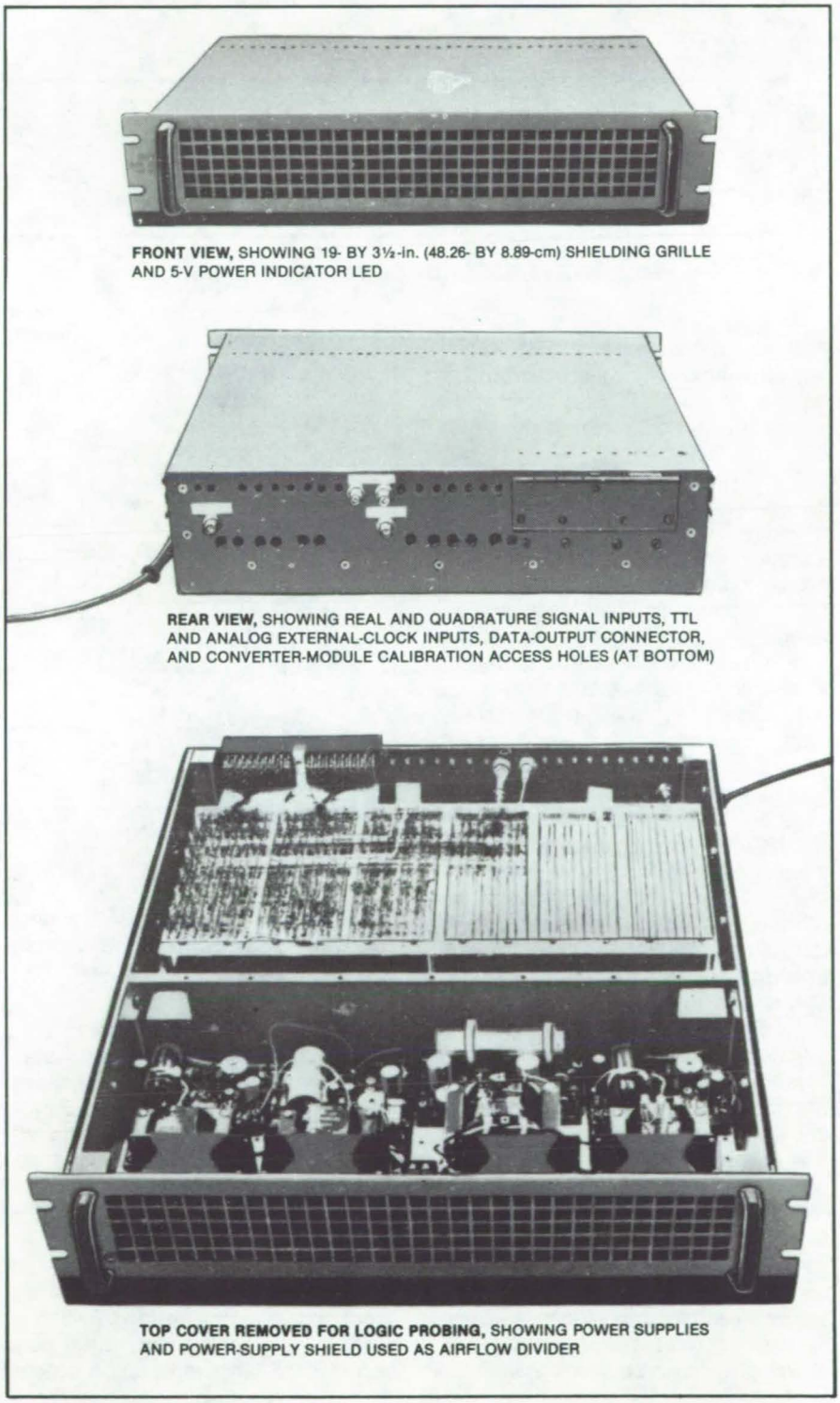

FRONT VIEW, SHOWING 19- BY 3½-in. (48.26- BY 8.89-cm) SHIELDING GRILLE AND 5-V POWER INDICATOR LED

REAR VIEW, SHOWING REAL AND QUADRATURE SIGNAL INPUTS, TTL AND ANALOG EXTERNAL-CLOCK INPUTS, DATA-OUTPUT CONNECTOR, AND CONVERTER-MODULE CALIBRATION ACCESS HOLES (AT BOTTOM)

TOP COVER REMOVED FOR LOGIC PROBING, SHOWING POWER SUPPLIES AND POWER-SUPPLY SHIELD USED AS AIRFLOW DIVIDER

The **Digital-to-Analog Convertor Unit** is constructed in a standard rack-panel housing.

The calibration potentiometers of the two sections of the converter are accessible from the rear of the equipment box: They can be adjusted without opening the box. Each of the two converter channels is calibrated by connecting a precise voltage source to the coaxial input jack for the channel, reading the converter output under program control, and making the necessary potentiometer adjustment.

The converter, when under control of the external clock or computer, does real, quadrature, or real/quadrature pair sampling and then transfers one or both conversion results (as numbers) to any block of contiguous addresses in the computer memory system. A block can consist of from 1 to 32,768 words or word pairs.

This work was done by David E. Wallis and Richard R. Green of Caltech for **NASA's Jet Propulsion Laboratory.** *For further information, Circle 13 on the TSP Request Card.*
NPO-15006

Wire-Identification Instrument

Unit identifies unconnected wires in a cable and searches for preselected wires.

NASA's Jet Propulsion Laboratory, Pasadena, California

An instrument automatically tests each wire in a multiwire cable and identifies a specified wire so that it can be segregated or labeled. It also locates the wire connected to a specified connector pin.

The battery-powered instrument incorporates a digital display, a thumbwheel switch, an audio transducer, and a probe. The cable to be tested is connected to the instrument by an adapter cable wired to match the connector on the instrument. For example, if the cable to be checked has only 37 pins, the first 37 pins on the test instrument would be used. Each of the wires in the cable is routed, via the adapter cable, to one of the inputs of a digital multiplexer (see figure).

When the instrument is operated in the "identify" mode, the user touches the probe to one of the cable leads, and the multiplexer addresses each of the wires in turn. The probe places a logic "1" voltage on the wire that the user touches. When the multiplexer addresses that wire, the logic "1" voltage stops the clock, halting the counter and displaying the number of the wire touched.

In the "search" mode, the user sets the number of the desired lead on the thumbwheel switch. The number set by the thumbwheel switch is fed to the counter and replicated at the address line to the multiplexer. When the selected multiplexer input "sees" a logic "1" from the probe, the instrument sounds its audio alarm. The user touches each lead in sequence. When the user touches the desired lead, the instrument emits an audible signal.

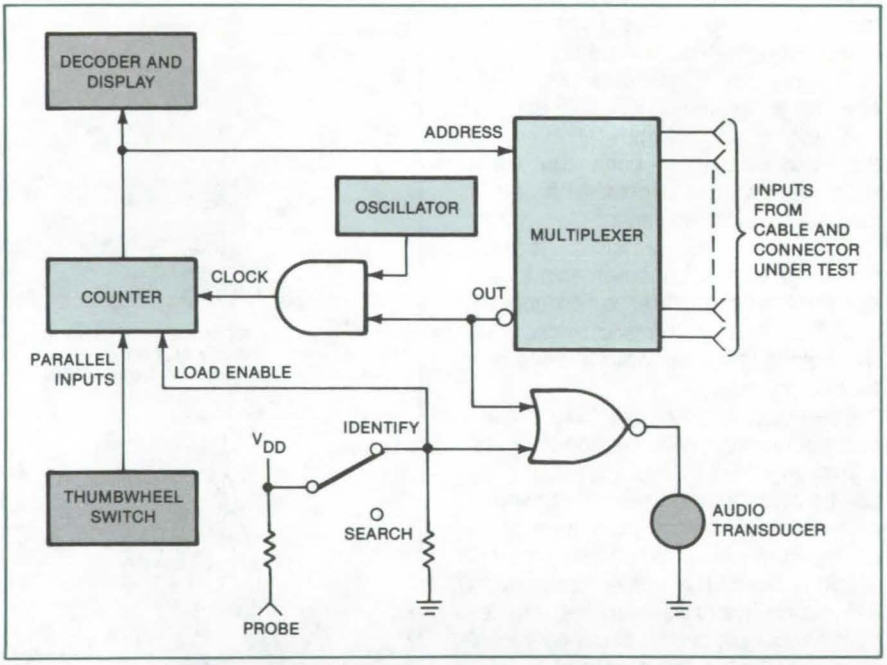

This **Wire-Finding Instrument** is made with readily-available CMOS integrated circuits. It is more efficient and reliable than conventional continuity testers and less expensive than computer-controlled units.

The instrument uses a liquid-crystal display and complementary metal-oxide-semiconductor (CMOS) chips throughout. It draws only about 3 milliamperes from the 6-volt battery. Its two binary-coded decimal counters can address up to 100 wires. At a 1-kHz clock rate, the maximum time to identify the selected wire is only 0.1 second.

Since the instrument produces no high voltages that could cause electrical overstress, no damage to the wires is possible. The multiplexer, when connected to the cable under test, functions simply as a passive receiver. Moreover, the supply voltage is low, and the current is limited by a series resistor. The test voltage is applied only to wires not yet connected to circuitry: No voltage is impressed on wires that have been connected previously.

This work was done by James O. Lonborg of Caltech for **NASA's Jet Propulsion Laboratory.** *For further information, Circle 14 on the TSP Request Card.*
NPO-15633

Automatic Monitoring of Switching Power Supplies

Fast analysis of switching waveforms would allow impending failures to be detected.

Marshall Space Flight Center, Alabama

The well-being of dc-to-dc switching power supplies would be determined with the aid of a proposed monitoring system. Based on fast analog-to-digital converters and microprocessors, the system would provide real-time information on such switching waveform characteristics as the amplitudes of selected spectral components, root-mean-square amplitude, and peak value. Comparisons of the values of these characteristics with nominal values yield early warnings of impending equipment failure or degradation.

The system concept was originally developed for space stations and spacecraft. It is also suitable for power-conditioning equipment in aircraft and in terrestrial photovoltaic power systems. The concept can be adapted to acquire and analyze time responses of such other subsystems as those for attitude control, heat control, propulsion, and life support.

A switching power conditioner converts dc power from a source such as a battery or solar-cell array to well-regulated dc at convenient voltages and currents. The converter is a high-gain feedback switching circuit with an output filter to recover the dc component and reduce the amplitude of the components at the 1- to 10-kHz switching frequency and its harmonics. The converter is subject to failures in the feedback loop and output filter. These failures often cause oscillations and increases in the output ripple voltage that may not have a large effect on the dc output or fundamental ripple component but have a significant effect on the overall spectrum of the output. The failures indicate deterioration of the equipment, but cannot be detected by examining the dc output.

The concept involves sampling the switching waveforms, storing the sampled waveforms, and extracting information from the samples. The key hardware required to implement the concept consists of fast analog-to-digital converters, memory, and a microprocessor. A converter can be combined with a personal computer to make a digital-storage oscilloscope with a 25-kHz bandwidth. A fast Fourier transform would be used to calculate the spectrum from samples of the waveform. An "expert" system would be used to analyze the waveform data both to determine the nominal spectral values and to correlate deviations from these values with specific circuit defects.

This work was done by Robert L. Moser of Martin Marietta Corp. for **Marshall Space Flight Center.** *No further documentation is available.*

Inquiries concerning rights for the commercial use of this invention should be addressed to the Patent Counsel, Marshall Space Flight Center [see page A5]. *Refer to MFS-25968.*

Intercomputer Communication Link

Interface units transmit, receive, and perform "handshaking" functions.

NASA's Jet Propulsion Laboratory, Pasadena, California

Two computers communicate over a distance up to 600 meters at average transmission speeds around 200 kilobaud with the help of a pair of programable interface units. The interfaces use a form of pulse modulation and are programed for full "handshaking" capabilities.

When transmitting, a unit converts digital signals from a computer-interface buffer into a serial data stream, adding a parity bit for each 8-bit byte. A bit is represented by the deletion of one cycle of a 1-MHz square-wave carrier, beginning at the leading edge of the positive or negative half cycle. The value of the transmitted bit (zero or one) is conveyed by the sign (positive or negative, respectively) of the last half cycle transmitted before the deletion (see figure).

The line receiver is a comparator with hysteresis. It switches its output state in response to the full peak-to-peak carrier-voltage transition but not in response to the half-peak voltage transition of the last half cycle before a deletion. A transition-absence detector produces pulses during the intervals when no pulses are observed in the line-receiver output. It therefore signifies either the presence of a data bit or the termination of the carrier. The combination of the transition-absence pulse and the polarity of the last half-peak transition (as determined by the output of the hysteresis circuit) gives the value (zero or one) of the received bit.

Each unit is controlled through a status register that coordinates the hardware and software of the communication link. There are many levels of control and interruption signaling. The net effect of the handshaking algorithms is to enforce the following protocol:

- One unit must not transmit data while the other does.
- One unit must not transmit to the other until the other and its computer are ready to receive data, the first unit and its computer are ready to transmit data, and the buffer of the first unit contains data to transmit.
- If both units attempt to initiate data transmission during one transmission-line delay interval, the first-arriving signal wins the race, and the unit that transmitted it is allowed to proceed first.

(continued on next page)

• When the computer at one unit has transmitted all its data, the computer at the other unit checks for error flags and odd bytes in its buffer. When all accounts have been settled, end-of-message indications are generated at both units.

The handshaking operations are normally performed automatically under the control of the unit program. However, an operator can intervene to prevent a unit from transmitting a carrier signal, to isue a "reset" command, or to set the value of a 2-bit control message in the receiving mode.

This work was done by Warren A. Lushbaugh and James W. Layland of Caltech for **NASA's Jet Propulsion Laboratory.** *For further information, Circle 15 on the TSP Request Card.*
NPO-13446

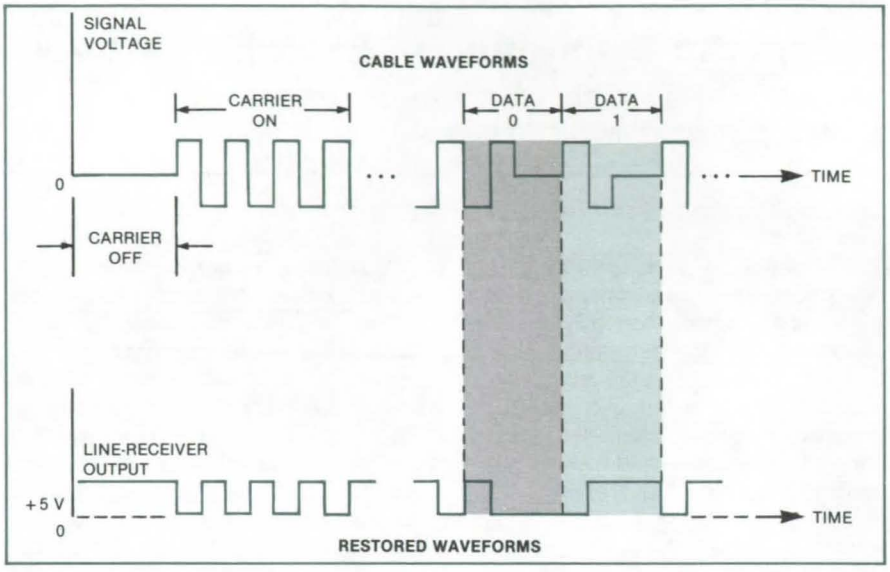

Deletion of a Carrier Cycle is the modulation used to transmit a data bit. The value of a bit is represented by the polarity of the last half cycle transmitted before the deletion.

Optical Quantum Receiver for Binary Signals

Both phase and amplitude are measured to detect ones and zeros.

NASA's Jet Propulsion Laboratory, Pasadena, California

A proposed receiver for binary phase-modulated optical signals would perform at a level approaching that of an optimum quantum receiver. In essence, the received optical field interferes constructively or destructively with a replica of itself generated in an optical Costas phase-locked-loop local oscillator. Constructive interference corresponds to binary "1," while destructive interference corresponds to binary "0."

The received field and the replica field are combined in a beam splitter (see figure) and focused on a photomultiplier tube. The combined fields either cancel each other or add to produce double the received amplitude, depending on whether the phase information in the received field represents a 0 or a 1.

To assure complete destructive interference during the reception of a "0," it is necessary to equalize the amplitudes of the received and locally generated signals at the photomultiplier. Assuming that this kind of receiver would be used in places where the received-field amplitude changes slowly, there is a relatively long time available for estimating the amplitude accurately.

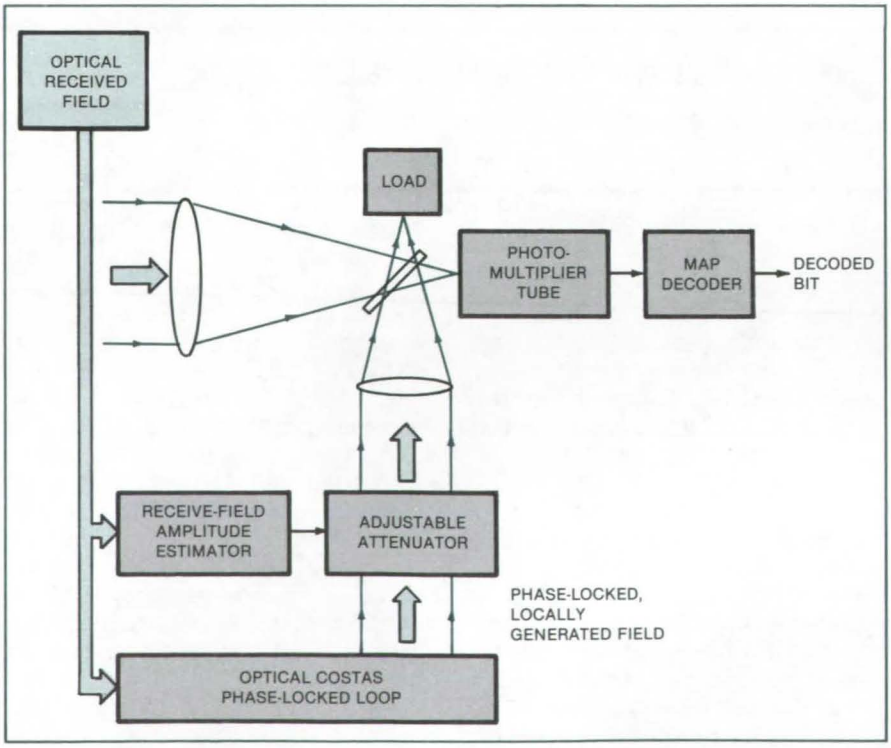

In the **Quantum Optical Receiver**, both the amplitude and phase of the received optical signal are measured to extract as much information as possible, thereby reducing the error probability. The phase-modulated received signal is mixed with an equal-amplitude replica of the optical carrier generated in a phase-locked loop. The two signals interfere with each other at the photomultiplier cathode.

The amplitude estimate is used to adjust an attenuator (such as a pair of polarizers) through which the locally-generated optical signal passes, thereby equalizing the two signals.

The photomultiplier output represents a count of the photoelectrons produced by the combined fields. A "maximum a posteriori" (MAP) decoder observes the count during each bit interval and determines whether the received signal is a 1 or a 0.

In the absence of background radiation, the probability of error with this scheme is close to the theoretical minimum. In contrast, the probability of error for a simple photon counter observing an on/off field would be greater for the same average received-signal power. The difference is that the proposed receiver examines both the amplitude and phase of the signal, whereas the photon counter examines only the amplitude.

To aid in designing a working system, the effects of phase error and background fields were investigated in detail. It is believed that this type of receiver can be implemented with current technology.

This work was done by Victor A. Vilnrotter of Caltech for **NASA's Jet Propulsion Laboratory.** *For further information, Circle 16 on the TSP Request Card.*
NPO-15122

Books and Reports

These reports, studies, and handbooks are available from NASA as Technical Support Packages (TSP's) when a Request Card number is cited; otherwise they are available from the National Technical Information Service.

Monitoring Performance of Complex Systems

Computers analyze measurements and verify events and commands.

A 33-page report describes the use of computers in automatic online monitoring of the Centaur rocket prior to launch. The software techniques are transferable to such industrial uses as batch-process control and production-line automation.

The Centaur monitoring system keeps track of the performance of a system characterized by over 200 analog measurements and 150 scheduled events. It uses adaptive software so that only real problems are detected and brought to the attention of engineers.

The monitor checks on these critical characteristics: tank and pressurization-bottle quantities and pressures, propellant quantities, propellant-line temperatures, hydraulic-control pressures and temperatures, environmental temperatures, battery voltages and temperatures, bus voltages and currents, heater currents, presence or absence of commands, radio-frequency signal strengths, purge flow rates and pressures, guidance-platform alinement, and ground and airborne-computer communication.

Two sets of computers monitor these parameters. One set consists of two computers that are in active control of the vehicle-guidance and airborne-computer systems. The set continuously monitors the analog parameters and the events. If an analog measurement is outside its predefined limits or if an event measurement is not at its predefined state, the computer set removes its permission for launching. If such a situation occurs during the last 3 seconds before launch, the computer set shuts down the engines.

The second set consists of a computer with a large memory. This computer is used strictly for monitoring measurements: It has no control ability. It displays its measurements of vehicle and ground-support systems on video consoles for human review. Engineers at the consoles can look at events and analog parameters as they are measured or can call past events and parameters from the computer memory. Analog measurements can be displayed as graphs or as listings.

The basic data-sampling method employed for analog measurements by the active-control computers consists of taking five samples, rejecting the highest and lowest, and averaging the remaining three. For event data, the control computers report the state of three out of five samples.

The monitor-only computer samples analog parameters at various rates, decided in advance by the system engineer according to the noisiness of the environment. Each measurement must change by a predetermined magnitude for the computer to recognize a new value. In addition, both analog and event measurements must remain at a certain level for a specified number (usually two) of consecutive samples before the computer will accept the value.

This work was done by William F. Thomas of **Kennedy Space Center.** *To obtain a copy of the report, Circle 17 on the TSP Request Card.*
KSC-11273

Report on Satellite Radar for Detecting Ocean Currents

Good resolution and high signal/noise ratio are anticipated.

A report describes an orbiting side-looking radar that would measure ocean currents in the direction toward or away from it. The radar relies on the relationship between Doppler shifts and the lengths and frequencies of ocean waves. Neglecting surface tension, a low surface wave over deep, still water has a phase speed of $v_p = \sqrt{g\lambda/2\pi}$, where g = the gravitational acceleration, and λ = the wavelength. If there is a current, the velocity of which has a component v_c along the direction of wave propagation, then the wave crests are observed to travel at $v_t = v_p + v_c$.

In the ocean area of interest, the radar system must first single out a train of waves separated by wavelength λ. It does this by selecting signals separated in frequency by an amount $\Delta f = c/2\lambda$ (where c = the speed of light), the frequency difference of the Bragg-scattering peaks of the ocean waves of wavelength λ. The radar system must then measure the total speed v_t from the Doppler shift of the return signal. The current speed is then estimated from $v_c = v_t(\text{measured}) - \sqrt{g\lambda/2\pi}$.

The SAR return signal is passed through a chirp filter before further processing so that an image of the scanned region is obtained at a sequence of frequencies corresponding to the sampled increments of the chirp frequency. To simplify the problem, the Bragg frequency difference Δf is taken as the frequency difference between a pair of chirp-filter frequencies.

(continued on next page)

Within each rectangular subdivision of the scanned region of the ocean surface, the overlapping images are deconvolved to obtain the signal for each frequency in that area. Next, products are formed by multiplying the signals of two different selected frequencies for the same area. The product for each area is Fourier-transformed, squared, and added to the like quantities obtained from all the other areas for the selected frequency pair. The result should be a spectrum with a high signal/noise ratio.

The shift of the peak of the spectrum from the radar center frequency is taken as the Doppler shift. Using this shift to calculate v_t and the difference between the selected frequencies as the Bragg frequency difference, v_c can then be estimated.

This work was done by Atul Jain of Caltech for **NASA's Jet Propulsion Laboratory.** *To obtain a copy of the report, Circle 18 on the TSP Request Card.*

Inquiries concerning rights for the commercial use of the technology described in this report should be addressed to the Patent Counsel, NASA Resident Office-JPL [see page A5]. Refer to NPO-15704.

Computer Programs

These programs may be obtained at very reasonable cost from COSMIC, a facility sponsored by NASA to make new programs available to the public. For information on program price, size, and availability, circle the reference letter on the COSMIC Request Card in this issue.

Cost and Performance of Distributed Photovoltaic Systems

Program compares the net present worth of a PV system to the cost of purchasing electricity.

The Lifetime Cost and Performance (LCP) Model assists in the design of Photovoltaic (PV) systems. LCP is a simulation of the performance, cost, and revenue streams associated with distributed PV power systems. It provides the user with substantial flexibility in specifying the technical and economic environment of the PV application.

User-specified input parameters are available to describe PV system characteristics, site climatic conditions, utility purchase and sellback rate structures, discount and escalation rates, construction timing, and lifetime of the system. Such details as PV array orientation and tilt angle, PV module and balance-of-system performance attributes, and the mode of utility interconnection are user-specified.

LCP assumes that the distributed PV system is utility-grid interactive without dedicated electrical storage. In combination with a suitable economic model, LCP estimates the expected net present worth of a PV system to the owner, as compared to electricity purchased from a utility grid. Similarly, LCP might be used to perform sensitivity analyses to identify those PV-system parameters having significant impact on net worth.

The user describes the PV configuration to LCP through the basic electrical components. The module is the smallest entity in the PV system that is modeled. A PV module is defined in the simulation by its short-circuit current, which varies over the system lifetime due to degradation and failure. Modules are wired in series to form a branch circuit. Bypass diodes are allowed between modules in the branch circuits. Branch circuits are then connected in parallel to form a bus. A collection of buses is connected in parallel to form an increment to capacity of the system. By choosing the appropriate series/parallel wiring design, the user can specify the current, voltage, and reliability characteristics of the system.

LCP simulation of system performance is site-specific and follows a three-step procedure. First, the hourly power produced by the PV system is computed using a selected year insolation and temperature profile. For this step it is assumed that there are no module failures or degradation.

Next, the monthly simulation is performed involving a month-to-month progression through the lifetime of the system. In this step, the effects of degradation, failure, dirt accumulation, and operations/maintenance efforts on PV system performance over time are used to compute the monthly power-capability fraction. The resulting monthly power-capability fractions are applied to the hourly power matrix from the first step, giving the anticipated hourly energy output over the lifetime of the system.

PV system energy output is compared with the PV system, electricity owners demand for each hour. The amount of energy to be purchased from or sold to the utility grid is then determined. Monthly expenditures on the PV system and the purchase of electricity from the utility grid are also calculated. LCP generates output reports pertaining to the performance of the PV system and system costs and revenues.

The Lifetime Cost and Performance Model is written in Simscript II.5 for batch execution and has been implemented on an IBM 370-series computer. This program was developed in 1981.

This program was written by Chester S. Borden and Michael C. Davisson of Caltech for **NASA's Jet Propulsion Laboratory.** *For further information, Circle D on the COSMIC Request Card.*
NPO-16001

Electric/Hybrid Vehicle Simulation

Performance and costs are analyzed for user-specified operating conditions.

The ELVEC computer program provides the vehicle designer with a simulation tool for detailed studies of electric and hybrid vehicle performance and cost. (A hybrid vehicle is one that can be powered by either electric power or internal combustion engine power using various component connections and control strategies.) ELVEC simulates the performance of a user-specified electric

or hybrid vehicle under a user-specified driving schedule profile or operating schedule. In addition, ELVEC can perform a vehicle-design and life-cycle-cost analysis.

ELVEC simulates the electric/hybrid vehicle as a collection of component models. These models include such components as batteries, motors, engines, transmissions, and flywheels. Also included are models for road load and coastdown.

ELVEC operates in the interactive mode and guides the user in performing a simulation. An experienced programer should be able to modify the code to accept new features as required.

ELVEC is written in ASCII FORTRAN 77 for interactive execution and has been implemented on a UNIVAC 1100-series computer with a central memory requirement of approximately 63K of 36-bit words. This program was developed in 1980 and was last updated in 1982.

This program was written by Ronald A. Slusser and C. Phil Chapman of Caltech and John P. Brennand of General Research Corp. for **NASA's Jet Propulsion Laboratory.** *For further information, Circle F on the COSMIC Request Card.*
NPO-15229

LRU Voltage Analysis

Program predicts the minimum supply voltages that give predetermined LRU voltages.

A program for analyzing Line Replaceable Unit (LRU) voltages in the Shuttle orbiter predicts the minimum voltage level of the main power distribution bus needed to meet the predetermined LRU voltages. The loads can be constant-power or resistive. In some cases, they may be fed from two or three sources through diodes.

Computations for each LRU are performed using direct analytical calculations based on known network losses until the required main distribution bus voltage is determined. Although primarily intended for analysis of the Shuttle distribution bus minimum voltage, this program could be adapted for voltage analysis in other situations.

This program is written in PL/1 for batch execution and has been implemented on an IBM 370-series computer with a central memory requirement of approximately 660K of 8-bit bytes. This program was developed in 1981.

This program was written by T. S. Oepomo and T. V. Prouty of Rockwell International Corp. for **Johnson Space Center.** *For further information, Circle G on the COSMIC Request Card.*
MSC-20699

Front-End Program for SYSGEN

The interactive Front-End Program for SYSGEN (FEPS) is used to create and modify data bases for SYSGEN simulations.

SYSGEN, the Power Generation System Production Costing and Reliability Analysis program, simulates the production costs and reliability of an electric utility with and without time-dependent generating units. FEPS transforms inputs into the proper formats, builds the data files, and adds the Job Control Language necessary for running the SYSGEN program. In addition, all inputs are checked for internal consistency and for program limits. An extensive update option permits easy modification and duplication of data files for the running of parametric analyses. The data prompting in FEPS corresponds directly with the model input worksheets for the SYSGEN program.

The original SYSGEN package was developed at the MIT Energy Laboratory as a production costing and reliability model for thermal, hydro, and storage units on an electric power system. The SYSGEN package has been modifed at the Jet Propulsion Laboratory and has been used in calculating the break-even cost of photovoltaic and solar/thermal electric systems in grid-connected applications.

SYSGEN computes the minimum-cost operating schedule and system reliability based on the operating and cost characteristics of each generating unit and on the load on the system. The FEPS package allows the user to easily prepare input for SYSGEN. FEPS permits the user to interactively build and modify utility data bases for use with SYSGEN.

FEPS can format hourly utility load and load reduction data, create load duration curves, format the utility production and cost variables, sort all data into the appropriate files, and generate the control stream for running SYSGEN. The FEPS/SYSGEN system does not require a sophisticated knowledge of computer programing or utility engineering.

FEPS is written in FORTRAN 77 for interactive execution and has been implemented on a DEC VAX-11/780 computer. SYSGEN is written in FORTRAN for batch execution and has been implemented on an IBM 370-series computer with a central memory requirement of approximately 700K. The FEPS/SYSGEN system was developed in 1981.

This program was written by Cynthia R. Carlson and Michael Davisson of Caltech for **NASA's Jet Propulsion Laboratory.** *For further information, Circle E on the COSMIC Request Card.*
NPO-15782

MiniBriefs describe NASA innovations and reports in an abbreviated format. Readers desiring additional information on these items should request the Technical Support Packages (TSP's), available in most cases, which can be obtained by using the TSP Request Card at the back of this issue.

Multiple-User Adaptive-Array Communication System

The weights for a K-beam system can be computed K/6 times faster.

In a single-frequency adaptive-array communication system in which K mobile users communicate with a central station (such as a satellite) equipped with an n-antenna array (n>K), each of the K signals is recoverable by taking a specific weighted sum of the n complex antenna voltages. Assuming that the users provide the central station with sufficiently frequent updates of their positions, the required weights can be determined in a straightforward manner. The new algorithm, however, performs this task much faster: specifically, it yields the K sets of n complex weights in

(continued on next page)

a time that is K/6 times shorter than that required by currently known techniques. For a 60-user system, this is an order-of-magnitude improvement. Such a system could handle more or faster-moving users.

This work was done by Shalhav Zohar of Caltech for **NASA's Jet Propulsion Laboratory.** *For further information, Circle 36 on the TSP Request Card.*
NPO-15765

Capacitor-Test System

A microprocessor-based capacitor-test system simultaneously monitors 80 capacitors.

Polycarbonate-film capacitors can be tested for leakage paths with a microprocessor-controlled multiplexer test sequence. The system indicates leakage factors and capacitor quality by sampling and sequentially measuring the voltage across a resistor in series with each capacitor under test. The measurements are taken at the rate of 20 times per second. Any change in voltage across the capacitors, such as that produced by an internal breakdown, is immediately detected. Up to 80 capacitors can be tested simultaneously for momentary microdischarge pulses as low as 10 microjoules of energy.

This work was done by Frank M. Ott and Roy A. Summers of Caltech for **NASA's Jet Propulsion Laboratory.** *For further information, Circle 37 on the TSP Request Card.*
NPO-15485

Improved Ultrasonic Resolution Via Analog Technique

Single-sideband analog processing is simpler than digital processing.

High spatial resolution is obtained from reflected or transmitted ultrasonic pulses by an analog technique that produces a signal proportional to the magnitude of the complex-plane analytic representation of the signal. This magnitude represents the bare time-dependent scattering amplitude, unmodulated by the fundamental ultrasonic frequency. Without such modulation, it is easier to resolve closely spaced peaks.

The return signal is heterodyned to a frequency much higher than the fundamental ultrasonic frequency, then filtered to obtain the upper sideband. The envelope of the upper sideband is the desired magnitude and is obtained by ordinary peak rectification. This technique is simpler and faster than digitally computing the Hilbert transform to obtain the quadrature signal.

This work was done by Paul M. Gammell of Caltech for **NASA's Jet Propulsion Laboratory.** *For further information, Circle 38 on the TSP Request Card.*

Inquiries concerning rights for the commercial use of this invention should be addressed to the Patent Counsel, NASA Resident Office-JPL [see page A5]. Refer to NPO-15707

Removing Drift From Frequency-Stability Measurements

An estimate of the frequency drift is used to remove the effects of this drift.

A method for eliminating frequency drifts from frequency-stability measurements produces a more accurate indication of stability of such a frequency standard as a hydrogen maser. Random phase fluctuations that were masked by the frequency drift can be seen by removing an accurate estimate of drift so that stability is observable from an Allan variance plot. The stability is measured by a pairwise comparison of the stability of two masers in an Allan variance plot and estimating the frequency-drift rate to remove the effects of the drift from the plot.

The average drift rate equals the average frequency near the end of a record, minus the average frequency near the beginning of a record, divided by the length of the record, where the averaging time is optimized for flicker-frequency noise. This average drift rate is then removed from the plotted data.

This work was done by Charles A. Greenhall of **NASA's Jet Propulsion Laboratory.** *For further information, Circle 39 on the TSP Request Card.*
NPO-15833

Remote-Imaging Parameters

Transmission parameters for remote-imaging systems can be operator controlled.

Image resolution, image quality and data-transmission rate of remote-imaging systems can be continuously controlled by operator intervention. A set of levers allows the operator to control independently frame rate, frame size, and image quality in bits per pixel. This provides flexibility to vary dynamically these parameters to maximize the usefulness of a limited and changing data rate. In addition, particular portions of the image may be selected for detail or brightness enhancement. Autonomous preselected operator parameters can further reduce the need for operator intervention. The system could be used for imaging systems in aircraft or remotely piloted vehicles.

This work was done by Robert F. Rice of Caltech for **NASA's Jet Propulsion Laboratory.** *For further information, Circle 40 on the TSP Request Card.*
NPO-14689

Programable Multicrate Controller

Weight and power consumption are minimized.

A high-speed, environmentally hardened controller has been developed for use with commercially-available system crates for both experiment control and data handling. The programable crate controller consists of three functional areas — the control section that utilizes high-speed bit-slice circuitry; memory that includes 1,024 16-bit words of EPROM, 1,024 16-bit words of RAM, and 1,024 48-bit words of SPROM; and a data-way interface. The system is programed in microcode, has an instruction cycle time of 400 nanoseconds, and offers the user maximum flexibility in data multiplexing and formatting, time-line sequencing, and in the control functions of multicrate operation.

This work was done by Gerald L. Mook and Melvin R. Phillips of McDonnell Douglas Corp. for **Marshall**

Space Flight Center. *For further information, Circle 41 on the TSP Request Card.*
MFS-25533

Eye-Movement Tracker Would Reduce Video Bandwidth

A small high-resolution image zone is centered in the viewer's gaze.

The bandwidth required to transmit a closed-circuit-television image would be reduced by transmitting a small portion at high resolution and the remainder at low resolution. The high-resolution portion would be centered in the viewer's gaze, so that the entire image would seem to be of high resolution.

According to the concept, the viewer's eye movements are tracked by reflected infrared light to determine the location of the spot on the display screen at which the viewer is looking. This location is transmitted to the control circuits, causing the camera to scan and the receiver to reconstruct the image at high resolution in the vicinity of the location.

This work was done by Carl F. Ruoff of Caltech for **NASA's Jet Propulsion Laboratory.** *For further information, Circle 42 on the TSP Request Card.*

Inquiries concerning rights for the commercial use of this invention should be addressed to the Patent Counsel, NASA Resident Office-JPL [see page A5]. Refer to NPO-15432.

Eliminating False Signals From Electromechanical Keyboards

"Bounce" eliminator scavenges its power from keyboard lines.

Contact switches in electromechanical keyboards are prone to "bounce" — the creation of unwanted pulses that interfere with digital systems. A new adapter unit eliminates bounce without a separate power supply.

The debouncer is placed in series, via standard connectors, with the cable joining the keyboard to the digital system. No other modification is needed. The debouncer draws its electric power from the unactivated keyboard signal lines. Because complementary metal-oxide-semiconductor (CMOS) integrated circuits are used in the unit, the power consumption is very low.

In the unit, one CMOS circuit serves six keyboard lines. The circuits are commercial devices specifically designed for bounce elimination. Diodes connected to the lines provide power for the circuits. Because only one line is activated at a time on a keyboard, the power is essentially constant.

This work was done by Charles F. Schott of Rockwell International Corp. for **Johnson Space Center.** *For further information, Circle 43 on the TSP Request Card.*
MSC-20429

Low-Frequency Navigational System

An automated low-frequency navigational system locates vehicles over large areas.

Accurate vehicle-position determination over a 50 by 50-km service area is accomplished by a low-frequency-radio navigational system comprised of four frequency/phase-comparison transmitters and receivers. The all-weather, 24-hour navigational system uses a keyed CW format operating at 300 kHz and represents the service area on an orthogonal grid display. Phase ambiguity is resolved by maximum-likelihood combination of phases from the four frequencies or by operator entry of an initial position. Use of a grid-calibration table permits accurate position determination in the vehicle receiver system.

This work was done by David E. Wallis of Caltech for **NASA's Jet Propulsion Laboratory.** *For further information, Circle 44 on the TSP Request Card.*

This invention has been patented by NASA [U.S. Patent No, 4,396,918]. Inquiries concerning nonexclusive or exclusive license for its commercial development should be addressed to the Patent Counsel, NASA Resident Office-JPL [see page A5]. Refer to NPO-15264.

Transfer-Function Simulator

Transfer function may be simulated and adjusted to simplify feedback-control loop analysis.

A transfer-function simulator constructed from analog or both analog and digital components can be used to substitute for a device that may have faults that confound analysis of a feedback-control loop. Two simulators with Lorentzian transfer functions have been designed for use in testing a laser frequency-stabilization loop. In that application the simulator is a substitute for a laser and spectrophone. A total of nine transfer-function variations that can be simulated is described.

This work was done by Michael J. Kavaya of Caltech for **NASA's Jet Propulsion Laboratory.** *For further information, Circle 45 on the TSP Request Card.*

Inquiries concerning rights for the commercial use of this invention should be addressed to the Patent Counsel, NASA Resident Office-JPL [see page A5]. Refer to NPO-15696.

Optical Mass Memory System Specification

Fiche magazines store 10^{13} bits off-line, 10^{12} bits on-line.

Specifications are given for a computer-controlled optical mass memory system that stores and retrieves data from silver halide fiches 148-mm-square and 7 mils (0.18 mm) thick at a user bit density of 30 Mbit/in.^{2} (4.7 Mbit/cm^2) with an uncorrectable bit-error rate of 10^{-9} or less. Data can be simultaneously read from one fiche and recorded on another at rates of approximately 5×10^7 bits/second.

Fiches are developed off-line in an automated processor; photographic duplication of fiches is also provided. Access to on-line fiche magazines is automated, but access to off-line magazines requires an operator. System design allows for expansion to 10^{15}-bit capacity.

This work was done by Harris Corp. for **Marshall Space Flight Center.** *For further information, Circle 47 on the TSP Request Card.*
MFS-25592

Reed-Solomon Encoder

VLSI structure incorporates a bit-serial algorithm.

A report presents the mathematical principles of the Berlekamp bit-serial

(continued on next page)

multiplier algorithm and its application to the design of very-large-scale integrated (VLSI) encoders for Reed-Solomon error-correcting codes. In contrast with conventional Reed-Solomon encoders for long codes, those employing Berlekamp's algorithm do not require look-up tables to multiply two elements: instead, they function with only shifting and exclusive-OR operations.

The report describes a VLSI structure for a code of 8 bits per symbol in code words of 255 symbols, of which 32 are check symbols and 223 are information symbols. The structure can be made readily on a single chip of negatively-doped-channel metal-oxide semiconductor.

This work was done by Trieu-Kie Truong, Irving S. Reed, Leslie J. Deutsch, In-Shek Hsu, Ke Wang, and Chiunn-Shyong Yeh of Caltech for **NASA's Jet Propulsion Laboratory.** *To obtain a copy of the report, Circle 48 on the TSP Request Card.*
NPO-16074

Normalizing VFO Frequency by Non-Power-of-2 Division

PLL oscillator with VFO operating at one frequency yields any one of four frequencies by dividing by 4, 7, 21, or 52.5.

A radiation-resistant phase-locked-loop oscillator that generates an output frequency 32 times any 1 of 4 specific input reference frequencies can be constructed without increasing component count over that of a conventional circuit. The radiation resistance of the voltage-controlled oscillator in the loop is maximized by designing the loop so that the oscillator works at the same relatively low frequency (12.9024 MHz) for each of the four output frequencies. The divider circuit has sections that can divide by 4 or 7, 3, and 2.5: These are cascaded to produce an overall division by 4, 7, 21, or 52.5.

This work was done by Carl R. Anderson of Odetics, Inc., for **NASA's Jet Propulsion Laboratory.** *For further information, Circle 46 on the TSP Request Card.*
NPO-15330

Physical Sciences

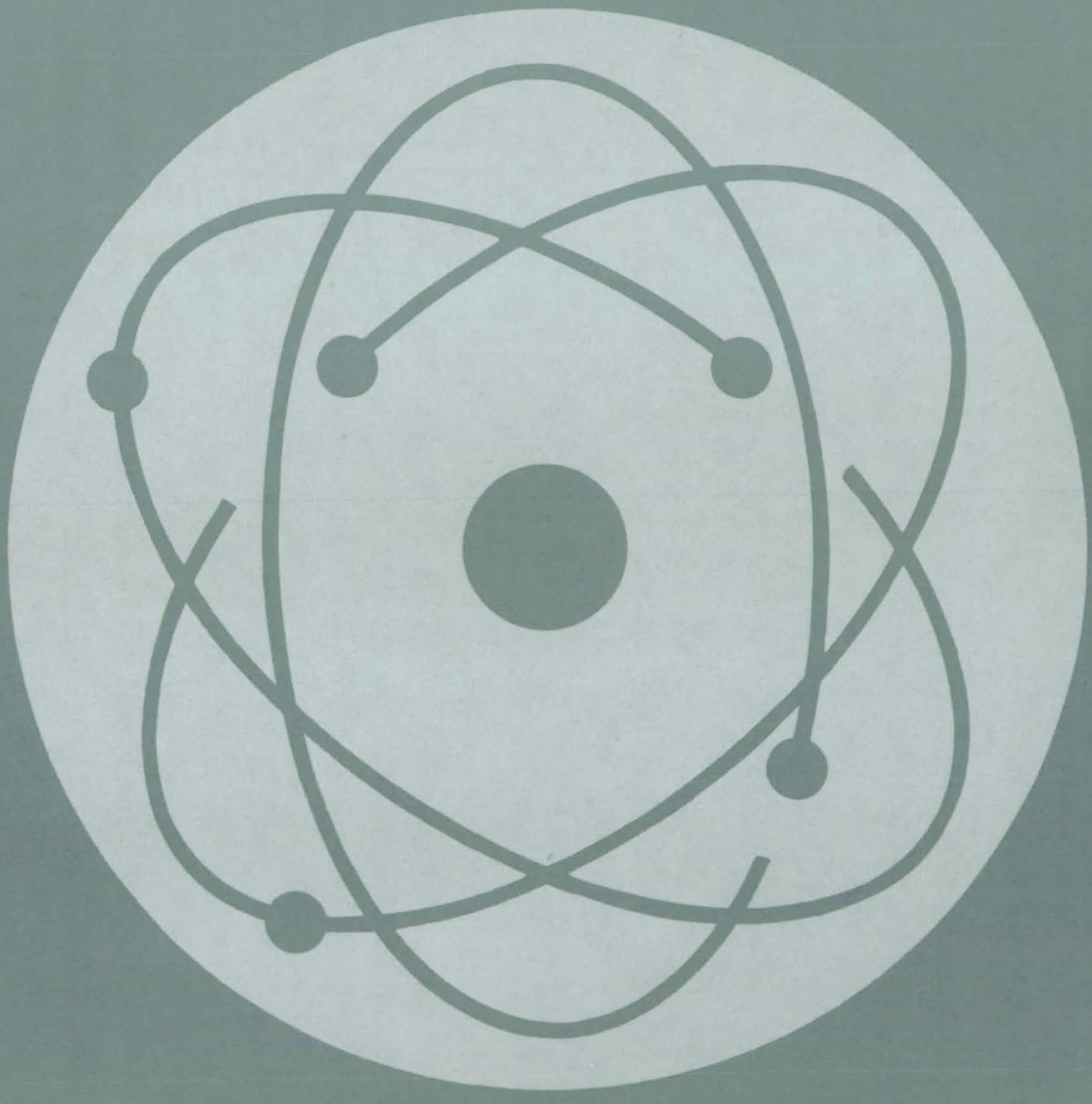

Interferometer Measures Broadband Surface Acoustic Waves

Two pairs of orthogonally-polarized optical beams produce a two-dimensional surface-wave profile.

Langley Research Center, Hampton, Virginia

A dual differential interferometer uses two pairs of orthogonally-polarized optical beams to measure the amplitude and orientation of broadband ultrasonic surface acoustic waves. Each of the two pairs of focused laser-probe beams is used in a separate wideband differential interferometer to detect independently the component of surface wave motion along one direction. By combining the two signals, the interferometer determines a two-dimensional surface-wave profile and its variation as a function of time. The system has an optically-adjustable acoustic bandwidth from the kilohertz to megahertz range and can detect peak-to-peak displacements in the subangstrom range; it is insensitive to low-frequency specimen translations.

The dual two-beam interferometer (see figure) is modular. The laser source module generates two pairs of parallel beams, each having a 45° polarization angle to the horizontal. The light source and polarization angle are obtained by appropriately rotating a singly-polarized He/Ne laser. The two pairs of beams depart at right angles to each other, and a Dove prism mounted at a 45° angle to the horizontal in one leg rotates one pair of beams to a perpendicular orientation with respect to the other pair. Both pairs are then alined in parallel and centered by a polarizing beam splitter.

The alinement also results in the beams being polarized by pairs and in beams of equal intensity. The beams propagate to the surface through another beam splitter oriented so that the reflected, modulated beams are reflected toward the detectors. A second polarizing beam splitter separates the reflected pairs. Each pair is individually spatially filtered and measured for modulation.

Both beam pairs may be expanded and refocused on to the surface by a variable-focus lens system, allowing variable separation of the focused spots.

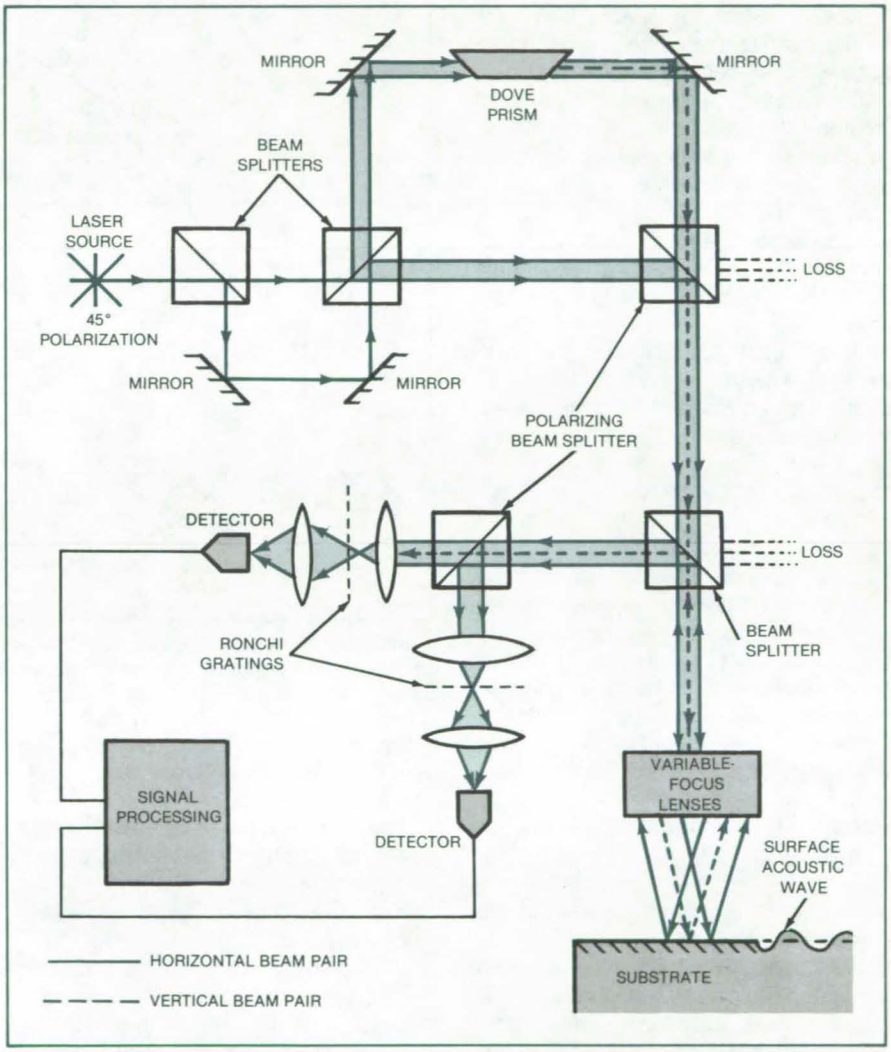

A **Dual Differential Interferometer** measures the amplitude and orientation of broadband surface acoustic waves. The instrument is modular, and its sensitivity is limited only by the optical detector used.

However, beam spot separation is more easily manipulated by appropriately separating the pairs when generated at the front of the system. This separation is accomplished by a translation of the mirror adjacent to the pair of beam splitters.

This work was done by Richard O. Claus and T.M.Turner of Virginia Polytechnic Institute and State University for **Langley Research Center.** *For further information, Circle 19 on the TSP Request Card.*

This invention is owned by NASA, and a patent application has been filed. Inquiries concerning nonexclusive or exclusive license for its commercial development should be addressed to the Patent Counsel, Langley Research Center [see page A5]. Refer to LAR-12966.

Acoustic Gaussian Far-Field Pattern

A Gaussian profile is achieved by using annular electrodes.

Langley Research Center, Hampton, Virginia

A new ultrasonic transducer produces a far-field beam with a Gaussian spatial profile for materials evaluation applications. The transducer is constructed by depositing a circularly-symmetric metallic multielectrode array on a 12.7-mm-diameter X-cut quartz disk. Each electrode is independently connected to an impedance network optimized to produce the Gaussian distribution with less than 2 percent error.

An electric-field distribution that is exclusively a function of radius is produced by the set of concentric ring electrodes. If the circumferences of the rings are large with respect to the spacing between successive electrodes, the electric field in the gaps may be considered to be a linear function of radius. From this model, a piecewise linear function that approximates the Gaussian may be then generated on the face of the piezoelectric crystal by applying proper voltages on the electrodes. The degree to which this function fits the desired Gaussian is determined by the width of each electrode ring, the number of electrodes, and the distribution of the electrode radii on the radius of the transducer crystal.

Because the ideal Gaussian voltage distribution is a smooth function of the radius, the electrode width should be as small as possible. The photoetching techniques used, however, required a minimum electrode width of approximately 0.5 mm. The degree of fit to the desired Gaussian shape may also be improved by using a large number of electrodes; but this approach requires that the interelectrode spacing be small, thereby increasing the possibility of electrical breakdown between adjacent rings when high voltages are applied.

Considering these practical limitations, it was found that with as few as five electrodes, the mean absolute fit error may be reduced to less than 1.5 percent of the peak. Because the radii of the rings are the variables over which greatest control may be exercised during design, an iterative computer routine was developed to minimize absolute error by varying ring placement.

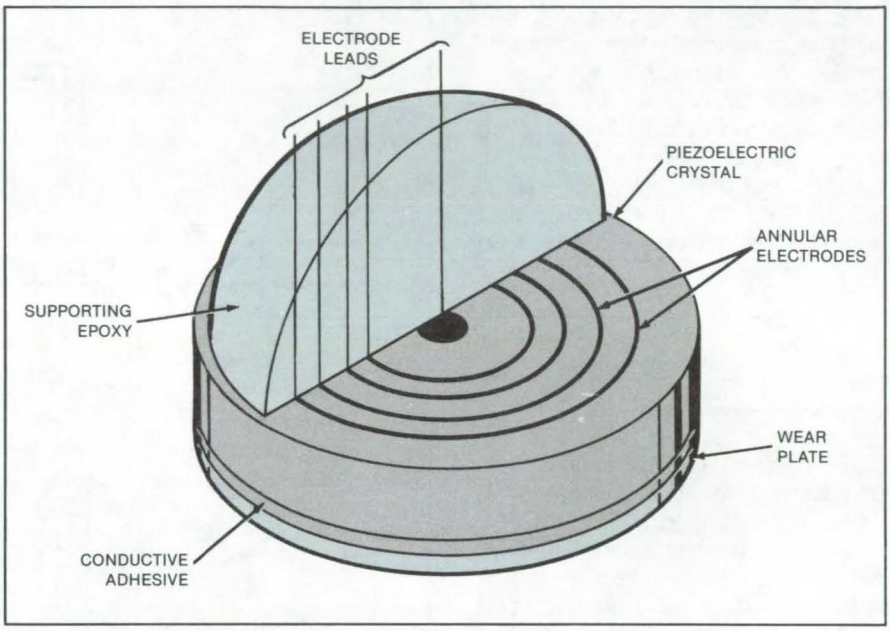

Concentric Electrode Rings in the ultrasonic transducer produce a beam with a Gaussian profile. The transducer is used for materials evaluations.

The designed electrode pattern was photoetched onto a layer of chromium and gold on a circular 2.25-MHz X-cut quartz transducer. Capacitance between electrodes and the wear-plate ground plane was calculated and later empirically verified to be less then 2 pF, producing a negligible reactive impedance at the 2.25-MHz operating frequency. Because this impedance is low, a simple resistive network may be used to fix the desired set of electrode voltages.

Construction details of the transducer are shown in the figure. The leads are attached to the electrodes with a conductive adhesive, and a dome of epoxy is applied to the electrode side of the crystal to provide mechanical support for the leads and to attenuate and disperse resonant surface-wave modes. Further damping is accomplished by a thin semi viscous layer of electrically conductive adhesive placed on the opposite uncoated side of the transducer disk and under a thin aluminum-foil electrode/wear plate. The electrode leads are connected to the resistive network and coaxial cable, and the entire transducer assembly is placed in a 1.3-cm-I.D. cylindrical PVC (polyvinyl chloride) case and potted in filler-loaded epoxy.

This work was done by Richard O. Claus and Paul S. Zerwekh of Virginia Polytechnic Institute and State University for **Langley Research Center.** *For further information, Circle 20 on the TSP Request Card.*

This invention is owned by NASA, and a patent application has been filed. Inquiries concerning nonexclusive or exclusive license for its commercial development should be addressed to the Patent Counsel, Langley Research Center [see page A5]. *Refer to LAR-12967.*

Receiver for Solar Air Turbine

Heat-exchanger design should assure long life.

NASA's Jet Propulsion Laboratory, Pasadena, California

A proposed solar receiver (see figure) would heat air to a temperature high enough to drive a gas turbine. The receiver would have a thermal output of about 70 kilowatts.

The concept is based on alloys, insulators, and heat-storage mediums that are commercially available and have been proved in industry for high-temperature service. The materials are weather-resistant. Moisture, dust, sand, ice, and snow will not cause appreciable damage or long-term degradation of performance. The receiver is designed for 30-year life without scheduled maintenance or replacement.

The receiver consists essentially of a cylindrical shell and rear bulkhead containing serpentine heat exchangers and a thermal-storage unit. Air flowing through the serpentine tubes is heated by Sunlight entering the receiver aperture. The hot air flows through a bed of alumina pebbles in the thermal-storage unit, then passes into the turbine. When supplied with air at 1,050° F and 35 lb/in.^{2} absolute pressure (566° C and 241 kPa) at a rate of 0.533 lb (0.242 kg) per second, the receiver will furnish air to the turbine at 1,500° F (816° C).

The primary design problem was reducing thermal stresses below those that would cause creep rupture in 30 years or less. The problem was a difficult one because of the high temperatures in the receiver and because the receiver undergoes a nightly cooling cycle. The solution was to design the heat-exchange tubes in the serpentine shape; in this shape, the tubes have freedom of movement for heat-induced expansion and contraction, and thermal stresses are thereby minimized. For maximum heat absorption, the relatively-cool incoming air is introduced into the serpentine tubes near the region of highest solar flux. Finite-element stress analysis of this peak-flux area predicts that stress will be below that allowable for 30-year life expectancy.

Air enters the receiver inlet after passing through a recuperator, where it is preheated by exhaust air from the turbine. The inlet air is uniformly distributed among the four serpentine heat exchangers in the receiver. All internal-airpath connections are welded.

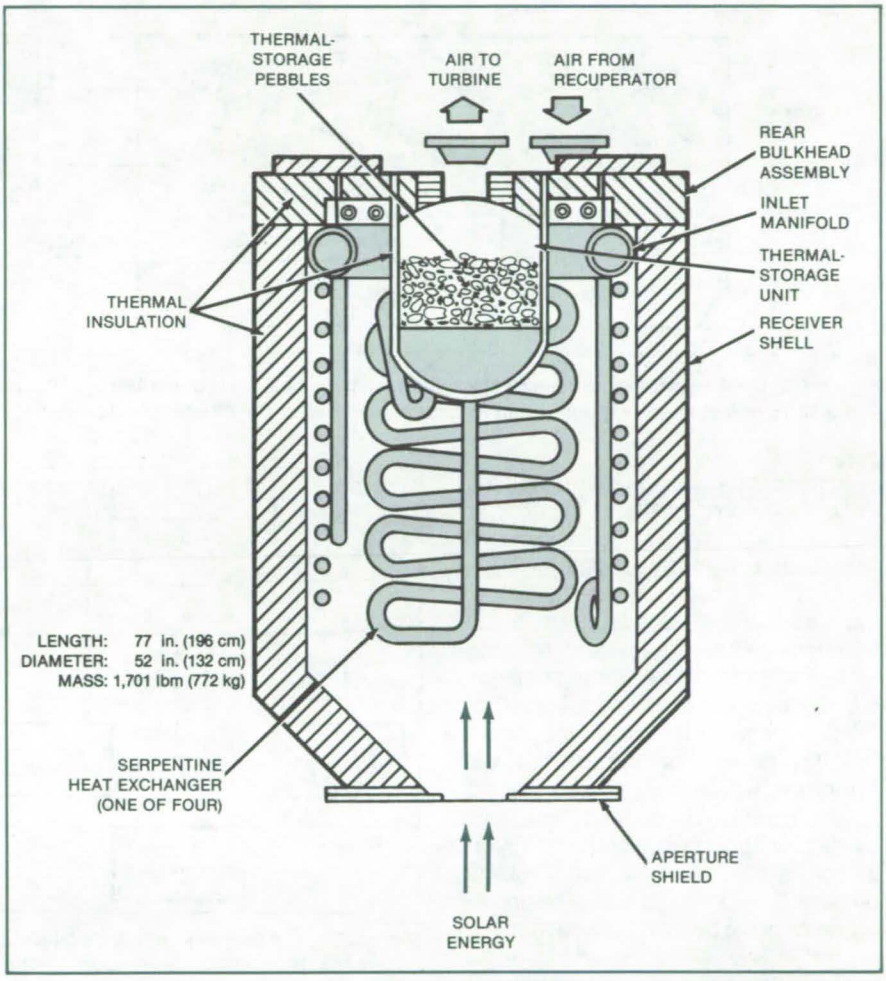

Pointing Downward at the Focal Position of a solar reflector, the proposed receiver accepts intense concentrated Sunlight. Although temperatures in the receiver may rise to 1,500° F (816° C) or more, calculations show that the receiver should lose less than 10 percent of the insolation by convection through the aperture.

The receiver shell and rear bulkhead are insulated with 6 inches (15.2 cm) of rigid, vacuum-formed insulation. The aperture shield is a composite of zirconia board, alumina board, and a nickel-alloy sheet. It is fastened to the receiver shell by bolts so that it can be replaced easily if it is damaged.

Four thermocouples sense the heat-exchanger-tubing temperature. If the airflow drops or the insolation rises excessively, the thermocouple signals will cause part of the inlet air to bypass the recuperator so that it is not preheated, thus protecting the receiver. Other than the thermocouples, the receiver requires no sensors or controls.

This work was done by A. E. Kofal, R. G. Shannon, and Donald K. Zimmerman of The Boeing Co. for **NASA's Jet Propulsion Laboratory.** *For further information, Circle 21 on the TSP Request Card.*
NPO-15124

Angle-Measurement and Ranging System

Projected "rainbows" and stereo ranging determine altitude and position.

Marshall Space Flight Center, Alabama

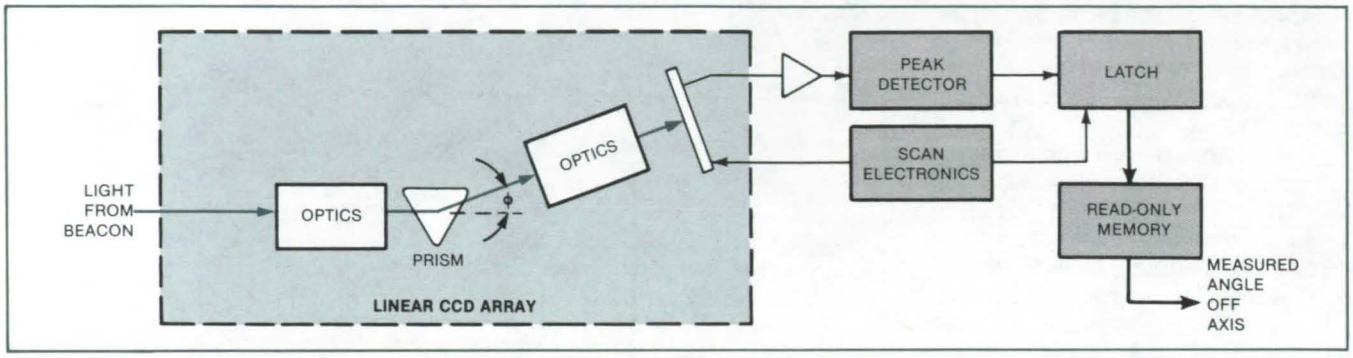

Figure 1. In the Angle-Measurement System, light from the beacon is deflected by the prism by an angle ϕ, which depends on wavelength. The electronics convert this deflection to a measurement of the chase vehicle angular separation from the docking axis.

A proposed optical system automatically supplies information on the angular position and range of an object. Although originally developed for spacecraft rendezvous and guidance, features of the system can be adapted to angle-measurement and ranging problems on Earth. For example, these techniques could be used for tool alinement, inspections and color recognition.

In the new optical system, it is assumed that a "chase vehicle" is seeking out a "target" to dock with it. To do this, it needs relative postion and range information. A beacon on the target vehicle projects "rainbows" of light. The apparent color of the beacon, viewed from the chase vehicle, depends on the angle between the docking axis and the line of sight. If the light from the beacon appears blue, the chase vehicle is to the left of the docking axis; if the light appears yellow, the chase vehicle is on the docking axis; if the light appears red, the chase vehicle is to the right of the axis.

The beacon also projects a second rainbow and rapidly alternates between the two. The second rainbow shows whether the chase vehicle is above or below the docking axis. For synchronization, the chase vehicle could send a radio signal to indicate which rainbow is active, or the chase vehicle guidance system could synchronize to a one-two-off flashing sequence.

The color detection system on the chase vehicle uses a prism spectrometer, as shown in Figure 1. Light from the beacon is refracted in the prism, and the angle of refraction is a function of the wavelength or color of the light. A linear charge-coupled-device (CCD) array behind a grating detects this deflected light; the position of the brightest spot along the array indicates the color. The system locates the bright spot with a peak detector that monitors the video signal from the CCD array.

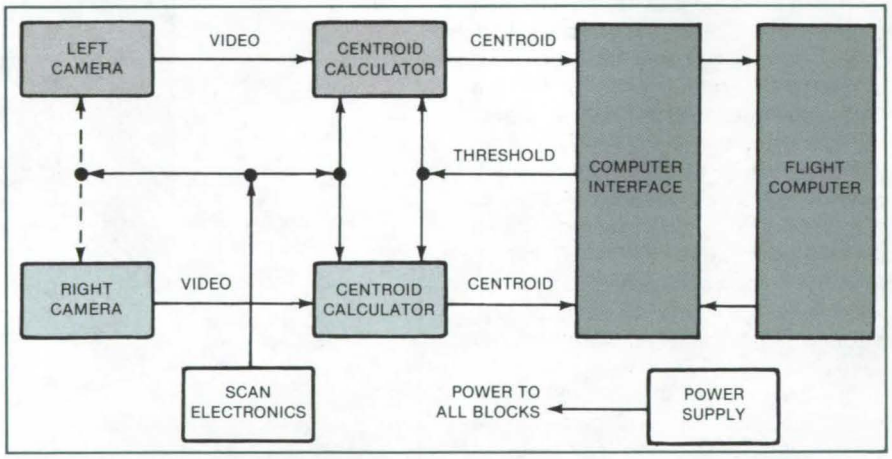

Figure 2. In the Stereo Rangefinder the video signals from the cameras are processed to determine the center of brightness for the images of a beacon on the target vehicle. The range is updated by an onboard computer.

The rangefinder uses two television cameras mounted on opposite sides of the chase vehicle. Both cameras find the center of brightness, and the range to the target is computed by comparing the center-of-brightness calculations from the two cameras.

Figure 2 is a block diagram of the rangefinder. Two centroid calculators compute the image-plane coordinates of the image of the beacon, and an onboard computer uses the coordinates to calculate the distance to the target and to keep the cameras pointed at the target. The system makes 30 range measurements per second. The center-of-brightness information is also used to point the color detector, which has a much smaller field of view than the cameras.

This work was done by John C. Tietz of Martin Marietta Corp. for **Marshall Space Flight Center.** *For further information, Circle 22 on the TSP Request Card.*

MFS-25912

Zero-Net-Charge Air Ionizer

Positive and negative ion outputs are controlled to produce neutral ionized air.

NASA's Jet Propulsion Laboratory, Pasadena, California

An instrument monitors the air supplied by an air ionizer and regulates the ionizer to ensure that the net charge is neutral. It is useful where integrated-circuit chips are manufactured, inspected, tested, or assembled since it prevents a localized buildup of electric charge and thus protects against damage from electrostatic discharge.

The instrument includes a probe, an electrometer, and an amplifier (see figure). As the ionizer blows air over a metal plate attached to the probe, the electrometer continuously measures the probe voltage and sends the measurement signal to the amplifier. The amplifier then sends a control signal to each of the ionizer high-voltage supplies, adjusting the outputs of positive and negative ions so that they are equal.

This work was done by William R. Woods, Jr., of Caltech for **NASA's Jet Propulsion Laboratory.** *For further information, Circle 23 on the TSP Request Card.*
NPO-15937

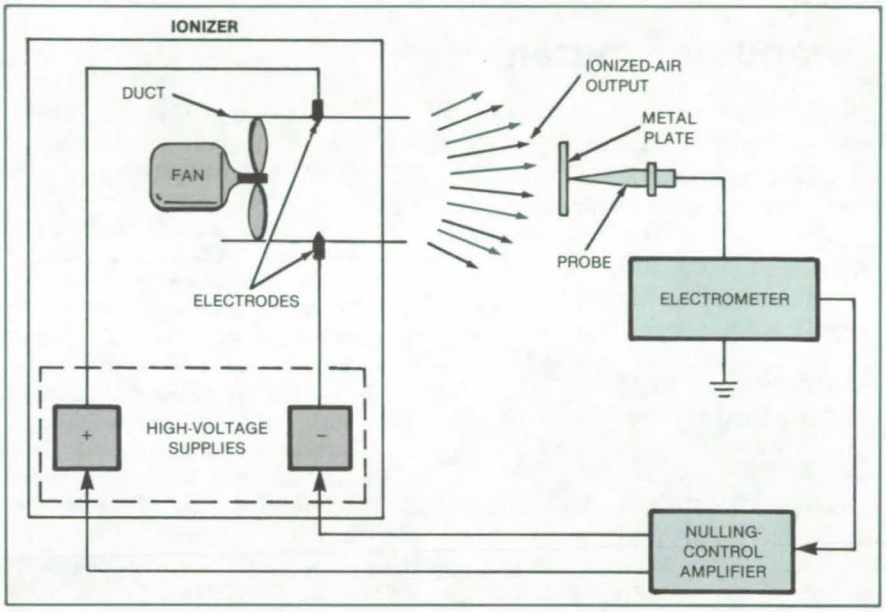

A High-Impedance Electrometer (about 10^{14} ohms) and a nulling-control amplifier regulate the output of an air ionizer. Although primarily intended to furnish ionized air having no net charge, the instrument could be adapted to generating air with a positive or negative net charge if so desired.

Books and Reports

These reports, studies, and handbooks are available from NASA as Technical Support Packages (TSP's) when a Request Card number is cited; otherwise they are available from the National Technical Information Service.

Convective Oscillations at Crystal/Melt Interface

An instability arises from coupled fluid-dynamical and solidification effects.

An oscillatory instability in the shape of the solid/liquid interface geometry was observed in heat-transfer experiments in a long, thin vertical cylinder filled with succinonitrile, according to a research report. This novel fluid-flow configuration with cylindrical symmetry was developed to permit detailed heat-flow experiments in a geometry that would also be mathematically tractable.

Succinonitrile was selected because it is a low-melting-point, transparent, single-component substance with a solidification behavior similar to that of metals. Thus, gravitationally caused effects could be studied in the absence of some of the other complicating effects, such as opacity, concentration gradients, and less tractable geometries that typically occur in production systems for growing doped semiconductor crystals.

The low-frequency oscillatory behavior that has been discovered may help in the interpretation of other crystal-growth processes. The new instability is the first confirmed case where a self-excited oscillation on a crystal/melt interface leads to traveling waves. Such waves had not been predicted: They may indicate the existence of more-general low-frequency oscillatory phenomena during crystal growth.

A mathematical analysis of the system was carried out after discovery of the oscillation. The new analysis is based on the linear perturbation of the Navier-Stokes and diffusion equations, taking into account the compliant nature of the solid/liquid phase boundary at the outer wall of the liquid annulus.

Both the experimental data and the mathematical analysis show that the oscillation occurs whenever the dimensionless Grashof number calculated for the melt exceeds about 200. The Grashof number is defined as

$$Gr = g\beta\Delta TL^3/\nu^2$$

where g = the gravitational acceleration, β = the temperature coefficient of bulk expansion of the melt, ν is the viscosity, ΔT = the temperature drop across the liquid, and L = the radial width of the liquid gap.

(continued on next page)

The Grashof number was tested because many natural convection problems scale with this number, which represents the ratio of buoyancy forces to viscous forces. The correlation between theory and experiment suggests that the oscillation is caused by an interaction between convective heat flow in the melt and heat flow from latent heat of fusion, which is absorbed as the crystal phase melts or released as the liquid phase solidifies. The analysis also predicts, a new instability with an axisymmetric eigenmode at about Gr = 500.

This work was done by M. E. Glicksman of Rensselaer Polytechnic Institute and S. R. Coriell and R. F. Boisvert of the National Bureau of Standards for **Marshall Space Flight Center.** *To obtain a copy of the report, Circle 24 on the TSP Request Card.*
MFS-25892

Computer Programs

These programs may be obtained at very reasonable cost from COSMIC, a facility sponsored by NASA to make new programs available to the public. For information on program price, size, and availability, circle the reference letter on the COSMIC Request Card in this issue.

Assessing Energy-Generating Systems

The economics of user-specified thermal and electrical systems are analyzed.

OMEGA, a program for the economic evaluation of energy-generation systems under a variety of tax environments is now available from COSMIC. OMEGA finds normative prices and break-even values of system parameters. It applies to electrical and thermal energy-generation systems owned by a utility, a business, or a consumer.

The systems under evaluation may be new construction or retrofit construction. They may be grid-connected or stand-alone. Owners of grid-connected systems have the option of selling all of the electricity generated and buying electricity back at utility rates, or of selling excess electricity and buying backup power as needed. OMEGA can perform parametric studies and compare systems. Use of the system as a tax shelter is among the issues that can be studied.

The OMEGA approach is a straightforward modeling of all the financial benefits and costs throughout the system life and beyond, assuming that components are replaced when necessary and that the performance follows a predictable pattern. Capital expenditures are assumed to recur at the end of component lifetimes. The performance pattern is assumed to repeat with a known period. Most of the cost elements are derived from the capital expenditures, while others are supplied directly by the user of the program. Financial benefits are assumed to grow at the rate of energy price escalation. Thus, an OMEGA assessment of a system produces time sequences of benefits and costs, expressed in nominal dollars.

OMEGA is written in Microsoft BASIC-80 for interactive execution and has been implemented on a Z80-based microcomputer with CP/M. The program requires 64K of memory and about 200K bytes of disk storage. The OMEGA program was developed in 1982.

This program was written by Robert G. Chamberlain, Kirby M. McMaster, and Michael C. Davisson of Caltech for **NASA's Jet Propulsion Laboratory.** *For further information, Circle H on the COSMIC Request Card.*
NPO-16159

A General Optical Systems Evaluation Program

Program evaluates optical systems by geometrical ray tracing.

The General Optical Systems Evaluation Program, GENOPTICS, aids the analysis and evaluation of optical systems that employ lenses, mirrors, diffraction gratings, and other geometrical surfaces. GENOPTICS uses geometrical ray tracing based on Snell's law. It can trace as many as 800 rays through as many as 40 surfaces. These surfaces may be planar, conic, or toric or polynomial-shaped lenses, mirrors, and diffraction gratings. Each surface may be tilted about as many as three axes and may be decentered. Surfaces having bilateral symmetry may also be analyzed. GENOPTICS provides for user-oriented input and for a wide range of output for the evaluation of the optical system being analyzed.

GENOPTICS provides a wide range of features for the optical system analyst. It performs paraxial ray tracing and computation of the third-order aberrations including aspheric contribution. Graphical output can be generated for spot diagrams, radial energy distributions, and modulation transfer functions, for each object point and each color. Sag tables may be generated for any rotationally symmetric surface, with options to obtain the sag differences from a reference sphere in units of lengths or wavelengths. Statistics and plots of ray intercepts with any surface in the system may be obtained for use in vignetting analysis and beam distribution analysis.

Afocal systems can be examined with image statistics generated in terms of tangents of angles with respect to the optical axis. For exact ray tracing, a ray pattern at the entrance pupil can be specified as a rectangular or polar grid, where each ray samples an equal amount of area, or as a pattern, where each ray samples an equal amount of solid angle for a finite object. This latter pattern is useful in radiometric work. A "ray-aiming" feature, which directs incoming real rays so that they fill the aperture at an internal surface, is also available.

Input to GENOPTICS includes program-control statements, system definition data, surface data, and task data. Multiple cases may be examined in a single run. Output includes printed and graphical results. The user can specify which portions of an analysis are to be printed. The Software II version provides for an input format similar to that of ACCOS V (Scientific Calculations, Inc.).

Optional printout includes system data, surface-to-surface printout of each ray, modulation transfer-function values, radial energy-distribution values, and paraxial ray date including aberrations. GENOPTICS is coded to generate plotted output for ZETA plotting system but should be readily adapted to other plotting systems.

The GENOPTICS program is written in FORTRAN IV for batch execution and has been implemented on a DEC VAX-11/780 computer and an IBM 3081. GENOPTICS was developed in the

mid-1970's and was last updated in 1983 (Software II).

This program was written by M. E. Wilson and B. J. Howell of **Goddard Space Flight Center.** *For further information, Circle J on the COSMIC request Card.*
GSC-12823

Solar/Thermal Powerplant Simulation

Program provides for consistent comparison of powerplant configurations.

A simulation program evaluates the performances and energy costs of diverse solar/thermal powerplant configurations. The methodology provides for a consistent comparative evaluation of solar/thermal powerplants. The approach is based on optimizing the sizes of the collector and storage subsystems to give the minimum energy cost for specified plant rating and load factor. The simulation assumes a continuous utility demand characteristic, with power being supplied by the solar plant, by the storage subsystems, or by both. This program has proved very useful in the study of solar/thermal powerplants such as the one constructed at Barstow, California.

The solar/thermal powerplant simulation is accomplished by dividing the task among three computer programs linked to operate as one. The FIELD computer program calculates the performance of the solar collector field. Input includes extensive insolation and meteorological data for a given geographical location. Ouput includes data on the field efficiency and the amount of energy collected.

The POWER program uses output from FIELD and user-supplied powerplant characteristics to determine the performance of the fixed-rating powerplant for various collector and storage sizes operating under the conditions input to the FIELD program. The ECONOMICS program uses output from the POWER program and user-supplied cost data to determine energy costs for the powerplants of various collector and storage sizes.

A major feature of this program is the connection between the performance and economics codes that allows for the optimization of the solar/thermal powerplant configuration. The ECONOMICS program determines an optimum plant for each size of total collector area and an envelope of these optima. The optimum solar/thermal powerplant for a given rated output may be determined by interpolation to the intersection of the envelope of optima with the line representing a constant specified load factor.

This program is written in FORTRAN V and Assembler for batch execution and has been implemented on a UNIVAC 1100-series computer with a central memory requirement of approximately 20K of 36-bit words. This program was developed in 1978.

This program was written by James M. Bowyer, Nabil El Gabalawi, Gerrie M. Hill, and Marie L. Slonski of Caltech for **NASA's Jet Propulsion Laboratory.** *For further information, Circle K on the COSMIC Request Card.*
NPO-15440

MiniBriefs describe NASA innovations and reports in an abbreviated format. Readers desiring additional information on these items should request the Technical Support Packages (TSP's), available in most cases, which can be obtained by using the TSP Request Card at the back of this issue.

Thermoelectric Generator

A thermoelectric generator features conversion efficiency of up to 40 percent.

A small modular alkali-metal thermoelectric generator with no moving parts directly converts heat to electrical energy with an efficiency of 20 to 40 percent. The unit uses a closed regenerative electrochemical concentration cell based on the sodium-ion conductor, beta alumina. The unit promises simplicity, high power-to-weight ratios, and potentially long maintenance-free life. Power-density efficiency and electrochemical performance characteristics are outlined in a published report.

This work was done by Terry Cole of Caltech for **NASA's Jet Propulsion Laboratory.** *For further information, Circle 35 on the TSP Request Card.*
NPO-16164

Soft-X-Ray Prefilter for Hot, Bright Objects

Detectors are protected at higher radiation levels.

Prefilters consisting of beryllium foil supported on conductive silver mesh transmit soft X-rays (2 to 60 Å), but are nearly opaque (neutral density >2) to visible and infrared light. The new Be/Ag filters protect imaging X-ray detectors from damage by visible and longer wavelength radiation when viewing such hot, bright emitters as the Sun or possibly certain industrial processes.

The new prefilters are about twice as thick as aluminum prefilters of comparable X-ray transmission. This extra thickness, combined with the greater tensile strength of beryllium, makes the new prefilters stronger and able to withstand radiation loads up to 7.5 dB higher.

This work was done by John M. Davis and Jens A. Ortendahl of American Science & Engineering, Inc., for **NASA's Jet Propulsion Laboratory.** *For further information, Circle 88 on the TSP Request Card.*
NPO-15972

Frequency-Modulation Correlation Spectrometer

Electro-optical phase modulator sinusoidally shifts frequencies of sample transmission spectrum.

A new type of correlation spectrometer eliminates the need to shift between two cells, one empty and one containing a reference gas. Instead, the effect of an empty cell is obtained when needed by phase modulating the beam transmitted by the sample at an amplitude and frequency that shift a given absorption line into sidebands on either side of the original line, reducing the absorption dip at the original line position. If the given line is coincident with one in the

(continued on next page)

reference cell, the net energy transmitted through the reference cell will change when the incoming light is modulated and will not change if the lines are not coincident. The change will be an increase if the incident line is in emission and a decrease if it is an absorption line.

This work was done by Jack S. Margolis and John V. Martonchik of Caltech for **NASA's Jet Propulsion Laboratory.** *For further information, Circle 49 on the TSP Request Card.*

Inquiries concerning rights for the commercial use of this invention should be addressed to the Patent Counsel, NASA Resident Office-JPL [see page A5]. Refer to NPO-15558

Pump-Fed Versus Pressure-Fed Propulsion

A pumping system may have lower mass.

Equations have been worked out to compare the masses of pump and pressure-fed bipropellant propulsion systems. The equations were developed specifically for interplanetary spacecraft, but the analysis technique may be adaptable to advanced automative energy-storage techniques; for example, pressurized versus metal-adsorption hydrogen storage.

If the conclusions of the spacecraft analysis are considered to indicate a trend, it appears that as the propellant mass increases, the total system mass increases more steeply in a pressure-fed system. The difference is due mainly to the larger mass of the pressurant and of the thicker tank walls required to contain liquids under pressure.

This work was done by Paul N. Estey of Caltech for **NASA's Jet Propulsion Laboratory.** *For further information, Circle 50 on the TSP Request Card.*
NPO-15190

Monitoring of Reactive Atmospheric Species

Reactive atmospheric species are produced and detected to provide reference spectra.

A laser-based apparatus for atmospheric studies generates short-lived, unstable or highly reactive atoms or molecules of interest in a radio-frequency discharge or electrical discharge and uses optogalvanic detection as a simple, sensitive, and reliable means of providing precise wavelength calibration spectra. The compact device is insensitive to scattered light and has low power consumption.

This work was done by Christopher R. Webster of Caltech for **NASA's Jet Propulsion Laboratory.** *For further information, Circle 51 on the TSP Request Card.*
NPO-15981

Thermal-Expansion Measurement

A laser-based system measures coefficients of thermal expansion.

A precise, stable laser system determines coefficients of thermal expansion. The dual-beam interferometer arrangement monitors changes in sample length as a function of temperature by following the changes in optical path lengths. Vacuum measurements in the range of $-150°$ to $120°$ F ($-101°$ C to $49°$ C) made over a 6-month period on graphite/epoxy tubes yielded thermal-expansion coefficients in the range of 2.5×10^{-7}/°F (4.5×10^{-7}/°C).

This work was done by Jack H. Davis and Carol Rives of the University of Alabama for **Marshall Space Flight Center.** *For further information, Circle 52 on the TSP Request Card.*
MFS-27000

Integrated System for Environmental Simulation

Wind, rain, vibration, and other factors closely resemble those of actual use.

An integrated testing system subjects ground-support equipment for the Space Shuttle to the conditions that prevail during a launch. The concept may also apply to testing other equipment that must function faultlessly in a difficult environment.

The system simulates engine ignition, wind and weather, cryogenic cooling, and solar heating, among other service conditions. It includes a support pad for a solid rocket booster, 18 small support pads for equipment, a pumphouse containing four high-capacity hydraulic pumps, a random-motion simulator, a simulated tower, liquid and gaseous nitrogen and liquid hydrogen, and communication; monitoring; and control units. Testing is performed under conditions simulating vehicle motion before launch, fueling and purging, power startup and power shutdown, emergency, hold, and other situations.

This work was done by R. T. Uda, S. R. Dandage, and D. C. MacDonald of Planning Research Corp. for **Kennedy Space Center.** *For further information, Circle 53 on the TSP Request Card.*
KSC-11274

Flexible Mirror Mount for Michelson Interferometer

Interferometer mirrors are mounted on flexible spring strips.

Front-surface mirrors for an airborne Michelson interferometer are mounted on flexible spring strips. The strips lie in the vertical plane of the instrument, and set screws allow adjustment of the angle of elevation. Azimuth and vertical elevation are adjusted with conventional clamps. The mirror mounts are unusually compact and rugged. The spring strips hold the mirrors rigidly in place, but allow easy alinement. The mounts are used in a folded-beam Michelson interferometer designed to monitor pollutants at an altitude of 40,000 meters.

This work was done by Gerald S. Perkins of Caltech for **NASA's Jet Propulsion Laboratory.** *For further information, Circle 54 on the TSP Request Card.*
NPO-15746

Adjustable-Frequency Spectrophone Laser Stabilization

Loop with spectrophone sensor stabilizes gas laser at any desired frequency within the gas spectral line width.

A gas-laser frequency-stabilizing system includes a sensitive spectrophone that senses a dither modulation of the frequency of the laser beam, producing a Lorentzian, Voigt, or Doppler spectral tuning response. The spectrophone

signal is divided by a laser power output signal to remove power dependence. The first or second derivative of this signal is used as a detector characteristic curve in a lock-in frequency-correction loop. An adjustable dc bias added to an error signal in the feedback loop offsets the laser to any desired frequency within the gas spectral line width. The dither feedback signal drives a piezoelectric transducer to tune the laser.

This work was done by Michael J. Kavaya and Robert T. Menzies of Caltech for **NASA's Jet Propulsion Laboratory.** *For further information, Circle 55 on the TSP Request Card.*

This invention has been patented by NASA [U.S. Patent No. 4,434,490]. Inquiries concerning nonexclusive or exclusive license for its commercial development should be addressed to the Patent Counsel, NASA Resident Office-JPL [see page A5]. Refer to NPO-15516.

Evaluating Solar Collectors

Analytical methods are compared.

A published survey discusses several methods for assessing the performance of solar-concentrator designs to determine whether a given design is suitable for a given high-temperature solar-powered-generator system. The survey considers the rationale and limitations of each method and provides a basis for selecting the proper method.

Simple formulas are suggested for a quick, inexpensive assessment of solar concentrator designs that are in a concept-development stage. For example, a focal-plane flux distribution of the concentrator assessed by simple formulas can be approximated with sufficient accuracy to determine whether a design is suitable, without resorting to the time-consuming rigorous analytical procedures. More rigorous analytical treatment becomes necessary only when a selected concentrator design has passed the simple analytical treatment and is ready for a detailed-design phase.

This work was done by Liang-Chi Wen, Peter T. Poon, and William J. Carley of Caltech and L. Huang of the U.S. Navy for **NASA's Jet Propulsion Laboratory.** *For further information, Circle 56 on the TSP Request Card.*
NPO-15733

Solar-Powered Water Distillation

Automatic unit removes minerals from well water.

A solar-powered still produces pure water at a rate of 6,000 gallons (23,000 liters) per year. The still is fully automatic and gravity-fed. The only outside electric power it needs is for a timer clock and a solenoid-operated valve. The still saves $5,000 yearly in energy costs, and will pay for itself in only 3 1/2 years.

Local well water with high mineral content is supplied from an elevated tank to solar panels. Heated by Sunlight, the water in the panels evaporates. The vapor is condensed and stored in an underground pure-water tank. Once a day, the solar panels are flushed with freshwater to remove minerals left by the evaporated water.

This work was done by Fred J. Menninger and Robert J. Elder of Caltech for **NASA's Jet Propulsion Laboratory.** *For further information, Circle 57 on the TSP Request Card.*
NPO-15894

Assessing the Performance of Solar Arrays

Selected environmental conditions can be more effective than traditional parameters.

A report available on request analyzes the selection of reference criteria for comparing the performances of photovoltaic arrays. Traditionally, the intensity and spectral composition of the incident radiation have been key variables, along with the cell junction temperature. However, for modules and arrays, these parameters are strongly influenced by the site environmental conditions and the module design. There are, therefore, advantages in choosing a set of selected environmental reference conditions (e.g., air temperature, wind velocity, and irradiance) appropriate for the array or module being studied. Examination of the commonly-used air mass 1.5 solar-irradiance spectrum indicates that it is excellent when assessing the performance of concentrating arrays, but is not as effective for flat-plate arrays.

This work was done by Ronald G. Ross, Jr., and Charles C. Gonzalez of Caltech for **NASA's Jet Propulsion Laboratory.** *To obtain a copy of the report, Circle 58 on the TSP Request Card.*
NPO-15277

Solar-Thermal-Desalination Study

Desalination technologies are compared and evaluated.

A survey assessing the economic feasibility of advanced solar-thermal technologies for desalination is described in a report available on request. Desalination schemes that are suitable for thermal applications are reviewed and their potential conversion efficiencies and development needs are estimated. Potential markets, system efficiencies, and capital operating costs are compared to identify the most promising solar-desalination technology to produce fresh water at low cost.

This work was done by Louis D. Leibowitz, Tsong-Mou Liu and Hung Q. Pham of Caltech for **NASA's Jet Propulsion Laboratory.** *To obtain a copy of the report, Circle 59 on the TSP Request Card.*
NPO-15795

Support System for Solar Receivers

Hinged split-ring mounts insure safe support of heavy receivers.

Solar receivers mounted on conventional rigid ring supports that have stationary struts can be easily damaged when installed in the field. A split-support mounting ring held in place by hinged legs allows the support-ring assembly to open and in effect to lock the two split rings into position. With this split ring the receiver can remain on cable mounts and still slip between openings provided by the split-ring arrangement. In addition to safer operation and damage-free mounting, this system provides more accurate focusing, and small incremental adjustments of the ring are more easily made.

This work was done by Taras Kiceniuk of Caltech for **NASA's Jet Propulsion**

(continued on next page)

Laboratory. *For further information, Circle 60 on the TSP Request Card. NPO-15749*

Testing for Solar-Array Hotspots

A standardized procedure predicts resistance to faults.

Circuit faults such as partial shading, cracking of cells, and open circuits between cells must be expected even in highly reliable arrays of solar cells. However, when such faults occur, the resultant heating from reverse biasing should not propagate the fault or create electrical safety hazards through solder melting or encapsulant deterioration.

Now, laboratory procedures have been developed for evaluating the hotspot endurance of photovoltaic modules under field-service conditions. The procedures can be used for qualification testing of modules.

Evaluations based on the procedures suggest certain circuit-design provisions that reduce the susceptability of modules to faults. For example, the number of cells per bypass diode should be limited to no more than 12 to 15. This will limit hotspot temperatures to less than 120° C, even on hot, sunny days.

This work was done by Charles C. Gonzalez and James C. Arnett of Caltech for **NASA's Jet Propulsion Laboratory.** *For further information, Circle 61 on the TSP Request Card. NPO-15596*

Materials

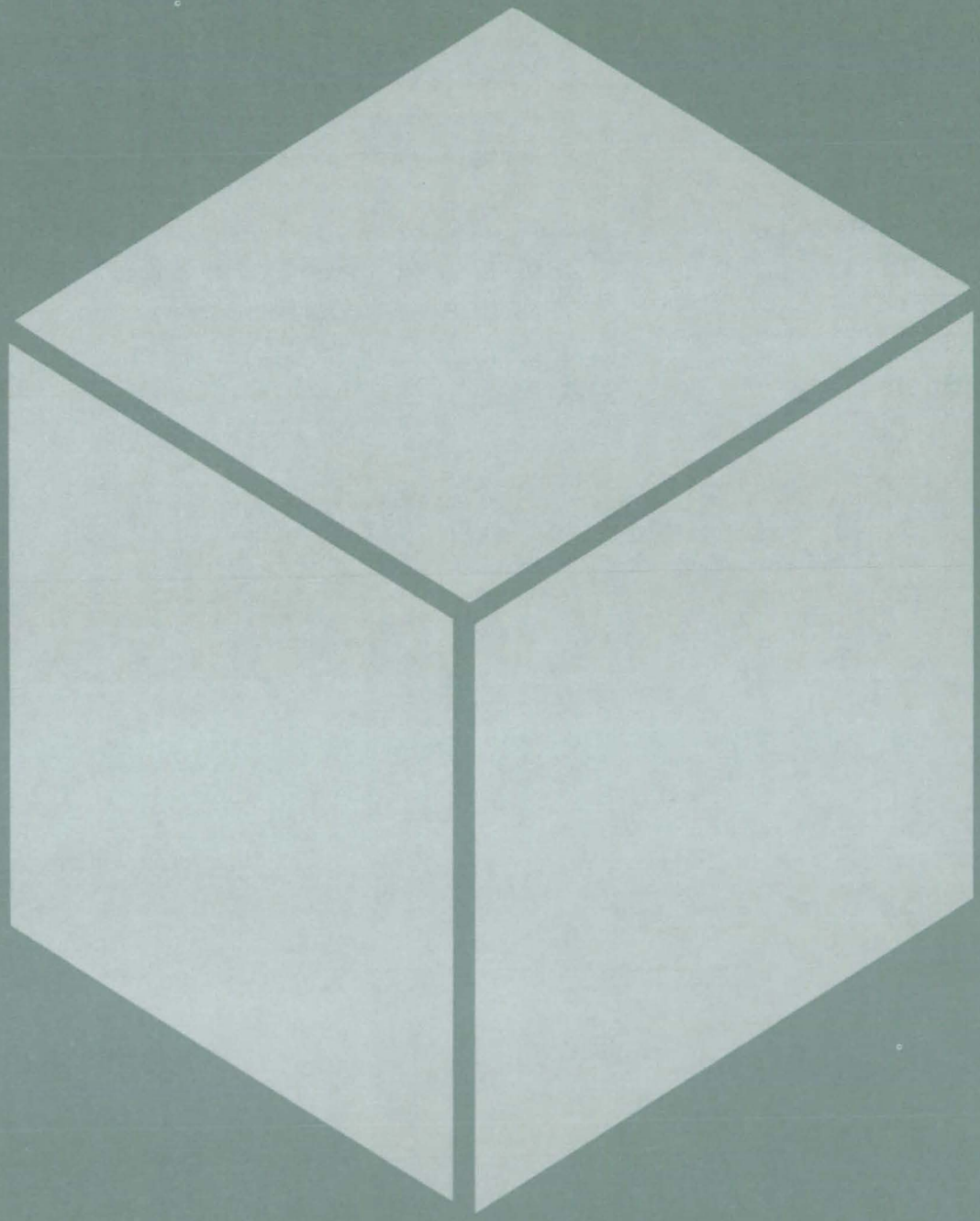

Upgrading Metallurgical-Grade Silicon

A proposed closed-loop process would produce semiconductor-grade silicon.

NASA's Jet Propulsion Laboratory, Pasadena, California

A closed-loop thermal-decomposition process is proposed that converts metallurgical-grade silicon into ultrahigh-purity (semiconductor-grade) silicon. The process produces a mixture of heterogeneously- and homogeneously-nucleated polycrystalline silicon that would be used in semiconductor device applications and in silicon photovoltaic solar-cell fabrication; all other products are recycled in the process, except for impurities, which are discarded.

The essence of the process is the manipulation, in the first stage of the process, of the equilibrium of the chemical reaction:

$$Si + 2H_2 + 3SiX_4 \underset{750^\circ C}{\overset{650^\circ C}{\rightleftharpoons}} 4SiHX_3$$

where X represents either chlorine or bromine. In the second stage of the process, the trihalosilane ($SiHX_3$) is purified; and in the third stage it is thermally decomposed into ultrapure silicon. The byproducts of the second and third stages are recycled as feed to the first stage.

The process is illustrated in the figure. The metallurgical-grade silicon, of about 95-percent purity or greater, is converted in the first stage in a fluid-bed reactor at 400° to 650° C and at atmospheric pressure or greater. The reaction products are then separated. Silicon tetrahalide (SiX_4) is first condensed from the overhead stream and returned to the reactor feed stream. The trihalosilane is next condensed from the overhead stream and fed to the next stage, and impurity metal halides are removed from the bottom of the first stage. Because the forward reaction has a positive free energy, it is a nonequilibrium reaction and the reaction products must be continuously removed from the first stage.

In the second stage, a simple multiple distillation column purifies the trihalosilane. The first-stage feed is separated into a mixture of less than 5 percent silicon tetrahalide in trihalosilane and is fed to the third stage.

The feed is thermally decomposed into silicon, hydrogen, and silicon tetrahalide in the third stage at 600° to 800° C and at atmospheric or reduced temperature in a fluid or moving-bed reactor. The wall temperature of the reactor is held above 900° C to prevent thermal-decomposition deposits on the wall, and subsequent reactor plugging, while the reactor bed temperature is maintained in the range of 700° to 800° C.

The silicon from the decomposition is a mixture of homogeneously-nucleated fine particles and heterogeneously-nucleated silicon growth upon the reactor bed substrate particles. To grow self-perpetuating substrate particles and maximize the conversion efficiency and rate, it is important to control the ratio of homogeneous and heterogeneous nucleation. The relative proportion is controlled by several factors, including the type of feedstock (tribromosilane or trichlorosilane), decomposition temperature and pressure, bed particle-size distribution and surface pretreatment, bed velocity, and bed depth and residence time.

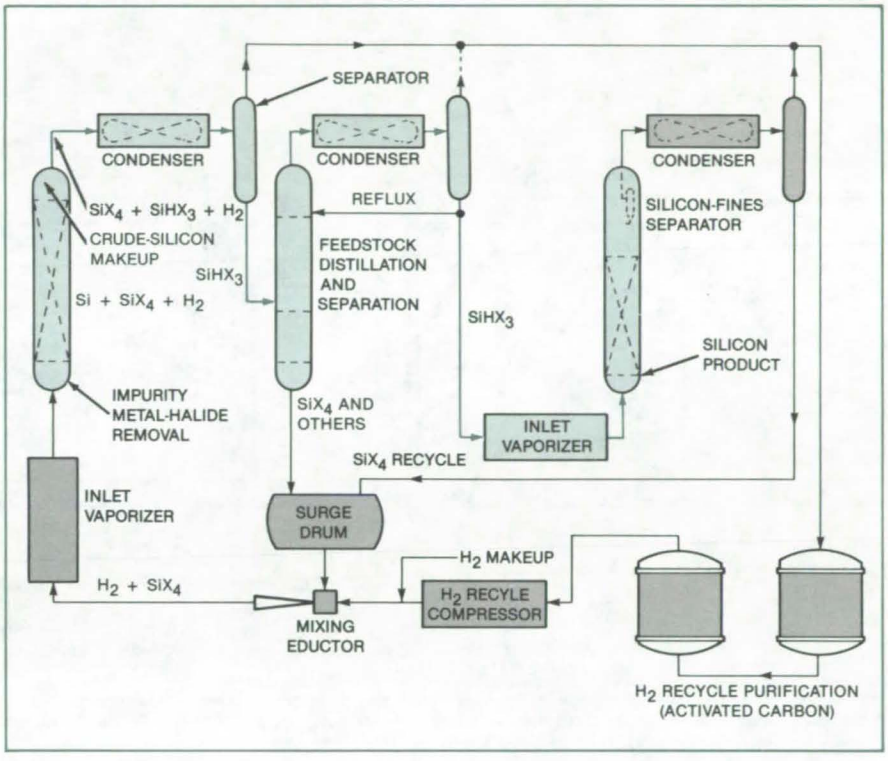

Metallurgical-Grade Silicon Is Converted to Ultrapure Silicon by reacting with hydrogen and silicon tetrahalide to form trihalosilane, purifying this intermediate, and again decomposing to high purity silicon in a third stage. The ultrapure silicon is produced along with byproduct hydrogen and silicon tetrahalide. The byproducts of the second and third stages are separated by a condenser and separator in each stage and are recycled through a surge drum as feed for the first stage. The recycled hydrogen is purified in an activated carbon filter and compressed before passing to a mixing eductor, where it is mixed with the tetrahalide from the surge drum and fed to the first-stage reactor.

This work was done by Lloyd M. Woerner and Edward B. Moore of J. C. Schumacher Co. for **NASA's Jet Propulsion Laboratory.** *For further information, Circle 62 on the TSP Request Card.*

NPO-15076

Containerless Manufacture of Glass Optical Fibers

Contamination and crystallization are reduced in a proposed process.

Marshall Space Flight Center, Alabama

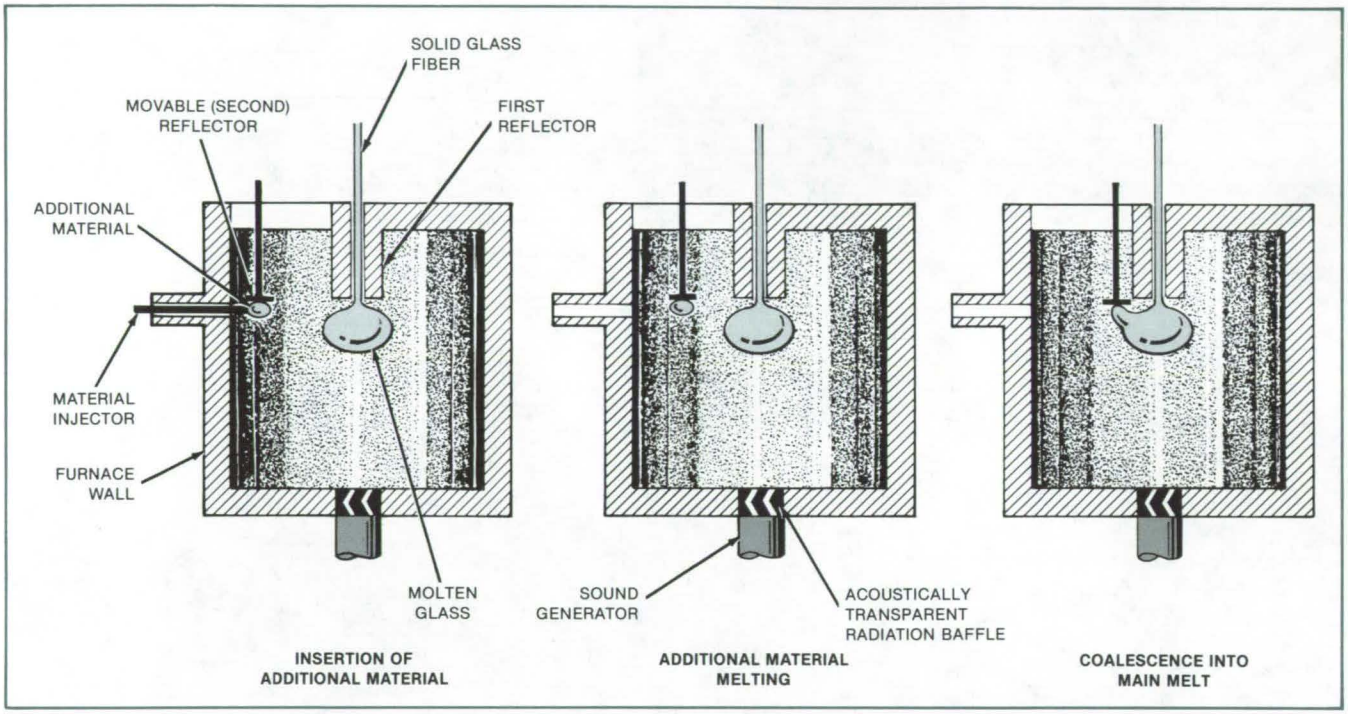

A **Solid Optical Fiber Is Drawn** from an acoustically levitated lump of molten glass. New material is added in solid form, melted, and then moved into the main body of molten glass.

Glass optical fibers of the high purity needed to reduce signal losses to near the theoretical minimum would be made in a proposed new containerless process. Since the molten glass would not make contact with any solid object except the glass fiber in formation, there would be no opportunity for solid contaminants to dissolve in the melt. Moreover, without contaminants and solid objects to serve as nucleation sites, the tendency of the melt to crystallize (and thereby preclude glass formation) would be suppressed.

The glass-forming material would be melted in a single-axis-interference acoustic-levitation furnace. Heating would be done with SiC or other resistance-type elements capable of withstanding an oxidizing atmosphere. High-intensity sound at a single frequency would be introduced through a radiation baffle at the bottom of the furnace.

Acoustic standing waves would cause a levitation equilibrium region just below a first acoustic reflector at the top of the furnace (see figure). A glass fiber would be drawn from the melt in this region through a hole along the acoustic axis of the first reflector. The hole would be lined with copper or other high-thermal-conductivity material that acts as a heat sink to cool the fiber. A quenching gas may also be fed through the hole.

Cold new glass-forming material would be added to the furnace by placing it under a second acoustic reflector. The pellet of material would be allowed to melt while levitated under the second reflector. Then the second reflector would be moved near the first reflector so that the new material will coalesce with the melt from which the fiber is drawn.

Single-axis acoustic-levitation furnaces can levitate glass melts at temperatures up to about 700° C. Since acoustic-levitation forces decrease with increasing temperature, it is likely that this kind of processing in unit gravity will be limited to low-melting-temperature glasses. It may be necessary to operate in low gravity to use higher temperatures or low-viscosity melts or to eliminate gravity-driven phase separations in multiple-component melts.

This work was done by Robert J. Naumann and Edwin C. Ethridge of **Marshall Space Flight Center.** *For further information, Circle 63 on the TSP Request Card.*

Inquiries concerning rights for the commercial use of this invention should be addressed to the Patent Counsel, Marshall Space Flight Center [see page A5]. Refer to MFS-25905.

Equation for Electrolyte Viscosity

Equation agrees with measurements over a wide concentration range.

NASA's Jet Propulsion Laboratory, Pasadena, California

An equation for the viscosity of aqueous electrolyte solutions matches experimental data closely and is valid for a wide range of electrolyte concentrations. Other equations do not match the data quite as well and are limited to dilute solutions.

The new equation is an empirical one of the form

$$\frac{\eta}{\eta_0} = \left(1 + \frac{1.25\phi}{1 - \phi/\phi_m}\right)^2$$

where η and η_0 are the viscosities of the solution and the solvent, respectively; ϕ is a parameter related to the concentration of the electrolyte; and ϕ_m is a parameter related to the maximum volume fraction to which the solute particles can be packed.

Researchers have found that ϕ_m for dense random packing is approximately equal to 0.637. The parameter ϕ can be expressed as the product $\phi = cV_e$, where c is the concentration of electrolyte in moles per liter of solution, and V_e is related to the volume occupied by a mole of electrolyte while in solution.

The equation can be rewritten and plotted as shown in the figure. The fit of calculated values to measured values is very close except for the measurement point in the upper right corner. This point represents a very dilute solution, for which the equation becomes sensitive to small errors in relative viscosity.

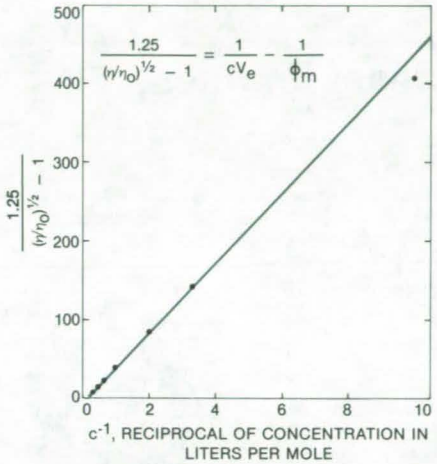

A Plot of Calculated Values from the equation (indicated by the solid line) and measured values (indicated by dots) shows a close match except at an extremely low concentration of electrolyte. Data are for sodium bromide solutions.

This work was done by Robert F. Fedors of Caltech for **NASA's Jet Propulsion Laboratory.** *For further information, Circle 64 on the TSP Request Card.*

NPO-15096

Pressure-Letdown Plates for Coal Gasifiers

Rotating plates would reduce erosion and clogging.

NASA's Jet Propulsion Laboratory, Pasadena, California

A variation of the pseudoporous plates used with coal gasifiers in the pressure-letdown stage of processing would minimize clogging. Rotating plates containing variable-gap annuli continually change the the flow path to enable an erosionless reduction of gas pressure. Particles that otherwise would clog the porous plugs pass through the gaps.

The pressure-letdown plates of coal-gasification processors must accommodate gas mixtures at temperatures up to 1,600° F (870° C) as the pressure is reduced from 3,000 psi (2.1×10^7 N/m^2) to atmospheric pressure. Mixed with the gas is the slurry emanating from the coal processor, carrying coal particles up to

(continued on next page)

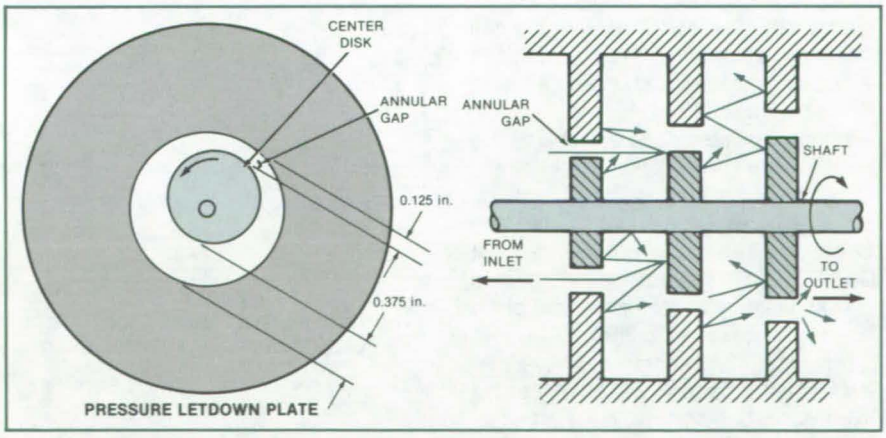

The **Pressure-Letdown Plates** create a tortuous path for the gas as it decompresses from 3,000 psi at the inlet to atmospheric pressure at the outlet. The center disk of each plate is mounted on a common shaft so that shaft rotation changes the path from plate to plate. The shaft rotation is intended to break apart clinging particulates, not to grind them.

one-eighth in. (3.2 mm) in diameter. Since the slurry particles tend to adhere to the plates as the temperature drops during letdown, clogging may result.

As shown in the figure, a set of the proposed pressure-letdown plates is mounted on a common shaft. Each of the plates contains a single annulus. The central disk is offset slightly from the centerline so that a nonuniform gap exists in each stage. Each annulus on successive plates increases in diameter from the inlet to the outlet.

The rotation of the plates changes the tortuous path from plate to plate. This rotation discourages agglomeration of the exiting particulates and minimizes the tendency for them to clog the plates.

This work was done by Earl R. Collins, Jr., of Caltech for **NASA's Jet Propulsion Laboratory.** *For further information, Circle 65 on the TSP Request Card.*
NPO-15965

Testing Ceramics for Diesel Engines

Concept offers safe, convenient simulation of operating conditions.

NASA's Jet Propulsion Laboratory, Pasadena, California

A proposed adaptation of a diesel engine would allow prestressed ceramic materials to be evaluated under realistic pressure, temperature, and stress without introducing extraneous stress. Such materials are under consideration as cylinder liners for diesel engines because they would allow operation at higher temperatures and therefore higher efficiencies. They tend to be brittle, however; and careful evaluation is necessary.

The ceramic specimen is a part of the prechamber of the research engine (see figure). The specimen is held in place by a clamp that introduces the required axial compressive stress. The specimen—a cylindrical shell — is surrounded by a chamber that may be vented or pressurized to introduce the requisite radial stress in the ceramic. The pressure chamber also serves as a safety shield in case the specimen disintegrates.

When the diesel engine is running, the specimen is subjected to essentially the same temperatures and pressures as in the combustion chamber, and the axial and radial stresses can be varied by the experimenter. The effects of stress risers can be determined by introducing notches, holes, or impurities into the specimens. The mounting arrangement can be varied to subject the specimen to tension instead of compression or to eliminate axial stress entirely.

This work was done by Horst W. Schneider of Caltech for **NASA's Jet Propulsion Laboratory.** *For further information, Circle 66 on the TSP Request Card.*
NPO-15824

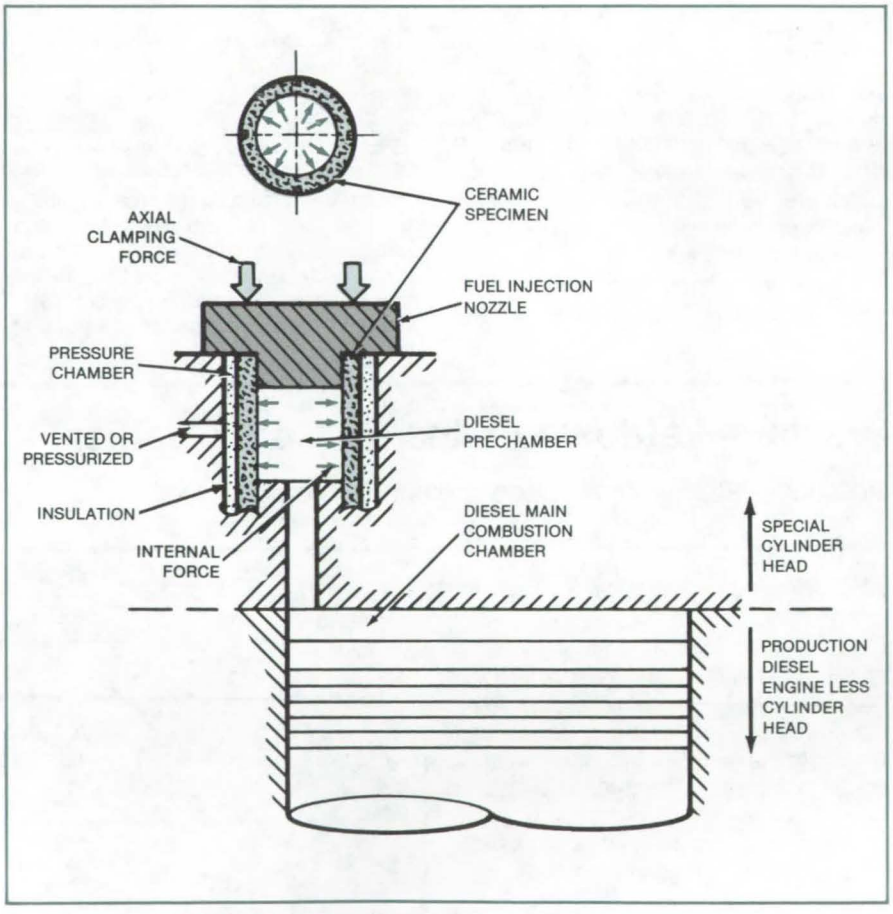

A Burst-Loaded Cylindrical Ceramic Specimen in the prechamber of a research engine is exposed to much the same conditions as in the main chamber. Testing specimens will be less costly than testing full-size functional components in operating engines.

Books and Reports

These reports, studies, and handbooks are available from NASA as Technical Support Packages (TSP's) when a Request Card number is cited; otherwise they are available from the National Technical Information Service.

Pure Glasses From Multicomponent Gels

Containerless melting of gels could yield low-loss glass for optical fibers.

A report now available describes experiments with multicomponent gels for the preparation of pure glass. The experiments are aimed at developing a zero-gravitation process for the fabrication of low-loss optical fibers.

In the proposed containerless process, the chemical precursors of the glass are mixed at low temperature, and a gel is formed to keep the precursors properly mixed. The gel is heated to form the glass, thus maintaining the original purity. Because the components are already intimately mixed in the gel, no further mixing is required.

Several glasses have been produced from gels. The alkaliborosilicate glass $Na_2O/B_2O_3/SiO_2$ was the first to be studied because its properties (including its attenuation coefficient in the 0.8- to 0.9-μm wavelength region) were already available in the literature.

The sol-gel process used is based on the polymerization of alkoxysilane with other metal alkoxides or with suitable metal salts. Gel formation occurs at room temperature where contamination from the container can be avoided. Many alkoxides are liquids and thus can be purified by distillation.

Gels of different compositions in the soda/borosilicate system were prepared by three different procedures using three different sources of Na_2O. The physicochemical nature of the gels was strongly influenced by process parameters, such as the chemical nature of the reactants, the pH of the medium, and the concentrations of water and reactants.

The ease of removal of organics from the gel powders depended on gel-preparation procedures and gel compositions. The variations in times and temperatures required for the removal of organics may be due to differences in the entrapment of residual organics in pores, which would be affected by the nature of the porosity and the rate of pore closing during the thermal treatment.

Infrared absorption spectra of gels produced by different procedures indicate some differences in the molecular structure of the gels. However, melting the gels at temperatures greater than 1,200° C results in near equilibrium in the melts for each of the gels.

The microstructures differed among the phase-separated glasses obtained from the gels prepared by the various procedures. These differences are probably due to differing concentrations of hydroxyl groups, which affect phase separation. Hydroxyl concentration was reduced by passing dry oxygen or other reactive gases through the porous gel powders at temperatures below the point of pore closure.

Hydroxyl concentration was further reduced to about 10 ppm by bubbling dry N_2 through the glass during melting. It is expected that an optimum choice of temperature, time, and reactive-gas composition during treatment of the gel powders could further reduce hydroxyl concentration in the glass. The high concentration of B_2O_3 in the glasses studied would necessitate tight control of experimental conditions to reduce hydroxyl concentration further. Rayleigh-scattering studies of the glasses are being undertaken to determine which gel preparation procedure is most suitable.

This work was done by Shyama P. Mukherjee of Battelle (Columbus Laboratories) for **NASA's Jet Propulsion Laboratory.** *To obtain a copy of the report, Circle 67 on the TSP Request Card.*
NPO-16160

Vacuum Baking To Remove Volatile Materials

Outgassing is reduced in some but not all nonmetallic materials.

Eleven polymeric materials were tested by determining the outgassing species as the temperature of conditioned and unconditioned materials was raised to 300° C. The conditioning process consisted of a vacuum bake for 24 hours at 80° C in addition to the usual cure. A report available on request describes the test program.

Conditioning significantly reduced outgassing in six commercial tapes and paint products. The latter were tested either primed or unprimed. Conditioning had no effect on outgassing in two other products, and it is recommended that the costly vacuum-baking step be eliminated for these materials. Baking at atmospheric pressure instead of in vacuum was found to reduce outgassing in some products. In no case did the baking change the residual gas percentage of water molecules.

This work was done by Joseph A. Muscari of Martin Marietta Corp. for **NASA's Jet Propulsion Laboratory.** *To obtain a copy of the report, Circle 68 on the TSP Request Card.*
NPO-15648

Solution Potentials Indicate Aluminum-Alloy Tempers

Potential is plotted as a function of aging time.

A report from the Marshall Space Flight Center discusses the use of solution potential as a measure of the temper of aluminum alloys. The technique is based on the fact that different tempers or heat treatments exhibit different solution potentials as a function of aging time.

Samples were solution-heat-treated to the desired tempers by heating in an oven at the temperatures and for the times of the temper specifications, then quenched in cold water. After potential measurements were made, the samples were placed in an oven for aging.

The surfaces of the aged samples were wet-sanded with silicon carbide paper, then degreased with boiling trichloroethylene. The samples were then placed in the measuring solution of NaCl and H_2O_2 in water and allowed to stand for 20 minutes before measurements were taken.

Solution potentials were measured with a commercial corrosion-measurement console and a saturated calomel reference electrode. Curves showing potential vs. time were plotted for each alloy tested. In general, the curves show a sharp rise in the magnitude of the solution potential during the first few hours of

(continued on next page)

aging. This is followed by a "knee" where the slope of a curve changes rapidly and after which the magnitude of the potential increases slowly with further aging. Times of aging reported in the literature are consistent with the positions of the slope changes except for one alloy.

This work was done by Merlin D. Danford of **Marshall Space Flight Center.** *Further information may be found in NASA TM-82459 [N82-22345/NSP], "Solution Potentials for Several Aluminum Alloys as a Function of Aging Time" [$7]. A paper copy may be purchased [prepayment required] from the National Technical Information Service, Springfield, Virginia 22161. The report is also available on microfiche at no charge. To obtain a microfiche copy, Circle 69 on the TSP Request Card.*
MFS-25846

MiniBriefs describe NASA innovations and reports in an abbreviated format. Readers desiring additional information on these items should request the Technical Support Packages (TSP's), available in most cases, which can be obtained by using the TSP Request Card at the back of this issue.

Properties of Low-Expansion Laminates

Mechanical and thermal properties of thermally stable laminates are calculated.

Laminate elastic constants and coefficients of thermal expansion have been calculated for near-zero-expansion graphite/aluminum and graphite/magnesium composites. Analysis was performed using a micromechanical approach to determine properties of unidirectional core material and the lamination theory for total laminate properties. A report presents results in graphic form for these properties as a function of laminate angle and fiber volume fraction for four high-modulus continuous-pitch fibers.

This work was done by M. Kural of Lockheed Missiles & Space Company, Inc., for **Marshall Space Flight Center.** *To obtain a copy of the report, Circle 70 on the TSP Request Card.*
MFS-25859

Elastomer Encapsulant for Solar-Cell Arrays

Liquid encapsulant polymerizes to a transparent, protective rubberlike coat.

Butyl acrylate syrups are useful potting compounds for encapsulating photovoltaic cells in modular arrays. The material is a pourable liquid that can be pumped into a module, then cured to a rubbery consistency. The cured material is a thermoset elastomer that is highly transparent, low cost, flexible, and with good low-temperature properties.

The basic butyl acrylate syrup is modified to increase greatly the gel content, decrease the time and temperature for curing, and give the user a wide range of formulations and properties. The cured surface is nontacky. These desirable characteristics are provided by the addition of small amounts (about 5 percent) of diacrylate compounds.

This work was done by Bernard Baum and Paul B. Willis of Springborn Laboratories, Inc., for **NASA's Jet Propulsion Laboratory.** *For further information, Circle 71 on the TSP Request Card.*
NPO-15663

Eutectic-Alloy Morphology

Lower solidification limit for controlled growth of Bi/Mn alloys is 1 centimeter/hour.

A deviation in controlled-rod eutectic morphology anticipated for diffusion-only crystal growth has been characterized at low solidification velocities. Naturally-induced, gravity-related convective instabilities result in nonalined irregularly-dispersed fibers or platelets. This determines a lower useful growth-velocity limit of 1 centimeter/hour for cooperative growth of eutectic bismuth/manganese and other related alloys.

This work was done by Ron G. Pirich and William J. Poit of Grumman Aerospace Corp. for **Marshall Space Flight Center.** *For further information, Circle 72 on the TSP Request Card.*
MFS-25937

Reliability Studies for Fatigue-Crack Detection

Different nondestructive evaluation techniques can be compared.

Reusable test panels are available to assess the reliability of techniques that use a fluorescent penetrant to detect fatigue cracks. The two materials selected for fabricating the panels, a nickel-base alloy and a cobalt-base alloy, are representative of high-temperature structural alloys that have critical fatigue requirements.

Each panel measures 4 by 16 by 0.25 in. (10.2 by 40.6 by 0.64 cm) and contains flaws ranging in size from 0.01 to 0.25 in. (0.25 to 6.35 mm) in sufficient numbers and size distribution to accommodate testing at 95-percent reliability with a 95-percent confidence level. An ultrasonic cleaning method was developed for removing the penetrant from the panels prior to reuse.

This work was done by Brent K. Christner, Ward D. Rummel, and John Knadler of Martin Marietta Corp. for **Marshall Space Flight Center.** *For further information, Circle 73 on the TSP Request Card.*
MFS-27031

Making Pure Fine-Grained Inorganic Powder

An RF plasma technique introduces few impurities.

A sustained-arc plasma chemical reactor fabricates very-fine-grained inorganic solids having low thermal conductivity. The powder-fabrication method, based on the plasma-tube technique, produces pure solids without the contamination commonly produced by grinding.

The method, used in the fabrication of powder for thermoelectric energy conversion systems, produces an average particle size between 50 and 100 Å. Because the particle size is small, the surface reactivity is high, and much lower temperatures and pressures are required in the subsequent hot-pressing step. Consequently, grain growth is reduced. The resulting fine-grained

material has significantly lower thermal conductivity.

This work was done by Charles Wood of Caltech for **NASA's Jet Propulsion Laboratory.** *For further information, Circle 74 on the TSP Request Card.*
NPO-16398

Fluidized-Bed Reactor System

Fluidized-bed reactor design minimizes gas pyrolysis through use of selective radiation.

Gas pyrolysis in hot fluidized beds is minimized by use of selectively filtered radiation and a parabolic cavity. Reactor walls are kept cool while radiant heat is provided to the reactor and the reacting particles themselves by utilizing the region of the spectrum to which the reactor walls are transparent. The radiant heat supplied is filtered by quartz envelopes to prevent heating of the reactor walls. The reactor is a parabolic cavity of two or more axes in which the light emanating from one axis bounces off the walls of the cavity and passes through the object axis to heat the sample.

This work was done by Andrew D. Morrison of Caltech for **NASA's Jet Propulsion Laboratory.** *For further information, Circle 75 on the TSP Request Card.*
NPO-15975

Samarium/Cobalt Magnets

High coercivities of $SmCo_5$ magnets are achieved by eliminating oxygen contamination.

Intrinsic magnetic coercivities of samarium cobalt magnets can be made to approach their theoretical limit of 350 kA/m by carefully eliminating oxygen from the finished magnet by hot isostatic pressing (HIP). The HIP process is a viable alternative to the currently-used sintering process. Since there is substantial lowering in oxygen pickup during densification of the powder compact, there is little grain growth from processing, and much coarser powder size can be used. The composition range over which the magnet properties remain more or less constant eliminates the necessity of careful and costly composition control.

This work was done by D. Das, K. Kumar, R. T. Frost, and C. W. Chang of Charles Stark Draper Laboratory, Inc., for **Marshall Space Flight Center.** *For further information, Circle 76 on the TSP Request Card.*
MFS-27006

Reducing Liquid Permeation Through Polymer Sheets

Solute inclusions in polymer sheets may reduce permeability to liquids.

Permeation of a liquid through polymer sheets may be retarded by including in the polymer a solute for the excluded liquid. The concept has been studied experimentally in the case of water permeating rubber. Three conditions must be satisfied for it to be successful with other solvents and polymers. First, the liquid must not dissolve or swell the polymer. Second, the inclusion should be highly soluble in the liquid. Finally, the inclusion must not be too miscible or soluble in the polymer. Long-term or steady-state permeability would not be reduced by the solute inclusions.

This work was done Robert F. Fedors of Caltech for **NASA's Jet Propulsion Laboratory.** *For further information, Circle 77 on the TSP Request Card.*
NPO-15802

Coal-Face Fracture With a Two-Phase Liquid

Flash vaporization of a dissolved gas would fracture the coal.

In a proposed method for mining coal without explosives, a two-phase liquid, such as CO_2 and water, would be injected at high pressure [e.g., 5,000 psi (34 MN/m^2)] into the deeper ends of holes drilled in the coal face. The liquid would permeate the coal seam through existing microfractures. As the liquid seeps back toward the face, the pressure would eventually drop below a critical value at which the dissolved gas should flash-vaporize, breaking up the coal.

Flash vaporization has been used previously to improve hydrojet cutting of coal. The propagation speed of the vaporization was shown to be faster than in a black-powder explosion.

This work was done by Earl R. Collins, Jr., of Caltech for **NASA's Jet Propulsion Laboratory.** *For further information, Circle 78 on the TSP Request Card.*
NPO-15849

Polyurethane-Foam Maskant

Handling difficulties and contamination are substantially reduced.

The brown wax previously used to mask hardware can now be replaced with a polyurethane foam in electroplating and electroforming operations. The foam is much easier to apply and remove than the wax (which must be hot), and does not contaminate the electrolytes.

The foam resin is applied to sections of the part where metal deposition is not desired and is allowed to foam in place. The foam can then be cut after hardening to shape the material and obtain precise patterns. A protection coating is then applied to protect the foam during processing and prevent electrolyte contamination.

This work was done by Ronnald Bodemeijer of Rockwell International Corp. for **Marshall Space Flight Center.** *For further information, Circle 79 on the TSP Request Card.*
MFS-19786

Streaming-Potential Studies

Surface coatings reduce electro-osmotic flow.

An apparatus and experimental technique that is based on measurements of streaming potentials evaluates the effects of surface coatings for reducing or eliminating electro-osmotic flow. The streaming-potential apparatus design as well as the variables involved in measurement show that coating the glass capillaries with a glycidoxy silane base upon which the methylcellulose is applied shows a sixfold decrease in

(continued on next page)

streaming potential over those of uncoated glass tubes. Treating the surface with such hydrophilic synthetic polymers as methacrylate gels shows similar streaming-potential behavior. The introduction of positively- or negatively-charged comonomer groups into the hydrophilic methacrylate gels produces a wide range of streaming-potential values.

This work was done by D. E. Gregonis, R. Van Wagenen, S. M. Ma, and J. D. Andrade of the University of Utah for **Marshall Space Flight Center.** *For further information, Circle 80 on the TSP Request Card.*

Inquiries concerning rights for the commercial use of this invention should be addressed to the Patent Counsel, Marshall Space Flight Center [see page A5]. *Refer to MFS-25657.*

Mathematical Model for Gas Dissolution in Glass

This model calculates dissolution of gas bubbles in glass melts.

A mathematical model calculates the rate of small oxygen-bubble contraction in soda/lime/silicate melts in the presence of a foreign nondiffusing gas. The process is of interest in optical-glass fabrication. Gas bubbles must be removed from this type of glass before it is optically acceptable. The rate of change of bubble radius with time is calculated by the quasi-stationary approximation, taking into account the effects of melt undersaturation and the initial fraction of foreign gas in the oxygen bubble.

This work was done by Michael C. Weinberg and Paulette I. K. Oronato of GTE and Donald R. Uhlmann of MIT for **NASA's Jet Propulsion Laboratory.** *For further information, Circle 81 on the TSP Request Card.*
NPO-15104

Life Sciences

Transducers for Heart Research

Miniaturization reduces damage
and interference with heart function.

NASA's Jet Propulsion Laboratory, Pasadena, California

A series of transducers with seven different configurations enables the measurement of forces and displacements in the wall of the heart. The new transducers are small, cause minimal perturbation of the heart function, and can be attached and detached without causing excessive tissue damage.

The transducers have performed well in experiments on dogs. Most are made for implantation during open-chest surgery. A few are small enough to be inserted by a catheter through a vein or artery leading into a heart chamber. All units can be implanted or removed during a single heartbeat: This permits rapid relocation for detail mapping.

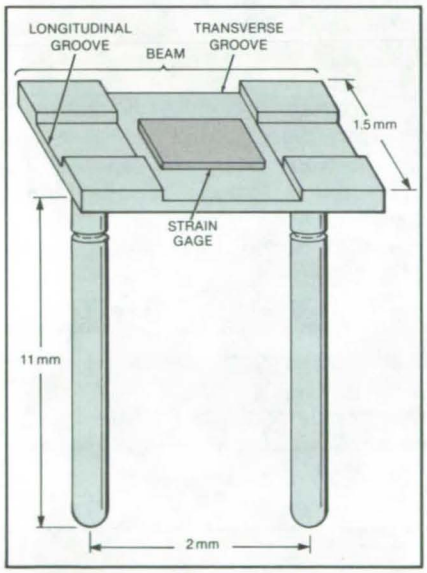

Figure 1. A **Myocardial Force Transducer** measures the local force of contraction along a line between two tines embedded in the heart wall. The longitudinal groove in the beam serves as a protective recess for the strain gage. The transverse groove is shallow enough to keep the beam compliance low, yet deep enough to allow the beam to bend slightly about the sensitive axis of the strain gage.

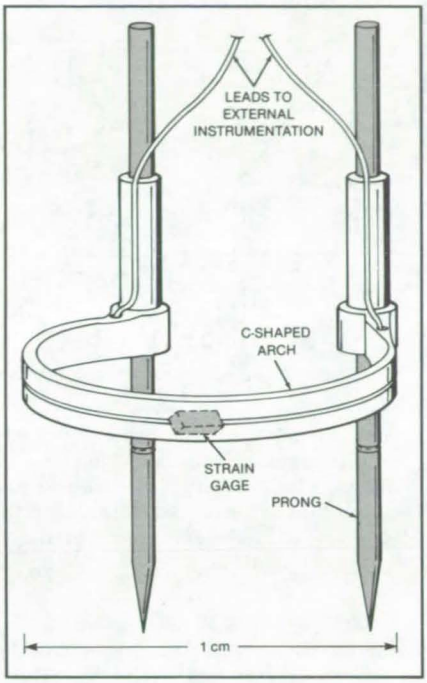

Figure 2. A **Displacement Transducer** includes a high-compliance strain member that reacts as gently as possible against the tissue being measured. The strain-gage output is proportional to the change in distance between the prongs embedded in the heart wall.

Figure 1 shows one type of force transducer that measures an averaged localized wall contraction. The unit is usually aligned with the axis between the tines along a myocardial fiber. Once the tines are implanted in the heart wall, the wall contraction or expansion exerts a bending moment on the beam. The resulting strain in the beam is detected by a piezoresistive strain gage.

The transducer has a high linear output (about 0.8 V/N) with less than 1 percent hysteresis. The output is constant with frequency up to at least 8 Hz and possibly as high as 15 Hz. The unit has a mass of only 0.3 g.

Figure 2 shows one type of displacement transducer. The C-shaped arch between the two prongs flexes compliantly with local muscle movements. Sharp tips facilitate insertion into the muscle. A piezoresistive strain gage is bonded to the arch, preferably at the point of greatest curvature. The prongs are maintained parallel during insertion with the aid of an alinement tool.

Both gages are inserted or removed by simply pushing into or pulling out of the heart wall. Tissue that is parted during insertion snaps back into the detent groove, thus holding the transducer in place. The groove is shallow enough to permit the transducer to be withdrawn with minimal trauma. Thus, a gage can be installed, removed, and reinstalled in the same or a different position.

The transducers are constructed with materials that resist chemical interaction with bodily fluids. Tines and prongs are made of stainless steel. Waterproofing agents must be selected with care because blood and water are corrosive, causing the deterioration of bonds between components as well as insulation breakdowns.

Other transducers in the series include a wall-thickness gage, intravascular force transducer, combination force-and-displacement units for open-chest surgery, intravascular force-and-displacement units, and a trifunctional (force, displacement, and thickness) gage. As a "bonus," the connection of electrical leads to the tines or prongs makes it possible to take electrocardiograms.

This work was done by Cyril Feldstein, Samuel Meerbaum, Gilbert W. Lewis, and Virgil H. Culler of Caltech for **NASA's Jet Propulsion Laboratory.** *For further information, Circle 82 on the TSP Request Card.*
NPO-15095

Aquatic Plants Aid Sewage Filter

Superior water treatment is obtained at low cost.

Marshall Space Flight Center, Alabama

A method of wastewater treatment combines micro-organisms and aquatic-plant roots in a filter bed. In the first step of the process, anaerobic settling takes place in a septic tank, a covered anaerobic lagoon, an Imhoff tank, or any sludge-collecting and sludge-digesting chamber. After a minimum treatment period of 6 hours, the supernatant liquid from the sludge-collecting tank is pumped into the bottom of the hybrid filter system consisting of micro-organisms and plants (see figure).

Treatment occurs as the liquid flows up through the system. Micro-organisms that have attached themselves to the rocky base material of the filter act in several steps to decompose organic matter in the wastewater under treatment.

The first step involves the hydrolysis of organic compounds into simple organic acids, primarily by facultative (having aerobic and anaerobic viability) and obligate anaerobic bacteria. In the second step, strictly anaerobic bacteria convert these acids into CH_4 and CO_2, with trace amounts of H_2 and H_2S. The last step involves the action of aerobic micro-organisms to convert odorous sulfides to sulfates. The vascular aquatic plants (typically, reeds, rushes, cattails, or water hyacinths) absorb nitrogen, phosphorus, other nutrients, and heavy metals from the water through their finely divided roots.

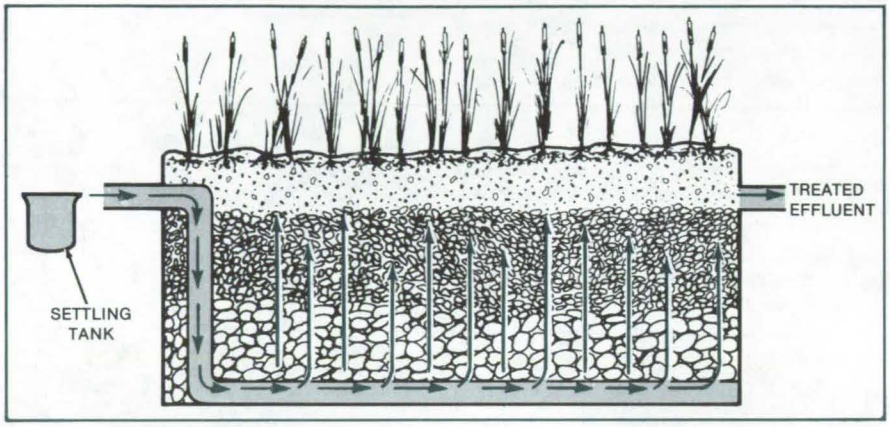

This **Filtering System** includes a sludge-collecting tank and a rock filter. Supernatant liquid from the collecting tank is pumped or flows under gravity into the bottom of the filter, then progresses upward through layers of rock on which micro-organisms are attached. The bottom layer consists of rocks 7.5 to 15 cm across. The second layer is made of 2.5- to 7.5-cm railroad rocks. Vinyl core material can also be used for these layers. The top layer consists of pea gravel (0.25 to 1.5 cm) in which the plants are anchored.

Two versions of a small-scale prototype system were set up: one with and one without plants in the filter bed. The system without plants required about 24 hours to bring the biological oxygen demand below the limit set by the Environmental Protection Agency for secondary treatment. The system using plants brought the level below the limit in 6 hours. The system without plants did not reduce levels of Kjeldahl nitrogen, nitrogen in ammonia, and phosphorus, even after 24 hours. Concentrations of all three were markedly reduced with 24 hours of residence time in the rock filter planted with reeds.

This work was done by Billy C. Wolverton of **Marshall Space Flight Center.** *For further information, Circle 83 on the TSP Request Card.*
MFS-25808

This invention has been patented by NASA [U.S. Patent No. 4,415,450]. Inquiries concerning nonexclusive or exclusive license for its commercial development should be addressed to the Patent Counsel, [see page A8]. Refer to MFS-25808.

Monitoring Marine Microbial Fouling

An epifluorescence-microscopy method takes only 10 minutes.

Marshall Space Flight Center, Alabama

Two techniques have been developed for studying marine fouling, the biological colonization of surfaces by such micro-organisms as bacteria, diatoms, fungi, or protozoa. The methods were originally developed to study fouling of materials to be used in the Space Shuttle solid-fuel booster rockets, which are recovered after they parachute into the ocean. These methods can be used to determine both the relative fouling rates and the efficacy of cleaning methods to remove fouling on various surfaces including paints, metals, and sealants intended for marine use.

The first technique requires 1 to 2 days for sample preparation, but provides qualitative and quantitative assessment of biofouling. The surfaces of the samples are viewed directly with scanning electron microscopy. These observations are combined with those from standard microbial-isolation methods in

which samples are streaked across solid agar media designed to support the growth of marine micro-organisms for enumeration and identification.

The second technique, which uses epifluorescence microscopy, requires as little as 10 minutes for sample preparation and is suitable for shipboard use, but is limited to the study of flat surfaces that do not give off excessive background fluorescence. The sample surfaces are fixed in a 2- to 2.5-percent glutaraldehyde solution, rinsed, and stained with acridine orange in a 0.01-percent solution for 3 minutes. After a final rinse, the surface is viewed under an ordinary light microscope adapted for epifluorescence illumination.

The acridine orange binds to nucleic acids (DNA and RNA) found in living organisms. Under ultraviolet illumination, the acridine orange fluoresces (green for DNA, orange for RNA), making the organisms visible against a dark background.

In the rocket-booster study, sample stubs 0.5 inch (12.7 mm) in diameter were prepared to fit in either the scanning electron microscope or the epifluorescence microscope. The stubs were made from the same aluminum and steel alloys to be used in the booster rockets. They were coated with various primers, paints, and sealants. Glass-surfaced stubs were also included: Glass proved to be a good choice for cross-reference between tests because its fouling rate fell toward the high end of the range spanned by the other materials under test and because glass is smooth, easily cleaned, and free of fluorescence.

Samples were examined after exposures to seawater ranging from 2 hours to nearly 2 days at 1 m below the surface. Higher fouling rates were found in summer than in winter in apparent correlation with water temperature. Fouling rates were high for a polysulfide sealant, woven parachute nylon, and glass. However, all surfaces tested suffered significant fouling even in winter.

This work was done by R. R. Colwell of the University of Maryland for **Marshall Space Flight Center.** *For further information, Circle 84 on the TSP Request Card.*
MFS-25928

Books and Reports

These reports, studies, and handbooks are available from NASA as Technical Support Packages (TSP's) when a Request Card number is cited; otherwise they are available from the National Technical Information Service.

Experimental Ecosystems Sealed in Glass

Analogs of the Earth's biosphere survive in isolation for years.

A report now available describes an investigation of the dynamics of microbial ecosystems sealed in 1-liter flasks and exposed to Sunlight or artificial light for extended periods. Many of the organisms survived for more than 15 years. Such systems have primary productivity and quantum efficiencies comparable to estimates for Earth's ecosystems.

Material closure with sustained biological activity is not restricted to microbial systems but can be extended at least to crustacea and macroalgae. For example, crustacea to 14 mm in length have so far kept in synthetic brackish water with a variety of algae under absolute material closure for more than 3 years. Data reveal that such ecosystems cannot only persist but have biodynamics, chemodynamics, and thermodynamics that are measurable. These systems appear to offer a wide variety of potential miniature worlds that can closely model or depart from the world of the global biosphere and can potentially serve as experimental analogs of closed ecological life-support systems (CELSS) — the focus of a NASA program to develop life-support systems for extended human space travel and planetary colonization.

After material closure, divergences in observable species lists among separate systems occur more frequently than not. These changes are noted in both heterotrophic and autotrophic populations. In microbiological systems, measured O_2 pressure levels become asymptotic within about 60 days. The initial experiments indicate that with given masses of inorganic resources in materially-closed, energetically open ecosystems, no more than some maximum level of biological activity can be supported.

Measurements show that such ecosystems achieve an apparent quantum efficiency of 1.3 percent. Given sufficient metabolic diversity at closure, these systems are expected to continue biological activity with some balanced network of oxidative/reductive processes (balanced bioelemental cycling) indefinitely; i.e., so long as adequate radiant energy is provided and the systems are maintained within physical conditions tolerable by living organisms.

Phonoacoustic spectroscopy can be employed to generate a spectrum of flagellar and ciliary frequencies for the sealed organisms that might produce a rapid nonintrusive index of species diversity. In addition, an integrated phonoacoustogram could provide an indication of total biological activity. NMR spectrometry can measure the amount of adenosine triphosphate and guanosine triphosphate, again in a nonintrusive fashion. Various infrared remote-sensing devices are under development that might be applicable to the determination of entropy production by materially closed ecosystems.

This work was done by Joe A. Hanson of Caltech for **NASA's Jet Propulsion Laboratory.** *To obtain a copy of the report, Circle 85 on the TSP Request Card.*

Inquiries concerning rights for the commercial use of the technology described in the report should be addressed to the Patent Counsel, NASA Resident Office–JPL *[see page A5].* *Refer to NPO-15712.*

Computer Programs

These programs may be obtained at very reasonable cost from COSMIC, a facility sponsored by NASA to make new programs available to the public. For information on program price, size, and availability, circle the reference letter on the COSMIC Request Card in this issue.

Estimating Health Services Requirements

Population statistics are used to predict local hospital and physician demand.

In the computer program NOROCA, population statistics from the National Center for Health Statistics are used with a computational procedure to estimate health service utilization rates, physician demands (by specialty), and hospital bed demands (by type of service). The computational procedure is applicable to a health service area of any size and may even be used to estimate statewide demands for health services. The program provides planners with the capability to use existing data to estimate future physician and hospital bed demands.

Starting with a sample population statistic set derived from National Center for Health Statistics Health Interview Survey tapes, the relative frequency of population, age, and sex groups is calculated for the health service region of interest. Multiplying these statistics by the actual population of the hospital service area yields the estimated population to be served. The product of this estimated population and the health service utilization rate is adjusted to derive the estimated service demands.

To obtain age-group frequency by sex, the number of persons in each of five age groups, by sex, is divided by total population by sex. Age-group frequency is then used to yield the estimated population at risk by age and sex. Next, the hospital admission rates by diagnosis, age, and sex are calculated from previous hospital admissions per year. The estimated population at risk is then multiplied by the admission rates to obtain the estimated number of hospital admissions by diagnostic category, age, and sex.

The diagnostic categories include medical/surgical, obstetrics/gynecology, pediatrics, and psychiatry. The average number of physician visits is calculated for the categories of general practice, internal medicine, pediatrics, surgery, obstetrics/gynecology, and other. Various adjustments and undercount parameters may be applied to the estimate to account for out-of-area admissions, overnight hospitalization that does not require formal admission, and other bed and physician demands not included in the general statistics.

This program is written in MARK IV Release 5 and has been implemented on an IBM 370 with a central memory requirement of approximately 260K of 8-bit bytes. Data required to run this model include Health Interview Survey tapes from the National Center for Health Statistics. These tapes are not available from COSMIC and must be purchased from NCHS.

This program was written by Hosea M. Alexander of Caltech for **NASA's Jet Propulsion Laboratory.** *For further information, Circle aa on the COSMIC Request Card.*
NPO-14151

MiniBriefs describe NASA innovations and reports in an abbreviated format. Readers desiring additional information on these items should request the Technical Support Packages (TSP's), available in most cases, which can be obtained by using the TSP Request Card at the back of this issue.

Parameters Affecting Electrophoresis

The influences of particle size, concentration, and charge are discussed.

Various experimental approaches and problems facing successful continuous particle separation by electrophoresis are outlined in a short report. Results of particle-interaction studies indicate that a number of key factors yield predictable increases in electro-osmotic mobilities and separations.

A combination of coatings for the separation chamber of the continuous particle electrophoresis unit may result in osmotic flow that, based on theoretical calculations, yield maximum resolution of separation. Increasing the particle concentration linearly decreases the migration distances. Use of latexes of the same size but different mobilities would be very helpful in determining what effects particle size, concentration, and charge have on band-separation distance.

This work was done by J. W. Vanderhoff and F. J. Micale of Lehigh University for **Marshall Space Flight Center.** *To obtain a copy of the report, Circle 86 on the TSP Request Card.*
MFS-25593

Dialysis Extraction for Chromatography

Batch or continuous processing would be done in the field.

A proposed chromatographic-sample pretreatment by dialysis would detect traces of organic contaminants in water samples analyzed in the field, with minimal analysis equipment and minimal quantities of solvent. The aqueous sample solution is placed on one side of a dialysis bag or membrane while a nonpolar solvent such as dichloromethane is placed on the other side. Low levels of lipophilic, high-boiling-point organic compounds (for example, polychlorinated biphenyls, identified as carcinogens) readily dialyze into the solvent.

With a slow, uninterrupted flow of the sample or solvent or both, this pretreatment technique could enable the continuous chromatographic or other monitoring of pollution in water. The technique may also be of value wherever the aqueous sample and the solvent must not make direct contact.

This work was done by Vilhelm J. Jahnsen of Caltech for **NASA's Jet Propulsion Laboratory.** *For further information, Circle 87 on the TSP Request Card.*
NPO-15691

Mechanics

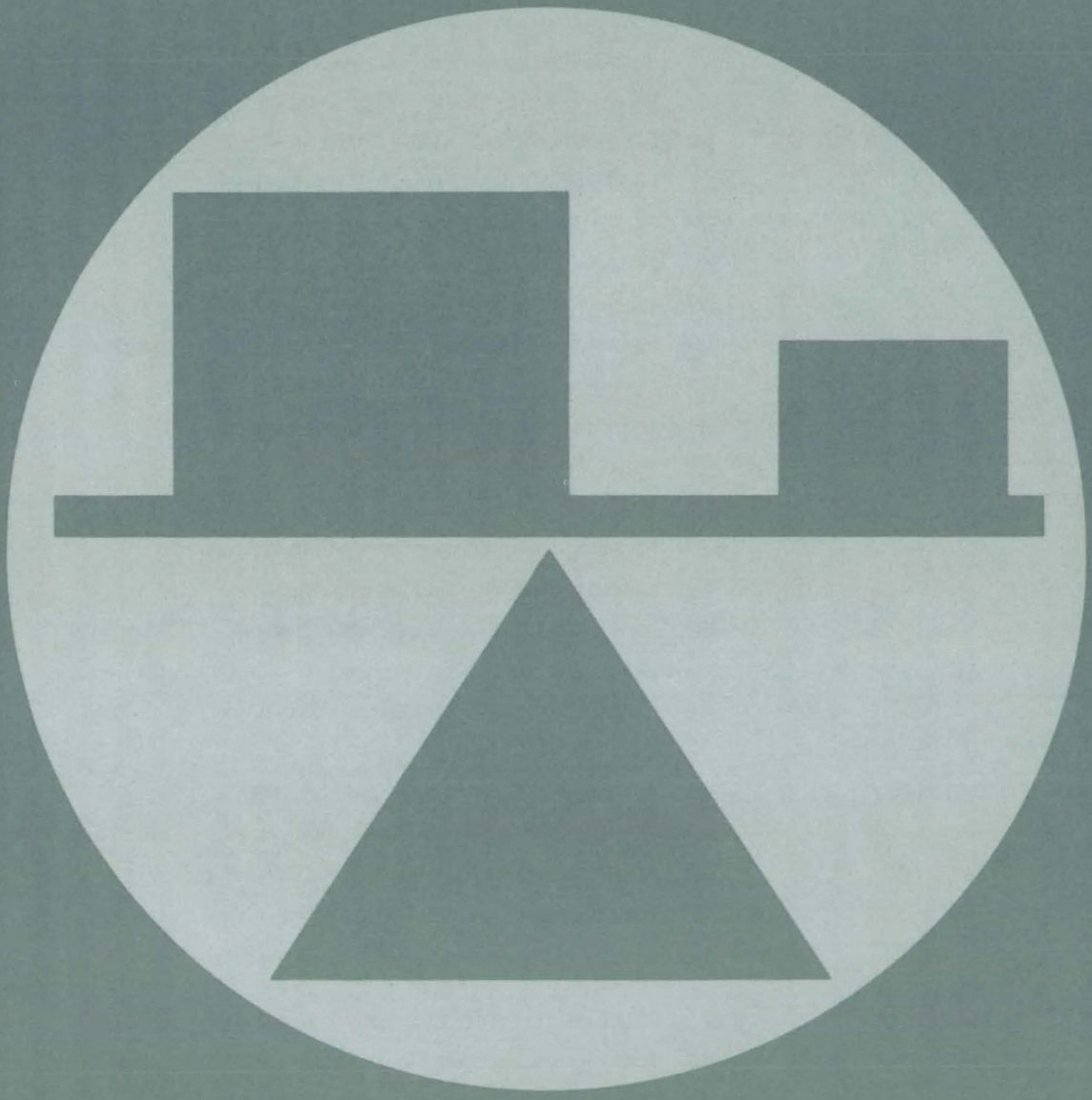

Hardware, Techniques, and Processes

Computer Programs

MiniBriefs

Temperature-Gradient Furnace for Solidification Experiments

Gradients are controllable from zero to 500° C/cm.

Marshall Space Flight Center, Alabama

A cylindrical furnace provides axial temperature profiles for material-processing experiments. Temperature gradients inside the central ceramic furnace tube can be varied locally from isothermal (zero gradient) to 500° C per centimeter by controlling the electric power to five independent heating elements and a heat-removal plate.

The furnace is made up of eight zones. A zone is heated, cooled, or passive, depending on the required temperature profile (see figure).

Zone 1, the hot guard heater, makes up for the heat loss at the end of the hot zone. It can be used to extend the hot zone or, with its temperature raised above that of the hot zone, to provide a slight positive temperature gradient beyond the strictly defined end of the hot zone. The hot guard heater is 1 inch (2.54 centimeters) long and operates at high power.

Zone 2, the hot zone, heats the material specimen to the proper starting temperature and maintains it there. In steady-state operation this zone draws little power — just enough to make up for heat losses. The zone is 8 inches (20.3 centimeters) long.

Zone 3, the hot passive zone, generates no heat. Instead, it allows the point at which the temperature profile starts to drop sharply to extend closer to the gradient zone without an excessive temperature in the hot zone. The hot passive zone is 1 inch (2.54 centimeters) long.

Zone 4, the booster heater, works in conjunction with the hot passive zone to extend the hot zone closer to the gradient zone so that the gradient can be made as steep as possible. The booster heater is only 0.135 inch (0.343 centimeter) long. It operates at a temperature higher than that of the other heaters and provides a large portion of the total energy required by the furnace.

The large thermal gradient occurs in zone 5. In this zone, there is no heater and the central tube is well insulated to minimize the axial heat flow. This makes it possible to have large axial thermal gradients and planar isothermal surfaces perpendicular to the axis. After heating in the hot zone, the specimen is moved to this zone for high-gradient experiments.

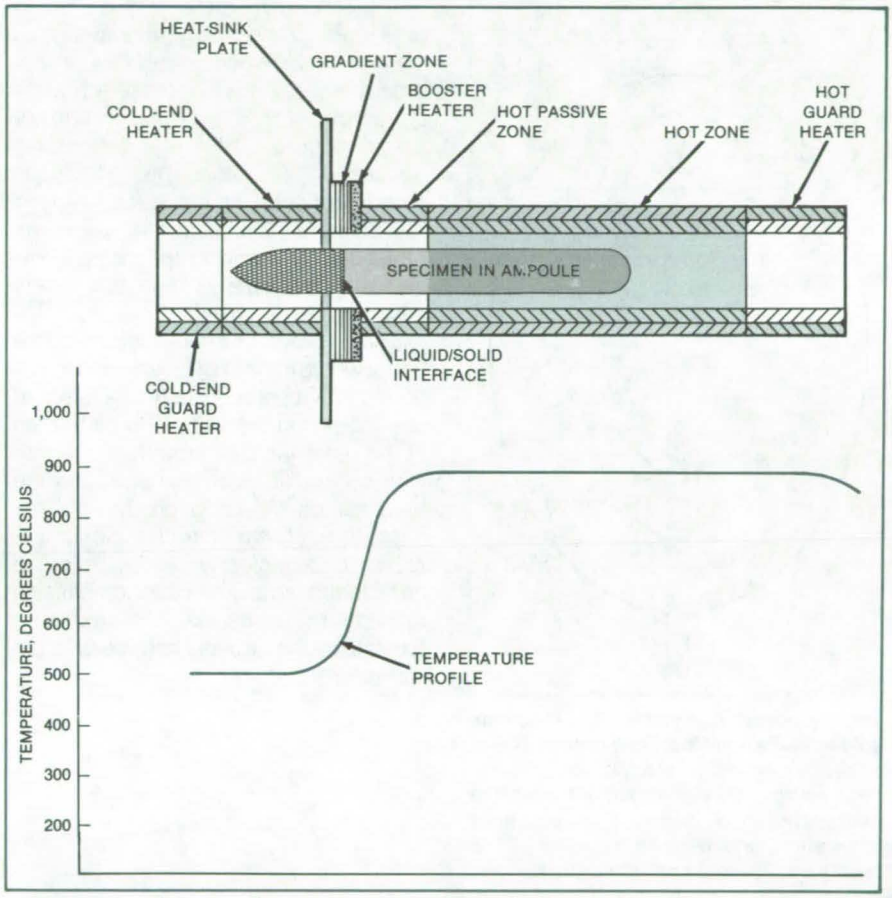

A **Typical Temperature Profile** is superimposed on a partial cross section of the furnace. The steepness of the gradient can be varied by adjusting the flow of energy to and from the different zones of the furnace. The specimen is placed in an ampoule that is moved inside the ceramic tube according to the needs of the experiment.

Zone 6, the heat-sink plate, extracts heat from the specimen and transfers it to a liquid coolant. It is 0.25 inch (0.635 centimeter) long.

Zone 7, the cold-end heater, works in conjunction with the heat-sink plate to establish the temperature of the relatively cold end of the furnace. The cold-end heater is 5 inches (12.7 centimeters) long.

Zone 8, the cold-end guard heater, adds heat to reduce the axial heat loss from the cold-end heater. It extends the isothermal length of the cold-end heater. It is 1 inch (2.54 centimeters) long.

An important feature of the furnace is that its zones are modular, allowing it to be assembled in different configurations. Since the end flanges of the major segments — such as hot section, heat-sink plate, and end caps — are identical, they can be interchanged. For example, two hot sections can be joined to make a long isothermal zone.

This work was done by Billy R. Aldrich and William D. Whitt of **Marshall Space Flight Center.** *For further information, Circle 90 on the TSP Request Card.*

This invention is owned by NASA, and a patent application has been filed. Inquiries concerning nonexclusive or exclusive license for its commercial development should be addressed to the Patent Counsel, Marshall Space Flight Center [see page A5]. Refer to MFS-25963.

Improved Ellipsoidal Radiation Furnace

A spherical reflector around the heat source increases efficiency and minimizes power requirements.

Marshall Space Flight Center, Alabama

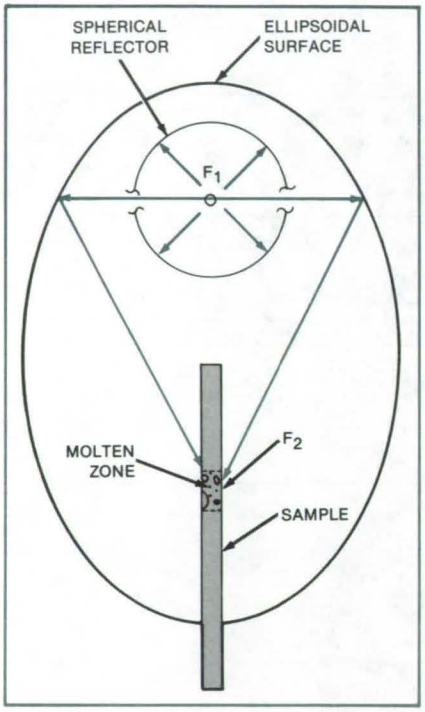

The proposed **Axisymmetric Monoellipsoidal Radiation-Heating Furnace** has a spherical reflector around the "point" heat source. This arrangement uses the heat efficiently, reduces waste heat generation, and permits full view of the specimen. The heat reflected back to the source helps to maintain the equilibrium temperature with much less power input.

A proposed radiation furnace would heat a small zone of a cylindrical sample while reducing waste heat. It is an improvement over ellipsoidal furnaces developed for the zone growth of semiconductors at NASA's Marshall Space Flight Center. These furnaces have a reflector shield placed around the sample. The reflector prevents radiation from striking the sample, except for a small band of light that enters a window in the shield.

The improved furnace shown in the figure would consist of an ellipsoid with a "point" heat source, such as a lamp, at one focus and the sample to be heated at the other focus. A spherical reflector with a circular slit would surround the heat source. All radiation that did not pass through the circular slit in the spherical reflector would be reflected back to the lamp. The radiation passing through the spherical slit would be focused by the ellipsoid surface onto the sample.

The spherical reflector reconcentrates the heat radiation that is normally lost as waste heat. Since most of the heat radiation is reflected back onto the heat lamp, the power could be greatly reduced; yet the lamp would run at maximum temperature. This would result in power saving and less wasted heat.

In addition, no reflector would be required around the sample, and it would be possible to observe the sample as it is being processed. Since only a small portion of the ellipsoid is used, a much smaller ellipsoidal surface is required. This would reduce the total weight of the furnace, resulting also in cost savings.

This work was done by Edwin C. Ethridge of **Marshall Space Flight Center.** *No further documentation is available.*

Inquiries concerning rights for the commercial use of this invention should be addressed to the Patent Counsel, Marshall Space Flight Center [see page page A5]. Refer to MFS-25933.

Double Linear Damage Rule for Fatigue Analysis

Crack initiation and propagation are predicted for cyclic loads.

Lewis Research Center, Cleveland, Ohio

The Double Linear Damage Rule (DLDR) is a method for use by structural designers to determine fatigue-crack-initiation life when a structure is subjected to unsteady, variable-amplitude cyclic loadings. Using the method a designer can calculate, in advance of service, just how many loading cycles can be imposed on a structural component before a macroscopic crack initiates.

From a knowledge of the magnitude of the unsteady loading spectrum to be applied to the component, and a knowledge of the constant-amplitude fatigue resistance of the material, the DLDR predicts the synergistic life-degrading interactions of the high- and low-loading levels. A designer can assess the severity of any complex service-loading cycle and thereby arrive at the most efficient design for resisting cyclic failures for the particular problem at hand.

The DLDR is a significant technical advance in the field of fatigue life prediction. It has a physically correct basis, does not require that material tests be conducted to evaluate constants in the DLDR equation, is extremely simple to apply, and is considerably more accurate than the overly simplified Linear Damage Rule that is used extensively in industry today. Interaction between high- and low-loading levels can produce reductions in cyclic lifetime of a factor of 10 or more under extreme circumstances. In such cases the Linear Damage Rule would be grossly unconservative, while the DLDR would predict a much more accurate lifetime.

The DLDR name derives from the basis of the method — the initiation of a macroscopic crack can be partitioned into two phases, microcrack initiation and microcrack propagation. A linear damage rule is then applied serially to each phase. Hence, a nonlinear problem is represented by simpler double-linear functions.

To date, the DLDR has been applied to laboratory specimen results for many different alloys with a high degree of success. The approach eventually will be used in the design of high-performance systems, and likely will be incorporated into design handbooks and codes.

This work was done by G. R. Halford of **Lewis Research Center** *and S. S. Manson of Case Western Reserve University. Further information may be found in NASA TM-81517 [N80-23684/NSP], "Practical Implementation of the Double Linear Damage Rule and Damage Curve Approach for Treating Cumulative Fatigue Damage" [$8.50]. A copy may be purchased [prepayment required] from the National Technical Information Service, Springfield, Virginia 22161.*
LEW-14058

Eddy-Current Inspection of Ball Bearings

A custom eddy-current probe locates surface anomalies.

Marshall Space Flight Center, Alabama

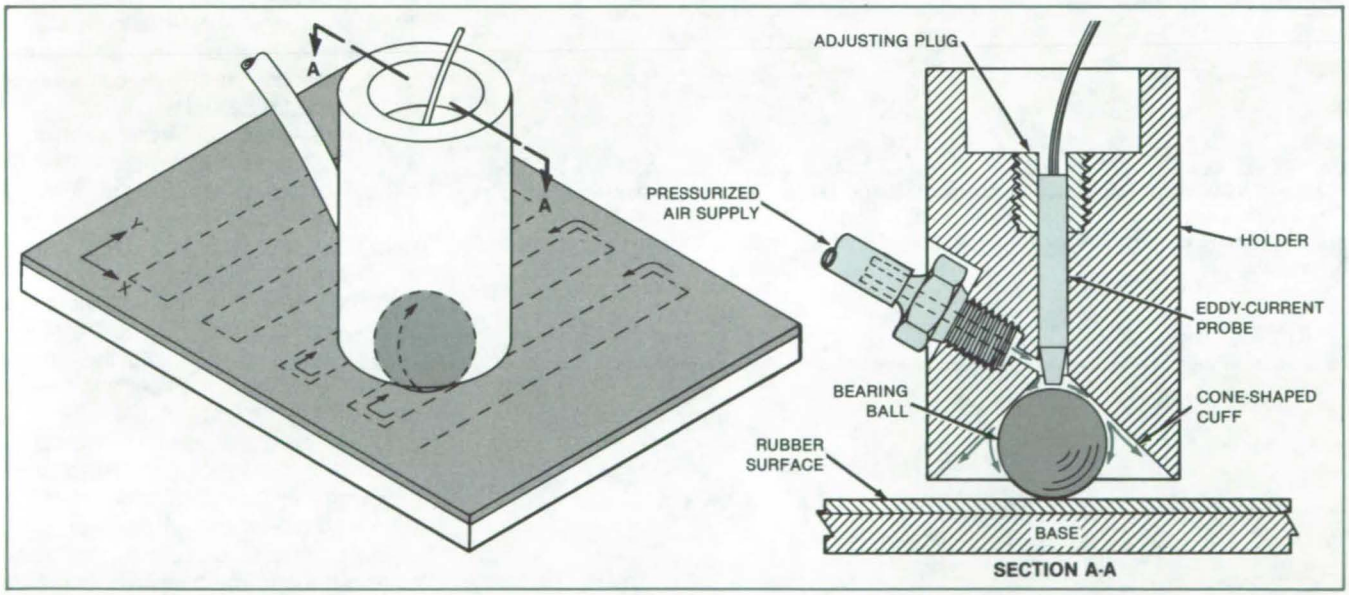

In the new Bearing-Ball Inspection Apparatus, an eddy-current probe inspects the ball for defects. The low-friction air cushion within the cone allows the ball to roll easily.

An eddy-current probe reliably detects surface and near-surface cracks, voids, and material anomalies in bearing balls or other spherical objects. Because of the small size of the bearing balls and the minute nature of the defects, an accurate inspection of the entire ball surface has previously been a problem.

The new inspection apparatus shown in the figure includes a nonabrasive high-friction base and a ballholder with an eddy-current probe mounted on one side. A recess in the holder in the shape of an inverted cone accommodates different ball sizes.

During inspection, the probe is normally spaced about 0.08 mm from a ball. A regulated supply introduces pressurized air at about 1 psi (6.9×10^3 N/m^2) to reduce the friction between the surface of the cone-shaped cup and the ball. When the holder is moved over the base in a predetermined pattern, the eddy-current probe inspects the entire surface of the ball. An X-Y scanner can be used to move the holder, or the holder can be moved manually over a pattern imprinted on the surface of the base.

Defects in the ball surface detected by the probe can be displayed on a CRT and recorded on a strip-chart recorder.

This work was done by B. F. Bankston of **Marshall Space Flight Center.** *For further information, Circle 91 on the TSP Request Card.*
MFS-25833

Surface-Streamline Flow Visualization

Streaks in an array of ink dots show key flow characteristics.

Lewis Research Center, Cleveland, Ohio

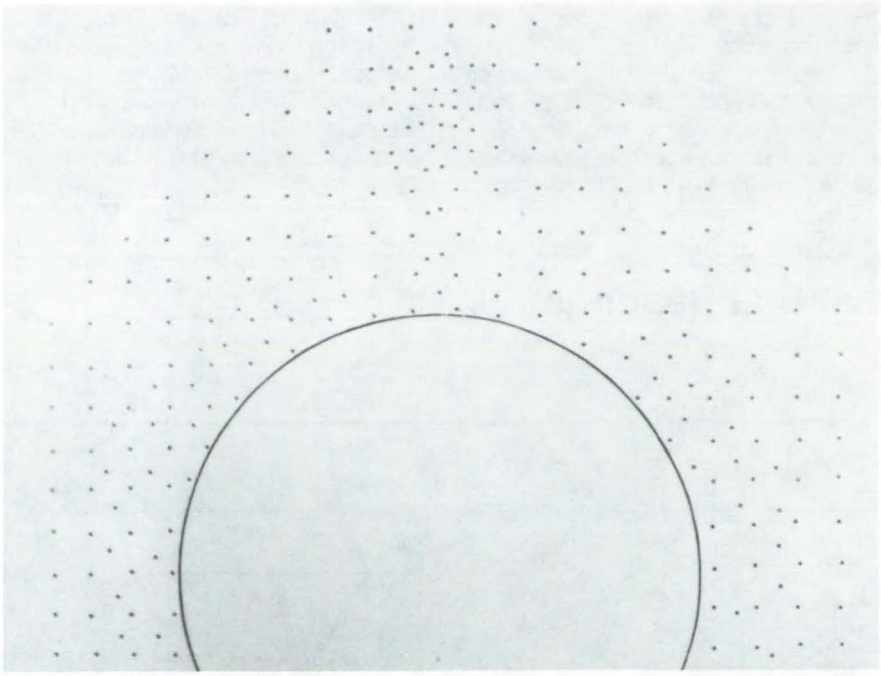

Figure 1. A **Matrix of Ink Dots** covers the matte surface of a polyester drafting film. The film is placed against the wind-tunnel wall, with the cylinder installed at the position shown. A layer of methyl salicylate (oil of wintergreen) is then sprayed over the dotted area.

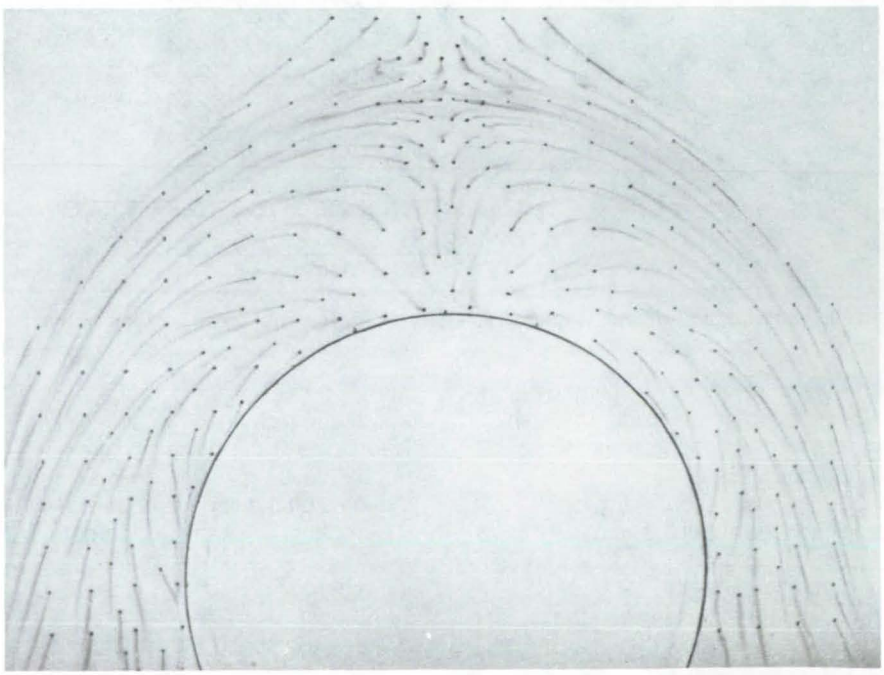

Figure 2. The **Ink-Dot Streaklines** show several characteristics of the flow, including the primary saddle point of separation, the primary horseshoe vortex, and a smaller vortex at the cylinder/endwall junction.

A new surface-streamline flow-visualization technique has been developed that is suitable for use in low-speed wind tunnels or other low-speed gas flows. The technique provides a permanent record of ink traces that show surface streamline direction and shape. The new technique is suited to the low-speed (up to a hundred meters per second) flow of a gas; e.g., flow over surface in a low-speed wind tunnel.

The ability to visualize the fluid flow near a solid surface is a valuable experimental technique. When properly interpreted, the flow visualization can provide an experimenter with a great deal of information about the flow fairly simply and in a relatively short period of time. There are a number of techniques available, all with their particular advantages and limitations. This new technique is more simple to use and is more accurate.

To more fully describe this technique, an endwall surface flow visualization of a horseshoe vortex system formed around the base of a cylinder by a separating turbulent boundary layer is used as an example. The cylinder (0.304 m high and 0.16 m diameter) was mounted in a low-speed wind tunnel (0.304 by 1.83 m test section) along the tunnel centerline between the floor and ceiling (endwalls) of the test section.

Figure 1 is a photograph of the matte side of a polyester drafting film (0.008 cm thick) on which the base of the cylinder has been traced. A matrix of ink dots is marked around the circles to act as flow tracers. The dots are made with a felt-tipped pen containing permanent (water insoluble) blue ink. Depending on the type of flow to be visualized, a dot is made with one application of the felt-tipped pen, or several applications with drying in between each application. In any event, the dots are not protuberances but are smooth to the touch.

The drafting film is then securely fastened to the lower horizontal endwall of the wind tunnel (the floor) using double-sided adhesive tape or rubber cement. The cylinder is mounted in place on top of the drafting film with the ink-dot matrix on the upstream side of the cylinder.

Just before the wind tunnel is turned on, the dotted area of the drafting film is sprayed with oil of wintergreen (synthetic methyl salicylate), so that the dotted area is completely covered with a thin but continuous liquid film. A small, handheld aerosol sprayer was used, but an artist's air brush would also work. It is important that the dotted area be covered with a continuous film of oil, for a discontinous film can give erroneous results.

After spraying, the matrix of dots becomes "blurred" as the ink dots dissolve and diffuse into the film of oil of wintergreen. The wind tunnel is then turned on and quickly brought up to operating conditions. The turbulent boundary layer on the tunnel floor separates in front of the base of the cylinder to form a horseshoe vortex system.

The oil of wintergreen film is then acted upon by wall/shear forces and flows in response to them. The ink that has dissolved into the oil of wintergreen film now acts as a tracer, with each dot acting as a stationary source of ink, producing a streakline. In a few minutes the oil of wintergreen has evaporated or has been moved downstream, leaving a permanent picture of ink traces of the surface streaklines on the drafting film, as shown in Figure 2.

The streaklines in Figure 2 clearly show the primary saddle point of separation (a point of zero wall/shear stress), the primary horseshoe vortex with one sense of rotation, and a smaller countervortex with an opposite sense of rotation at the cylinder/endwall junction. The flow visualization picture is much clearer than those obtained by most conventional techniques.

Since the oil of wintergreen is colorless, different colored dots can be used in different areas to produce a picture that clearly shows where surface flows originated. This is particularly useful when several surfaces are being tested simultaneously.

If care is taken to spray a thin and continuous oil film, the technique can be made to work on vertical and downward-facing surfaces if the wind tunnel is quickly turned on after oil film application.

The results of the new technique were compared with those obtained from a conventional flow visualization technique. Good agreement was found between the two, with the new technique appearing to give more accurate surface streamlines.

This work was done by L. S. Langston and M. T. Boyle of the University of Connecticut for **Lewis Research Center.** *For further information, Circle 92 on the TSP Request Card.*
LEW-13875

Structural Turnbuckle Bears Compressive or Tensile Loads

The length of a structural member is readily adjusted.

Marshall Space Flight Center, Alabama

A proposed column-length adjuster is based on the turnbuckle principle. The new device differs from the conventional turnbuckle in that it is more stable under compressive loads and requires less clearance for installation. Like the turnbuckle, it is readily accessible for adjustments.

The device consists of an internally and externally threaded bushing, a threaded housing, and a threaded rod (see figure). The housing is attached to one part of a structure, and the threaded rod is attached to the other part of the structure.

Normally, the internal and external threads are oppositely handed for relatively-coarse length adjustments. In that case, rotating the bushing through one turn adjusts the length of the device by an amount equal to the sum of the pitches of the internal and external threads. Finer adjustments can be made if the internal and external threads on the bushing are both left-handed or both right-handed but of slightly different pitch: The length adjustment for one turn is then the difference of the thread pitches.

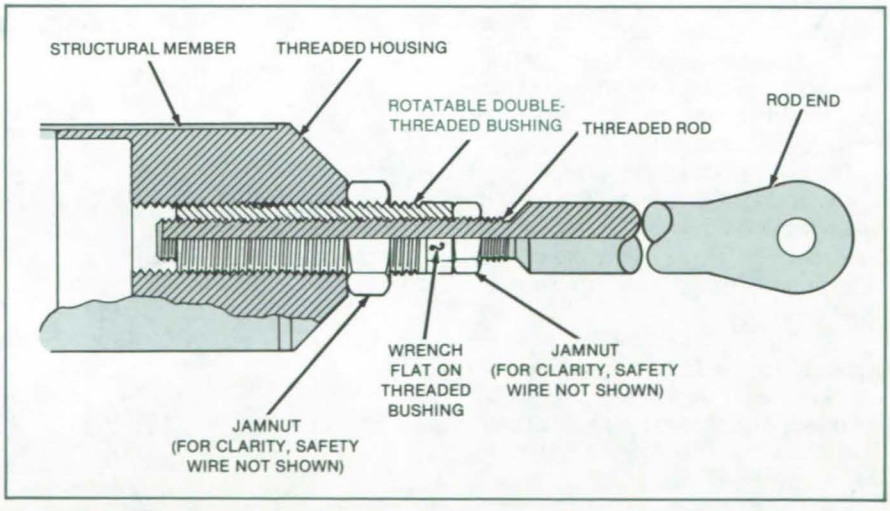

Turning the Double-Threaded Bushing contracts or extends the rod in relation to the housing. Once adjusted, the bushing is secured with jamnuts.

With its more-direct load path and shorter overall length, the device makes a stiffer structural member than does a conventional turnbuckle. The device can be used for axially loaded members requiring length adjustment during installation.

This work was done by William A. Bateman and Clifford H. Lang of Rockwell International Corp. for **Marshall Space Flight Center.** *No further documentation is available.*
MFS-25939

Beam Window for Pressure Chambers

Window resists products of combustion experiments.

Marshall Space Flight Center, Alabama

A sodium chloride window seals over chamber pressures from 0.1 to 13.8 MPa while absorbing minimal energy from a CO_2 laser beam that passes through it into the chamber. The window is inexpensive and easily replaceable.

The chamber is used for combustion experiments in an oxygen atmosphere. The window resists clouding by smoke particles produced in the experiments. It also resists damage by droplets of molten material ejected from the combustion zone.

The window-mounting assembly is placed in the top plate of the pressure chamber. The assembly consists of a seal-retaining ring, a spring- and pressure-energized seal, a backup ring, an upper seal-retaining ring, and a retaining plate (see figure). The window and a thrust washer fit inside the assembly. The thrust washer, composed of glass-fiber-filled polytetrafluoroethylene (PTFE), cold-flows under pressure to conform to the window surface: It therefore prevents excessive point stresses from acting on the load-bearing surface of the window. The lower retaining ring prevents excessive movement of the seal when the chamber is evacuated.

The NaCl window piece is 25.4 mm in diameter and 20 mm thick. The clear diameter of the window when mounted is 12.7 mm. The window therefore can accommodate easily a 9-mm-diameter laser beam.

Thus far, the window has shown no signs of failure, even at points where obvious surface damage has occurred. The window is expected to be usable at pressures well beyond the maximum for which it was designed.

This work was done by James W. Bransford and John G. Austin, Jr., of the National Bureau of Standards for **Marshall Space Flight Center.** *For further information, Circle 93 on the TSP Request Card.*

Inquiries concerning rights for the commercial use of this invention should be addressed to the Patent Counsel, Marshall Space Flight Center [see page A5]. *Refer to MFS-25961.*

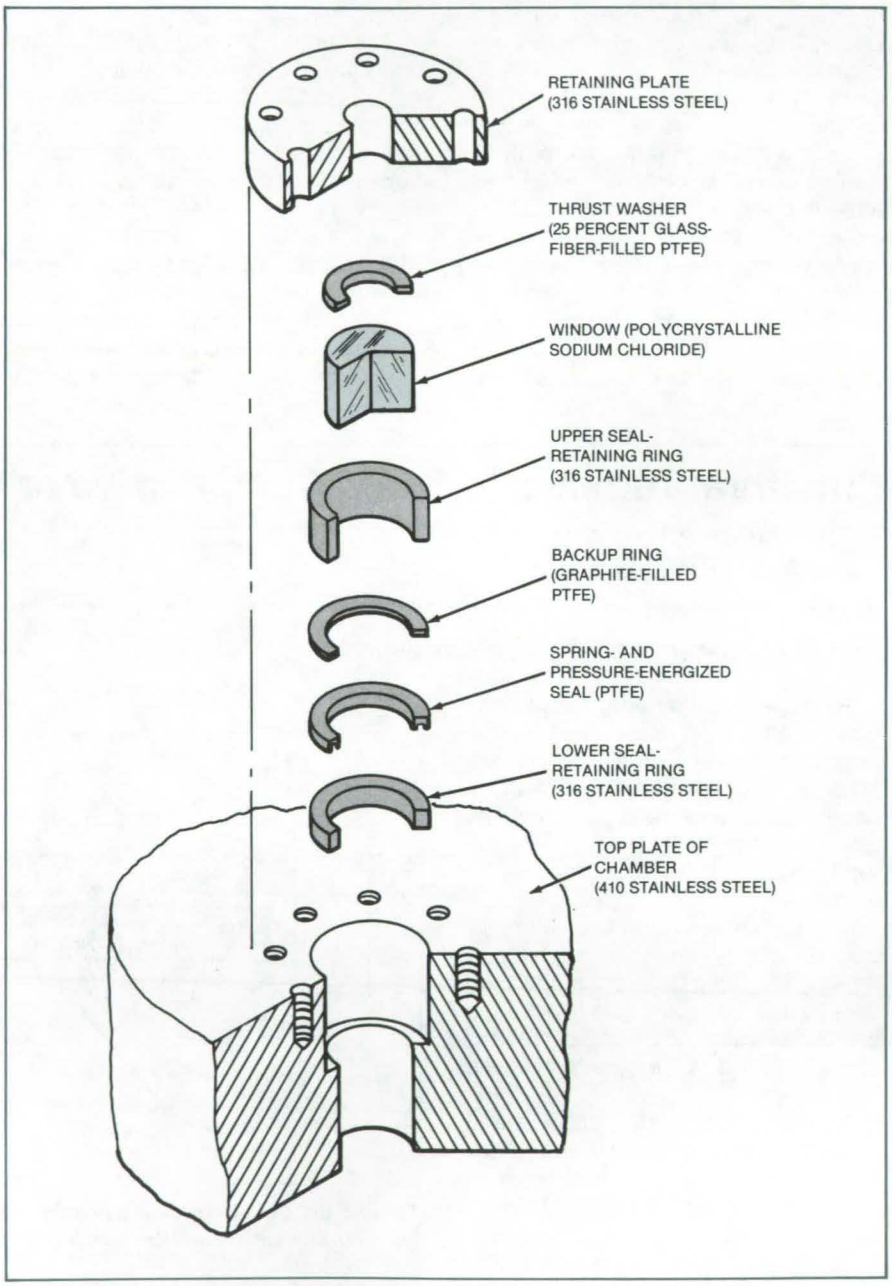

This **High-Pressure Window of Polycrystalline NaCl** transmits a laser beam at a wavelength of 10.6 μm. Despite its relatively low mechanical strength and hygroscopic nature, the sodium chloride window material has performed well.

Fabricating Thin-Shell Heat-Transfer Models

Freestanding shells have been produced for experimental aerodynamic-heating tests.

Langley Research Center, Hampton, Virginia

Heat-transfer effects from aerodynamic heating generated in the intertile gaps of the Space Shuttle orbiter thermal-protection system can be studied using freestanding shells as models. Such models have become available recently through a new fabrication technique that is an extension of earlier techniques developed at the Johnson Space Center. The result is a 6- by 6- by 2.5-in. (15- by 15- by 6.4-cm) freestanding shell, 0.025 in. (0.64 mm) thick, instrumented with single-wire thermocouples. This fabrication is not limited to any particular geometry and results in a seamless heat-transfer model.

The heat-transfer shells require several steps and several precise molds. First, interlocking aluminum male and female molds are fabricated. Holes for thermocouples are drilled through the male mold at the desired locations. Wires having the same diameter as the thermocouple wire are then placed through these holes in the male mold flush to the female mold.

Epoxy that has been exposed to a vacuum to remove air bubbles is poured between the male and female molds to form a thin female mold. Once the mold is cured, the wires are removed and the aluminum molds separated. Thermocouple wires are then fed from the inside of the mold through the cast holes and anchored on the outside. The mold is placed in a vacuum furnace for 24 hours prior to casting a mandrel in the mold. The mandrel is then cooled in a furnace at a very slow rate. Once cooled, the mold is removed, leaving a smooth mandrel with thermocouple wires protruding from the surface.

Initially, the mandrel is sealed with a copper strike and a nickel-alloy strike; then the nickel alloy is plated to one-half of the desired shell-wall thickness as shown in the diagram insert. The protruding thermocouple wires are clipped and polished flush with the surface. The surface is reactivated, and the nickel-alloy plating is completed to obtain the prescribed wall thickness. Finally, the mandrel is removed by melting, and the nickel-alloy shell is cleaned in an acid solution followed by sandblasting.

Two thin-shell heat-transfer models have been fabricated to simulate a Shuttle tile, each having 256 single-wire thermocouples. The heat-transfer tile model was installed in an array of other simulated Shuttle tiles and successfully tested in the 8-Foot High Temperature Tunnel.

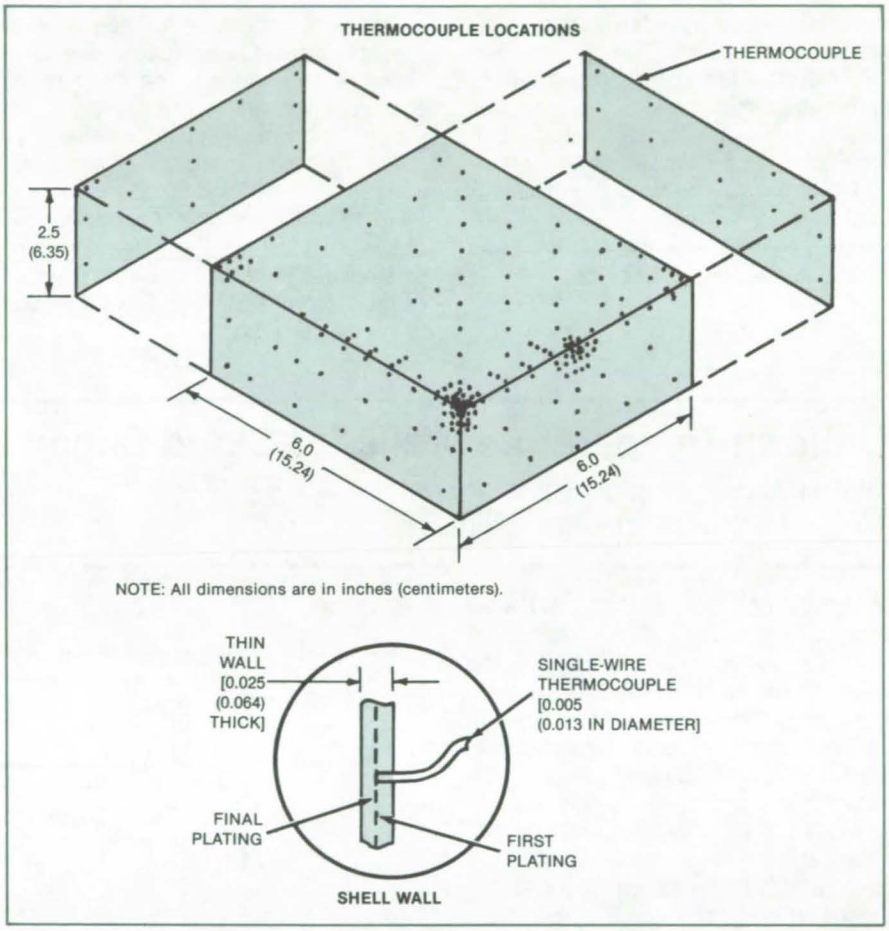

A **Freestanding Shell** with wall thickness of 0.025 in. (0.64 mm) is used as a model to obtain heat-transfer effects on Space Shuttle tiles. Earlier models were very small and not freestanding.

This work was done by Don E. Avery, Gary K. Ballard, and Maywood L. Wilson of **Langley Research Center** *and John H. Allen, Sr., of Johnson Space Center. For further information, Circle 94 on the TSP Request Card.*
LAR-13087

Flexible Heat Pipe

A narrow tube carries 10 watts or more to moving parts.

Goddard Space Flight Center, Greenbelt, Maryland

A flexible heat pipe carries heat to articulating machinery. Such a pipe can conduct heat to the moving segment of a thermal switch, for example.

The heat pipe is 12 inches (30.5 cm) long and has a diameter of 0.312 inch (7.92 mm). It can be bent to a minimum radius of 2.5 inches (6.35 cm). Its tapered evaporator and condenser ends plug into mating copper blocks.

The flexible section is made of 321 stainless-steel tubing (Cajon Flexible Tubing or equivalent). The evaporator and condenser are made of oxygen-free copper. The working fluid is methanol.

The heat pipe operates at temperatures between 20° and 50° C and carries 10 to 16 watts at a typical conductance of 1 watt per Celsius degree temperature difference. The conductance at 16 watts ranges from 0.97 W/°C at 20° C to 1.60 W/°C at 50° C.

This work was done by Walter B. Bienert and David A. Wolf of Dynatherm Corp. for **Goddard Space Flight Center.** *No further documentation is available.*

This invention is owned by NASA, and a patent application has been filed. Inquiries concerning nonexclusive or exclusive license for its commercial development should be addressed to the Patent Counsel, Goddard Space Flight Center [see page A5]. *Refer to GSC-12864.*

Uniform-Temperature Walls for Cloud Chambers

Flat heat pipes rapidly transfer heat to and from experimental volumes.

Marshall Space Flight Center, Alabama

Flat-plate heat pipes are used as the walls of spaceborne atmospheric cloud chambers. On Earth, they might find use as isothermal floors for environmental test chambers. The heat pipes offer the advantages of flat walls, low thermal mass, vibration resistance, and strength. They allow precise control of the temperature in the volumes they enclose, resulting in uniform wall temperature.

The inner wall of the experimental volume wall is called the "critical surface." A critical surface is divided into zones according to the degree of required temperature uniformity. The temperature of zone 1 is controlled within ±0.01° C, that of zone 2 within ±0.1° C, and that of zone 3 within ±1.0° C.

An envelope of thin stainless steel encloses the vapor chamber (see figure). Adjacent to the critical surface is a heat-pipe wick consisting of a single layer of diffusion-bonded, 150-mesh (sieve opening 0.104 mm, wire diameter 0.066 mm), stainless-steel screen. The interior of the vapor chamber is bridged by studs 0.125-in. (3.2-mm) in diameter, wrapped with 120-mesh (opening 0.125 mm, wire diameter about 0.09 mm) sock wick. The studs are in an array 1 inch (2.54 cm) square. They provide strength as well as a transport medium for the working fluid

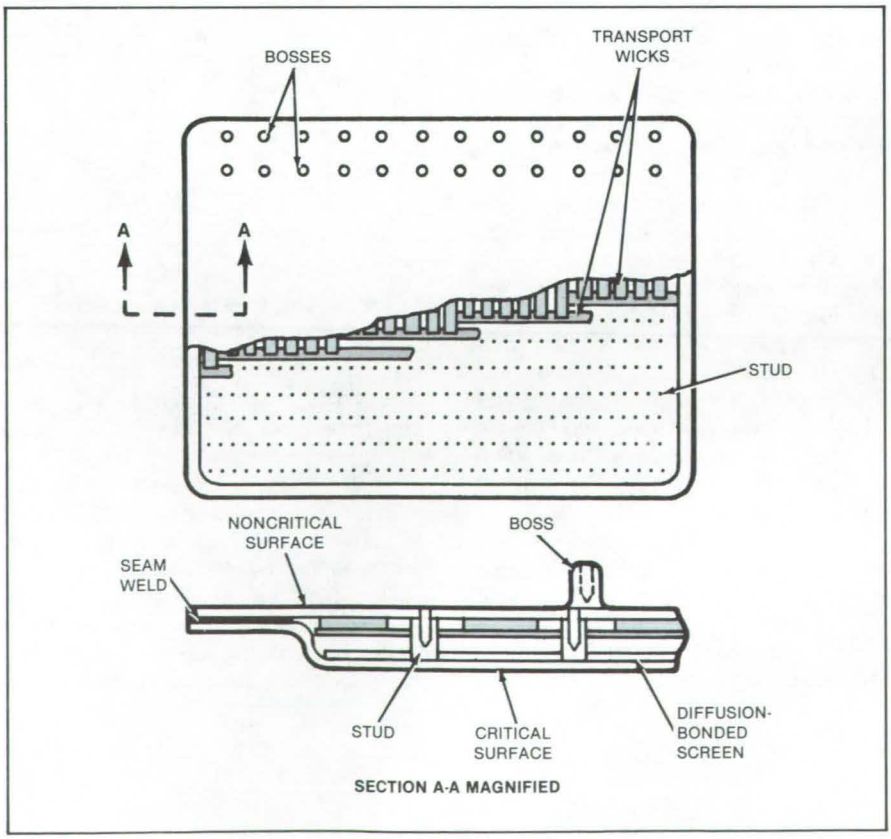

A **Heat-Pipe Vapor Chamber** carries heat to and from thermoelectric modules. The critical surface can act as either an evaporator or a condenser in cloud-physics experiments.

between the critical and noncritical surfaces.

The noncritical surface is covered with a layer of coarse-mesh wicks to provide both liquid transport and reservoir capacity for working-fluid expansion. Wells for temperature sensors are drilled through selected studs from the outside toward the critical surface.

Thermoelectric modules along one edge of the chamber control temperature by adding or removing heat. The wicks provide side-to-side heat-transport capacity for adequate working-fluid distribution between the critical surface and the thermoelectric modules. The modules also act with a linear heater on the opposite edge of the vapor chamber to sweep noncondensable gas to harmless areas under the modules.

Methanol was selected as the working fluid for its favorable thermal characteristics and its low vapor pressure in the operating-temperature range of -25° to +30° C. The stainless-steel, all-welded construction of the vapor chamber is strong and is compatible with the working fluid.

Vapor chambers constructed thus far have been 1 cm thick, up to 44 cm wide, and up to 72 cm long. They have masses of about 2.8 g per cm^2 of wall area.

This work was done by G. L. Fleischman of Hughes Aircraft Co. for **Marshall Space Flight Center.** *For further information, Circle 95 on the TSP Request Card.*
MFS-25931

Energy-Absorbing Airframes for General Aviation

The fuselage subfloor collapses under crash impact.

Langley Research Center, Hampton, Virginia

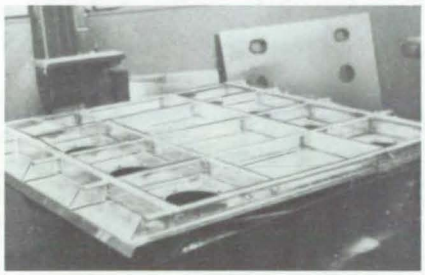

STRUCTURAL FLOOR

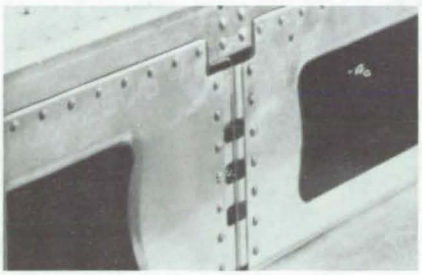

NOTCHED CORNERS

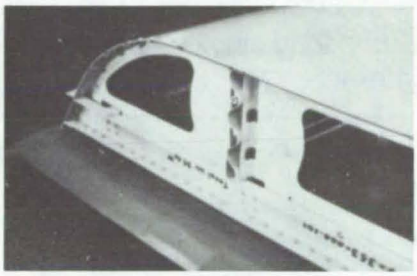

CORRUGATED BEAMS
NOTCHED CORNERS

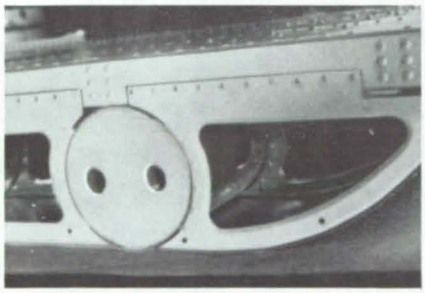

FOAM-FILLED CYLINDERS

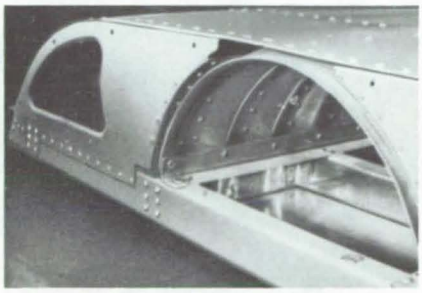

CORRUGATED HALF SHELL

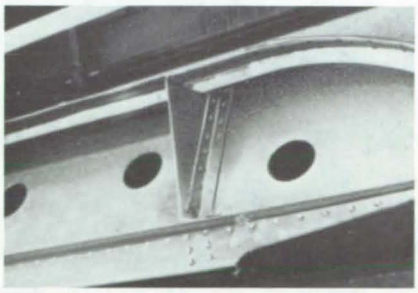

CANTED BULKHEADS

Energy-Absorbing Subfloors reduce the forces transmitted to people inside the aircraft.

A promising concept for protecting people in lightweight airplane crashes involves redesigning the area between the interior floor and the outer skin of the airplane belly to create a subfloor that would be strong enough to bear the stresses of flight but that would crush under the force of impact. The general configuration of the lower fuselage section consists of two major areas: the first, a strong structural floor, strong enough to retain the occupant seats without breaking up, heaving, or decreasing the cabin volume; the second, an energy-absorbing section or crush zone to control the load application to the strong floor.

Several concepts were evaluated, and five were selected and designed as lower fuselage sections that could be tested in NASA's crash-testing program. The structural floor for each concept was identically the same. The structural floor and five energy-absorbing subfloors are shown in the photograph inserts:

1. The *Notched Corner* concept incorporates conventional metal airframe structure with sheet-metal skins, beams, frames, and stringers. The shear clips that tie the beams to the frame members have been struc-

(continued on next page)

turally tailored to reduce their column stiffness and to promote an accordion-style buckling mode for the beams and frame members during the crush stroke.

2. The *Corrugated Beam* concept resembles conventional airframe structure with sheet-metal skins, beams, frames, and stringers except that the beam web material has been longitudinally corrugated to promote controlled collapse during the crush stroke. Notched-corner shear clips are also incorporated in this configuration.
3. The *Foam-Filled Cylinder* concept uses two longitudinal cylinders for primary fore/aft structure. The cylinders are filled with PVC foam material appropriately vented for absorbing energy. The cylinders and outboard frames support the exterior skin.
4. The *Corrugated Half Shell* concept differs completely from conventional structure. The primary fore/aft structural member resembles one-half of a large corrugated sewer pipe. It and outboard frames support the exterior skin.
5. The *Canted Bulkhead* concept incorporates conventional metal airframe structure with sheet-metal skins, beams, frames, and stringers except that all frames are canted at an angle of 30° from vertical to promote collapse during the crush stroke.

Experimental and analytical results indicate that all five concepts perform well; the upper floor remains structurally intact whereas the crush zone collapses under essentially constant load. The unmodified subfloor structure, under the same test conditions, produces undesirably high loads with minimal crush and with the loss of structural integrity.

This work was done by Huey D. Carden and Robert J. Hayduk of **Langley Research Center** *and J. D. Cronkhite and V. L. Berry of Bell Helicopter Textron, Inc. Further information may be found in NASA CR-3603 [N82-33735/NSP], "Crashworthy Airframe Design Concept — Fabrication and Testing" [$19]. A copy may be purchased [prepayment required] from the National Technical Information Service, Springfield, Virginia 22161.*
LAR-12808

Interferometer Detects Acoustic Emissions in Composites

Embedded single-mode optical fibers sample internal-stress fields directly.

Langley Research Center, Hampton, Virginia

Acoustic emission in prestressed composite panels has been detected using embedded single-mode optical fibers. A statically loaded composite matrix emits pulsed ultrasonic waves, which mechanically modulate the embedded fiber and phase-modulate the transmitted optical field. This modulation, detected by optical interferometry and Fourier optical processing, is converted to an electronic signal proportional to the acoustic field amplitude integated along the length of the fiber embedded in the specimen.

Previous acoustic-emission detectors relied on surface measurements, using piezoelectric or other conventional transducers. Internal stress-field transients were inferred from measurements of surface displacements. However, these transducers mechanically load the sample and scatter and reflect the acoustic signal. They also have limited frequency response.

In the optical technique, the embedded fibers sample the internal stress fields directly. Wave motion therefore is not inferred from surface motions, and surface loading is eliminated.

The sensitivity of the technique is comparable to that of standard Michelson and differential acoustic/optic interferometers. In addition, the resolution of the interferometer is restricted only by the fiber diameter, eliminating the time-bandwidth and spatial resolution problems associated with pulsed acoustic techniques.

The fiber-sensing technique may be used for measurements of both high- and low-frequency CW acoustic fields as well as high-frequency transients. The system lends itself to absolute calibration. Because the optical fibers can be embedded during fabrication of the composite, the test sample is immediately available for evaluation.

The interferometer (see figure) uses a 0.5-mW adaptively-stabilized He/Ne laser as the monochromatic source, which is focused on to the input ends of two single-mode fibers having nominal 4.5-μm-diameter cores. The external plastic jacketing and inner RTV (room-temperature-vulcanized) sleeving are re-

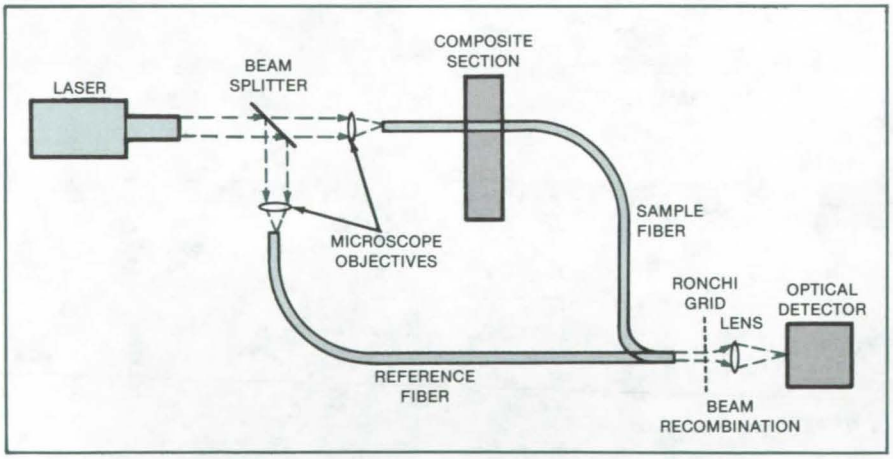

An **Optical Fiber Interferometer** directly measures acoustic emission in composite materials.

moved from the first several centimeters of both ends of both fibers, and approximately 4 cm of exposed fiber are painted with index-matching mode-stripping fluid. Approximately 2.5 cm at the ends of each fiber are not painted. The sample and reference optical signal are optically recombined, spatially filtered, and detected through an electronic output signal proportional to the instantaneous stress in the fiber.

This work was done by John H. Cantrell, Jr., of **Langley Research Center** *and Richard O. Clause, Janet C. Wade, and Paul S. Zerwekh of Virginia Polytechnic Institute and State University. For further information, Circle 96 on the TSP Request Card.*
LAR-12965

Measuring Absolute Oxygen Pressure

A reference voltage or current replaces a reference pressure.

NASA's Jet Propulsion Laboratory, Pasadena, California

A sensor determines the absolute pressure of oxygen without the need for a reference pressure source. A prototype measures oxygen pressure to control the air/fuel ratio of an automobile.

The device has a small sensing volume and one or two solid-electrolyte membranes through which oxygen enters the sensing volume (see figure). The oxygen flows back into the surrounding atmosphere through a narrow duct. Electrodes on both sides of the membranes sample the current through or voltage across each membrane.

Since the flow of oxygen across a solid-electrolyte membrane is directly proportional to the electrical current flowing through it, a known rate of gas flow into the sensing volume is enforced by applying a known current to the electrodes of one membrane. After the short time required for pressure and flow equilibrium to be established, the rate of inflow is assumed equal to the rate of outflow along the duct. The latter rate is proportional to the pressure difference between the sensing volume and the surrounding atmosphere. Finally, since the voltage across a solid electrolyte is proportional to the logarithm of the ratio of partial oxygen pressures on the two sides, the voltage across a membrane is measured to determine the ratio of oxygen pressure in the sensing volume to that in the surrounding atmosphere. Combining these relationships, it is possible to eliminate the pressure in the sensing volume as an unknown and arrive at an equation for the oxygen pressure in the surrounding atmosphere.

The measuring device can be operated either with a constant-current source or with a constant reference voltage. In the former case, the measured potential determines the measured pressure. In the latter case, the current needed for matching the output potential with a reference voltage is directly proportional to the oxygen partial pressure in the combustion gas.

The measuring device can be adapted for direct control of the oxygen pressure in a combustion mixture. For example, the measured potential is compared with a reference potential as oxygen is being pumped into the sensing volume at a constant current. The output voltage of a differential amplifier drives the control device (stepper motor, torque motor, or the like) until both potentials are equal.

This work was done by Robert Richter of Caltech for **NASA's Jet Propulsion Laboratory.** *For further information, Circle 97 on the TSP Request Card.*
NPO-16131

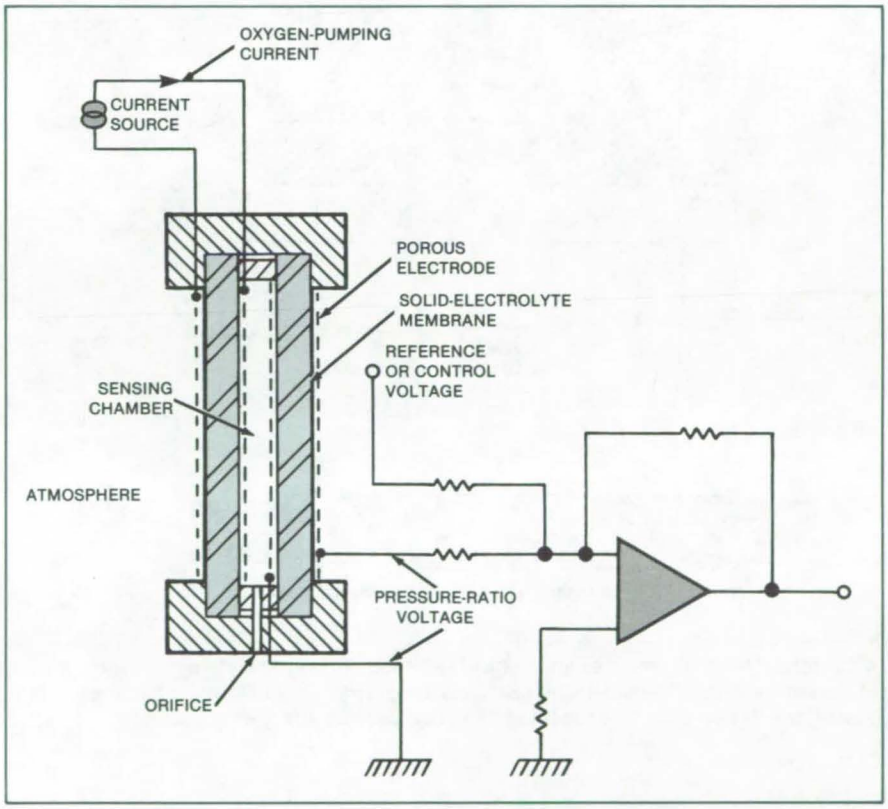

The Absolute-Oxygen-Pressure Transducer, shown with a control circuit, enables measurement without a reference pressure. The transducer, a two-port device, combines a solid-electrolyte-membrane sensor with a diffusional orifice.

Low-Stress Sealing of Pressure Transducers

Compliant washer seals high pressures without excessive compressive stress on transducer.

Marshall Space Flight Center, Alabama

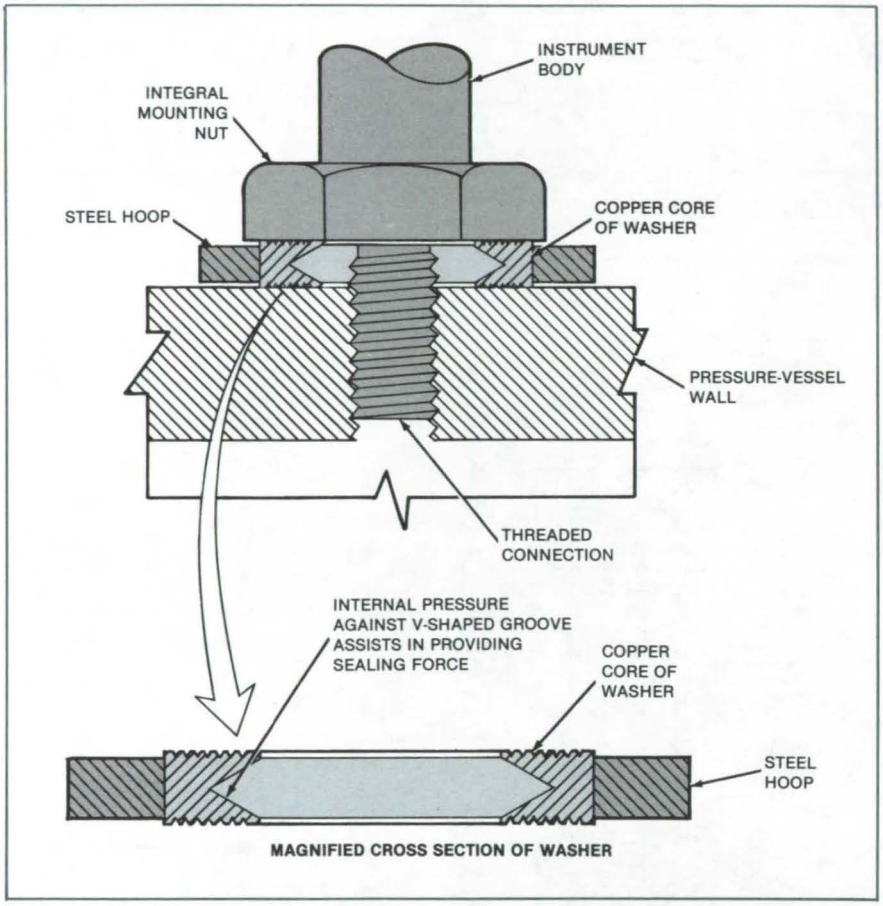

A **Conformal Washer** serves as an effective seal for a transducer passing through the walls of a pressure vessel. The washer makes it unnecessary to tighten the mounting nut to a high torque, which could damage the transducer or adversely affect its accuracy.

A washer for pressure transducers seals at high-pressure without subjecting the transducer to excessive stress. The transducer may be used at pressures of 15,000 lb/in.^{2} (103 MN/m^2) or more. Yet only a low torque — about 15 lb-in. (1.7 N-m) — need be applied to the nut that holds the transducer on the pressure vessel. The washer can also be used to seal mountings for temperature sensors and other devices.

The washer includes a core ring of such low-yield-strength material as copper surrounded by a hoop of such high-strength material as steel (see figure). Under internal pressure the core distorts outward, pressing against the transducer, the hoop, and the vessel. Serrations on the core increase the sealing pressure and help the core to conform to the surrounding surfaces so that it provides an effective barrier against high-pressure gases. The steel hoop restrains the copper core, preventing a blowout.

This work was done by Ralph E. Kroy of Rockwell International Corp. for **Marshall Space Flight Center.** *No further documentation is available.*

Inquiries concerning rights for the commercial use of this invention should be addressed to the Patent Counsel, Marshall Space Flight Center [see page A5]. *Refer to MFS-19877.*

Preventing Fires in Cryogenic Oxidizer Lines

Friction- and compression-induced ignition is prevented by a heat-dissipation layer.

Marshall Space Flight Center, Alabama

It is proposed to plate a thin layer of copper on the inside surfaces of pipes (see figure) and other parts in contact with flowing liquid oxygen, fluorine, or other oxidizers. A copper layer of only 0.001 to 0.005 inch (0.0254 to 0.127 mm) will ensure that heat is carried away from hotspots, thereby discouraging ignition.

When liquid oxygen at pressures of 2,000 to 8,000 lb/in.^{2} (14 to 55 MN/m^2) flows through tubes of stainless steel or nickel alloy, there is danger of the wall material igniting. The friction of flow and the highly reactive nature of the liquid combine to create the danger, which is especially great in small pipes, bends, valves, and flange junctures because of the higher velocity in such sections. The low thermal conductivity of high-nickel steel alloys permits local heat buildup

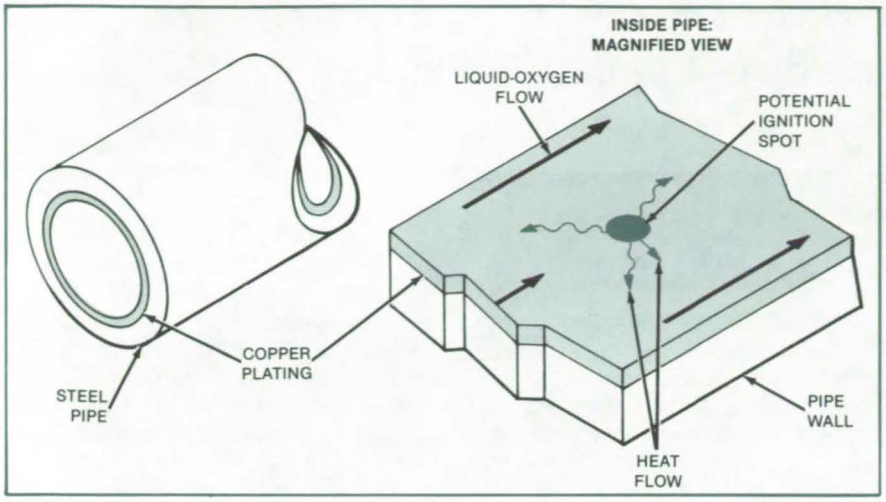

A **Thin Layer of Plated Copper** allows heat to spread out quickly, away from a potential hotspot.

that can raise temperatures above the ignition point.

The high thermal conductivity of the copper layer should quickly dissipate local hotspots, dispersing the heat into the larger thermal mass of the surrounding wall. Moreover, the copper layer becomes chemically inert by virtue of the tenacious oxide that forms on its surface. In effect, the copper layer increases the oxygen ignition threshold of the pipe by 5 to 20 times.

This work was done by William R. Wagner of Rockwell International Corp. for **Marshall Space Flight Center.** *For further information, Circle 98 on the TSP Request Card.*
MFS-19830

Measuring Rind Thickness on Polyurethane Foam

Hardness is a good indicator of thickness.

Marshall Space Flight Center, Alabama

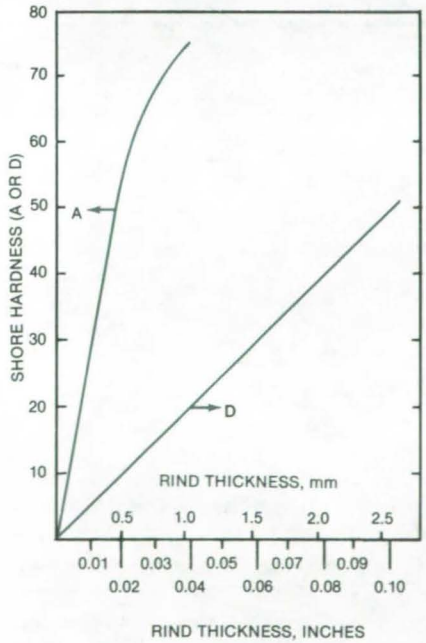

Shore D Hardness of the surface rind on polyurethane foam varies linearly with rind thickness. Shore hardness measured on the A scale is also a useful indicator of thickness, particularly at lower thickness values.

A nondestructive test determines the rind thickness of polyurethane foam. The surface hardness of the foam is measured by the Shore durometer method: The hardness on the Shore D scale correlates well with the rind thickness (see figure). A Shore D hardness of 20, for example, indicates a rind thickness of 0.04 inch (1 millimeter).

The thickness of the rind — the tough, relatively-unfoamed surface layer — affects the properties of the polyurethane foam. It may be desirable to minimize rind thickness to improve the shock-absorption characteristics, for example. On the other hand, it may be desirable to maximize rind thickness in applications requiring greater dimensional stability or improved surface appearance and paintability. The new hardness test makes it easy to determine the rind thickness of a sample nondestructively and to adjust the fabrication variables accordingly.

The technique was developed by comparing hardness measurements of specimens with optical and scanning-electron photomicrographs of their cross sections. The microscopic methods are not suitable for production quality checks or process adjustments, however, because they are destructive (entailing the removal of samples of foam), require time-consuming sample preparation, and give variable results due to subjective interpretation of the rind thickness in the photomicrographs.

Other techniques were also evaluated. Ultrasonic scanning could not be used since the sound energy could not penetrate deeply enough. X-ray inspection was too sensitive to variations in the composition and temperature of X-ray-plate processing solutions to provide reproducible results.

This work was done by C. B. Johnson, J. D. Miller, and H. J. Brown of Martin Marietta Corp. for **Marshall Space Flight Center.** *For further information, Circle 99 on the TSP Request Card.*

Inquiries concerning rights for the commercial use of this invention should be addressed to the Patent Counsel, Marshall Space Flight Center [see page A5]. Refer to MFS-25941.

Reducing Thermal Expansivity of Composite Panels

Finished parts are heat-treated.

Marshall Space Flight Center, Alabama

The coefficient of thermal expansion of laminated graphite/epoxy composite panels can be altered after the panels have been cured by a postcuring heat treatment. The treatment makes it possible to reprocess costly panels for the requisite thermal expansivity instead of discarding them.

The panels for which the treatment was developed were originally cured at 275° F (135° C). The resulting coefficient of thermal expansion was greater than about $+0.125 \times 10^{-6}(°F)^{-1}$ [0.225×10^{-6} $(°C)^{-1}$], whereas the application required a coefficient in the range of $+0.05$ to -0.15×10^{-6} $(°F)^{-1}$ [$+0.09$ to -0.27×10^{-6} $(°C)^{-1}$]. A post-curing bake at 290° to 350° F (143° to 177° C) was found to produce the required shift in the thermal-expansion coefficient.

Previously, it had been assumed that once a thermosetting epoxy resin was cured, its physical properties were fixed. Apparently, however, the postcure decreases the coefficient of thermal expansion by increasing the cross-linking between molecules.

For specific laminates having exacting dimensional requirements, the postcuring procedure can be used to lower the coefficient of thermal expansion until it is in the desired range. Temperature-vs.-time curves for the postcure can be developed analytically and confirmed with the aid of test specimens. Such curves will depend on initial cure temperature, the laminated materials, and the ply orientation.

This work was done by Dennis D. Smith of Boeing Aerospace Co. for **Marshall Space Flight Center.** *No further documentation is available.*
MFS-25793

Sintered Lining for Heat-Pipe Evaporator

Hotspots should be eliminated by lining the inner wall.

NASA's Jet Propulsion Laboratory, Pasadena, California

The distribution of heat-transfer liquid in a heat-pipe evaporator should be improved by lining the inner wall with a layer of sintered metal. The sintered layer takes the place of a layer of screen wick that was formerly sintered or bonded to the wall.

A prototype of the evaporator was fabricated from an existing stainless-steel evaporator tube for which sodium was the working fluid. First, the inside of the pipe was machined to increase the diameter by 0.030 in. (0.76 mm). The inside of the tube was then built down to its original diameter by sintering nickel powder onto the inside surface in an atmosphere of dry hydrogen (see figure).

It is expected that the sintered layer will provide adequate circumferential distribution of liquid and that loose contact between this layer and the arteries will suffice to spread liquid evenly throughout the evaporator. Since the sintered layer would always be full of liquid, there would be no hotspots of the type that previously arose where the former screen wick did not fit properly against the wall.

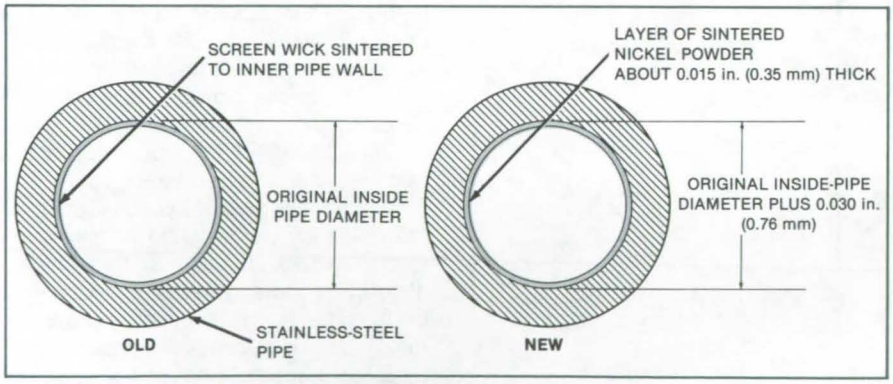

The **Old Heat-Pipe Wall and Lining Are Reworked** to give a new sintered lining that would assure a more even distribution of working fluid.

This work was done by Donald M. Ernst and G. Yale Eastman of Thermacore, Inc., for **NASA's Jet Propulsion Laboratory.** *For further information, Circle 100 on the TSP Request Card.*
NPO-16172

Joint for Erectable and Collapsible Frames

Mechanism is self-energized, rigid, and reversible.

Lyndon B. Johnson Space Center, Houston, Texas

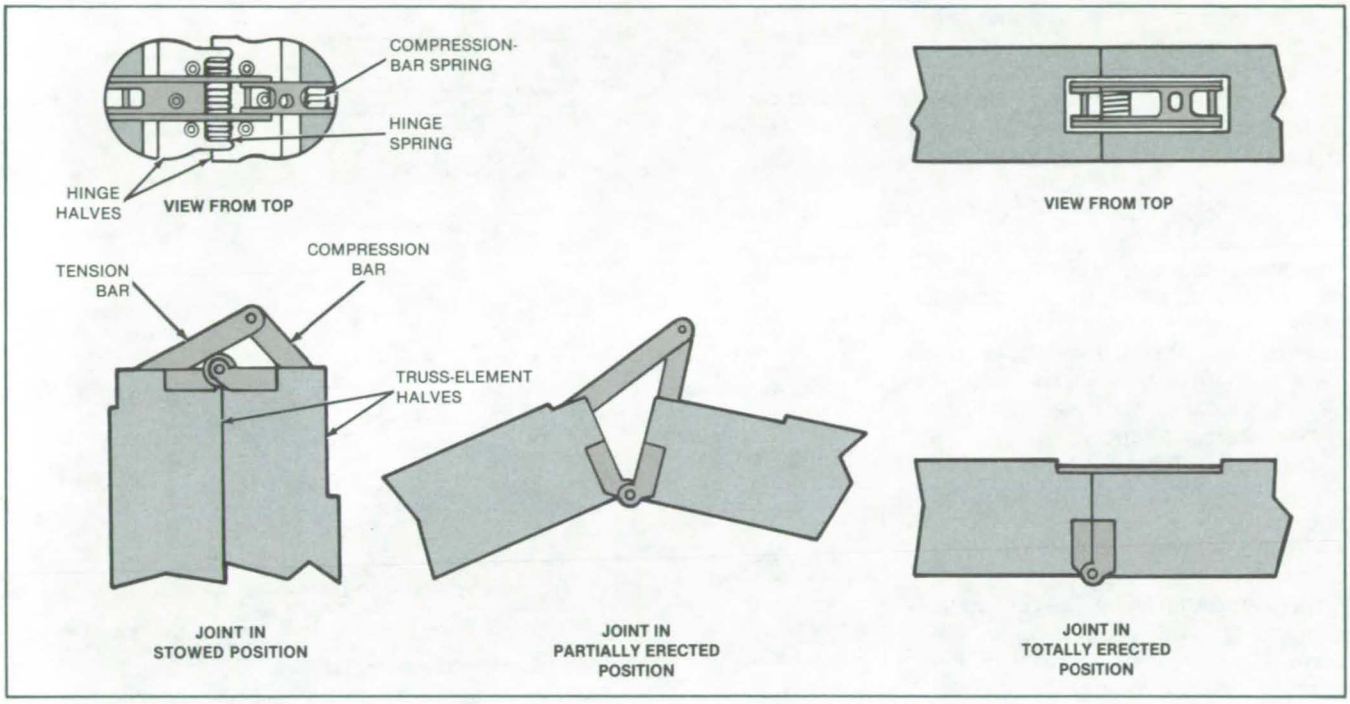

Stages in the Automatic Erection of truss members illustrate the operation of the new joint mechanism. The springs in the mechanism cause the members to pivot about the hinge until they lock in alinement.

A joint mechanism allows a truss structure to be folded and stowed in a small space. On command, the joint mechanisms unfold, erecting the structure and locking its members in place. The joints can also be collapsed so that the structure can be restowed. Developed for structures to be erected in space (for example, antennas, solar panels, solar sails, and masts), the joint mechanism can be readily adapted to window-opening struts, folding furniture, and television antennas.

The joint mechanism includes a hinge attached to two truss elements that are also connected by two links, a tension bar, and a compression bar (see figure). When the folded elements are released, the springs in the joint mechanism rotate the truss elements about the hinge and lock the mechanism to form a single member.

When the joint is locked, there are no protrusions to snag clothing or equipment. The joint cannot be triggered accidentally by vibration as can other hinge joint mechanisms. A bending moment created by buckling or initial crookedness does not open the joint. Harmful outgassing of volatile substances — common in glued ball-and-socket erectable joints — does not occur. Since the mechanism has stored energy in the springs, an external force is not required for erection.

This work was done by Timothy E. Pelischek of **Johnson Space Center.** *No further documentation is available.*
MSC-20635

Pressure-Letdown Plates for Coal Gasifiers

A variation of the pseudoporous plates used with coal gasifiers in the pressure-letdown stage of processing would minimize clogging. Rotating plates containing variable-gap annuli continually change the flow path to enable an erosionless reduction of gas pressure. Particles that otherwise would clog the porous plugs pass through the gaps.
(See page 355.)

Sealing Mechanical Cryogenic Coolers

Metal bellows are used to seal Vuilleumier and Stirling-cycle cryogenic coolers, replacing sliding seals. The bellows, which are mechanically attached to the moving piston and the stationary cylinders, are fully collapsed when the piston reaches the position of minimum volume. They are expected to have a long service life.
(See page 397.)

Angle-Measurement and Ranging System

A proposed optical system automatically supplies information on the angular position and range of an object. Although originally developed for spacecraft rendezvous and guidance, features of the system can be adapted to angle-measurement and ranging problems on Earth.
(See page 344.)

Lightning Protection for Composite Aircraft Structures

A secondarily applied system nullifies the destructive right-angle effect.

Langley Research Center, Hampton, Virginia

A lightning-protection system (see figure), consisting of two layers of aluminum foil separated by a layer of dielectric material protects graphite/epoxy composite structures on aircraft. These structures are vulnerable to lightning, especially at or near wingtips, stabilizer tips, vertical fin tips, rudders, elevators, and ailerons. At these locations the composite may be subjected to the initial-attachment lightning strike characterized by the the fast-rise, high peak current (200 kA) and large energy transfer (2×10^6 A^2-s), which can produce severe structural damage to the unprotected graphite/epoxy.

The protective layer is a secondarily-applied lightning-protection system, the prime advantage of which is the nullification of the thermal and right-angle effect of the lightning-arc attachment to a graphite/epoxy laminate. The right-angle effect is the interaction of forces between the current paths taken by the lightning; that is, if the arc attachment is normal to the surface, the lightning current flows away from the attachment point along the direction of the graphite fibers. These structures are angle-ply laminates (0°, ±45°, and 90°). Therefore, in addition to the right-angle effect, buckling forces are created between the plies of the laminate when the current is forced to flow in different directions in each ply at the arc attachment point.

Lightning tests performed on five prototype systems applied to test panels have shown that almost all damage was confined to the lightning-protection system. Because this system is secondarily applied, it can be removed and replaced after the damgage.

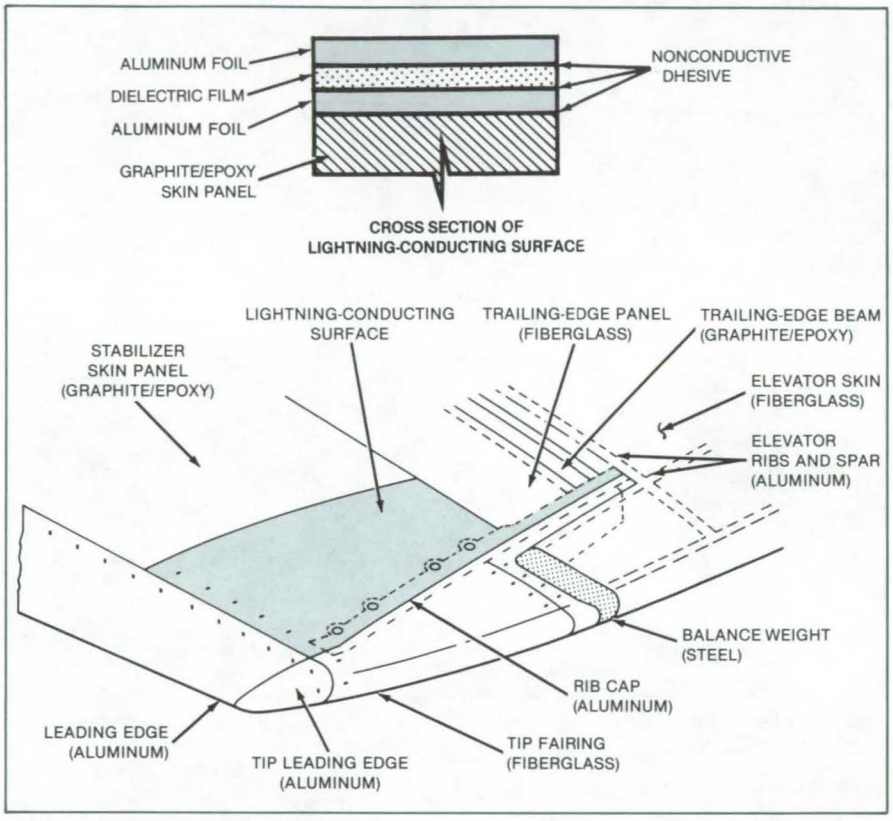

A Lightning-Protection System prevents damage to composite graphite/epoxy structures on aircraft surfaces. The system struck by the lightning is readily replaced, leaving the composite undamaged.

This work was done by Glenn O. Olson of The Boeing Co. of **Langley Research Center.** *For further information, Circle 101 on TSP Request Card.*

Title to this invention, covered by U.S. Patent No. 4,352,142, has been waived under the provisions of the National Aeronautics and Space Act [42 U.S.C. 2457(f)], to The Boeing Company, Seattle, WA 98124.
LAR-12879

Interferometer Measures Broadband Surface Acoustic Waves

A dual differential interferometer uses two pairs of orthogonally-polarized optical beams to measure the amplitude and orientation of broadband ultrasonic surface acoustic waves. By combining the two signals, the interferometer determines a two-dimensional surface-wave profile and its variation as a function of time. The instrument is modular, and its sensitivity is limited only by the optical detector used.
(See page 341.)

Acoustic Gaussian Far-Field Pattern

A new ultrasonic transducer produces a far-field beam with a Gaussian spatial profile for materials evaluation applications. The transducer is constructed by depositing a circularly-symmetric metallic multielectrode array on a 12.7-mm-diameter X-cut quartz disk. Each electrode is independently connected to an impedance network optimized to produce the Gaussian distribution with less than 2 percent error.
(See page 342.)

Isolation Mounting for Charge-Coupled Devices

A support for small imaging devices provides both cooling and vibration isolation. Developed for charge-coupled devices (CCD's) in infrared telescopes, the support is adaptable to sensors in a variety of environments — for example, sensors in nuclear reactors, engine exhausts, and plasma chambers. The CCD's are suspended by wires under tension.
(See page 316.)

Efficient Joints for Graphite/Epoxy Structures

Bonded joints perform well through a wide temperature range.

Langley Research Center, Hampton, Virginia

Single lap joints that minimize stress concentrations were designed for graphite/polyimide material. Tests indicate that a significant improvement in joint efficiency is available through geometric modifications and hybrid material additions at the adherend interfaces.

Specimens were fabricated for baseline single lap joints and for joints with geometric or material modifications at the bonding interface. Two geometric concepts were investigated: preforming adherends and scalloping the ends of the adherends. The preformed-adherend concept consisted of single lap joints with the adherend angled at the lap ends (5°, 10°, and 15°). The material modifications consisted of placing S-glass/polyimide fabric in the joint between the adherends.

Testing was conducted at −250°, 70°, and 550° F (−157°, 21°, and 288° C). The preformed-adherend tests demonstrated a significant increase in load-carrying capacity compared to the baseline configuration. For the preformed adherends, increases ranged from 92 to 262 percent at 70° F (21° C) and from 46 to 234 percent at 550° F (288° C).

Scalloping the single lap joints, however, gave a slight reduction in failure loads. Placing fabric interfaces, S-glass/polyimide and graphite/polyimide, between the single lap joints resulted typically in 28- to 70-percent increases in average failure load. Most of the fabric interface specimens delaminated between the two fabric plies as opposed to failing in the base adherends.

This work was done by Donald E. Skoumal and James B. Cushman of Boeing Aerospace Co. for **Langley Research Center.** *Further information may be found in NASA CR-3602 [N83-16787/NSP], "Test and Analysis of Celion 3000 PMR-15, Graphite/Polyimide Bonded Composite Joints" [$11.50]. A copy may be purchased [prepayment required] from the National Technical Information Service, Springfield, Virginia 22161.*

LAR-13091

Computer Programs

These programs may be obtained at very reasonable cost from COSMIC, a facility sponsored by NASA to make new programs available to the public. For information on program price, size, and availability, circle the reference letter on the COSMIC Request Card in this issue.

Acquisition of Dynamic Stress/Strain Data

Program computes average strains, modulus of elasticity, and the Poisson ratio.

This computer program enables real-time data acquisition and plotting of stress-strain by a small, desk-top computer. The program monitors a load cell and multiple-strain gages during tension or compression loading. Its scan routine is triggered by a specified change of applied load or longitudinal strain.

The load cell and strain gage feedback voltages are converted to stress and microstrain values that are displayed on the CRT, plotted, and stored. At the conclusion of the test, the program plots the average back-to-back gage values from the longitudinal and the transverse gages. In addition, the program calculates the modulus of elasticity and the Poisson ratio. All data and specimen parameters may be printed and stored on magnetic disk. A replot routine enables the test data and specimen parameters to be recalled from disk, modified, and replotted with the same or different scales.

This program is written in BASIC for interactive execution and has been implemented on a Hewlett-Packard HP 9845 desk-top computer. The data acquisition system also requires an HP 9872A plotter, an HP 3455A digital voltmeter, an HP 3495A scanner, a line printer, a disk drive, and signal conditioners. This program was developed in 1982.

This program was written by Robert G. Mines and Robert J. Demonet of Rockwell International Corp. for **Johnson Space Center.** *For further information, Circle L on the COSMIC Request Card.*

MSC-20589

Dynamic Simulation and Stability Analysis

Actively-controlled, coupled multiflexible systems are simulated.

The Dynamic Interaction Simulation of Controls and Structure (DISCOS) program was developed for the dynamic simulation and stability analysis of passive and actively controlled spacecraft. In the use of DISCOS, the physical system undergoing analysis may be generally described as a cluster of contiguous flexible structures (bodies) that comprise a mechanical system, such as a spacecraft. The entire system (spacecraft) or portions thereof may be either spinning or nonspinning. Member bodies of the system may undergo large relative excursions, such as those of appendage deployment or rotor/stator motion.

The general system of bodies is, by its inherent nature, a feedback system in which inertial forces (such as those due to centrifugal and Coriolis acceleration) and the restoring and damping forces are motion-dependent. The system may

(continued on next page)

possess a control system in which certain position and rate errors are actively controlled through the use of reaction-control jets, servomotors, or momentum wheels. Bodies of the system may be interconnected by linear or nonlinear springs and dampers, by a gimbal and slider block mechanism, or by any combination of these.

The DISCOS program can be used to obtain nonlinear and linearized time responses of the system, total system resonance properties, and frequency-domain response and stability information for the system. DISCOS is probably the most-powerful computational tool to date for the computer simulation of actively-controlled, coupled multi-flexible-body systems.

The program is not easy to understand and apply effectively and is not intended for simple problems. The DISCOS user is expected to have extensive working knowledge of rigid-body and flexible-body dynamics, finite-element techniques, numerical methods, and frequency-domain analysis. Various applications of DISCOS include simulation of the Shuttle payload deployment/retrieval mechanism, solar-panel array deployment, antenna deployment, analysis of multispin satellites, and analysis of large, highly flexible satellites, including the design of attitude-control systems.

The overall approach of DISCOS is unique in that any member body of the system may be flexible, and the system is not restricted to a topological tree configuration. The equations of motion are developed using the most general form of Lagrange's equations, including auxiliary nonholonomic rehenomic conditions of constraint. Lagrange multipliers are used as interaction forces/torques to maintain prescribed constraints.

Nonlinear flexible/rigid dynamic coupling effects are accounted for in unabridged fashion for individual bodies and for the total system. Elastic deformation can be represented by normal vibration modes or by any adequate series of Rayleigh functions, including "quasi-static" displacement functions. To "solve" Lagrange's equations of motion, one must define the explicit form of the kinetic and potential energy functions, the dissipation function, and the form of the transformation relating ordinary Cartesian position coordinates to the generalized coordinates.

The potential energy and dissipation functions for a structure may be determined with standard finite-element techniques, using the NASTRAN program. To use the computed functions, the Lagrange's equations and the system kinematic constraint equations are expressed in matrix format. These differential matrix equations are solved numerically by the DISCOS program. Provisions are included for environmental loading of the structure (spacecraft), including solar pressure, gravity gradient, and aerodynamic drag.

Input to DISCOS includes topological and geometrical descriptions of the structure under analysis, initial conditions, control-system descriptions, and derived structural matrices. Specialized routines are supplied that read the input data and redimension the DISCOS programs to minimize core requirements.

DISCOS output includes an extensive list of calculated parameters for each body of the structure, the system state vector and its time derivatives, Euler angles and position coordinates and their time derivatives, control-system variables and their time derivatives, and various system parameters at a given simulation time. For linearized system analysis, the output includes the various transfer matrices, eigenvectors, and calculated eigenvalues.

This program is written in FORTRAN IV for batch execution and has been implemented on a DEC VAX-11/780 computer. For plotted output an SC-4020 plotting system is required. DISCOS was developed in 1978 and adapted to a DEC VAX computer in 1982.

This program was written by Harold P. Frisch and Joan A. Sanborn of **Goddard Space Flight Center.** *For further information, Circle M on the COSMIC Request Card.*
GSC-12810

Aerodynamic Analysis of Low-Speed Wing-Flap Systems

Performance analysis includes the effects of leading-edge thrust and vortex lift.

The SUBAERF program was developed for the aerodynamic analysis and design of low-speed wing-flap systems. SUBAERF is based on a linearized-theory lifting-surface solution. The low-speed aerodynamic analysis method used in SUBAERF provides estimates of wing performance, which include the effects of attainable leading-edge thrust and vortex lift. This basic aerodynamic analysis method has been improved to provide for the efficient and accurate treatment of simple leading-edge and trailing-edge flap systems. Flap geometry may be input directly by the user. The program provides for the simultaneous analysis of up to 25 pairs of leading-edge and trailing-edge flap-deflection schedules.

The SUBAERF program is written in FORTRAN IV for batch execution and has been implemented on a CDC 6000-series computer with a central-memory requirement of approximately 110K (octal) of 60-bit words. This program was developed in 1983.

This program was written by Harry W. Carlson and Kenneth B. Walkley of Kentron International, Inc., for **Langley Research Center.** *For further information, Circle N on the COSMIC Request Card.*
LAR-13116

Turbine-Engine Transient-Rotor Analysis

The response to blade loss or transients is calculated.

A computer program has been developed to predict the structural dynamics of a rotor system in gas-turbine engines subjected to sudden unbalance. The TETRA computer code calculates transient structural response of turbine engines due to blade loss or other time-dependent events.

Based on a modal synthesis approach, the component-element method employed in TETRA follows a modular or building-block scheme both in the construction of the mathematical model of an engine to be analyzed and in the architecture of the program and subroutines.

The turbine engine is described by a reduced system of second-order differential equations, and a solution for the transient response is obtained through an explicit numerical-integration scheme — the central finite-difference method. Global stiffness and damping matrices are not assembled, and only the right-hand side of the system of equations; i.e., the forces, is updated at each time step.

The differential equations are formulated in terms of generalized coordinates, model-elastic and rigid-body elements, and elements obtained through the coordinate transformations that are associated with the free-free modes and

partially constrained modes computed for engine-subsystem structures (rotors, case, pylon). In the latter case, the elements describe the physical connections between the subsystem structures. These connections can be nonlinear and are defined with bearing/frame springs and dampers, engine support elements, link elements, rotor-case rub springs or stop elements, and gyroscopic cross-axis coupling elements. The rotor-case rub springs are used to model the additional load path between the rotor and the case that exists for the large rotor excursions caused by high rotor unbalance. For this element, the effect of the nonlinear restoring force associated with the structural clearance is included in the formulation.

Running this program is automatic with the modal data file, created earlier, of each major component. Output are time histories of deflections and loads at any desired point or points of the engine structure. Outputs can be plotted also.

This program is written in FORTRAN IV for use on a UNIVAC 1100/41 computer. TETRA can be used to calculate transient response of an entire engine or just one structural component of two or more connected components. It can be used on structures other than turbine engines with little or no modification.

This program was written by V. Gallardo, Jr., M. J. Stallone, A. Storace, and G. Black of General Electric Co. for **Lewis Research Center.** *For further information, Circle P on the COSMIC Request Card.*
LEW-13726

Heat-Exchanger Computational Procedure for Temperature-Dependent Fouling

Fuel-vaporizer exchanger performance is evaluated.

A computer program has been generated under NASA contract that predicts heat-exchanger performance under a variety of conditions. This novel computational procedure was developed for use with a heat exchanger that vaporizes fuel prior to the fuel ignition. It provides a rapid means of calculating the distribution of fluid and wall temperatures, fuel deposit formation, and pressure losses at various locations in the heat exchanger.

The computational procedure is unique in that it is capable of treating wide variations in system geometry without unduly restrictive assumptions concerning heat-exchanger type (e.g., coflow, counterflow, and crossflow). This program also permits consideration of the variation in fluid properties, including rapid changes in liquid viscosities. The procedure has been adapted to the special case of a phase change in the fluid and to the evaluation of transient inflow conditions in heat-exchanger performance.

A specific application involved a heat exchanger composed of a core of unfinned stainless-steel tubes that are heated by burning Jet A fuel and bleed air. The heat energy is transferred to atomized engine fuel (prior to combustion). The two engine conditions are assumed to be acceleration and cruise. Other applications of this program are possible.

This program was written by L. M. Chiappetta and E. J. Szetela of United Technologies Corp. for **Lewis Research Center.** *For further information, Circle Q on the COSMIC Request Card.*
LEW-13874

Structural Analysis of Cylindrical Thrust Chambers

Extrapolation, plot, and restart routines for use with the BOPACE program

A system of three computer programs was developed for use with the BOPACE finite-element program for analyzing cumulative plastic deformation of structures subject to high thermomechanical load cycles. An extrapolation program is used to predict finite-element model nodal displacement over a range of user-specified cycles by using BOPACE-computed nodal-displacement rates. A plot package is used to display predicted configurations. A BOPACE restart tape-reader routine is included for retrieving the computed nodal displacements from BOPACE restart tapes for extrapolation or plotting.

The extrapolation method was developed to estimate finite deformation and low-cycle fatigue damage in hot structures without a complete cycle-by-cycle analysis over the life of the structure. The method provides a predictor/corrector technique wherein BOPACE-computed deformation rates are used to predict configuration changes over a user-specified number of loading cycles. The predicted configuration is analyzed in BOPACE, and the computed deformation rates in the deformed model are read by the extrapolation program to establish another selected state of the deformed model. The procedure may be repeated as required.

The extrapolation procedure utilized a linear least-squares approximation to establish the computed displacement rate of each node in the finite-element model. The program provides the option of extrapolating up to and including three components of the computed nodal-displacement vector. The input and output of the extrapolation program are compatible with BOPACE Version 6.0. Card input/output is used as the transfer medium between BOPACE, the extrapolation program, and the plotting program. This provides the user with complete flexibility in the choices of configurations to plot, extrapolate, and feed back to BOPACE for additional computation.

The three programs are written in FORTRAN and are compatible with IBM 370 and UNIVAC 1108 computers. The computer programs can be used to analyze finite plastic deformation and low-cycle fatigue damage in the hot section of pumps or compressors as well as static equipment used in power generation. Other possible applications are the analyses of equipment used to process fossil or nuclear fuels.

This program was written by W. H. Armstrong and M. L. Pearson of Lockheed Missiles & Space Co., Inc., for **Lewis Research Center.** *For further information, Circle R on the COSMIC Request Card.*
LEW-13655

Turbulent Recirculating Flows in Isothermal Combustor Geometries

Improved analyses of the combustor flow fields are accomplished.

A computer program has been developed that provides a mathematical solution to the design and construction of combustion chambers for jet engines.

(continued on next page)

Improved results in the area of the combustor flow fields are accomplished by this computer-program solution, which is cheaper and quicker than experiments involving real systems or models. This computer program presents details of the mathematical procedure used to evaluate effects of combustor geometry and the boundary conditions, physical properties, and turbulence of the gases.

The computer program is code-named STARPIC (swirling turbulent axisymmetric recirculating flows in practical isothermal combustor geometries). The technique involves a staggered-grid system for axial and radial velocities and a line-relationship procedure for efficient solution of the equations. It also includes a two-equation k-ε turbulence model, a stairstep boundary representation of the expansion flow, and a realistic accommodation of swirl effects.

The computer program report is a user's manual and deals with the computational problem showing how the mathematical basis and computational scheme may be translated into a computer code. The user's guide also includes a flow chart and notes about various subroutines.

This program is written in FORTRAN IV for use on an IBM 370/3033 computer.

This program was written by D. G. Lilley and D. L. Rhode of Oklahoma State University for **Lewis Research Center.** *For further information, Circle S on the COSMIC Request Card.*
LEW-13894

Computation of Three-Dimensional Combustor Performance

Modified program includes computations of soot and nitrogen oxide emissions.

An existing steady-state 3-D computer program for calculating gas-turbine flow fields was modified to include computation of soot and nitrogen oxide emissions. In addition, the radiation calculation was corrected for soot particles. Significant advances have been made in combustor analytical modeling. These advanced tools, while still in their early stages, offer the potential of reducing the design and development time required for gas-turbine combustors. Also, the analytical models increase the understanding of the phenomena affecting combustor performance.

The existing computer program is fully elliptic, capable of handling recirculating flows and of analyzing a variety of combustor configurations, including can, can/annular, and annular designs. The program solves for the three velocity components, u, v, and w, species concentrations, CxHy, CxHy-2, C(S), CO, CO_2, H, H_2, O, O_2, OH, H_2O, N, N_2, NO, and NO_2, turbulence quantities from the k-E turbulence model, and three radiation fluxes. In addition, the use of primitive variables makes modifications to the boundary conditions easy, allowing the user to analyze complex inlet geometries. The program also calculates the trajectories and evaporation rates of a fuel-nozzle spray.

The final report presents calculations for a JT8D can combustor for idle, cruise, and takeoff conditions. The computations agree reasonably well with the limited experimental data available.

This program was written by S. K. Srivatsa of Garrett Turbine Engine Co. for **Lewis Research Center.** *For further information, Circle T on the COSMIC Request Card.*
LEW-13930

Generating Tables of Thermodynamic Properties

Tables are obtained over a wide range of environmental conditions.

The Thermodynamic Property Generation program produces tables for any fluid for which the state equation, vapor pressure equation, specific heat equation, and critical constants are known. The program calculates thermodynamic properties at any state, providing a way of obtaining properties at extreme environmental conditions.

Input to the program consists of the fluid critical constants, vapor pressure equation, specific heat equation, and state equation. Either of two forms of the state equation may be used, the Benedic-Webb and Rubin or the Beattie-Bridgeman. Either metric or English units may be used. Output consists of either properties for a specific state or a table of temperature, pressure, specific volume, internal energy, enthalpy, and entropy.

The program is written in FORTRAN V for batch execution and has been implemented on a CDC CYBER 170-series computer with a central memory requirement of approximately 40K (octal) of 60-bit words. It was developed in 1983.

This program was written by Son N. Nguyen of Rockwell International Corp. for **Johnson Space Center.** *For further information, Circle U on the COSMIC Request Card.*
MSC-20701

Trajectory Analysis and the Orbit Determination

Two programs aid in trajectory analysis.

The Double-Precision Trajectory Analysis Program (DPTRAJ) and the Orbit Determination Program (ODP) is used at NASA's Jet Propulsion Laboratory for navigation of deep-space missions such as *Voyager*. DPTRAJ and ODP work together. DPTRAJ, ODP, and their supporting utility programs are capable of handling the massive amounts of data and performing the numerical calculations required for solving the navigation problems associated with planetary fly-by and lander missions. They are used extensively in support of *Voyager*.

DPTRAJ produces a spacecraft ephemeris by numerical integration of the equations of motion, which can be formulated using a full set of acceleration models. For each trajectory, the extent of the modeling employed and the precision of the integration process are controlled by user input specifications.

The equation of motion inlcudes four types of terms: An acceleration term accounts for the basic conic motion of the spacecraft with respect to the central body. Terms that measure the attraction of the perturbing bodies on the spacecraft and terms that indirectly affect the motion as perturbations on the central body may be included. Terms are also provided to account for other gravitational and nongravitational effects of the motion.

The function of the ODP subsystem of the navigation system is the processing of the observational data in order to compute precise estimates of the spacecraft, or lander, position-

coordinate histories. This function is executed by processing the observation data and auxiliary calibration information to compute a spacecraft state vector, or a lander position vector, along the parameters that define the acceleration. The heart of the ODP process is a data-fitting subprocess in which validated, edited, and corrected observational data are transformed into a state-vector estimate. The derived state-vector estimate may then be used to generate an estimated trajectory, which contains the final product of the orbit determination process: the time evolution of the estimated spacecraft, or lander, position coordinates.

DPTRAJ and ODP are written in FORTRAN V, SFTRAN, and Assembler, for batch execution (SFTRAN is a structured FORTRAN for which a preprocessor is supplied). These programs have been implemented on a UNIVAC 1100-series computer. The DPTRAJ and ODP programs were last updated in 1980.

This program was written by Daniel J. Alderson, Franklyn H. Brady, Peter J. Breckheimer, James B. Collier, John E. Ekelund, Jordan Ellis, David E. Hilt, Ahmad R. Khatib, Victor N. Legerton, Susan K. McMahon, Robert T. Mitchell, Patricia M. Molko, Theodore D. Moyer, Melba W. Nead, Nick D. Panagiotacopulos, Theodore Pavlovitch, Richard F. Sunseri, and Thomas D. Talbot of Caltech and John W. Zielenbach of The John W. Gross Co. for **NASA's Jet Propulsion Laboratory.** *For further information, Circle V on the COSMIC Request Card.*
NPO-15586

Orbital Mechanics Analysis Program

Program computes position, velocity, range, and range rate.

The Orbital Mechanics Analysis Program provides the engineer with a simple tool for the analysis or synthesis of any orbital maneuvering function involving a vehicle and a target. The program is useful in such applications as proximity operations and rendezvous maneuvers.

The program keeps track of orbiting objects by means of state vectors (time, position, and velocity). An absolute state vector (Earth-related) and a relative state vector (vehicle-related) are used by the program. The movement of the orbiting objects is computed by utilizing an elliptical predictor algorithm independently for each object. The position and velocity of each object are computed at each time point of interest. The line-of-sight range and range rate from the vehicle to the target are also computed.

The program is written in FORTRAN 77 for interactive execution and has been implemented on a Data General ECLIPSE C/350 computer with a central memory requirement of approximately 40K of 8-bit bytes. The program was developed in 1983.

This program was written by William C. Simon, Stephen C. Jankowski, and Thomas B. Hughes of Rockwell International Corp. for **Johnson Space Center.** *For further information, Circle W on the COSMIC Request Card.*
MSC-20700

Thermal Radiation Analyzer

Program handles internode radiation exchange and heat from environmental radiant sources.

The Thermal Radiation Analyzer System, TRASYS II, solves the radiation-related aspects of thermal analysis problems. When TRASYS II is used in conjunction with a generalized thermal analysis program such as the Systems Improved Numerical Differencing Analyzer (SINDA), any thermal problem that can be expressed in terms of a lumped parameter RC thermal network can be solved.

TRASYS II provides for the calculation of internode radiation interchange data and for the calculation of incident and absorbed heat-rate data originating from environmental radiant heat sources. Data of both types are provided by TRASYS II in a format directly usable by such thermal analyzer programs as SINDA.

TRASYS II consists of two major components: the preprocessor and the processor library. A primary feature of TRASYS II is that it allows users to write their own executive, or driver, programs, which organize and direct the library routines to an efficient solution of the problem. The preprocessor first reads and converts the user's geometry input data into the form used by the library routines. Next, the preprocessor accepts the user's driving logic, written in the TRASYS II-modified FORTRAN language, which directs the user-provided and library routines in the solution of the problem.

The processor library consists of FORTRAN routines that perform the functions commonly needed to solve thermal-radiation problems. In many cases, the user has a choice of solution techniques to perform the same function. As previously mentioned, users may provide their own routines where desirable. In particular, the user may write output routines to provide for an interface between TRASYS II and any thermal-analyzer program using the RC network concept.

Input to the TRASYS II program consists of edit/control data and model data. The edit/control data do not participate in the definition of the thermal-radiation problem but provide for basic program control and provide the user with an editing capability. The model data provide for the definition of the mathematical model of the thermal radiation problem. The model data include surface geometry data, documentation data, nodal data, block coordinate system data, form factor data, operations data (the user's driver logic), and user-supplied subroutines.

TRASYS II currently allows problems with as many as 1,000 nodes and time-variable problem geometry. The edit capability allows for the easy modification of complex thermal-radiation problem models. Output from TRASYS II consists of two basic types of data: internode radiation interchange data and incident and absorbed heat-rate data. A plot package provides for the plotting of input geometry, orbit data (for on-station spacecraft problems), the two types of data described above, and any other data generated by the user's driver logic.

TRASYS II is written in FORTRAN V and Assembler for batch execution and has been implemented on a UNIVAC 1100-series computer under EXEC8 with a minimum central memory requirement of approximately 46K of 36-bit words. This latest revision of the TRASYS was developed in 1981.

This program was written by Robert A. Vogt of **Johnson Space Center** *and Carl L. Jensen, Richard G. Goble, and Robert J. Conner of Martin Marietta Corp. For further information, Circle X on the COSMIC Request Card.*
MSC-20448

Data-Generating Program for ASKA Modeling

Time and data requirements are reduced for finite-element thermal modeling.

The carrier-plate assemblies of the NASA Space Shuttle thermal protection system are provided for easy access to the protected vital parts of the Shuttle. Each assembly is mounted on the substructure with fasteners through holes in the protective tiles.

The Automatic System of Kinematic Analysis (ASKA) finite-element program is used to evaluate these assemblies. The PLATE.FORT computer program was developed as a data generator for ASKA modeling. PLATE.FORT greatly reduces the amount of time and data required for building an ASKA model of these assemblies. PLATE.FORT may be adaptable to other ASKA modeling situations.

This program is written in FORTRAN IV for batch execution and has been implemented on an IBM 370-series computer with a central memory requirement of approximately 420K of 8-bit bytes. PLATE.FORT was developed in 1982.

This program was written by Abdol Karimi-Dechesh and Tilden K. Cheng of Rockwell International Corp. for **Johnson Space Center.** *For further information, Circle Y on the COSMIC Request Card.*
MSC-20644

Transient Response Analysis

The damping characteristics of electromechanical devices are determined by analyzing transient response.

The Transient Response Analysis Program, TRAP, aids in the analysis of the frequency response of force-transmission and shock-damping devices. Devices that might by analyzed with TRAP include hydraulic actuators, automotive shock absorbers, and electromechanical actuators.

When an input load is stepped or changed suddenly, the displacement of the main component (such as a piston or armature) oscillates. The oscillation settles down and the new equilibrium position or steady-state trend is achieved. This behavior can yield information about the device damping characteristics. TRAP uses this approach to determine damping characteristics of both installed and separated devices.

TRAP handles second-order, nonlinear dynamic systems with a nonconstant steady-state response curve. The system may have variable damping characteristics with damping as a function of position.

Input to TRAP consists of output force and displacement histories from when the device was subjected to a stepped load. From these data, TRAP predicts the force magnification (transfer function) and response phase angles as functions of input frequency. The program generates output for graphical presentation of damping and stiffness characteristics as well as force magnification and phase angle.

TRAP is written in FORTRAN IV for batch execution and has been implemented on a CDC CYBER 170-series computer with a central memory requirement of approximately 70K (octal) of 60-bit words. The TRAP program was developed in 1982.

This program was written by Lawrence D. Blackman of Rockwell International Corp. for **Johnson Space Center.** *For further information, Circle Z on the COSMIC Request Card.*
MSC-20590

MiniBriefs describe NASA innovations and reports in an abbreviated format. Readers desiring additional information on these items should request the Technical Support Packages (TSP's), available in most cases, which can be obtained by using the TSP Request Card at the back of this issue.

Prewhirl Jet Model

A mathematical model provides information to design jet-mixing parameters.

A simple, accurate model of centrifugal or rocket-engine pumps provides information necessary to design the inducer backflow deflector, backflow eliminator, and prewhirl jet in jet-mixing zones. In this model, the axial- and whirl-velocity components are decoupled while the radial-velocity and boundary-layer effects are neglected. A jet design based on this model shows improvement in inducer suction performance and reduced cavitation damage.

This work was done by Sen Y. Meng, Masumi Jensen, and Eugene D. Jackson of Rockwell International Corp. for **Marshall Space Flight Center.** *For further information, Circle 89 on the TSP Request Card.*
MFS-19826

Measuring Side Loads on Bolts

Transverse loading can be correlated with torque data.

Side loads on a clevis bolt can be measured quickly and easily. Such loads can be introduced during assembly of the bolt and can affect its operation. Now, unwanted loads can be determined quantitatively and corrected.

A hexagonal wrench socket is machined into the end of the clevis bolt. The bolt and fittings are brought together at points where side loads are created, and the relationship of the side load versus torque is measured and plotted. The clevis bolt is then assembled to its mechanism, and with a torque wrench inserted in the hexagonal wrench socket, a torque reading is made. The load is estimated from the load-versus-torque calibration. If the load is too high, fasteners on the clevis are loosened, adjusted, and retightened.

This work was done by Thomas O. Killgrove of Caltech for **NASA's Jet Propulsion Laboratory.** *For further information, Circle 102 on the TSP Request Card.*
NPO-15705

Eddy-Current Reference Standard

An eddy-current reference standard is stable over long time periods.

Magnetic properties of metallic reference standards can be duplicated and stabilized for eddy-current coil measurements over long times. The concept uses precisely-machined notched samples of known annealed (austenitic) materials as reference standards. The dimensions of the machined notches result in the same amplitude of eddy-current response as in samples with variations in magnetic characteristics, and are stable over long time periods. The technique is useful in monitoring possible material transformations from austenite to martensite.

This work was done by Howard H. Ambrose, Jr., of Rockwell International Corp. for **Marshall Space Flight Center.** *No further documentation is available.*
MFS-19824

Flexible Liquid-Transport Tube

Tubes with zipperlike access allow addition or removal of liquid.

A flexible tube with zipper-type arrangements of U-shaped side ribs and top plates allows liquids to be both transported and removed. The individual sections are mounted on skids, which form flap seals with the flexible covers by holding the heads down against the tops of the U-shaped trough, thus maintaining the seal. As the access device moves along the top of the tube, the cover vertebra is lifted upward to allow material to be added to or removed from the flow within the tube.

This work was done by Earl R. Collins, Jr., of Caltech for **NASA's Jet Propulsion Laboratory.** *For further information, Circle 103 on the TSP Request Card.*
NPO-15761

Conserving Purge Gases

A two-step flow control adjusts to dimensional changes in purged equipment.

Programing the flow rate of helium purge gas in two steps helps conserve the supply of the gas. The helium flows over the seals in a turbopump, preventing oxidizing gases from contacting them. At the start of the operation, pump clearances are relatively large; however, as the parts heat up, the clearances decrease and less flow of purge gas is needed.

Two pressure-actuated valves provide the two-step control. When the turbopump starts, helium flows through both valves. As the pump operates, its parts expand, the clearances decrease, and back pressure builds up on the valves. At a preset back pressure value, one of the valves closes, reducing the helium flow.

Initially, the flow rate is 265 std ft^3/min. (75 $stdm^3$/min). This is reduced to 150 $stdft^3$/min (42 $stdm^3$/min) after 150 seconds.

This work was done by Ken Kan, Lorin Blewett, and Tom Nelson of Rockwell International Corp. for **Marshall Space Flight Center.** *For further information, Circle 104 on the TSP Request Card.*
MFS-19625

Selecting Flatpack Lead-Forming Dies

The die is selected optically.

An optical instrument accurately records the unformed-lead offset for each flatpack and provides better fit of the flatpack to the printed-wiring board. The lead-forming operator enters the data into a prepared tabular matrix to determine which lead-forming die is best to use. Due to the usually low variation in lead offset from sample to sample, the measurements of only one or two flatpacks per lot are sufficient to determine acceptance or rejection of the entire lot.

This work was done by Edwin L. Choate of Honeywell Inc., for **Marshall Space Flight Center.** *For further information, Circle 105 on the TSP Request Card.*
MFS-25951

Coilable-Column Development

Design changes for longeron columns allow fabrication of larger structures.

Double-laced, coilable lattice columns were manufactured in 20-ft. (6-m) lengths and 30-in. (0.9-m) diameters. The fiber content and the catalytic percentage are two independent variables, each affecting the properties of the final product. Parametric studies indicate that glass/epoxy composites are superior to graphite in this application because they exhibit higher strain limits. Pultrusion was selected as the manufacturing process for the evaluation of longeron materials and engineering and design changes.

This work was done by Peter R. Preiswerk, Laurence A. Dinley, and Karl Knapp of Astro Research Corp. for **Marshall Space Flight Center.** *For further information, Circle 106 on the TSP Request Card.*
MFS-27032

Maintaining Constant Load Cell Temperature

An insulated enclosure allows accurate weight measurements under varying environmental conditions.

A thermal-insulation and temperature-compensation device maintains a constant temperature environment for load cells. At constant temperature, the cells measure weight accurately and reproducibly.

A box encloses the load cell and allows an 8 in. (20 cm) clearance around the cell. A light bulb acts as the heat source to maintain the desired temperature. The box is insulated with fiberglass material attached to the inside surfaces. A copper thermocouple connected to a controller regulates temperature.

Both floor-type and hanging-type load cells use the same basic insulated box. Special holes must be added for supports or eyebolts for hanging.

This work was done by George D. Van Mark of Beech Aircraft Corp. for **Johnson Space Center.** *For further information, Circle 107 on the TSP Request Card.*
MSC-20333

Detection of Gas Slugs in Heat Pipes

Slugs 1 in. (25 mm) in length can be detected.

A temperature-sensing system detects the presence of gas slugs in heat

(continued on next page)

pipes. The system is designed for operation between zero and −70° C and can detect noncondensable pockets of gas that result from the decomposition of ammonia cooling fluid.

A manifold is positioned concentrically around the heat pipe. It contains holes 1/16 in. (1.6 mm) in diameter spaced 1/2 in. (13 mm) apart along a straight line for the entire length of the condensing section of the heat pipe. Vaporized liquid nitrogen is passed through the holes to produce a high, uniform heat-transfer rate along the pipe outer surface, and multiple thermocouples are used to detect the temperature discontinuities that result from internal gas slugs.

This work was done by Jack A. Jones of Caltech for **NASA's Jet Propulsion Laboratory.** *For further information, Circle 108 on the TSP Request Card.*
NPO-16064

A Positive-Shutoff Fuel Valve

This ball valve is shut by a pneumatic actuator.

A pneumatically-actuated ball valve utilizes continuous-contact ball-seat seals and dynamic delta seals in lieu of bellows to seal against low-pressure leaks in fuel-supply lines. The seat seal is pressure-balanced as well as spring-loaded by the delta seal springs. The higher the inlet pressure becomes, the better the sealing characteristics.

The ball-valve position is held open by an actuator until a signal is given. The actuator operates from a single three-way solenoid valve connected to a pneumatic supply. When the solenoid is activated, pressure is removed from one side of the actuator piston thus causing the actuator to close the valve.

This work was done by Jack Tolpen of Rockwell International Corp. for **Marshall Space Flight Center.** *For further information, Circle 109 on the TSP Request Card.*
MFS-19779

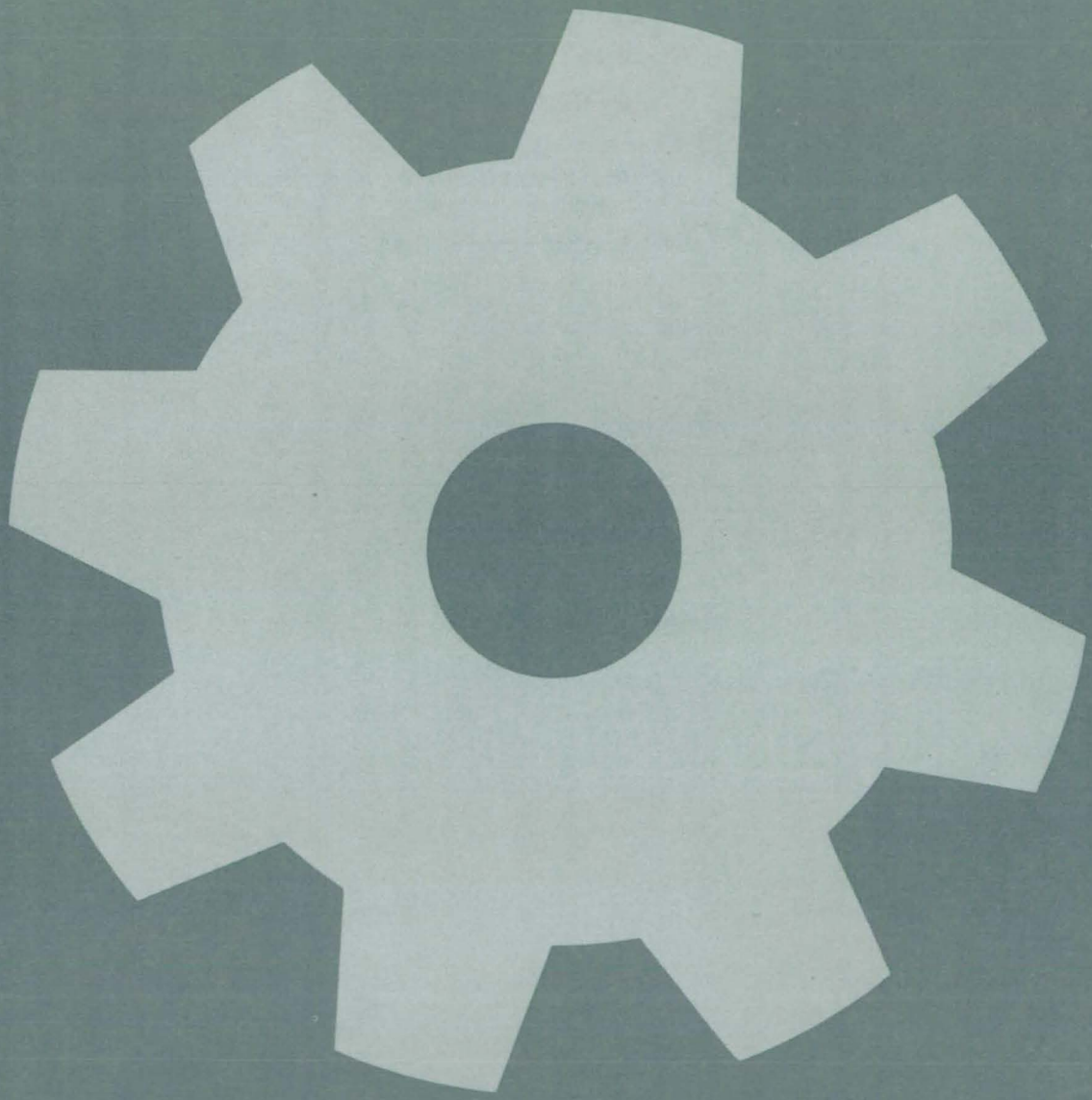

Stepped-Pin Clevis Resists Jamming

Pin modification may allow pyrotechnic release devices to operate more smoothly.

NASA's Jet Propulsion Laboratory, Pasadena, California

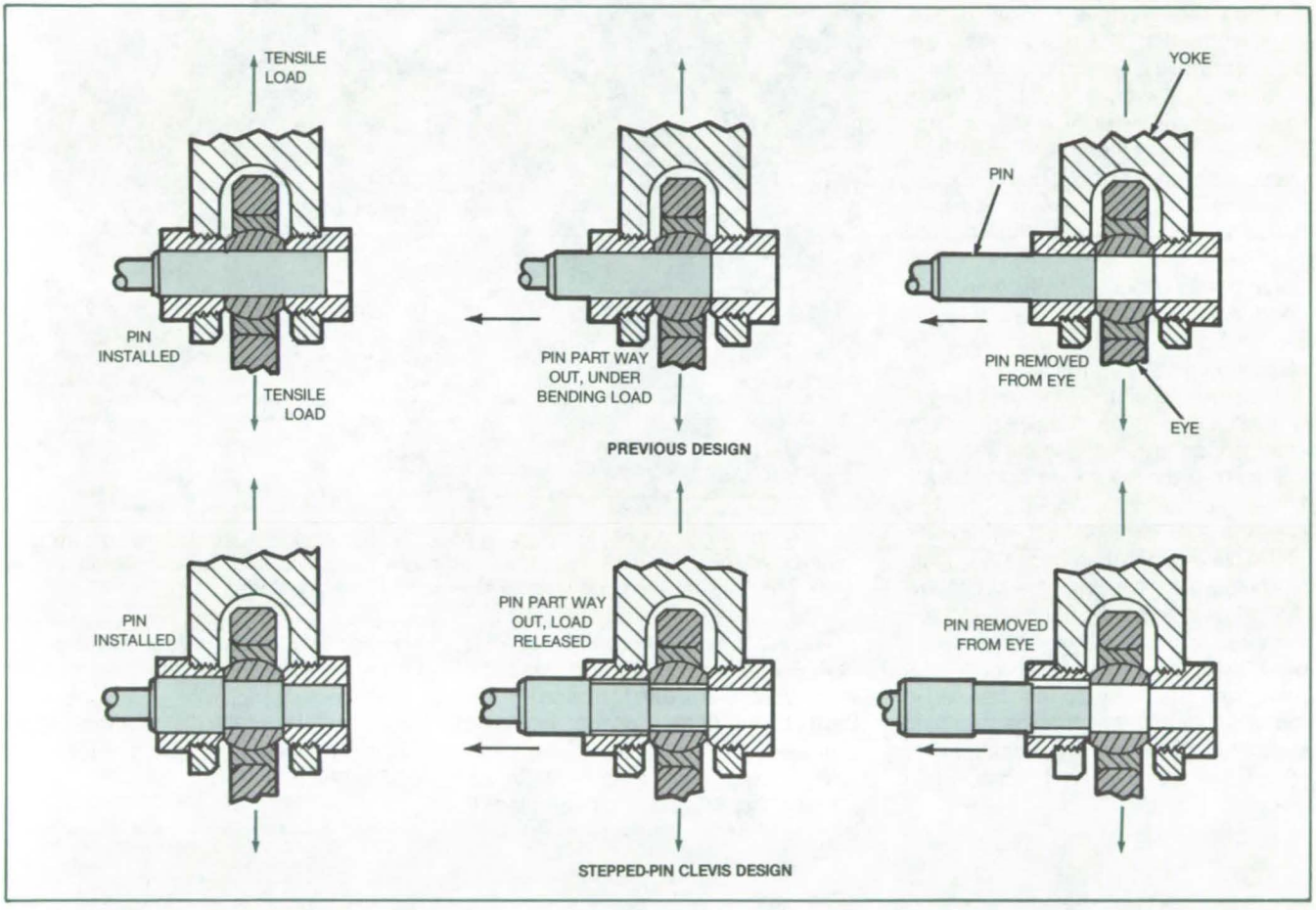

The **New Clevis Pin** (below) has stepped diameters to prevent it from bending as it exits the yoke. In contrast, a conventional unstepped clevis pin (above) may bend and jam as it is withdrawn.

Quick-release mechanisms that incorporate explosively-driven clevis pins may be less vulnerable to jamming with a new stepped-pin design. Pin ejection should also require less energy because the pin bears a frictional side load during a shorter portion of its travel.

As shown in the figure, the pin has three steps. The largest diameter fits in the yoke on the side from which the pin is pulled (the left side in the figure). The middle diameter fits in the clevis eye, and the smallest diameter fits in the other (right) side of the yoke.

When the pin begins to move out, the middle portion continues to bear the load of the clevis eye, while the large and small portions continue to transmit the load to the sides of the yoke. Since both ends of the pin remain in the yoke, the pin is restrained against bending and jamming in the left hole.

When the middle and smaller portions simultaneously pull out of the clevis eye and right yoke half, respectively, the load is suddenly removed from the pin and yoke. This permits the pin to be pulled the rest of the way out easily, without jamming.

The pin must be pulled quickly, before the vertical load pulls the eye against the small-diameter part of the pin. Thus, the stepped-pin design is suitable for explosive- and possibly hammer-driven pin pullers, but may not work with manual pin pullers.

This work was done by Thomas O. Killgrove of Caltech for **NASA's Jet Propulsion Laboratory.** *For further information, Circle 110 on the TSP Request Card.*

NPO-15834

Forklift Support Dolly

Long, heavy loads are handled safely.

Goddard Space Flight Center, Greenbelt, Maryland

Large metal plates [typical dimensions 6 ft by 12 ft by 3 in. (1.8 m by 3.6 m by 8 cm)] are safely moved between machine-shop work areas by a forklift truck, an auxiliary dolly, and four large C-clamps. These items are used if an overhead crane is not available.

Normally, a large metal plate has to be loaded on a forklift with the long side perpendicular to the direction of travel. Since the long side is wider than most doorways, aisles, or corridors, a forklift cannot be used to transport the large plate through these areas.

Instead, the plate is laid out lengthwise along the truck axis, with one end clamped to the forklift and the other end clamped to the dolly (see figure). With this arrangement, the minimum width of passage is determined by the short side of the plate rather than by the long side.

The pivoting wheels on the dolly allow the forklift to move the plate around corners and to maneuver it through doors or other tight spaces. As an additional advantage, the technique can be used to move plates that weigh twice the lifting capacity of the forklift, because the forklift and the dolly each support half the weight.

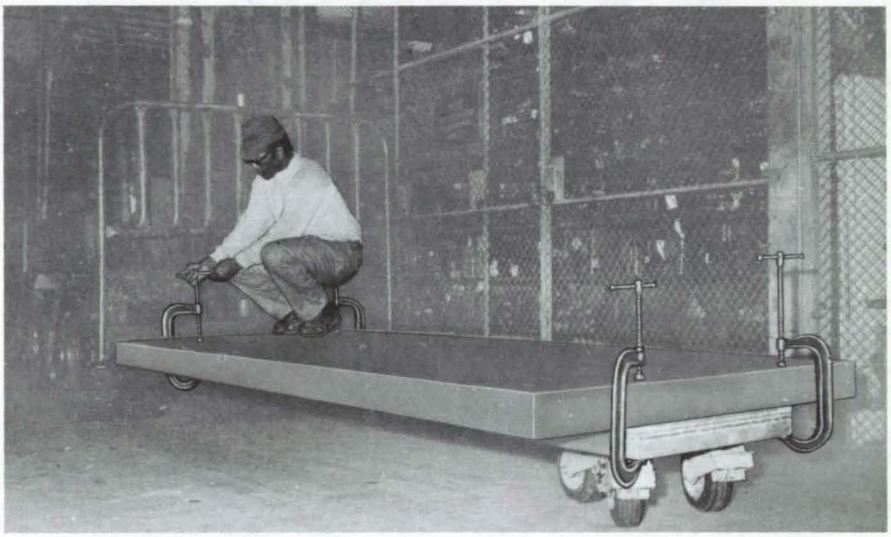

The **Forklift Support Dolly** enables an operator to manipulate safely large sections of material (in this case, metal plate) around corners and through narrow aisles and doorways. The dolly has pivoting tandem wheels for maneuverability.

This work was done by William Young of A. & M. Machine Co. and Howard C. Witcher of **Goddard Space Flight Center.** *No further documentation is available.*

This invention is owned by NASA, and a patent application has been filed. Inquiries concerning nonexclusive or exclusive license for its commercial development should be addressed to the Patent Counsel, Goddard Space Flight Center [see page A5]. *Refer to GSC-12916.*

Faster Response for Memory-Metal Actuators

Cooling is accelerated by attaching a Peltier junction.

NASA's Jet Propulsion Laboratory, Pasadena, California

Active thermoelectric cooling via the Peltier effect has been proposed to speed the response of memory-metal actuators. The operation of these devices is based on cycling between rigidity or springiness above the critical temperature and limpness or malleability at lower temperatures.

The response of a memory-metal actuator can be made very rapid during the heating portion of the cycle because the electrical heating current can be made to flow in the memory element itself. The heating response can also be speeded by maintaining the element at a standby temperature slightly below critical. In either case, passive cooling by contact with the surroundings usually takes longer than heating and is characterized by an asymptotic approach to the standby temperature.

To speed cooling, a Peltier junction is mounted in thermal contact with the actuator element. In the Peltier effect, an electric current carries heat to or from a junction between two dissimilar metals, the direction of heat flow depending on the direction of the current and the particular metals used. The direction of the current is opposite to that of the same two metals operating as a thermocouple.

Almost any pair of dissimilar metals could be used, and the memory metal could even serve as one of the Peltier elements. The cold plate of the Peltier

junction would be shaped and situated for optimum thermal contact with the memory metal. The design might call for permanent contact, intermittent contact depending on the actuator position, flexing with the actuator motion, or other configurations.

With active cooling, the actuator would be rapidly cycled by alternately turning on the heating and Peltier (cooling) currents. Depending on the relative heating and cooling parameters of the memory metal and the Peltier junction, it may be possible to use the Peltier junction for both heating and cooling by simply reversing the junction current at the actuation-cycle frequency. In that case, only one power supply or pulse source would be needed.

This work was done by Carl F. Ruoff of Caltech for **NASA's Jet Propulsion Laboratory.** *For further information, Circle 111 on the TSP Request Card.*

Inquiries concerning rights for the commercial use of this invention should be addressed to the Patent Counsel, NASA Resident Office-JPL [see page A5]. Refer to NPO-16120.

Sealing Mechanical Cryogenic Coolers

A thin-walled metal bellows eliminates sliding surfaces.

NASA's Jet Propulsion Laboratory, Pasadena, California

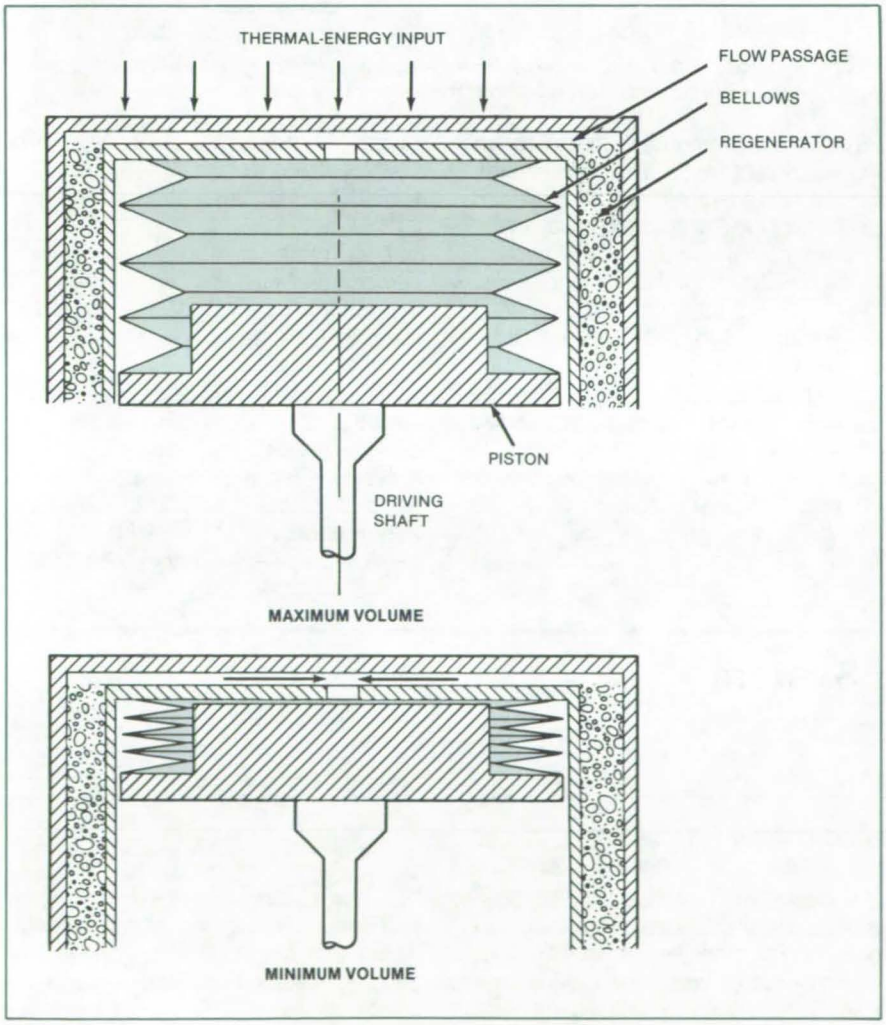

Metal Bellows, incorporated in the displacer design, provide a nonrubbing dynamic seal. The lifetime of a cryogenic cooler will no longer be limited by the loss of the sealing material and by the deterioration of the regenerators due to clogging by seal debris.

Metal bellows are used to seal Vuilleumier and Stirling-cycle cryogenic coolers, replacing sliding seals that failed after only 3,000 hours of service. The bellows are expected to have a much longer service life, although test data are not yet available.

A seal for the displacer of a cryogenic cooler is shown in the figure. The volumes in the hot and cold cylinders of the Vuilleumier cooler increase and decrease during the cycle by the expansion and contraction of the bellows. The bellows, which are mechanically attached to the moving piston and the stationary cylinders, are fully collapsed when the piston reaches the position of minimum volume. As a result, dead volume in the cycle is minimal.

This work was done by Robert Richter of Caltech for **NASA's Jet Propulsion Laboratory.** *For further information, Circle 112 on the TSP Request Card.*
NPO-15139

Vacuum Seal Permits Limited Rotation

All-metal seal allows ±45° rotation.

NASA's Jet Propulsion Laboratory, Pasadena, California

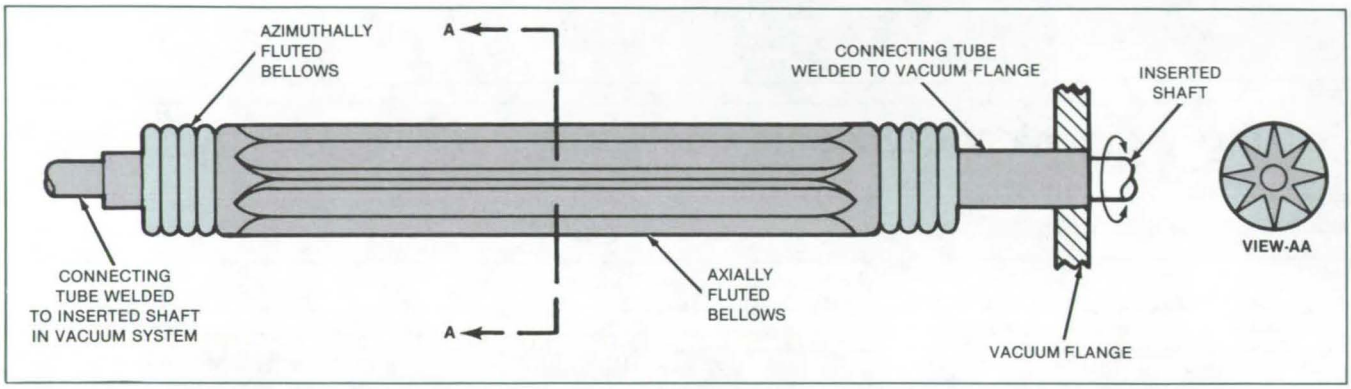

The **Axially Fluted Portion** of the bellows assembly permits 45° of relative rotation of the ends about the cylindrical axis. Thus, a sample on a rod extending through the bellows into the vacuum system can be rotated without the loss of vacuum.

A flexible metal seal permits ±45° rotation of an object in a vacuum chamber. It was originally designed for rotation of sample probes in electron spectroscopy for chemical analysis (ESCA), although other applications are likely.

The seal is made from two cylindrical azimuthally fluted bellows attached to the ends of a cylindrical axially fluted bellows, with connecting tubes at both ends (see figure). In ESCA, the sample probe is inserted into the connecting tube at one end and welded in place. The connecting tube at the other end is inserted into the vacuum system through a vacuum-tight flange. With the vacuum-system end fixed against rotation, the flexibility of the axially fluted bellows permits the sample tube to rotate approximately ±45° about the cylindrical axis.

The bellows sections can be made of 3 to 5 mils (0.08 to 0.13 mm) thick nickel or other metal compatible with the vacuum system. The parts can be fastened together by inert-gas-shielded arc welding. It may also be possible to make the seal as a single piece by electrodeposition or pressure forming. The all-metal construction is bakable and outgasses less than do conventional O-rings on a rotary shaft. The seal should be vacuum tight to 10^{-11} torr (10^{-9} N/m^2).

This work was done by Frank Lombardi of Caltech for **NASA's Jet Propulsion Laboratory.** *For further information, Circle 113 on the TSP Request Card.*

This invention has been patented by NASA [U.S. Patent No. 4,311,057]. Inquiries concerning nonexclusive or exclusive license for its commercial development should be addressed to the Patent Counsel, NASA Resident Office-JPL [see page A5]. Refer to NPO-15115.

Automatic Coal-Mining System

Coal cutting and removal would be done with minimal hazard to people.

NASA's Jet Propulsion Laboratory, Pasadena, California

A proposed automatic coal-mining system would cut coal, grind it, mix it with water to make a slurry, and transport the slurry to the surface. The system would include closed-circuit television monitoring, laser guidance, optical obstacle avoidance, proximity sensing, and other features for automatic control.

The system is intended for longwall mining, in which the coal seam is divided into several blocks at least 600 feet (183 m) wide by corridors or "entries," which allow the movement of equipment and materials. Moving along an entry, an extracting machine cuts coal from the face of a block (see figure) to a depth of a few feet (about a meter). An extractor has two cutting heads, one at each end.The extractor moves on crawler tracks that are reversed at the end of each pass so that coal can be cut in the opposite direction. Thus, the extractor does not have to retreat in "deadhead" fashion to begin the next cut, and its productivity is increased.

The cut coal falls on loading ramps, where gathering arms move it to central screws. The screws crush the coal and feed it to the transport tube.

Water is sprayed on the extractor drums as they cut to keep down explosive dust and to promote visibility. More water is added in the screws to convert the coal powder into a low-viscosity slurry.

A laser beam guides the extractor along the face, ensuring a straight cut. Connected to the slurry-transport subsystem, the laser and its reflector are moved forward automatically with each pass of the extractor. Any deviation from the path set by the beam represents a change in the direction of travel of the extractor; and an onboard controller changes the speed of one crawler track relative to the other, thereby adjusting the direction of travel.

A sonic or optical proximity sensor detects the approach of an entry and stops the extractor to prevent a collision with the far wall of the entry. The proximity sensor also guides the reversing maneuver and the start of a new cut.

The transport tube is made in repeating sections, with each section mounted on an individual skid to allow lateral motion. As the extractor moves along, it pulls each section toward it and connects with that section in turn.

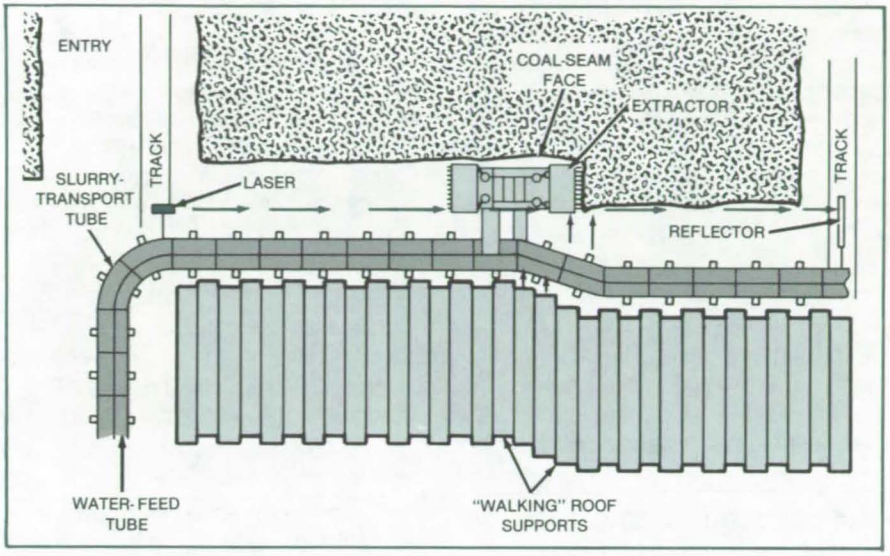

In the **Automatic Coal Mine,** the cutting, transport, and roof-support movement are all done by automatic machinery. The exposure of people to hazardous conditions would be reduced to inspection tours, maintenance, repair, and possibly entry mining.

The roof supports move forward in alternation, "walking" by being lifted off the floor by hydraulic pistons, then propelled by horizontal pistons. Each alternate support unit supports itself on adjacent neighbors and propels itself by pushing on its neighbors. The units that are not moving are holding up the roof. The movement of the roof supports may be controlled remotely by human operators watching via television, or they may be made to move automatically on the basis of the movement of the slurry-transport tube.

This work was done by Earl R. Collins, Jr., of Caltech for **NASA's Jet Propulsion Laboratory.** *For further information, Circle 114 on the TSP Request Card.*
NPO-15861

Computer Programs

These programs may be obtained at very reasonable cost from COSMIC, a facility sponsored by NASA to make new programs available to the public. For information on program price, size, and availability, circle the reference letter on the COSMIC Request Card in this issue.

The Effect of Wind on the Aerodynamic Resistance of Highway Vehicles

Program computes the effect on fuel consumption of statistical wind and vehicle speed.

CARYAW predicts the effects of wind on the aerodynamic resistance of vehicles. It can determine the effect of winds on fuel consumption. It can also determine the effects of vehicle speed on fuel consumption for a wide variety of wind conditions.

CARYAW uses simple formulations for the engine map and for the inertia of rotating masses. (These may be altered to suit the user, but with appropriate changes in the rest of the program.) Rolling resistance is assumed to be independent of time. Several representative wind spectra, which are assumed to be equally probable from any direction, are used for variations in wind speed and direction. The two EPA driving cycles, urban and highway, are contained within the program.

The effects of the wind on aerodynamic resistance are quantified in terms of fuel required to overcome aerodynamic resistance and overall fuel consumption. The results can also be interpreted as a correction factor to the zero-wind aerodynamic drag coefficient.

Many cases may be computed to develop statistical trends in the wind-effect data. The vehicle characteristics of frontal area, total weight, and lift-to-drag ratio must be selected for each case. Also, the power requirements of auxiliaries and accessories and the rolling resistance must be specified.

This program was written by Bain Dayman, Jr. of Caltech for **NASA's Jet Propulsion Laboratory.** *For further information, Circle bb on the COSMIC Request Card.*
NPO-14771

Standard Fastener Library

Fastener details are inserted as the drawing is constructed on a graphics terminal.

When available software packages do not provide for graphic representation of details of fastener hardware, the

(continued on next page)

operator must individually construct each nut and bolt used on the drawing. This is a time-consuming operation, especially when large assembly or installation drawings are involved.

A program for use with a graphics system creates a library of standard fastener hardware. The programs are categorized by fastener geometric shape with tabulated sizes. Fastener details may be recalled by configuration and size for insertion into a drawing on the screen. This program has been used in the production of engineering drawings for the Space Shuttle orbiter.

This program is written in PEP (Parametric Element Processor) for the Computer Vision Model 109S computer with the CADDS 3 graphics software. This program was developed in 1982.

This program was written by Judy J. Tejwani, Thomas R. Kelly, and Michael L. Marke of Rockwell International Corp. for **Johnson Space Center.** *For further information, Circle cc on the COSMIC Request Card.*
MSC-20645

MiniBriefs describe NASA innovations and reports in an abbreviated format. Readers desiring additional information on these items should request the Technical Support Packages (TSP's), available in most cases, which can be obtained by using the TSP Request Card at the back of this issue.

Aerodynamic Design of Road Vehicles

A guidebook presents design strategy and data for reducing the aerodynamic drag.

A guidebook discusses the design of road vehicles to reduce aerodynamic drag. Relatively little is known about the aerodynamics of bluff bodies in the vicinity of the ground. This body of knowledge is much less developed than that pertaining to aircraft. The book presents a strategy for integrating aerodynamic design into vehicle design. Supporting information and procedures are also presented. Elements of the procedures are based on wind-tunnel tests of generic small-scale models and full-scale prototypes of some vehicles. The book is written for readers who may lack expertise in aerodynamics.

This work was done by Donald W. Kurtz of Caltech for **NASA's Jet Propulsion Laboratory.** *Further information may be found in NASA CR-163744 [N81-12943/NSP], "Aerodynamic Design of Electric and Hybrid Vehicles: A Guidebook" [$11.50]. A copy may be purchased [prepayment required] from the National Technical Information Service, Springfield, Virginia 22161.*
NPO-15474

Inexpensive Pressure-Relief Valve

Simple device vents excess low-pressure gas.

An inexpensive pressure-relief valve can be built from polyvinylchloride pipe. The valve is suitable for low-pressure — 25 to 50 cm of mercury — and flow rates up to 14 m^3/min.

The valve operates on the principle of a deadweight plug in a gas column. A pipe 8 inches (20.3 cm) in diameter is mounted vertically on a horizontal pipe. The vertical pipe contains a ring of slots above the sealing surface. A pipe 6 inches (15.2 cm) in diameter and capped at its lower end is positioned inside the 8-inch pipe so that it rests on a sealing ring at the junction with the horizontal pipe. The 6-inch pipe is loaded with lead shot to press it tightly against a sealing ring. As the gas pressure increases, the weighted pipe rises, allowing gas to escape from the slots.

This work was done by Eugene A. Theordore of Rockwell International Corp. for **Johnson Space Center.** *For further information, Circle 115 on the TSP Request Card.*
MSC-20518

Bolt Inserts for Lightning Protection

Older, more complex grounding methods are eliminated.

Stainless-steel bolt fasteners have adequate grounding paths for the protection of structures against lightning strikes. The fasteners are particularly useful in sections where an insulating material is required, such as the thermal panels of an external storage tank.

Application involves threading and inserting the fasteners into drilled boltholes and tightening the bolts with 25 ft-lb (34 N-m) of torque. Conductivity through the fasteners ranges from 0.65 to 0.81 milliohm, which is well below the 2.5-milliohm specification required for adequate lightning protection.

This work was done by Kenneth O. Hambrock of Martin Marietta Corp. for **Marshall Space Flight Center.** *For further information, Circle 116 on the TSP Request Card.*
MFS-25918

Solar-Powered Flywheel

Energy-storage system has 20-year lifetime.

An electrical power source consisting of a flywheel and an electronic control system stores solar energy. The flywheel, developed for space vehicles, features good weight-to-energy-storage ratios and can be used as a control gyroscope for maneuvering.

Exposed to Sunlight, the flywheel accelerates while powering other loads in the vehicle. When Sunlight is not available, the control system regenerates electrical power from the moving flywheel and is able to maintain a constant-voltage output in the face of changing loads and changes in the flywheel speed.

This work was done by Frank J. Nola of **Marshall Space Flight Center.** *For further information, Circle 117 on the TSP Request Card.*

Inquiries concerning rights for the commercial use of this invention should be addressed to the Patent Counsel, Marshall Space Flight Center [see page A5]. Refer to MFS-25978

Clamp Secures Material to Cylinder Base

Two-part clamp can be assembled around a pipe or post, the ends of which are not free.

A two-part clamp effects repairs that require screen material to be clamped

around the base of a closed-end post. The clamp functions at temperatures from -360° to 1,040° F (-218° to 560° C). The clamp is forced against the screen material from one side of the post. To secure the clamp, its upper part, which is a knurled locking ring, is rotated 180° around the post. Resistance welding the clamp to the post and the locking ring to the lower part of the clamp permanently fixes the clamp in place, preventing thermal cycling from loosening the clamp.

This work was done by Yan S. Tam of Rockwell International Corp. for **Marshall Space Flight Center.** *For further information, Circle 118 on the TSP Request Card.*
MFS-19479

Remotely Operated Gripper Tracks Applied Force

Operator "feel" is incorporated into a new design.

A remotely controlled gripper grasps, holds, and maneuvers items that are not equipped with a grapple fixture and have no preplanned interface with the gripper. The parallel jaws of the gripper have elastic surface pads. Force sensors are mounted in the fixed jaw. The force applied by the operator at the control lever produces an output from the command potentiometer, which is proportional to the applied force. A potentiometer tracks the moving-jaw position. The command moves the jaw until the output of the force sensors in the jaw balances the command signal.

This work was done by Gene C.Burns of McDonnell Douglas Corp. for **Johnson Space Center.** *For further information, Circle 119 on the TSP Request Card.*
MSC-20241

Pillar-Trimming System

Trimming and reinforcing of coal pillars allows more coal recovery.

A conceptual coal-pillar-trimming machine uses two counterrotating cutting drums to take the corners off roof-support pillars in coal mines. The coal pillars trimmed to a stress-justified curved shape would enable recovery of more coal than by previous methods.

The machine wraps a restraining cyclone fence around the pillar to reinforce it and keeps the tension on the wire fence tight as the machine rocks back and forth, trimming the coal pillar. Having finished trimming, the machine closes the fence to provide permanent support to the pillar and thus to the mine roof.

This work was done by Earl R. Collins, Jr., of Caltech for **NASA's Jet Propulsion Laboratory.** *For further information, Circle 120 on the TSP Request Card.*
NPO-15848

Performance Testing of the DOE Electric Test Vehicle

Report describes the total system testing and evaluation of an electrically powered automobile.

The testing of the DOE ETV-1, an advanced electrically powered automobile, is described in a 14-page report. Road load data from controlled track tests were used to determine realistic parameters for dynamometer testing. Test results include an analysis of energy flow through the major subsystems and incorporate aerodynamic and rolling losses under various cyclic and constant-speed conditions.

Charge and discharge characteristics of the propulsion batteries were measured. Estimates of battery performance and automobile range as a function of vehicle speed are also presented. An appendix describes vehicle subsystems, including chassis, dc motor and drive train, electronics, and batteries.

This work was done by Donald W. Kurtz, James A. Bryant, and Theodore W. Price of Caltech for **NASA's Jet Propulsion Laboratory.** *To obtain a copy of the report, Circle 121 on the TSP Request Card.*
NPO-15660

Inert-Gas Electrical-Discharge Machining

A dry EDM process uses inert gas as the dielectric.

Holes in complicated hardware can be successfully drilled by a dry EDM process that uses a tubular copper electrode and argon or helium gas as the dielectric medium. In this procedure bright contamination-free holes have been drilled in a testpiece of a nickel alloy, using the inert gas to flush debris from the holes. The fittings and supplies required for this operation are simple and inexpensive; the apparatus is portable.

This work was done by Ven Ramani and Michael L. Cassidenti of Rockwell International Corp. for **Marshall Space Flight Center.** *No further documentation is available.*
MFS-19778

Countersink Drill

Tool performance and service life are increased.

An efficient drill design for countersinking or metal drilling uses only two flutes instead of three and is made of carbide instead of "high-speed" steel. This design improves the drill tolerance and increases effective tool life. Since the tool can operate at approximately twice the drill speed of previous three-flute, high-speed steel designs, the amount of drill time required is reduced. Improved tool wear and more accurate machining are projected.

This work was done by Rudolph J. Hernandez of Rockwell International Corp. for **Marshall Space Flight Center.** *For further information, Circle 122 on the TSP Request Card.*
MFS-19852

Two-Phase Wet/Dry Engine for Waste-Heat Recovery

A two-phase nozzle provides dry vapor by expansion from saturated liquid.

A novel supersonic fluid-expansion nozzle is used to vaporize toluene (or other drying-type organic liquid) by expansion through the two-phase region to drive an impulse turbine in a Rankine-cycle engine. The wet-to-dry expansion provided by the new nozzle eliminates the pinch-point limitations inherent in vapor-expansion Rankine-bottoming-cycle engines and eliminates the need for a boiler. When used to extract work from the heat energy in diesel exhaust at 340° C, the heat-utilization efficiency of the wet/dry engine is 0.19, versus 0.14 for a vapor expansion engine.

This work was done by David G. Elliott of Caltech for **NASA's Jet Propulsion Laboratory.** *For further information, Circle 123 on the TSP Request Card.*
NPO-15621

Kick-Free Pressure-Release Valve

A movable energy-absorbing sleeve improves safety.

A release valve for smoothly venting the buildup of gas pressure has been modified to reduce the kickback of the mechanism during discharge. The valve consists of a spring-loaded piercing lance connected to a pair of rollers that are held apart by a separator for keeping the lance in the cocked position. Removal of the separator actuates the lance to puncture a venting diaphragm and release the pressure.

A kickback force is imparted to the separator, however, which can present a safety hazard. A movable sleeve on the separator for absorbing the kickback effectively reduces or eliminates this force. The sleeve can be spring loaded or contoured to absorb high levels of force.

This work was done by Thomas O. Killgrove of Caltech for **NASA's Jet Propulsion Laboratory.** *For further information, Circle 124 on the TSP Request Card.*
NPO-16078

Magnetic Despinning System

Electrical coil reduces spinning and tumbling through eddy-current braking.

Based on the eddy-current phenomenon, a technique for stabilizing the orientation of Earth satellites may also have terrestrial applications. A large coil carrying many windings of insulated electrical conductors reduces the spinning or tumbling speed of orbiting satellites by one or two orders of magnitude. The coil or loop is loosely fitted around the satellite and is connected to a high-current power source. The induction of eddy currents into the skin of the satellite by the electromagnetic field produces torques that oppose the rotation.

This work was done by Georg F. Von Tiesenhausen of **Marshall Space Flight Center.** *For further information, Circle 125 on the TSP Request Card.*

Inquiries concerning rights for the commercial use of this invention should be addressed to the Patent Counsel, Marshall Space Flight Center [see page A5]. Refer to MFS-25966.

Memory-Metal Stepping Motor

A spring clutch is driven by a memory-metal actuator.

A compact stepping motor for applications that require high torque at slow speeds might be made with a helical-spring clutch and an electrically-heated memory-metal actuator. According to a proposal, the helical spring is anchored at one end and wound around the motor shaft. The other end of the spring is attached to an anchored memory-metal actuator that is horseshoe-shaped when hot, but relaxes to a straighter shape when cold.

An electric current heats the actuator, curling it into a horseshoe shape and causing it to pull on the spring. The spring tightens around the shaft and rotates the shaft slightly. When the current is turned off, the actuator relaxes, thereby loosening the grip of the spring on the shaft without rotating the shaft back to the original position.

This work was done by Robert S. Jamieson of Caltech for **NASA's Jet Propulsion Laboratory.** *For further information, Circle 128 on the TSP Request Card.*

Inquiries concerning rights for the commercial use of this invention should be addressed to the Patent Counsel, NASA Resident Office-JPL (see page A5). Refer to NPO-15482.

Diverter Lip for Seal

Thermal gradients in hydrogen-cooled platform seals are reduced.

A proposed one-piece design change for cooling turbine rotor disks eliminates the temperature differential that normally causes thermal stresses and cracks. The design adds a diverter lip to the platform seal, which strips off the cold boundary layer of hydrogen on the disk before the hydrogen gets to the shank region. Holes in the lip structure allow the hydrogen to exit. Analysis shows that average temperatures in the shank base area should increase from 583 R (324 K) to 1,300 R (2,340 K). This significantly reduces thermal gradients in the blade shank area and should eliminate cracks.

This work was done by E. D. Jackson, III and D. M. Johnson of Rockwell International Corp. for **Marshall Space Flight Center.** *For further information, Circle 127 on the TSP Request Card.*
MFS-19891

Measuring the Runout on a Rotary Shaft

The measuring system uses two orthogonal pistons.

The runout on a shaft, such as on a pump shaft in a liquid oxygen environment, can be measured by a device employing a pair of pistons placed 90 degrees apart and in contact with the shaft. The piston displacements are measured and compared to their initial positions to determine the total runout. Measurements with accelerometers will indicate if the runout occurred during a transient, a resonance, or a steady operation.

This work was done by R. F. Beatty and J. R. Fenwick of Rockwell International Corp. for **Marshall Space Flight Center.** *For further information, Circle 129 on the TSP Request Card.*
MFS-19694

Fabrication Technology

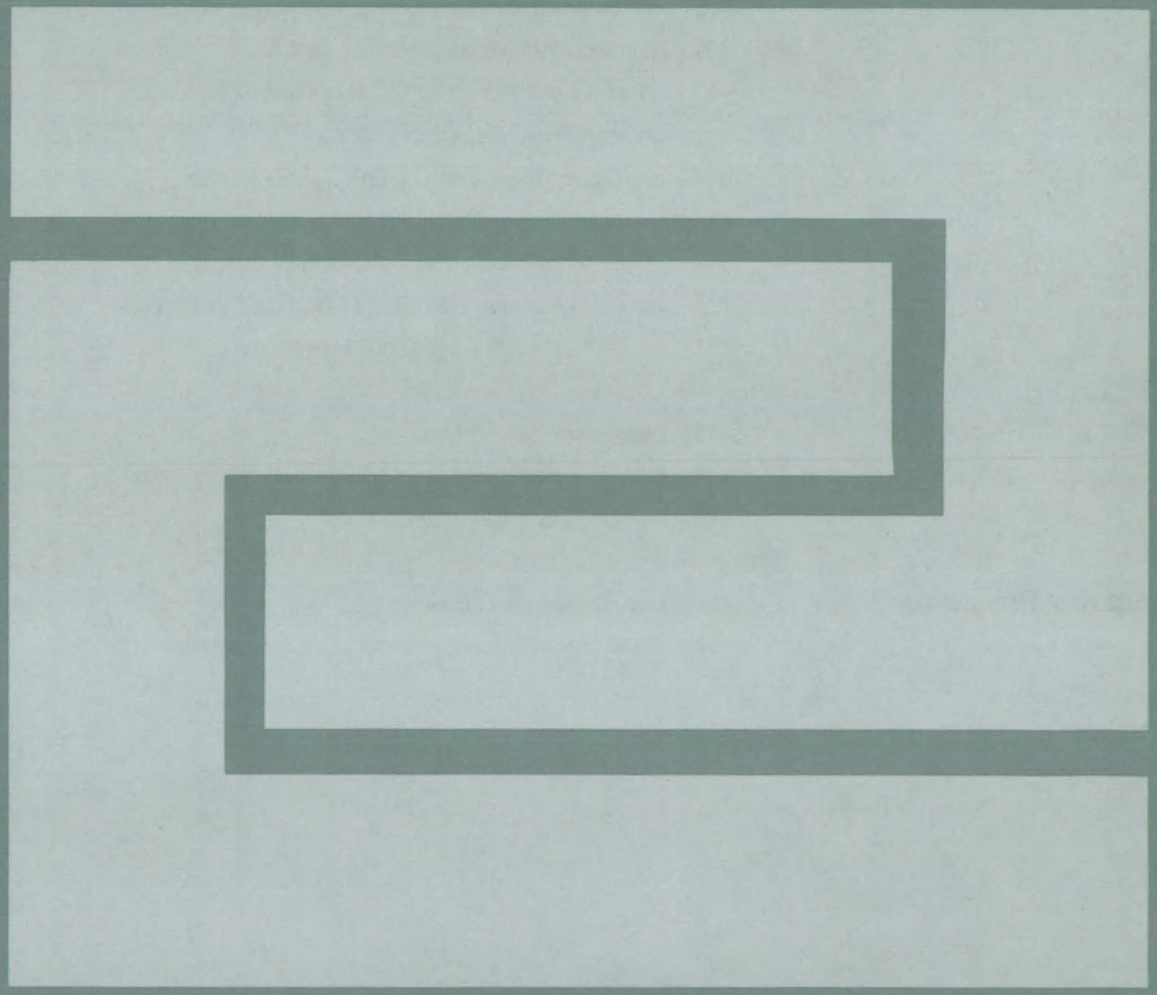

Two-Crucible Czochralski Process

The second crucible enables continuous melt replenishment.

NASA's Jet Propulsion Laboratory, Pasadena, California

A scheme for continuous melt replenishment increases the capacity of a Czochralski crystal-growing furnace. Since the melt is recharged during crystal growth, it is not necessary to shut down the furnace for recharging, and several boules can be drawn from the same melt. The results of this semicontinuous operation are higher production speed, lower cost, and good control of crystal quality.

A version of the improved Czochralski apparatus is shown in the figure. There are two crucibles: one from which the crystal is withdrawn and one for replenishment. For silicon growth, the crucibles would be made of quartz, with a typical inside diameter of 10 in. (30 cm).

Crystal growth is initiated by inserting a seed crystal into the melt on the end of the drawing rod, then slowly pulling the rod out. As in the conventional Czochralski process, the rod is slowly rotated as it is withdrawn, and the crucible is slowly rotated to stir the melt to compositional and thermal uniformity. Also as in the conventional Czochralski process, the diameter of the boule is controlled by an automatic system that varies the withdrawal speed in response to the optically sensed diameter of the meniscus between the melt and the boule.

A laser beam is reflected from the melt surface and focused by a lens onto an electro-optical position sensor. The beam is band-pass-filtered to suppress stray light and nonlaser wavelengths emitted by the incandescent melt. The position of the beam on the sensor, as indicated by the sensor output signal, indicates the melt level.

When the melt is lower than the preset level, the control system responds by turning on the auger motor to move silicon from the hopper into the replenishing crucible. (The replenishment silicon is doped to the concentration required in the grown crystal.) Alternatively or concurrently, the melt level can be adjusted by raising or lowering the replenishing crucible.

Liquid silicon flows through a thermally insulated, heated siphon to maintain equal melt levels in both crucibles. The siphon consists of the following concentric layers, inside to outside: a quartz tube of 7-mm inside diameter and 25-mm outside diameter, four series-connected lengthwise flexible graphite resistance heating tapes equally spaced about the circumference, a thermally and electrically insulating layer of silica tape, a protective layer of flexible graphite sheet, a second layer of silica tape, two layers of graphite felt one quarter of an inch (6 mm) thick, and a solid graphite shell. The inner quartz tube withstands the erosive and corrosive effects of the

(continued on next page)

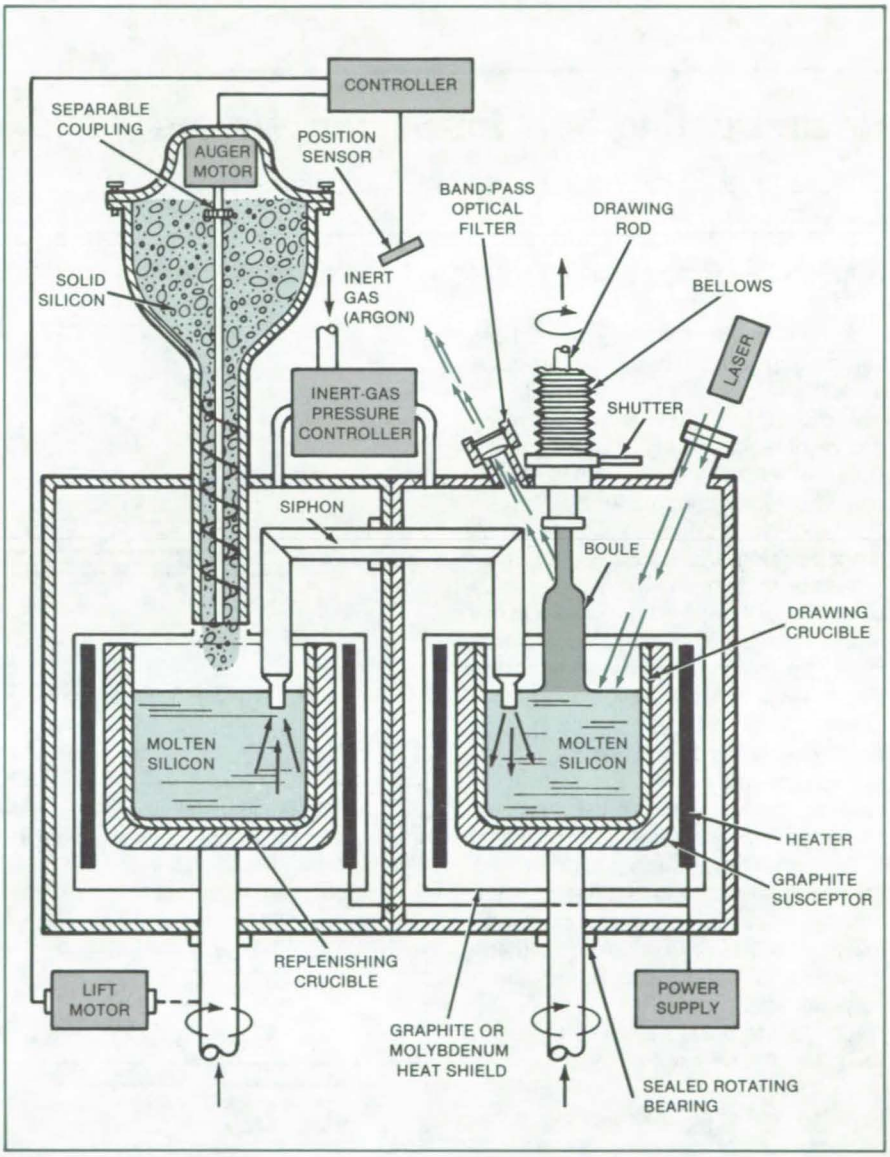

The **Replenishing and Drawing Crucibles** of this improved Czochralski apparatus are connected by a heated quartz siphon. When doped silicon is added to the replenishing crucible, liquid silicon flows into the drawing crucible, equalizing the two melt levels. The addition of new material is automatically controlled in response to the optically-sensed melt level.

1,500° C molten silicon. The silica and graphite layers provide thermal insulation and mechanical strength.

The entire furnace system is filled with argon or other inert gas to prevent the oxidation of the silicon. To start the siphon, the gas pressure in the replenishment chamber is raised above that of the withdrawal chamber until the liquid silicon flows through the quartz tube. Thereafter, the system is operated with equal gas pressure in both chambers.

When the boule has grown to full size (typically, 1 m long by 0.1 m in diameter), it is pulled up into the bellows. The shutter is then closed so that the boule can be removed from the bellows without exposing the furnace interior to the atmosphere. A new seeded rod can then be inserted into the bellows in preparation for drawing a new boule.

This work was done by George Fiegl and Walter Torbet of Siltec Corp. for **NASA's Jet Propulsion Laboratory.** *For further information, Circle 130 on the TSP Request Card.*
NPO-15110

Reciprocating Saw for Silicon Wafers

Concept would increase productivity and wafer quality.

NASA's Jet Propulsion Laboratory, Pasadena, California

A concept for cutting wafers from silicon ingots promises to produce smooth wafers at high rates with reduced blade wear. The concept involves a straight reciprocating saw blade and a slight rotation of the ingot between cutting strokes. Many parallel blades can be combined to cut many wafers simultaneously from the ingot.

In reciprocating cutting, a blade saws back and forth through the ingot. On the return stroke, however, there is a tendency for the diamond particles on the cutting edge of the blade to become dislodged. Consequently, the cutting edge quickly becomes dull and leaves a rough surface on the wafer: Productivity is reduced, and the wafer must therefore be put through a smoothing operation.

With the new cutting scheme the return stroke is through a different ingot. The blade passes between upper and lower ingots (Figure 1). As the blade moves to the left, the upper ingot engages the top cutting edge of the blade. As the blade moves to the right, the lower ingot engages the bottom cutting edge.

At the end of each stroke, the ingots are moved vertically as required to engage or disengage them with the blade. Each ingot is therefore sawed in one direction only; and the pulling out of diamond particles is minimized without wasting any of the blade movement.

Both upper and lower ingots are rotated slightly between cuts. This procedure distributes the cutting force over a smaller area of silicon, and more efficient cutting results (Figure 2).

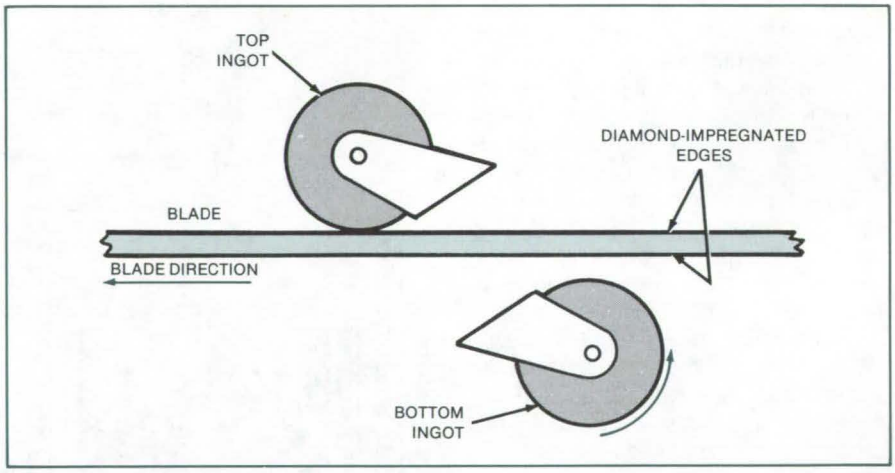

Figure 1. As the **Blade Moves Back and Forth,** it contacts first one and then the other of the two silicon ingots — but never both at the same time. The blade thus travels unidirectionally through a given ingot.

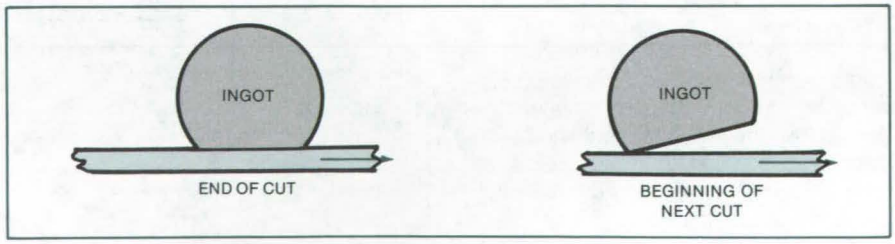

Figure 2. **Rotating an Ingot** slightly at the end of a cut presents a smaller contact area to the blade for the new cut. Cutting efficiency is thereby increased.

An ingot is rotated in a bracket. It is held in the bracket by a layer of wax or epoxy. As wafers are severed, they continue to be held in place individually by the layer. When the layer is removed by heat or a chemical reagent, the wafers are released.

This work was done by Andrew D. Morrison and Earl R. Collins, Jr., of Caltech for **NASA's Jet Propulsion Laboratory.** *For further information, Circle 131 on the TSP Request Card.*
NPO-15863

Production Line for Dendritic-Web Solar Cells

Proposed machinery would process 0.5 m^2 of silicon each minute.

NASA's Jet Propulsion Laboratory, Pasadena, California

A manufacturing concept has been worked out for producing 1- by 3-m solar-cell panels from dendritic-web silicon of 5-cm useful web width. The direct inclusion of web-growth furnaces in the production line is expected to result in lower costs than those of current production processes using silicon wafers sliced from Czochralski boules. The silicon-web input capacity of the line is 0.5 m^2/min, which corresponds to a total peak-power output of about 25 MW for 1 year of production. The line would employ about 18 production people per shift and would require about 3,650 ft^2 (340 m^2) of floorspace.

On its way to becoming part of a solar panel, the silicon is processed as follows (see figure): A total of 200 silicon-web furnaces is required to produce enough silicon web for one 25-MW processing line. As it emerges from a furnace, the web is wound on a reel. Fifty such reels are ganged on a mandrel for feeding through a laser cutter. The cut pieces, each 3 m long, are loaded into special frames, 50 pieces to a frame. To meet the throughput requirement, a frame must be processed every 15 minutes.

Each frame of web is washed in an organic solvent and dried in preparation for the junction-formation process. A protective oxide is formed on the front surface of the web and a boron-doped oxide on the back. After the boron is driven into the silicon, the material passes through a phosphorus-diffusion furnace and finally into an etching bath where the oxides are removed. This completes the formation of the photodiode junctions.

An antireflection coating and a photoresist layer are applied on the web material by dipping. A grid pattern is exposed onto the photoresist layer. The grid pattern is then etched through the photoresist and antireflection coating.

Before the remaining photoresist is removed, metalization layers are applied to both web surfaces using an evaporation process. Removing the remaining photoresist also removes the unwanted portion of the metalization, leaving the active, antireflection-coated surface of the web exposed. The remaining metalization is sintered and then plated with silver to form the current-carrying paths on the front of the solar cells. The webs are again cleaned.

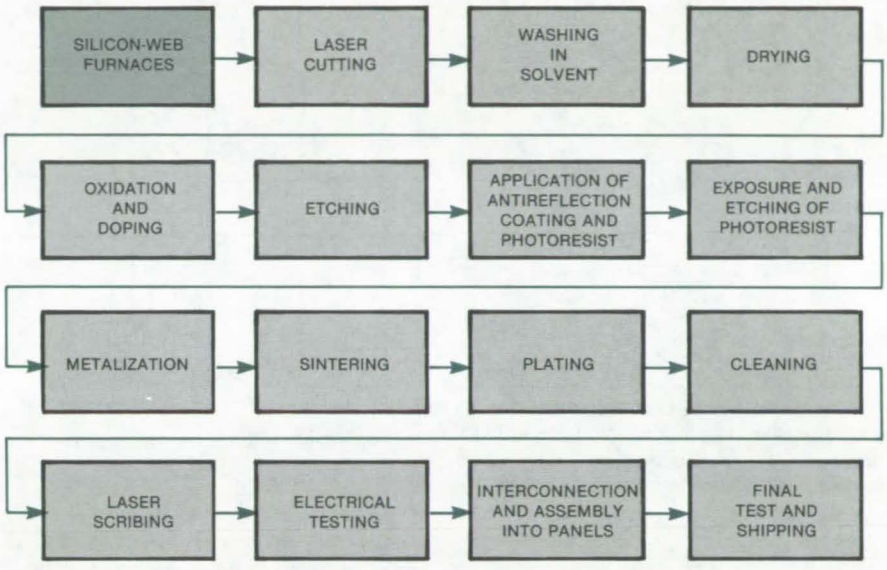

Lumps of Feed Silicon Would Be Processed into panels of solar cells in a production line that performs this sequence of steps.

Two laser-scribe lines are placed 5 cm apart, just inside the dendrite regions along the edge of the web, in preparation for the removal of the dendrites. The web is also laser-scribed transversely at 20-cm intervals along the length. The webs then run over rollers that break off the dendrites and fracture the web into individual 5- by 20-cm solar cells. The electrical characteristics of each cell are tested: The good cells are placed in cassettes, the bad discarded. Each 5- by 20- by 125-cm cassette holds 5,000 cells.

To prepare the cells for assembly into solar panels, aluminum-foil contact strips are ultrasonically bonded to the front of each cell. The active surfaces of the solar cells are placed face down on a layer of transparent adhesive on a 1- by 3-m glass panel. The contact strips from the front of each cell are then ultrasonically welded to the metalized layer on the back of the adjacent cell to form series strings running the length of the glass panel. Another layer of adhesive is applied to the rear of the cells, followed by a backing board that has the panel electrical connections attached to it.

This work was done by Derrick J. Page of Westinghouse Electric Corp. for **NASA's Jet Propulsion Laboratory.** *For further information, Circle 132 on the TSP Request Card.*
NPO-15098

Machining of Silicon-Ribbon-Forming Dies

Bevels and slot are alined automatically.

NASA's Jet Propulsion Laboratory, Pasadena, California

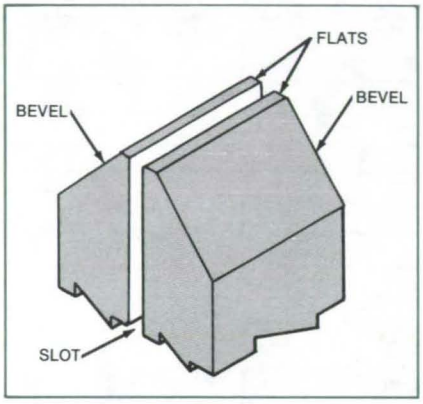

Figure 1. The **Die Extension** must have edges beveled toward narrow flats at the top, with a slot precisely oriented and centered between the flats and bevels.

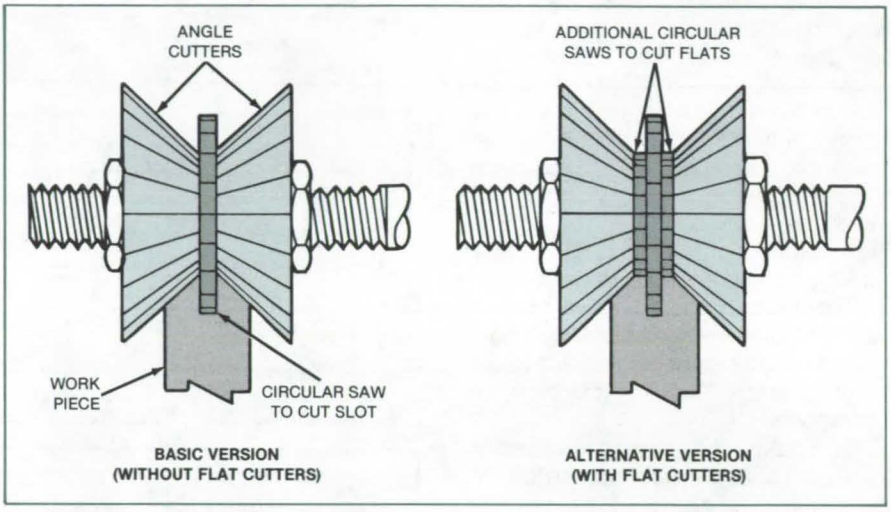

Figure 2. The **Cutting Tool** is assembled from standard angle cutters and a circular saw or saws. The angle cutters cut the bevels while the slot saw cuts the slot between them. In the alternative version, custom-ground edges or additional circular saws also cut the flats simultaneously.

Carbon extensions for dies used in forming silicon ribbon crystals are machined precisely with the help of a special tool. The centering of the die slot and the cutting of the flats to uniform and equal widths (see Figure 1) formerly required great care and long machining times. With the new tool, however, the bevel and slot cuts are automatically centered and are all made in one setup.

The tool is made from commercially-available angle cutters and a circular saw. With the pieces assembled as shown in Figure 2, the cut takes on the symmetry of the tool faces. No separate alinement is needed for the two bevels and the slot since all three cuts are made by the different parts of the compound tool simultaneously.

After cutting the workpiece with the special tool, the flats are formed by running an ordinary end, fly, or side cutter across the apex. Even this operation can be eliminated if the angle cutters are ground to include the two flats or if two circular saws of appropriate diameter and thickness are assembled into the tool on either side of the slot saw.

This work was done by Andrew A. Menna of Mobil Tyco Solar Energy Corp. for **NASA's Jet Propulsion Laboratory.** *For further information, Circle 133 on the TSP Request Card.*
NPO-15127

Automatically Dressing Blades in Silicon-Wafer Cutting

Dressing material is inserted into the beam supporting the silicon ingot.

NASA's Jet Propulsion Laboratory, Pasadena, California

Inserts incorporated in the support beams for silicon ingots automatically "dress" the cutting blade during wafer slicing. Manual dressing is thus eliminated, and production rates are increased.

In cutting silicon with a circular saw, a beam of graphite supports the silicon ingot. The inside edge of the blade plunges down through the ingot and into — but not through — the beam. The beam then supports the severed wafers.

If dressing is not done regularly, blade deflection becomes excessive and the quality of the sliced silicon wafer deteriorates. The surface of the wafer is roughened by saw marks, and the thickness of the wafer may vary from one edge to the other. Cutting takes longer than it should, the blade wears out quickly, and too much silicon is lost as kerf.

With the new method, segments of blade-dressing material are placed at regular intervals in the graphite beam (see figure). The blade cuts into the segments and is thus dressed without operator intervention and without interrupting regular machine operation.

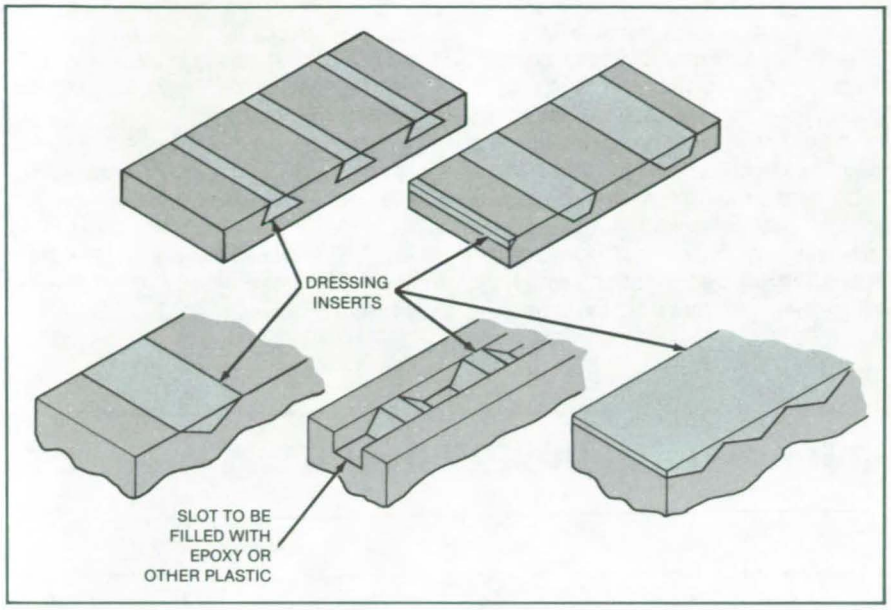

An Ingot-Support Beam containing doubly-tapered blade-dressing inserts would be used with inside-cutting-edge blades. A variety of insert beam configurations is proposed.

In one form of the automatic dressing method, a channel is cut in the support beam, and tightly fitting inserts of the dressing material are fixed in place with adhesive. The sides of the inserts are tapered to ensure symmetrical dressing. The spacing between inserts is determined by the dressing frequency required for a given cutting operation.

This work was done by Andrew D. Morrison of Caltech for **NASA's Jet Propulsion Laboratory.** *For further information, Circle 134 on the TSP Request Card.*
NPO-15745

High-Mobility Epitaxial Silicon Wafers

Multilayers of silicon and germanium have greater electron mobility than epitaxial silicon.

Langley Research Center, Hampton, Virginia

A new techique produces high-mobility multilayer films suitable for use on a silicon process line. Films grown thus far have electron mobilities 50 percent greater than those of epitaxial silicon films grown previously. The new material is a multilayer film of alternate layers of silicon and an alloy of silicon and germanium.

Active electronic devices have been fabricated using the multilayer structures. Both MESFET's (metal/semiconductor FET) and depletion-mode FET's have been built and successfully tested.

The multilayer film is grown on a silicon substrate in a standard silicon hydride epitaxial system. The silicon source is silicon (SiH_4), and the germanium source is germane (GeH_4). Dopants are diborane (B_2H_6) and phosphine (PH_3). Hydrogen was the carrier gas in all runs thus far.

In a typical run, the substrate temperature is 1,000° C, each layer is approximately 0.5 micron thick, the germanium content of the alloy layers is 15 percent,

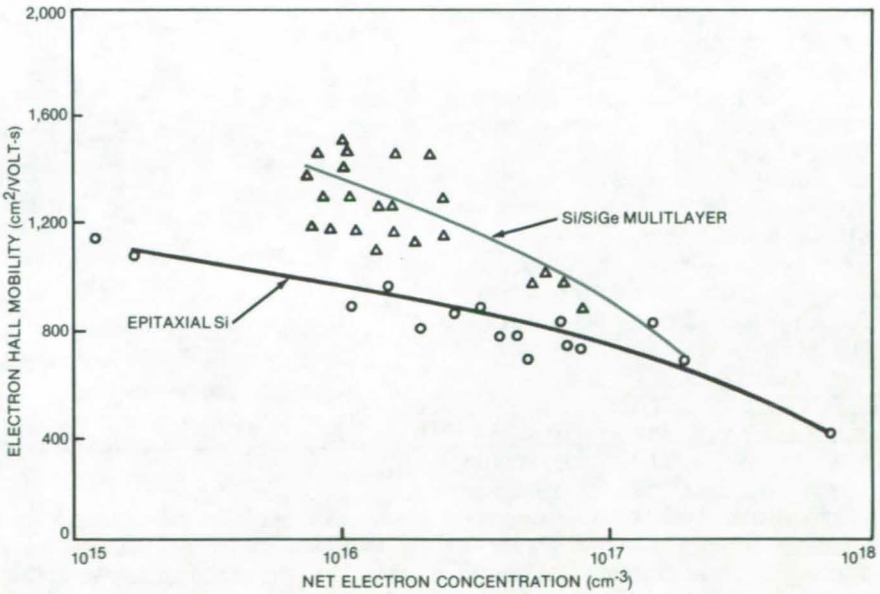

Electron Hall Mobilities of multilayer films are consistently higher than those of epitaxial silicon.

and between 50 and 100 layers are grown. The final layer is always silicon because of surface passivation, which is necessary to be compatible with a standard silicon-processing line. The figure shows a curve of the electron mobility plotted as a function of doping (phosphorus) level for both the multilayer film and the conventional epitaxial silicon films of approximately the same thickness.

Enhanced mobility has only been observed in phosphorus-doped films where each layer is greater than 0.04 micron thick and where the total film thickness is greater than 2 microns. No enhancement has been observed in single-layer-alloy films, regardless of thickness or dopant. It is believed that interdiffusion in both the vapor and solid phases eliminates the layered structure when the single-layer thickness is less than 0.04 micron; hence enhanced mobility may be possible in very thin (less than 0.04 micron) films grown by molecular beam epitaxy.

This work was done by R. L. Stermer, Jr., and A. L. Fripp, Jr., of **Langley Research Center** *and A. B. Jones, J. D. McMullen, H. M. Manasevit, I. S. Gergis, and S. I. Soclof of Rockwell International Corp. For further information, Circle 135 on the TSP Request Card.*
LAR-12846

Rapid Adhesive Bonding for Metals and Composites

A toroidal induction heater is the key element in a rapid bonding technique.

Langley Research Center, Hampton, Virginia

A technique similar to that used for spot welding in metallic structures has been used for rapid bonding of graphite/polyimide and graphite/epoxy composites, titanium and aluminum alloys, and metallic and composite specimens with adherends of unlike materials. High-strength adhesive bonds in standard overlap-shear specimens have been made with polysulfone and polyimide thermoplastic adhesives and with an epoxy/phenolic thermosetting adhesive. The technique is also suited to the bonding of end tabs onto material test specimens.

The rapid adhesive bonding equipment for laboratory shear specimens is shown in the figure. The press is identical to that for conventional specimen bonding, as are the load cell and the temperature and load indicators. Replacing the conventional heated platens is a toroidal high-frequency induction heater and its power controller. The specimen is located in a fixture for ease of alinement.

When power is applied, the toroid rapidly heats a metal susceptor, such as a metal screen, which has been impregnated with a thermoplastic adhesive or is sandwiched between thermosetting adhesive films. For lap-shear specimens, the metallic or fiber-reinforced plastic composite material adherends are placed above and below the susceptor in the sample fixture and bonding pressure is applied.

The susceptor heats the adhesive rapidly, usually within a minute, to the bonding temperature. The heat is maintained from 1 to several minutes to promote adherend/adhesive wetting. When power is turned off, the specimen rapidly cools to a temperature below which the adhesive is sufficiently set, and pressure is removed.

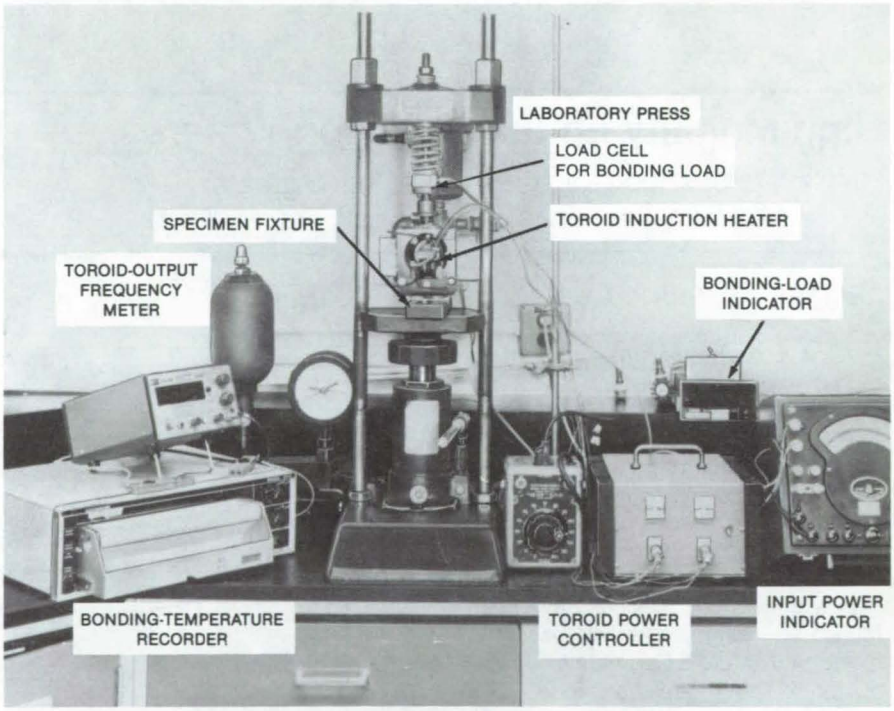

This **Rapid Adhesive Bonding Equipment** features a toroid induction heater for quick bonding of composites and metals. The process avoids damaging composites that cannot withstand high temperatures for long time intervals. The process can be scaled up for production.

Power and frequency indicators are optional and were used only for the equipment development phase of this technique. Rapid adhesive bonding was compared directly with laboratory-press/heated-platen bonding of titanium alloy adherends using an experimental thermoplastic adhesive, which was formulated to have good flow conditions while retaining good elevated-temperature properties. The strengths of the bonds were significantly higher than those obtained by press bonding.

With the present equipment, parts with bond areas up to 6 cm^2 have been joined. The technique may also be suitable for the buildup of an assembly of

components when the properties of a high-temperature-curing adhesive are needed but when the assembly cannot withstand the long time at temperature required for conventional processing. The process is more controllable and more energy conserving than conventional bonding with a heated-platen press or autoclave.

This work was done by Bland A. Stein, James R. Tyeryar, Robert L. Fox, S. Elmo Sterling, Jr., and John D. Buckley of **Langley Research Center**. *For further information, Circle 136 on the TSP Request Card.*

Inquiries concerning rights for the commercial use of this invention should be addressed to the Patent Counsel, Langley Research Center [see page A5]. Refer to LAR-13066

Collapsible and Deployable Trusses

Cable-controlled mechanisms allow large structures to be stored in small spaces.

Marshall Space Flight Center, Alabama

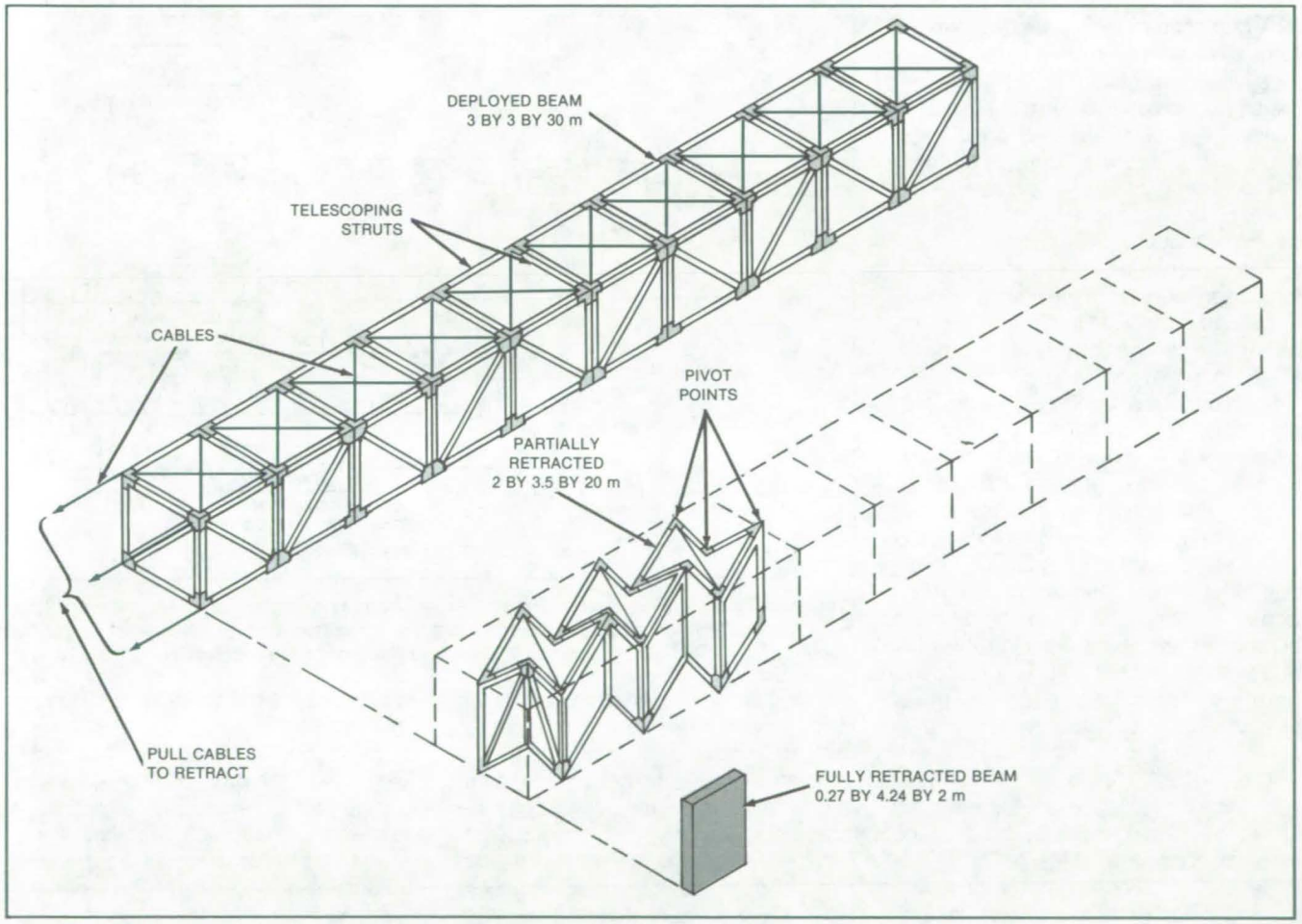

This **Combination of Telescoping Struts and Pivot Points** allows a very large structure to be collapsed into a very small one. The concept can be used not only for straight beams but for tapered or curved ones as well.

A proposed deployable and collapsible structure is strong and versatile. Originally designed for platforms to be erected in space, the structure is adaptable to such terrestrial uses as portable towers, scaffolds, and bridge beams that can be folded compactly for transportation or storage.

Called a biaxial double-fold structure, the deployed structure is collapsed by pulling retraction cables with a reel (see figure). This action compresses the main deployment springs in telescoping struts, thereby collapsing the struts. At the same time, the cable tension bends the deployment-initiating springs at pivot points on the struts so that all cells in the structure collapse simultaneously in scissorslike action.

Deployment follows the reverse sequence: When cable tension is released, the deployment-initiating springs unbend, opening up the cells and allowing

(continued on next page)

the main deployment springs to expand the telescoping struts and lock them in place.

The structure offers a high ratio of deployed volume to folded volume. For the dimensions shown in the figure, the ratio is 118. Utilities such as electric power and communication lines can be routed through the hollow interior of the structural members. The utility lines terminate in connectors at points where they are to join with equipment or other structural modules.

This work was done by Roy A. Nelson of Vought Corp. for **Marshall Space Flight Center.** *For further information, Circle 137 on the TSP Request Card.*

Inquiries concerning rights for the commercial use of this invention should be addressed to the Patent Counsel, Marshall Space Flight Center [see page A5]. Refer to MFS-25945.

Hot-Dipped Metal Films as Epitaxial Substrates

Cadmium or zinc layers show promise for low-cost solar cells.

NASA's Jet Propulsion Laboratory, Pasadena, California

A proposed multistep process would form semiconductor devices on macrocrystalline films of cadmium or zinc. The metal film would reside on a sheet metal substrate. Such devices as solar cells could be made economically by forming the desired surface substance (e.g., CdS) directly on the metal film by chemical reactions.

The silicon wafers used in manufacturing semiconductor devices are usually sliced from large single crystals, an expensive process that uses more silicon than that required for the thin surface layer containing the active device.

In laboratory experiments, cadmium macrocrystalline layers were readily formed by hot-dipping. The single crystals were 5 to 50 mm across and the crystal orientations were suitable for subsequent epitaxial deposition. With zinc films, experiments show that grain size in the film can be increased to arbitrarily large size by reducing the pull rate to a few feet per minute (a few centimeters per second). Lower melt temperatures seemed to favor the growth of large grains.

The process should also work with such other low-melting-point metals or alloys as tin, aluminum, lead, germanium, copper, and Mg_2Sn.

Several variations of the process for making solar cells are shown in the figure. The steps are as follows:

1. Sheet metal (such as steel) is coated with a macrocrystalline layer of a low-melting-point metal or alloy. For CdS cells, the coating would be cadmium.

2. The crystalline substrate is reacted with other substances by gas-phase or electrolytic reaction to form the desired epitaxial film on top of the metal grains. If possible, the reaction should be carried to the point where the macrocrystalline layer is completely consumed by the reaction or where the epitaxial film is thick enough to be self-supporting.

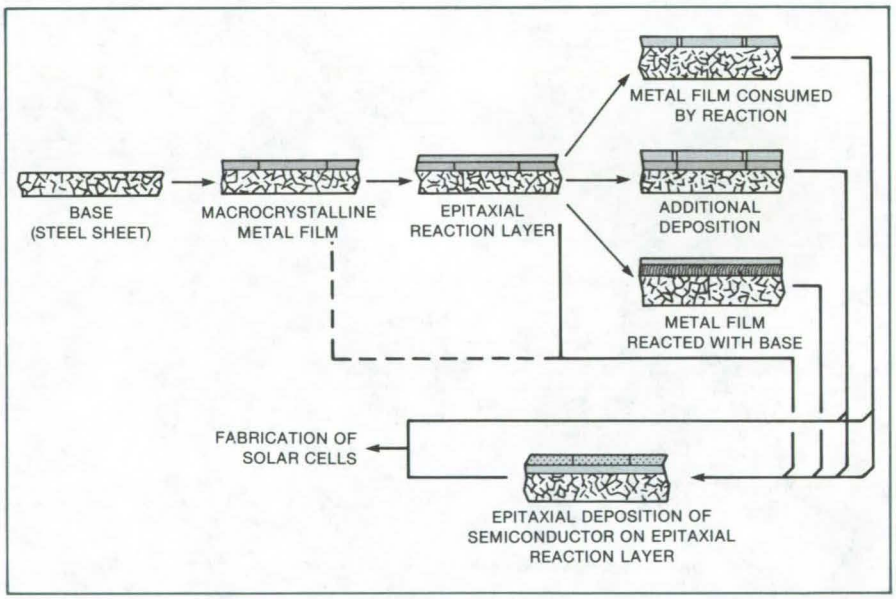

Proposed Solar-Cell Fabrication Processes would use hot-dipped macrocrystalline films on a low-cost sheet-metal base as substrates for epitaxy. Epitaxial layers would be formed by a variety of methods as shown by a number of alternative sequence paths.

As an example, the conversion of the cadmium to cadmium sulfide can be done using any of several processes to form CdS epitaxial films on Cd substrates, such as heating in a mixed H_2/H_2S reaction gas at 130° C, electrodepositing CdS, or immersion deposition of CdS using a mixed $CdCl_2$/thiourea solution.

3. The metal layer is then either depleted by exhaustive application of step 2 or passivated by reaction with the metal sheet. This prepares the substrate for subsequent chemical vapor deposition (CVD) steps.

4. The epitaxial film is used as the substrate for the epitaxial deposition of either more of the same material or else of a different material.

In addition to the case of CdS, other versions of the process show promise, although further experimentation is necessary. These include the following:

- GaAs solar cells on zinc-galvanized substrates could have considerable economic potential. A substrate for GaAs could be prepared starting with zinc-galvanized sheet. The subsequent steps are sulfidization to produce a ZnS film, CVD epitaxial growth of ZnSe on the ZnS, and CVD epitaxial growth of GaAs on the ZnSe.
- Substrates for silicon from sulfidized zinc-galvanized sheet would be possible if silicon can be deposited epitaxially on ZnS, as appears probable from

the match of crystal lattice dimensions. Silicon deposition would probably be restricted to low-temperature CVD techniques, such as SiI_4 decomposition. This method could have a major impact on the silicon-solar-cell industry, even allowing for the comparatively high cost of the silicon CVD step.

This work was done by Paul J. Shlichta of Caltech for **NASA's Jet Propulsion Laboratory.** *For further information, Circle 138 on the TSP Request Card.*

Inquiries concerning rights for the commercial use of this invention should be addressed to the Patent Counsel, NASA Resident Office-JPL [see page A5]. Refer to NPO-15904.

Decontaminating Aluminum/Ammonia Heat Pipes

Internal gas slugs are reduced or eliminated.

NASA's Jet Propulsion Laboratory, Pasadena, California

A manufacturing method increases the efficiency of aluminum heat pipes in which ammonia is the working fluid by insuring that the pipe is filled with a nearly pure charge of ammonia.

Such heat pipes are used to cool scientific instruments, operating at typical temperatures of $-70°$ to $+100°$ C. Often, a slug of noncondensable gas forms inside a pipe and is swept to the condensing end, where it interferes with condenser operation. The noncondensable gases include contaminants that remain from the manufacturing process, plus nitrogen or hydrogen that forms when some of the ammonia decomposes on trace catalysts or other metals in the pipe.

In the new manufacturing process, the heat pipe is initially closed with a stainless-steel valve instead of a weld, so that the pipe can be put through several cycles of filling, purging, and accelerated aging. After initial cleaning, the pipe is filled with 100 psia (0.7×10^6 N/m^2) oxygen plus 15 psia (0.1×10^6 N/m^2) steam and heated to 100° C for 4 hours. Then the pipe is evacuated and filled with 100 psia nitrogen at 100° C for 4 hours. This ensures adequate surface oxidation and nitriding to inhibit later reactions with the ammonia. To remove adsorbed gases, the heat pipe is heated again to 100° C while being evacuated to 1 micron pressure by an oilless liquid-nitrogen sorption pump. The heat pipe is then filled with 0.99999-pure ammonia and heated to 130° C for 7 days, to accelerate any possible chemical reaction with the ammonia.

Next, the heat pipe is cooled to room temperature and tilted such that the valve stem is somewhat higher than the rest of the pipe. By heating the lower end and cooling the upper end, any trace noncondensable gases are gathered near the valve. The valve is opened to "burp" out the noncondensable gas, taking care not to let out any liquid ammonia. The "burping" procedure is repeated.

The pipe is then permanently sealed: First, the valve stem is crimped flat. The stem is then recrimped with a narrower clamp at the base of the flat crimp. After the second crimp, the stem is cut with a clean hacksaw and welded shut at the cut edge.

This work was done by Jack A. Jones of Caltech for **NASA's Jet Propulsion Laboratory.** *For further information, Circle 139 on the TSP Request Card.*
NPO-16066

Polyurethane Masks Large Areas in Electroplating

Foam masking agent reduces contamination.

Marshall Space Flight Center, Alabama

Polyurethane foam provides an effective mask in the electroplating of copper or nickel. The material is especially suitable where large areas must be masked. If the usual waxy maskants are used on large areas, contamination of the plating bath can result.

First, a thin layer of Turco maskant (or equivalent) is painted on the area to be masked: This layer ensures that the polyurethane foam can be removed easily after it has served its purpose. Component A, isocyanate, and component B, polyol, are then mixed together and brushed or sprayed on the mask area. The mixture reacts, yielding the polyurethane foam.

The foam prevents the deposition of nickel or copper on the covered area. After the workpiece is removed from the plating bath, the masking materials are removed. The new method saves time, increases productivity, and uses less material than do older procedures.

This work was done by John L. Beasley of Rockwell International Corp. for **Marshall Space Flight Center.** *No further documentation is available.*
MFS-19825

Vented Compression Molding of Granule-Filled Resins

Production cost is reduced by a process that uses a perforated mold.

Marshall Space Flight Center, Alabama

Resins filled with granules are formed to final size and shape in a new process called vented compression molding. Suitable for making a variety of parts with simple shapes, vented compression molding takes less time and costs less than older processes. The new method will find use where low- and medium-density parts are to be molded from particulate composite materials.

The molding of particulates presents a complex problem. In its mechanical behavior, a typical particulate molding material resembles a lightweight, wet, rubbery sand. Large shear strength and compressibility make it difficult to achieve large material flows. Attempts at ordinary compression molding often result in nonuniform distribution in the molds and nonuniform compaction. One way to circumvent these difficulties is to use the labor-intensive process shown at the left in the figure.

In vented compression molding, the limitations of ordinary compression molding are overcome without introducing many time-consuming extra steps or complicated molding machinery. No attempt is made to have large material flows or to control the molding pressure

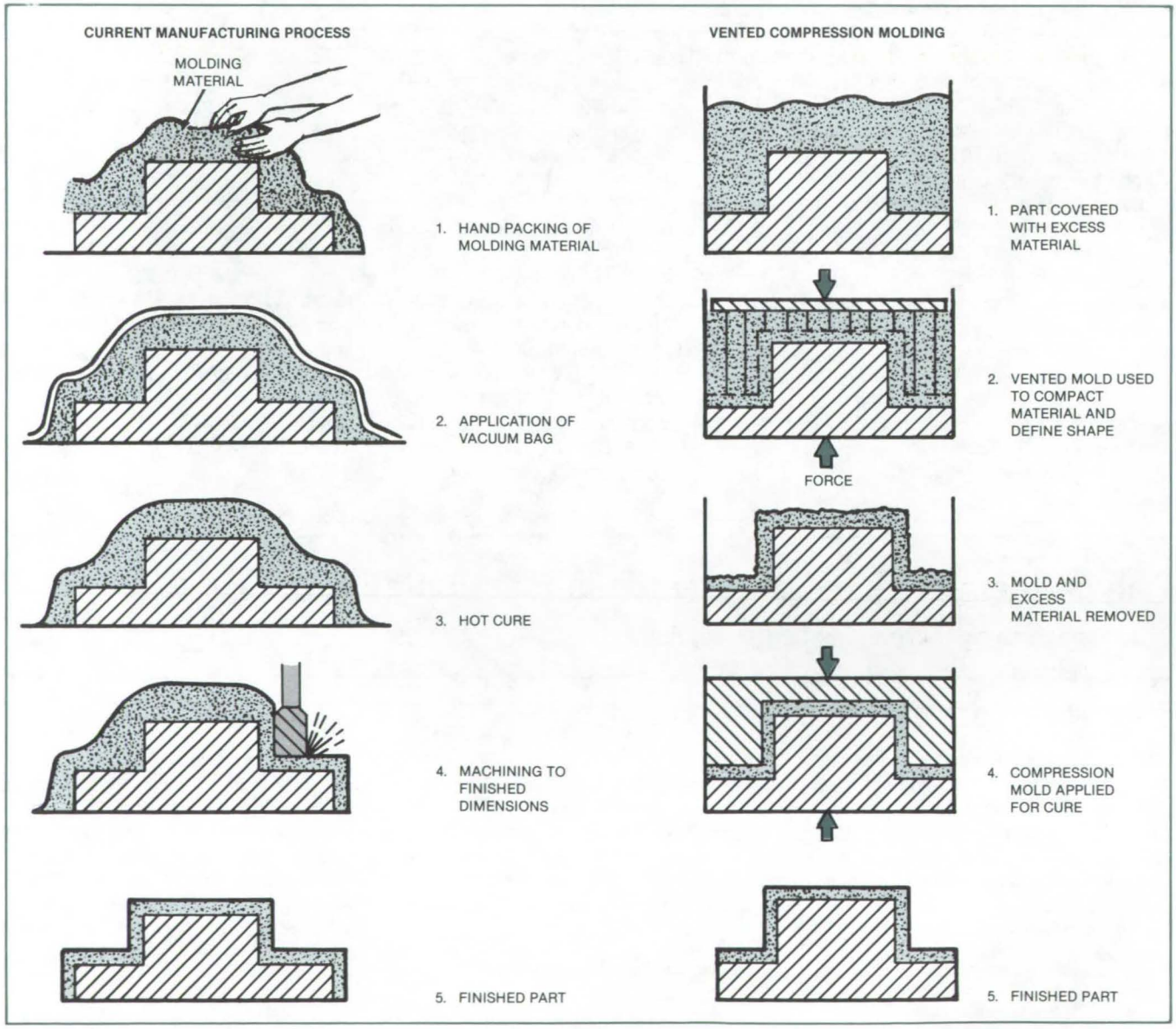

The **New Vented Compression Molding** method (right) takes less time than the conventional method shown at the left. The vacuum-bagging and machining stages are eliminated. The part emerges from the mold in the final size and shape.

directly. As shown in the right half of the figure, the new technique involves the use of a perforated mold. The mold cavity is filled (or the object to be covered is surrounded) with an excess of the molding material. As the mold is closed, excess material escapes through the holes.

The frictional forces in the escaping material generate a pressure in the mold that compresses the retained material to the desired density. The pressure and density in the mold are controlled by setting the sizes and locations of the ventholes.

Many variations of the process are possible, depending on the size and shape of the part and the type of material. For example, if the part is too large to be conveniently surrounded by a mold, a rolling vented surface can be used to cover large smooth areas. If a part is to be covered with a particulate of varying density, the size and distribution of ventholes might be made to vary with position on the mold. The design of an optimal vented-compression-molding apparatus for a given situation is probably best left to the tool designer, who will have to verify the design by experimenting with the molding material.

This work was done by John O. McCree and Lewis Erwin of Martin Marietta Aerospace Corp. for **Marshall Space Flight Center.** *For further information, Circle 140 on the TSP Request Card.*
MFS-25975

Alining Heat-Exchanger Tubes for Assembly

A simple support method makes costly jigs and fixtures unnecessary.

Marshall Space Flight Center, Alabama

An assembly method simplifies the alinement of many narrow flexible tubes in rocket nozzles, heat exchangers, and similar devices. Expensive jigs are not required.

"Dummy" tubes are installed at regular intervals to support the "real" tubes before the real tubes are installed. The dummy tubes are filled with Cerrobend (or equivalent) material, a metallic substance with a low melting point. The filler makes the dummy tubes rigid so that they brace the real tubes as they are installed. When all available spaces for the real tubes have been filled, the dummy tubes are removed and replaced with real tubes.

This work was done by Kirt A. Benson of Rockwell International Corp. for **Marshall Space Flight Center.** *No further documentation is available.*
MFS-19857

Books and Reports

These reports, studies, and handbooks are available from NASA as Technical Support Packages (TSP's) when a Request Card number is cited; otherwise they are available from the National Technical Information Service.

Beam-Cap-Forming Machine

Graphite-reinforced plastic strip is transformed into a continuous beam cap.

A report describes a machine that fabricates beam caps from graphite-reinforced thermoplastic materials supplied as strip stock. Suitable materials include graphite/polysulfone and graphite/polyethersulfone. The machine concept is described in "Forming Lightweight Beams From Composite Tape" (MFS-25880), *NASA Tech Briefs* Vol. 8, No. 2, page 277.

Beam caps are essentially long beams of generally V-shaped cross section with inward-folded flanges at the ends of the vee. The machine is a prototype of one that would function in space, producing caps for beams used in large truss-type space structures ranging from 400-meter-diameter radio reflectors to 13-kilometer-long solar-power satellites. On Earth, a version of the machine might be used to fabricate lightweight trusses at a remote site.

The composite materials were selected for their low thermal distortion, high stiffness, and low density. They lend themselves to fabrication in space and to low-cost continuous processing. Thermoplastic resins were selected rather than thermosetting ones because the latter produce gases during curing. In contrast, thermoplastic resins can be handled and formed in much the same way as sheet metal, for which much of the beam-cap-forming technology has already been developed.

A coiled strip of composite material is fed into a drive and roll-form tooling, where it is radiantly heated by quartz heaters. The tooling consists of four sets of steel rollers that progressively shape the heated strip into a cap. The rollers are coated with a fluorocarbon material to reduce friction and sticking.

A microcomputer and associated peripheral equipment perform the overall control of the servomotor operation for the rolling and of the event sequence for simulated truss fabrication. Four proportional controllers provide closed-loop servocontrol of the quartz lamps at the rolling-mill heating stations. Optical pyrometers furnish the feedback signal for the controllers and the microcomputer.

A control panel with a keyboard and video display allows manual as well as

(continued on next page)

automatic control of the prototype system. This would be removed from the deployed version of the beam builder.

This work was done by Warren Marx and others of Grumman Aerospace Corp. for **Marshall Space Flight Center.** *Further information may be found in NASA CR-170642 [N83-11158/NSP], "Space Fabrication Demonstration System Composite Beam Fabricator [$10]. A paper copy may be purchased [prepayment required] from the National Technical Information Service, Springfield, Virginia 22161. The report is also available on microfiche at no charge. To obtain a microfiche copy, Circle 141 on the TSP Request Card.*
MFS-27007

Matching Impedances and Modes in Acoustic Levitation

Temperature differences could be accommodated with tunable couplers.

A report now available discusses schemes for coupling sound efficiently from a cool outside atmosphere into a hot acoustic-levitation chamber. These theoretical studies have practical implications for material-processing systems that employ acoustic levitation.

For mathematical simplicity, the problem is treated as though the ambient and furnace temperatures are spatially uniform and that the interface region between them is infinitesimally thick — a plane surface for the purpose of the analysis. Since the speed of sound is proportional to the square root of the absolute temperature, the normal acoustic modes are calculated separately for the two temperature regions using the speed of sound applicable in each.

The mathematical solutions for the two regions are matched to each other through the requirement that both give the same pressure and displacement velocity at the interface. The resonant condition necessary for maximum acoustic coupling and most efficient levitation is achieved when the gradient of acoustic pressure across the interface is zero.

To maintain the resonance as the temperature of the heated region rises or falls, it is necessary to vary either the length of the cold part of the coupling tube, the length of the hot region, the total length, the position of the interface, the frequency of the sound, or perhaps the configuration of a tuning obstruction in the coupling tube. It is probably simplest to vary the length of the cold region. It can, for example, be constructed of two or more telescoping cylinders.

A long telescoping tube confers the additional ability to move a levitated object to and from the hot region. Adjusting the tube changes the mode structure, thereby altering the equilibrium levitation position. For example, suppose that it is desired to move the object out of the furnace along a vertical acoustic axis. One way to do this might involve first adjusting the coupling tube to the position for the new mode, then turning off the sound for a short time to allow the object to fall past the interface, and then turning the sound back on to levitate the object to the new position.

Making the length of the cold region adjustable also compensates for the mathematical error introduced by the fact that the temperature transition is not abrupt in practice. Although it is possible in principle to calculate the effect of a gradual interface, it is simpler to find the resonance by tuning the coupling tube.

This work was done by Martin B. Barmatz of Caltech for **NASA's Jet Propulsion Laboratory.** *To obtain a copy of the report, Circle 142 on the TSP Request Card.*

Inquiries concerning rights for the commercial use of the technology described in this report should be addressed to the Patent Counsel, NASA Resident Office-JPL [see page A5]. Refer to NPO-16022.

Acoustic Levitation With One Driver

The modes of a rectangular chamber are excited from one corner.

A brief report discusses acoustic levitation in a rectangular chamber using one driver mounted at a corner. The single driver excites vibrations along all three axes. The excitation scheme is an elaboration of concepts expressed in "Acoustic Levitation With Less Equipment" (NPO-15562), *NASA Tech Briefs*, Vol. 7, No. 3, p. 350 (Spring 1983).

As in earlier schemes of this type, the driver excites acoustic standing waves having pressure nodes that intersect at the center or other designated levitation position. The placement of the driver at a corner enables it to couple effectively to acoustic modes along all three axes.

The use of a single driver reduces the cost, complexity, and weight of the levitation system below those of a three-driver system. For an acoustic levitator that is part of a high-temperature material-processing system, the use of a single transducer eliminates some of the heat loss that would otherwise occur through the multiple excitation ports and reduces the parasitic thermal mass of the levitator.

The excitation signals for the three axes can be multiplexed into a single transducer or else introduced through the excitation port from three separate sources having the proper phase relationships. The separate sources must be well isolated from each other to preserve the phase differences among the signals. As discussed in the earlier article, the frequencies and phases of the modes are adjusted to control the rotation and location of the levitated object.

This work was done by Taylor G. Wang, Isadore Rudnick, Daniel D. Elleman, and James D. Stoneburner of Caltech for **NASA's Jet Propulsion Laboratory.** *To obtain a copy of the report, "Corner Mounted Single Transducer, Three Axis Acoustic Chamber," Circle 143 on the TSP Request Card.*
NPO-15793

Computer Programs

These programs may be obtained at very reasonable cost from COSMIC, a facility sponsored by NASA to make new programs available to the public. For information on program price, size, and availability, circle the reference letter on the COSMIC Request Card in this issue.

Price Estimation Guidelines

The cost of a manufactured product is calculated.

The Improved Price Estimation Guidelines, IPEG4, program provides a comparatively simple, yet relatively accurate, estimate of the price of a manufactured product. It facilitates extensive sensitivity studies of price estimates at considerably less expense than would be incurred by using the Standard Assembly Line Manufacturing Industry Simulation, SAMIS, program. A difference of less than one percent between the IPEG4 and SAMIS price estimates has been observed with realistic test cases. However, IPEG4 allows the analyst with limited time and computing resources to perform more sensitivity studies than SAMIS would allow. Although IPEG4 was developed for the photovoltaics industry (as was SAMIS), it is readily adaptable to virtually any assembly-line industry.

IPEG4 processes user-supplied input data to determine an estimate of the price per unit of production. The input data include equipment cost, space required, labor cost, materials and supplies cost, utility expenses, and production volume on an industry-wide or a process-wide basis. The IPEG4 input file is normally generated by a SAMIS simulation but may be prepared by the user.

Once the IPEG4 input file is prepared, the original price estimate is completed and then sensitivity studies may be performed. The IPEG4 user selects a sensitivity variable and a set of values. IPEG4 computes a price estimate and other cost parameters for every specified value of the sensitivity variable. IPEG4 is interactive and "prompts" the user for all required information. It offers a variety of output options.

The IPEG4 program is written in SIMSCRIPT II.5 for interactive execution and has been implemented on an IBM 370-series computer with a central memory requirement of approximately 300K of 8-bit bytes. The program was developed in 1980.

This program was written by Robert G. Chamberlain, Robert W. Aster, Paul J. Firnett, and Mark A. Miller of Caltech for **NASA's Jet Propulsion Laboratory.** *For further information, Circle dd on the COSMIC Request Card.*
NPO-15569

Assembly-Line Manufacturing Industry Simulation

It assists in the economic analysis of production-line manufacturing.

The Standard Assembly-Line Manufacturing Industry Simulation (SAMIS) program was originally developed to estimate the product price that would have to be received by a hypothetical U.S. industry that manufactures silicon solar modules for use in electricity generation. SAMIS has now been extended and generalized to the extent that it can simulate the operation of many different production-line manufacturing industries and/or companies.

The most important capability of SAMIS is its ability to simulate an industry based on a model developed by the user (with the aid of SAMIS). The result of the simulation is a set of financial reports that details the requirements, including quantities and costs of all of the companies and manufacturing processes that comprise the industry. Among other possible uses, SAMIS provides a fair, consistent, reliable way of comparing manufacturing processes being developed by competing, independent efforts. It can also be used to assess the industry-wide (or company-wide) impact of changes in financial parameters such as prices of resources and services, inflation rates, interest rates, tax policies, and required return on equity.

Because a large amount of data is needed to describe an industry, a major portion of SAMIS is dedicated to data entry and maintenance. This activity is referred to as "model management." Model management requires a significant amount of interaction between the user and SAMIS. SAMIS facilitates this interaction with a dialogue that makes it possible for persons not familiar with computers or the SAMIS program to provide all of the data necessary to perform a simulation.

The SAMIS program is written in Simscript II.5 and has been implemented on an IBM 370-series computer with a central memory requirement of approximately 2 million 8-bit bytes. The original SAMIS program was developed in 1978 and was last updated (Release 4) in 1982.

This program was written by Robert G. Chamberlain and Paul J. Firnett of Caltech for **NASA's Jet Propulsion Laboratory.** *For further information, Circle ee on the COSMIC Request Card.*
NPO-16032

MiniBriefs describe NASA innovations and reports in an abbreviated format. Readers desiring additional information on these items should request the Technical Support Packages (TSP's), available in most cases, which can be obtained by using the TSP Request Card at the back of this issue.

Two-Pulse Stitch Welding

A second welding pulse at about 20 percent higher energy repairs bad single-pulse welds.

A capacitance-discharge stitch-welding method makes a weld in the normal manner and then restrikes the weld with a second higher energy pulse. This two-step process repairs bad welds that may have occurred due to variabilities in the wire, terminals, and weld machine. The method has been used successfully to weld polytetrafluoroethylene-insulated nickel wire to stainless-steel terminals in back-plane wiring.

The two pulse levels used are selected on the basis of the results of prescribed physical and visual tests. The second pulse is added to a weld designed to be acceptable on its own.

This work was done by Charles J. Torborg of Honeywell, Inc., for **Marshall Space Flight Center.** *For further information, Circle 144 on the TSP Request Card.*
MFS-25716

Sonically-Welded Thermal Blankets

Insulating layers are joined by seams.

Assembling a multilayer insulating blanket by sonic welding saves time and reduces weight. The layers of the blanket are built up from alternating layers of polyester sheet and polyester net. A paper pattern showing lines along which the layers are to be joined together is placed over the top layer.

An operator runs a sonic welding tool along the pattern lines, bonding the layers. The pattern material does not bond to the blanket. The operator removes the pattern and reuses it for another blanket, or discards it.

Continuous sonic welding is much faster than joining the layers with conventional fasteners. Moreover, the sonically bonded blanket weighs no more than the individual layers; heavy conventional fasteners are avoided.

This work was done by R. Bettini and F. Citrin of The Perkin-Elmer Corp. for **Marshall Space Flight Center.** *No further documentation is available.*
MFS-25806

Fabrication of Thick Gold Strip Lines

Ion-beam etching and masking techniques fabricate micron-sized gold strip lines.

Ion-beam etching allows micron-sized gold strip lines and other micro-geometric structures to be deposited without edge damage. A strip-line electrode which is on top of SiO_2 consists of a 100-Å layer of Cr followed by a thick (3 μm) layer of gold, on top of which is deposited a Cr or Ti layer that is subsequently oxidized. The resulting CrO_2 or TiO_2 oxidized layer provides a mask for the strip-line pattern during subsequent etching of the gold. The gold strip lines, 3 μm thick, 13 μm wide, and 1.5 cm long, are fabricated by use of argon ion-beam milling.

This work was done by Caroline M. Gee, Hugh L. Garvin, and Klaus Robinson of Hughes Aircraft Co. for **NASA's Jet Propulsion Laboratory.** *For further information, Circle 145 on the TSP Request Card.*
NPO-16238

Magnetic Chuck for Precise Grinding

Handling time is substantially reduced.

A magnetic grinding chuck is used for fabricating parts that have thin, delicate geometries requiring close tolerances. Previously, the use of conventional clamps to produce such parts required highly-skilled machine operators and extensive setup and indication time.

The principal features of the chuck are the slots and forms that are milled onto its face for precise positioning of the workpiece. During grinding, the recessed slots hold tabs ground into the backside of the piece to secure it tightly. After grinding, the piece can be turned over, fit into another chuck, and finished without inducing the stresses that would occur from clamping.

This work was done by Richard A. Carver of Rockwell International Corp. for **Marshall Space Flight Center.** *For further information, Circle 155 on the TSP Request Card.*
MFS-19764

Improved Melt-Level Control System

Laser feedback control automatically maintains silicon melt levels.

During long-term growth of dendritic-web silicon, the silicon melt level can be controlled and held nearly constant using a laser feedback system to sense the level of the melt and control the silicon-pellet feed rate. A beam from a helium/ neon laser is reflected from the surface of the melt and detected by a silicon photodetector. The analog signal is filtered through a long-time-constant dc amplifier, to remove fluctuations, and sent to a gear-motor controller that drives the silicon-pellet-feed rotational mechanism.

This work was done by Daniel L. Meier of Westinghouse Electric Corp. for **NASA's Jet Propulsion Laboratory.** *For further information, Circle 147 on the TSP Request Card.*
NPO-15900

Silicon-Web-Growing Machine

Silicon is replenished automatically as the web is withdrawn.

The design of a semiautomatic silicon-web-growing machine has been set down in detailed engineering drawings. The machine has not been built in its entirety, but critical subsystems have been tested successfully on other web-growing machines.

The automatic melt-replenishment subsystem greatly reduces the demand upon the operator's time. The melt level is sensed with a He/Ne laser beam and the melt-level error signal is used to control a motor-driven pellet feeder, speeding it up when the level is low. With this feedback control system, the melt level

remains nearly constant, and silicon is replaced at about the rate at which it is consumed.

This work was done by C. S. Duncan of Westinghouse Electric Corp. for **NASA's Jet Propulsion Laboratory.** *For further information, Circle 148 on the TSP Request Card.*
NPO-15870

Minimizing Convection During Crystal Growth

Cell design uses novel geometry and quasi-adiabatic windows.

Buoyant convection during crystal growth from solution is minimized in an experiment cell using boundary-layer stabilizing configurations, such as downward isothermal growth or upward growth into a thermal gradient. Convection from horizontal thermal gradients is minimized by a novel control system. The master controller regulates the temperature of a ring of copper fins sandwiched between the inner windows to form the experiment chamber. The outer windows have transparent, resistively heated films that are regulated by a slave controller maintaining a preset chamber-window temperature difference, which minimizes heat flow through the windows.

Convection in Earth-based experiments is an order of magnitude lower than in conventional systems. Comparable reductions in residual convection are expected for spaceflight experiments.

This work was done by Paul J. Shlichta for **NASA's Jet Propulsion Laboratory.** *For further information, Circle 149 on the TSP Request Card.*

Inquiries concerning rights for the commercial use of this invention should be addressed to the Patent Counsel, NASA Resident Office-JPL [see page A5]. Refer to NPO-15811.

Automated Texturization of Silicon Wafers

Two-stage texturization of silicon wafers improves solar-cell efficiency.

"Texturization" of either single-crystal or polycrystalline wafers improves the conversion efficiency of the finished solar cells. The wafers are first cleaned with boiling Freon TMS, or an equivalent, in two sequential ultrasonic vapor degreasers. The wafers are then etched for 5 min at 90° C in a 20-percent aqueous NaOH in the presence of ultrasound and bubbled air. Next, the wafers are texturized for 15 min at 95° C in a solution of 2 percent NaOH in 80:20 water: isopropanol, in the presence of ultrasound. The texturized wafers are rinsed with distilled deionized water and dried in an air tunnel.

This work was done by Sanjeev Chitre, Chuck Snyder, Greg Jones, and Priscilla Marlowe of Photowatt International, Inc., for **NASA's Jet Propulsion Laboratory.** *For further information, Circle 150 on the TSP Request Card.*
NPO-15816

Reciprocating Crystallizer

Automatic crystallizer grows crystals from aqueous solutions.

A reciprocating crystallizer grows single triglycine sulfate crystals of good quality. Crystals are grown from aqueous solutions by slow cooling of the growth solution along with forced convection to increase mass transfer. The polyhedral seed crystals are mounted on a holding rod that is rotated through a threaded drive by a reversible small 48-rpm motor. Two 250-watt immersion heaters maintain the temperature of the crystallizer water bath to an accuracy of 0.01° C. The bath temperature is monitored by thermometers.

This work was done by Ravindra B. Lal and Manmohan Aggarwal of Alabama A & M University for **Marshall Space Flight Center.** *For further information, Circle 151 on the TSP Request Card.*
MFS-25948

Impurity Effects on Dendritic Growth

Effects of argon additions in succinonitrile agree with theory.

Measurements of the effects of soluble-impurity addition on dendritic-growth rates and morphology allow testing of the theoretical dendritic-growth models. Succinonitrile was used as the simplified model system to produce the solidification characteristics of dilute binary alloys. It was found that the presence of argon impurity enhanced the growth rates of the dendrites. Recent stability theories have yielded predictions of kinetics and morphologies in good agreement with the experimental data. The information collected may help in understanding the effects of controlled impurities on alloy-casting and solidification technology.

This work was done by Martin E. Glicksman of Rensselaer Polytechnic Institute for **Marshall Space Flight Center.** *For further information, Circle 152 on the TSP Request Card.*
MFS-25672

Acoustic Sorter for Small Parts

System provides inexpensive alternative for assembly lines.

A sorting system that uses an acoustic resonance chamber can detect and reject anomalous parts on an automated assembly line. The system is particularly suited to small nuts, bolts, pins, and assemblies, which previously required expensive three-dimensional television-monitoring systems to prevent misfeeds.

Detection is based on an acoustic frequency shift that occurs when an incorrect or misalined part passes through the resonance chamber and produces an acoustic pattern different from the standard pattern. Microphones located opposite the acoustic transducers in the chamber pick up the shifts and trigger rejection of the bad part.

This work was done by Taylor G. Wang and Emily W. Leung of Caltech for **NASA's Jet Propulsion Laboratory.** *For further information, Circle 153 on the TSP Request Card.*

Inquiries concerning rights for the commercial use of this invention should be addressed to the Patent Counsel, NASA Resident Office-JPL [see page A5]. Refer to NPO-15913.

Square-Cutting Grinder

A modified grinder easily makes square cuts in pipes.

An attachment to a grinder may be used to cut small pipe ends square and smooth, ready for welding. The attachment is a simple plate bracket fastened to an air pencil grinder, which is held against the pipe flange to guide the grinder. Using the flange face as a guide, the square cut could be made at the required position from either the in-

(continued on next page)

side or outside diameter. This technique is especially useful for cuts of short length.

This work was done by Gale B. Dennis of Boeing Services International for **Kennedy Space Center.** *For further information, Circle 154 on the TSP Request Card.*
KSC-11257

Holder for Straightening Bent Tubes

Metal tubes are straightened only where needed.

A one-piece holder restrains a bent metal tube against further bending during a straightening operation. The holder consists of a handle 16 in. (41 cm) long welded to a short, strong tube that fits around the tube to be straightened. For clearance, the handle axis is at an angle a few degrees from the tube axis.

The holder is slipped with one hand onto the bent tube and slid to the position at which bending is not allowed. A rod or tube with an end of smaller diameter is slid with the other hand into the tube and used to apply a corrective bend.

This work was done by Arthur R. Turner and Eric D. Polzien of Rockwell International Corp. for **Marshall Space Flight Center.** *For further information, Circle 156 on the TSP Request Card.*
MFS-19705

Annular-Tube Reinforcer

A tube inserts support sleeves between coaxial tubes.

A cylindrical tool inserts support sleeves into the annular space between coaxial tubes to provide local reinforcement. The tool is particularly useful when the space between the outer ends of the coaxial tubes is narrow, requiring a thin sleeve.

Both the sleeve and the tool are constructed to slip through the narrow annular opening and be pushed to the base of the inner tube. A soft metal, such as a copper ring, is used for the sleeve so that when the forward end of the tool is forced against the base of the inner tube, the ring expands to form a tight-fitting support sleeve.

This work was done by R. Pessin of Rockwell International Corp. for **Marshall Space Flight Center.** *For further information, Circle 157 on the TSP Request Card.*
MFS-19738

Mathematics and Information Sciences

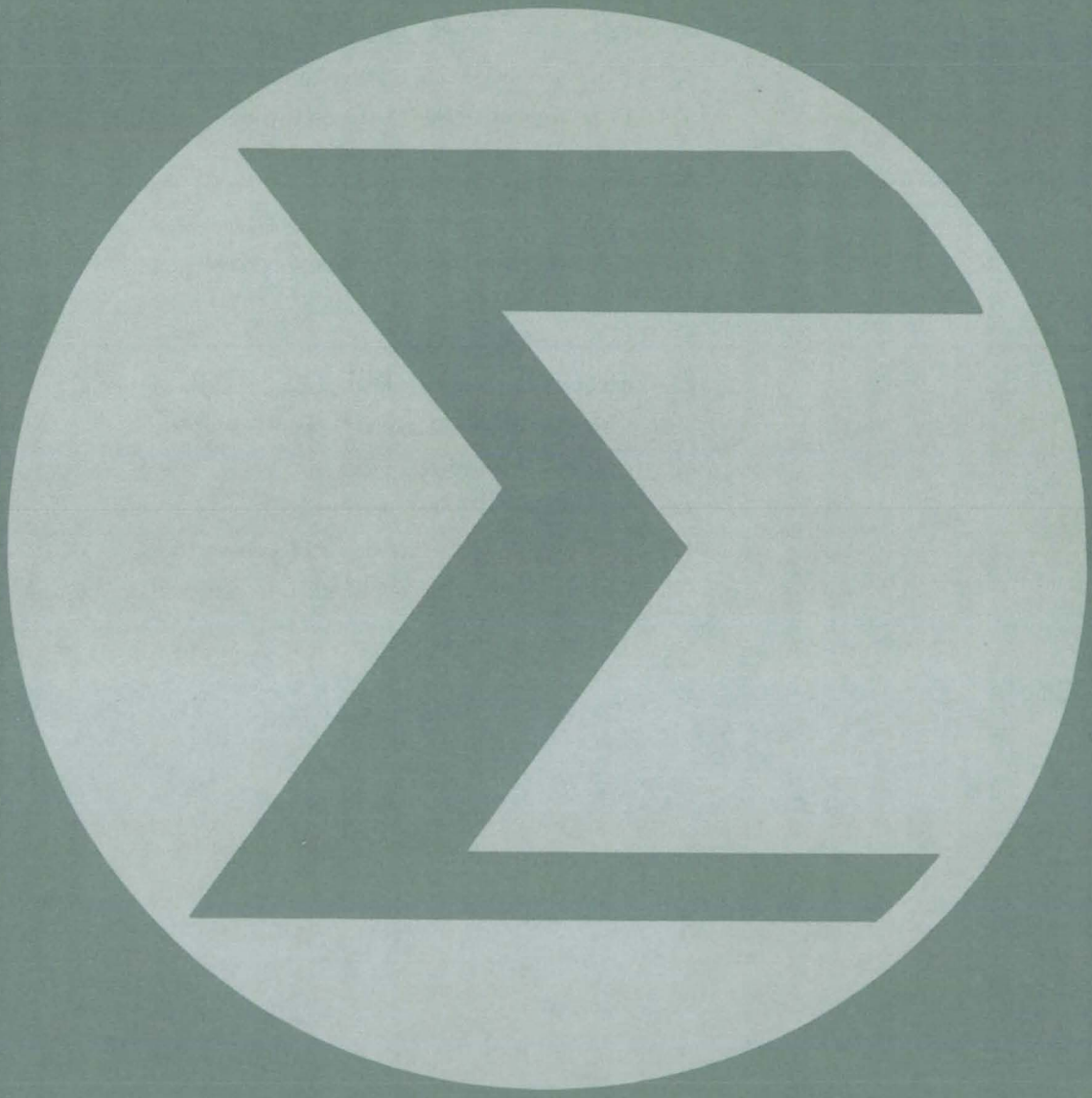

Calculating Closed-Loop Sensitivity to Parameter Variations

Performance sensitivity is calculated by back substitution.

NASA's Jet Propulsion Laboratory, Pasadena, California

The sensitivity to parameter variations of a closed-loop dynamic system employing a reduced-order controller can be calculated directly after doing only one eigensystem analysis. It is not necessary to solve a separate problem for each parameter change because the calculation can be put in a form that involves the same matrix solved in the original problem.

The sensitivity to parameter variations of a general dynamic system is related to the steady-state statistical response to white-noise inputs. This response is found by solving the Lyapunov equation. The solution of this equation requires a time-consuming calculation of the eigenvector matrix containing the dynamic parameters of the system.

The sensitivity to parameter changes could be calculated by slightly perturbing the original system and then solving the resulting Lyapunov equation as before. This, however, would require extensive computations.

The new derivation demonstrates a much shorter process. The original Lyapunov equation is differentiated two times with respect to a parameter p. Each differentiation turns out to yield a Lyapunov equation for the first and second derivatives with respect to the parameter p of the steady-state covariance of the state variables. These derivatives are the desired closed-loop performance sensitivities.

The feature that makes it economical to solve the equations for the two covariance derivatives is that they are the same as the original Lyapunov equation except that they have different right-hand sides. Since obtaining the eigenvectors for the solution of the original Lyapunov equation was the bulk of the computational load, the subsequent solution for the covariance derivatives is obtained at almost no additional cost.

This work was done by David B. Schaechter of Caltech for **NASA's Jet Propulsion Laboratory.** *For further information, Circle 158 on the TSP Request Card.*
NPO-15941

Books and Reports

These reports, studies, and handbooks are available from NASA as Technical Support Packages (TSP's) when a Request Card number is cited; otherwise they are available from the National Technical Information Service.

Techni-kits and Techni-kit Building Systems

Concepts and tools are discussed that improve software quality while reducing costs.

"Techni-kits" are described in a 16-page document. A techni-kit consists of theories, methods, standards, and computer-based tools that assist in the design of information-intensive systems. A techni-kit "building system" is a techni-kit that builds techni-kits.

The document is based on the premise that the human must be considered as an integral part of the process to develop informaton-intensive systems and that information systems engineering can be advanced by the development of a set of conceptual models for techni-kits. An information system, in the context of the document, is defined as a computer-based processing system in which the major inputs are data and information and the major output is information.

The two major physical components of such a system are as follows:

- Hardware, such as computers, communication lines, and terminals; and
- Humans.

The two major procedural elements of the system are the following:

- Software for the computers, and
- Procedures for the humans.

Examples of an information-intensive system are such diverse entities as a robot, a spacecraft, and a design and implementation team.

The concept and structure of a techni-kit are regarded as the framework for such a mix. Since it is important to specialize the tools for the designers and the job, it is necessary to be able to develop techni-kits quickly. A techni-kit building system provides a way to meet that necessity. The authors urge that the concept of the techni-kit be adopted along with such other major concepts as structured programing, and that attention be devoted not only to the computer-based tools but also to the intellectual concepts and the interplay between tools and concepts.

Section 1 of the document is an introduction. Section 2 discusses a development and implementation team as an information-intensive system. Section 3 presents a conceptual model of a techni-kit, and section 5 gives a similar model for a techni-kit building system. An example of a techni-kit is discussed in section 4.

This work was done by E. David Callender, Christopher Hartsough, Richard V. Morris, and Yuzo Yamamoto of Caltech for **NASA's Jet Propulsion Laboratory.** *To obtain a copy of the document, "Techni-Kits and Techni-Kit Building Systems," Circle 159 on the TSP Request Card.*
NPO-15956

Fast Two-Dimensional Digital-Filter Hardware

A 5-by-5 convolute-integer filter could process 4×10^6 image points per second.

A report describes the principles of the hardware implementation of a two-dimensional 5-by-5 convolute-integer low-pass filter. Such a filter could process 4×10^6 image data points per second, a speed fast enough for real-time use in image analysis and enhancement. The theory of such filters was discussed in "Digital Filters for Two-Dimensional Data" (MFS-25790) on page 481 of *NASA Tech Briefs,* Vol. 7, No. 4. A 4-by-4 hardware concept is presented in "Interstitial Digital-Image-Point Generator (MFS-25871) on page 183 of Vol. 8, No. 2.

By using sets of convolute integers, the hardware can perform low-pass (noise-reduction), high-pass, or band-pass filtering. Still other sets of convolute integers can be used to produce various partial derivatives of the data. The hardware can also be used for processing other two-dimensional data besides image data.

Most generally useful is the low-pass convolute-integer filter: It suppresses image noise with minimal loss of resolution. The procedure used is equivalent to fitting second-order surfaces to the data by regression calculations. The filtering process replaces each picture-element value by a weighted sum of the values of the 5-by-5 array of element values centered on the given element. The weighting factors are the convolute integers.

The filtering process is fast for two reasons: 1. The regression calculation is not to be done over at each element (it is done once in advance to determine the 5-by-5 coefficient array). 2. The coefficients in the array are all integers, so that integer arithmetic can be used rather than slower floating-point arithmetic.

The symmetry of the 5-by-5 coefficient array is exploited in the hardware. Although there are 25 elements in the array, only 6 multipliers are used, as that is the number of different magnitudes of coefficients: The other coefficients are derived from these by sign changes and symmetry principles.

Up to four picture-element values that are to be multiplied by a coefficient of a given magnitude are added together (taking proper account of signs by complementing the data) before performing the multiplication. All that is required to adapt the hardware to a different filter of the same size is to load the proper coefficients into the multipliers and to modify the complementing to take care of the signs on the coefficients.

This work was done by Thomas R. Edwards of **Marshall Space Flight Center.** *To obtain a copy of the report, Circle 160 on the TSP Request Card.*
MFS-25876

Design Primer for Reed-Solomon Encoders

Conventional and Berlekamp architectures are compared.

The design and operation of Reed-Solomon (RS) encoders are discussed in a document prepared for NASA's Jet Propulsion Laboratory as an instruction manual for computer designers and others in the data-processing field. Engineers who must equip computer memory chips with burst-error and drop-out detection and correction should find the report especially useful.

The text begins with the basic mathematical principles of RS codes. Practical RS codes of interest are described in terms of the number of bits (J) per symbol, the number of information (K) and check (2E) symbols per code word, the number of symbols ($N = 2^J - 1$) per RS code word, and the depth of interleaving (I). The error-correcting capabilities and error probabilities are described for various combinations of J, E, and I.

RS codes have a number of mathematical properties that are both interesting in themselves and useful in the design of hardware to implement them. One of the useful properties is that a code can be characterized by a generator polynomial, the appropriate choice of which can reduce the amount and complexity of hardware.

The development of concatenated codes for spacecraft telemetry is discussed briefly. The information bits are first processed through an RS encoder to form the "outer" RS code. The RS-coded data are then further processed into an "inner" convolutional code — a code used for transmission. Concatenated coding improves error correction at the receiving end because decoding errors due to the Viterbi decoder (used in decoding the "inner" code) tend to occur in bursts that affect relatively-few RS symbols.

Using the example of a code with N = 255, K = 223, the report discusses hardware considerations in the design of RS encoders. A block schematic diagram (in the conventional architecture) is developed for the logic needed to compute a general code-word polynomial that includes the information polynomial and the appended check symbols.

Next, an example is given of Berlekamp's architecture, which is based on a polynomial with 2E roots that occur in reciprocal pairs and on a hardware design of bit-serial multipliers compatible with the serial organization of RS encoders. The mathematical characterization is presented for the N = 255, K = 223 encoder designed by Berlekamp.

The complexity of hardware is compared for conventional and Berlekamp implementations of encoders for N = 255, K = 223. The comparison is based on experience with two existing designs using parts qualified for the Galileo spacecraft. All RS codes with the same N and K parameters are equivalent, although their mathematical representations may differ.

The report concludes with a chapter on testing RS encoders. Three classes of symbol sequences representing RS code words are investigated: the generator-polynomial-coefficient sequence, the constant-symbol sequence, and the iterative-symbol sequence. The leading segment of a given sequence comprised of all the information symbols is entered into the RS encoder. The output sequence (representing check symbols over distinct combinations of information symbols) is compared with the trailing segment of the given sequence. A favorable comparison validates the integrity of the encoding process.

This work was done by Marvin Perlman and Jun-Ji Lee of Caltech for **NASA's Jet Propulsion Laboratory.** *Further information may be found in NASA CR-169754 [N83-17141/NSP], "The Reed-Solomon Encoders: Conventional Versus Berlekamp's Architecture" [$10]. A copy may be purchased [prepayment required] from the National Technical Information Service, Springfield, Virginia 22161.*
NPO-15568

Computer Programs

These programs may be obtained at very reasonable cost from COSMIC, a facility sponsored by NASA to make new programs available to the public. For information on program price, size, and availability, circle the reference letter on the COSMIC Request Card in this issue.

Research-Concept Evaluation

Concepts are ranked according to their potential benefit/cost ratios.

The ARINC Research Concept Evaluation Methodology (ARCEM) program was developed to assist in the rank ordering of research concepts in terms of their potential benefit-to-cost ratios. In particular, ARCEM resulted from the development of a planning methodology that provides NASA with a framework for generating and analyzing control- and guidance-system concepts and for selecting concepts that maximize the benefits to the aviation community. The ARCEM program and the methodology it supports can provide a powerful tool for the organization and planning of research activities. It can indicate which concepts should provide the greatest benefit for the investment, and it can determine the number of concepts that must be implemented to justify expenditures for development of generic technologies.

Input to ARCEM consists of a list of concepts, each described in terms of expected costs, expected benefits, and their technology lines. The technology line indicates which generic technologies are needed for concept execution. ARCEM can accept up to 100 concepts and 20 generic technologies. ARCEM examines the benefits and costs of each concept, including the costs of required technology, and ranks them in order of descending benefits-to-cost ratio. ARCEM can then compute the cumulative benefits-to-cost ratio associated with implementing the concepts in order (the ranked order or a user-specified order). Thus, the computed ratio associated with the fifth concept is the cumulative ratio for the first five concepts. ARCEM results can be printed in tabular or bar-graph form.

The ARCEM is written in BASIC for the TRS80 Model III microcomputer with a minimum configuration requirement of 48K of memory and one disk drive. Program use also requires a light-pen input device such as the 3-G Company unit. The ARCEM program was developed in 1983.

This program was written by Michael J. White and William Kolb of ARINC Research Corp. for **Langley Research Center.** *For further information, Circle ff on the COSMIC Request Card.*
LAR-13143

Relational Information Management Data-Base System

A DBMS with several features useful to scientists and engineers

The Relational Information Management data-base system, RIM5, resulted from a NASA project aimed at improving the technology of managing engineering information. RIM5, a general-purpose data-base management system (DBMS) suitable for a wide range of data-processing applications, contains several features that make the system particularly useful to people working in scientific and engineering areas. The RIM5 command language offers the user direct online or batch access to information retained in the data base. RIM5 is a fully relational DBMS with data stored in tables instead of in hierarchical or network relations. As new applications arise, the RIM5 data base can be easily modified, allowing the DBMS to change as needs change.

In the RIM5 data-base system, data are stored in a two-dimensional table termed a relation. The table contains attributes of the relation and data occurrences. The relations and their attributes are defined as the schema of the data base. A full selection of RIM5 commands permits the user to create, update, and query the data base. The data-base structure is defined in terms of attributes, relations, constraints (rules), and passwords. Data in the RIM5 data base may be of fixed or variable length of the following types: text, integer, real, double precision, vectors (integer, real, double precision), and matrices (integer, real, double precision). The RIM5 user can easily load new relations, modify the data base, or modify the schema.

RIM5 commands are provided for querying the data base. Queries may contain up to 10 conditions, including arithmetic and logical comparisons. The user can generate a tally for any attribute giving each unique value and the number of times it occurs in a relation. Simple functional values of an attribute that can be computed include minimum, maximum, average, and sum. Relational algebra commands allow the RIM5 user to create new relations from existing relations. RIM5 commands also provide the user with a limited report-generator capability. Portions, or all, of a RIM5 data base may be off-loaded for communication to other computers supporting RIM5.

The RIM5 program is a stand-alone system and can be executed in a menu mode or a command mode. In the menu mode, the user is prompted for the inputs required to create, update, and query the data base. The menu mode offers the inexperienced user assistance and a chance to get acquainted with the RIM5 commands. In the command mode, RIM5 commands are directly input by the user. An extensive online HELP facility is available to both the new and experienced user.

RIM5 can also be interfaced with any application program that is written in a language capable of calling FORTRAN routines. RIM5 offers the data-base manager a password feature that can be used to restrict access to data and to restrict the use of RIM5 commands. Applications to date include management of data for the Space Shuttle *Columbia* tiles, aircraft flight tests, high-pressure piping, atmospheric chemistry, census, university registration, CAD/CAM geometry, and civil-engineering dam construction.

RIM5 is written in FORTRAN 77 (and some Assembler on the CDC version) for interactive or batch execution. RIM5 is available for implementation on DEC VAX (VMS), PRIME (PRIMOS), and CDC CYBER (NOS) computers. The RIM5 system was developed in 1981.

This program was written by Olaf O. Storaasli of **Langley Research Center** *and Wayne J. Erickson, Frederic P. Gray, Dennis L. Comfort, and Stig O.*

(continued on next page)

Wahlstrom of Boeing Commercial Airplane Co. and Geoffrey von Limbach of Boeing Computer Services Co. For further information, Circle gg on the COSMIC Request Card.
LAR-12943, LAR-12944, and LAR-12945

SDDL: Software Design Documentation Language

It promotes effective communications between the software designer and the user.

SDDL assists programers in writing effective software documentation. It results in documents that are easy to read and effective in communicating the designer's "creative thinking" to those who later use the software. SDDL has been successful on tasks ranging from small, one-person informal projects to large projects of hundreds of formally published pages of design.

The objective of SDDL — to support the communications requirements of the software design and documentation process — is met by providing:

1. A design and documentation language with forms and syntax that are simple, unrestrictive, and communicative;
2. A processor that translates design specifications, couched in SDDL syntax, into an intelligible, informative, machine-reproducible software design document; and
3. Methodology for effective use of the language and the processor.

SDDL is basically a language processor for handling the concepts of structure and abstraction that are fundamental to software development and documentation. The program is a batch processor that reads the design data base, reformats it to emphasize and clarify structure, compiles information about the data, and prints the resulting information enhanced software design document.

The reformatting step uses indentation to show structures and flow lines to highlight module escape (left arrow) and module invocation statements (right arrow). The result of the reformatting step is topologically equivalent to a flow chart and has the added advantages of having regular structure, no constraints on the amount of information in a structure node or body, and prohibiting the use of spaghettilike nonstructures. All SDDL output is produced in standard line-printer format, which can be output on a terminal or diverted for batched output on a high-speed line printer.

The SDDL processor is written in Pascal for batch execution. It has been implemented on a DEC VAX-11/780 computer under VMS and on a Z80-based microcomputer with CP/M. The Pascal version of SDDL was developed in 1981.

This program was written by Henry Kleine, E. David Callender, and Thomas M. Zepko of Caltech for **NASA's Jet Propulsion Laboratory.** *For further information, Circle hh on the COSMIC Request Card.*
NPO-16201/16202

Software Cost-Estimation Model

It provides an automated resource and schedule model for software development.

The Software Cost Estimation Model program, SOFTCOST, provides an automated resource and schedule model for software development. SOFTCOST was developed after the evaluation of a number of existing cost-estimation programs. It combines several software cost models found in the open literature into one comprehensive set of algorithms. SOFTCOST compensates for nearly fifty implementation factors relative to size of the task, inherited baseline, organizational and system environment, and difficulty of the task.

SOFTCOST produces mean and variance estimates of software size, implementation productivity, recommended staff level, probable duration, amount of computer resources required, and amount and cost of software documentation. The user can enter risk-biased values for effort, duration, and staffing to achieve higher confidence levels. SOFTCOST then produces a PERT-CP/M file with subtask efforts, durations, and precedences defined so as to produce the Work Breakdown Structure, WBS, and schedule having the asked-for overall effort and duration.

The SOFTCOST program operates in an interactive environment prompting the user for all of the required input. The program builds the supporting PERT data base in a file for later report generation or revision. The PERT schedule and the WBS schedule may be printed and stored in a file for later use.

SOFTCOST is written in Microsoft BASIC for interactive execution and has been implemented on a Z80-based microprocessor operating under CP/M with 64K bytes of memory and 8-inch floppy disk drives.

This program was written by Robert C. Tausworthe of Caltech for **NASA's Jet Propulsion Laboratory.** *For further information, Circle ii on the COSMIC Request Card.*
NPO-15862

Software Design Analyzer System

Programs support modular structured software development.

The CRISP80 software design analyzer system is a set of programs that supports top-down, hierarchic, modular, structured design, and programing methodologies. CRISP80 allows for the expression of the design as a "picture of the program." Its use is not constrained by the syntax of a computer language.

The quality of a computer program can often be significantly influenced by the design medium in which the program is developed. The medium must foster the expression of the programer's ideas easily and quickly, and it must permit flexible and facile alterations, additions, and deletions to these ideas as the design evolves.

A program design using CRISP80 consists of short, English textual descriptions of data, interfaces, and procedures that are embedded in a simple, structured, modular syntax. The output from CRISP80 displays the program as a set of modules hierarchically refined into algorithms, data structures, and interfaces. The display is formatted into two-dimensional flowchart-like segments for a graphic presentation of the design. Together with a good interactive full-screen editor or word processor, CRISP80 becomes a powerful tool for the serious programer.

CRISP80 also prepares material that would be tedious and error-prone if extracted manually, such as a table of contents, module directory, structure (tier) chart, cross-references, and a statistics report on the characteristics of the design. Another feature is the capability to

detect all changes that have been made between versions and to have automatic "change bars" placed in the output document together with a list of changed pages and a version-history report. All items marked "tbd" (to be determined) or appearing as "stub" modules are listed as a separate table of items to be supplied later.

CRISP80 is written in Microsoft BASIC-80 compiled for rapid interactive execution. The system has been implemented on a Z80-based microcomputer operating under CP/M with a memory requirement of approximately 39K of 8-bit bytes for the largest program. The CRISP80 program was developed in 1983. To run CRISP80, users must have the compiled BASIC-80 run-time support program BRUN.

This program was written by Robert C. Tausworthe of Caltech for **NASA's Jet Propulsion Laboratory.** *For further information, Circle kk on the COSMIC Request Card.*
NPO-16234

Integrated Procurement Management System, Version II

An online system for managing and disseminating procurement-related data

The Integrated Procurement Management System, Version II, (IPMS II) is an online/batch system for collecting, developing, managing, and disseminating procurement-related data at NASA's Johnson Space Center. Although it is specific to the needs of Johnson Space Center, portions of IPMS II may be adaptable to other procurement situations.

IPMS II takes into account the needs of procurement managers, the NASA field-center management, and NASA headquarters. IPMS II provides an extensive data-base-management and inquiry capability and a reporting capability to the procurement division. Access to IPMS II is through online terminals and batch processing.

IPMS II is an ASCII COBOL system using the multi-indexed sequential access method for storage and retrieval of information from mass-storage files. IPMS II consists of two major subsystems: online and batch. The online subsystem has three major functions: preprocessing, template processing, and recovery. Preprocessing ensures that the database is ready for the online user. Template processing provides online user-access to the database files. Recovery restores database files when necessary. The batch subsystem provides for batch reporting and year-end processing.

IPMS II is written in COBOL and Assembler and has been implemented on a UNIVAC 1108 computer operating under EXEC8 with a minimum memory requirement of 65K of 36-bit words. IPMS II uses Megadata CRT terminals for all online functions. It was developed in 1980.

This program was written by Louis J. Collier of Computer Science Corp. for **Johnson Space Center.** *For further information, Circle mm on the COSMIC Request Card.*
MSC-20278

Language for Allocation and Network Scheduling

Useful in scheduling, it is also an efficient high-level tree-manipulation language.

The Programing Language for Allocation and Network Scheduling, PLANS, handles the many scheduling requirements of the Space Shuttle program. It is also a generalized, high-level tree manipulation language.

PLANS allows for the easy, direct expression of the kinds of functions frequently found in scheduling and resource allocation programs. It has a unique capability to dynamically manipulate tree data structures at execution time. Another important feature is the ability to establish a close correspondence between basic scheduling functional operations and PLANS statements, making design and maintenance of PLANS programs a relatively simple task. These features also make PLANS applicable to many areas in addition to scheduling.

PLANS allows the designer of experimental or constantly changing scheduling and resource allocation algorithms to translate his designs into working code directly from their basic functional descriptions. For large, logically complex scheduling problems, the simplicity of PLANS encourages the truly experimental approach that can offer the greatest promise of convergence to good solutions.

Because it is intended to be used by problem-area experts, rather than programing experts, PLANS minimizes functionally nonessential details. While PLANS has quantitative capabilities, its emphasis is more on the manipulation of data structures, which is the principal activity performed in most scheduling algorithms. By eliminating the need for programing expertise and detailed intermediate program design, PLANS significantly cuts the cost and time required to develop scheduling and resource allocation programs.

The Program Library of Utilities for Scheduling, PLUS, is a collection of modules written in the PLANS language to provide a portion, or all, of the logic needed to construct a program to solve problems associated with scheduling and resource allocation. PLUS modules are not constrained to any particular application. They are methodological segments that may be used on any problem for which the corresponding methodology applies. The PLUS modules provide the PLANS programer with a resource that can make the development of scheduling and resource allocation algorithms even easier.

The PLANS/PLUS processing system is written in FORTRAN 77 for batch execution and has been implemented on a UNIVAC 1100-series computer with a central memory requirement of approximately 55K of 36-bit words. The PLANS/PLUS system was last updated in 1981.

This program was written by John K. Willoughby of Science Applications, Inc., for **Johnson Space Center.** *For further information, Circle nn on the COSMIC Request Card.*
MSC-20633

A Visually Oriented Text Editor

It includes special features for editing FORTRAN source programs.

HERMAN employs an Evans & Sutherland Picture System 2 to provide a screen-oriented editing capability for a DEC PDP-11-series computer. Text is altered by a visual indication of the characters to be changed. A group of HERMAN commands provides for higher level operations. Since FORTRAN is a widely used language on the PDP-11 series, HERMAN provides special features for editing FORTRAN source programs. HERMAN provides the user

(continued on next page)

with a two-area display: one for the text being edited and one for a menu area.

The HERMAN system is written in FORTRAN IV, FORTRAN IV Plus, and MACRO for interactive execution and has been implemented on a DEC PDP-11-series computer under the RSX-11M operating system. HERMAN was developed in 1980.

This program was written by Julian E. Gomez of Caltech for **NASA's Jet Propulsion Laboratory.** *For further information, Circle oo on the COSMIC Request Card.*
NPO-15088

Structured FORTRAN Preprocessor

A structured language for the design of effective FORTRAN code

SFTRAN3 supports structured programing in a FORTRAN environment. The SFTRAN3 language is intended particularly to support two aspects of structured programing — nestable single-entry control structures and modularization and top-down organization of code. Code designed and written using these SFTRAN3 facilities have fewer initial errors, are easier to understand, and are less expensive to maintain and modify.

The SFTRAN3 language provides seven nestable single-entry control structures (IF, CASE, WHILE, UNTIL, FOR, FOREVER, and BLOCK) to support the needs for selection and iteration as well as exceptional multilevel exiting from the structures. This eliminates almost all of the need for numeric statement labels and GO TO statements that otherwise carry the main burden of control flow in FORTRAN programs. Modularization and top-down organization of code within a single FORTRAN program unit are supported by statements to declare segments of code as named procedures that can then be invoked from elsewhere in the same program unit.

SFTRAN3 has useful auxiliary features that may be selected by preprocessor directives. For example, the portable INCLUDE feature supports the dynamic insertion of named segments of code. This is particularly useful for maintaining identical COMMON declaration statements in many subroutines of a complete program.

A dynamic analysis feature determines how many times each branch of the program logic is taken during execution. This can be useful in determining whether test cases have exercised all statements of a program. It can also be employed to identify those parts of the program that are most heavily used and thus may warrent additional design effort to achieve greater efficiency.

Those experienced with FORTRAN programing should have little trouble learning and employing the SFTRAN3 language. SFTRAN3 is run through the SFTRAN3 preprocessor to generate a program in FORTRAN that is the functional equivalent of the SFTRAN3 program. This FORTRAN code may then be compiled and executed. Any modifications, updates, or error corrections are applied to the SFTRAN3 code and a new FORTRAN source program is generated.

The SFTRAN3 preprocessor can be readily installed on any computer supporting the FORTRAN 66 or FORTRAN 77 standard and having at least 80K 8-bit bytes of primary storage. The SFTRAN3 preprocessor has been successfully installed on UNIVAC, IBM, CDC, DEC VAX, DEC PDP-11, and DEC-20 computers. The original SFTRAN language and preprocessor were conceived and developed in 1973. The present language, SFTRAN3, was defined in 1978. Level 13 of the SFTRAN3 preprocessor was released in June 1981.

This program was written by John A. Flynn, Charles L. Lawson, William Van Snyder, and Haralambo N. Tsitsivas of Caltech for **NASA's Jet Propulsion Laboratory.** *For further information, Circle pp on the COSMIC Request Card.*
NPO-15726

NASTRAN NASTPLT Plotting Post Processor

Post processor reads plot files, checks contents for validity, and translates commands for plotting systems.

The NASTRAN NASTPLT Plotting Post Processor reads NASTRAN-generated NASTPLT plot files, checks the file contents for validity, and translates the NASTPLT plot commands into appropriate calls to plotting routines for either CALCOMP, Tektronix PLOT10, or Versatec plotting systems. This program was originally written to generate a summary of the contents of a NASTPLT plot file for the purposes of debugging and checking the validity and characteristics of the file contents.

The summary information generated includes the following information for each plot on the NASTPLT file: plot number, draw-lines summary, draw-axis summary, draw-character summary, maximum and minimum values in the x-range and y-range, and pen change information. The summary information also includes the following information for the NASTPLT file as a whole: the number of records read, the number of commands, and the number of plots.

The summary generation program was extended to include the plot routine calls for the CALCOMP, Tektronix PLOT10, and Versatec plotting systems. The Post Processor is run interactively and prompts the user for all of the required input. The user may request the summary information and then use that information to determine which plots on the file are to be output. The Post Processor is compatible with either VAX or IBM NASTRAN-generated NASTPLT files.

The Post Processor is written in FORTRAN IV-PLUS for interactive execution and has been implemented on a DEC VAX-11/780 computer under VMS. This program was developed in 1981.

This program was written by Robert Strang of Computer Sciences Corp. for **Goddard Space Flight Center.** *For further information, Circle rr on the COSMIC Request Card.*
GSC-12833

Algorithm Solves Constrained and Unconstrained Optimization Problems

Algorithm features rapid convergence and good numerical stability.

The BFGS algorithm solves both constrained and unconstrained optimization problems. It is a quasi-Newton iteration utilizing the Broyden/Fletcher/Goldfarb/Shanno update on the inverse Hessian matrix. It is capable of solving constrained optimization, unconstrained optimization, and constraints-only problems with from one to five independent variables, from one to five constraint functions, and one dependent function to be optimized.

The BFGS update, sometimes called the complementary Davidon/Fletcher/Powell update, is a single-rank update. It preserves symmetry and positive definiteness and features superlinear

convergence near the solution, provided the functions are smooth. Designed to solve multidimensional optimization and constraint problems, BFGS provides fast convergence, good numerical stability, and good global convergence qualities.

BFGS is written in FORTRAN V for batch execution and has been implemented on a UNIVAC 1100-series computer with a central memory requirement of approximately 5K of 36-bit words. The algorithm requires access to basic matrix manipulation routines such as those provided in the UNIVAC MATHPACK library. The algorithm was developed in 1982.

This program was written by Mark A. Denson of McDonnell Douglas Corp. for **Johnson Space Center.** *For further information, Circle ss on the COSMIC Request Card.*
MSC-20683

MiniBriefs describe NASA innovations and reports in an abbreviated format. Readers desiring additional information on these items should request the Technical Support Packages (TSP's), available in most cases, which can be obtained by using the TSP Request Card at the back of this issue.

Handling Software Requests for Commands

Special software ensures orderly treatment of simultaneous requests.

A software component has been created expressly to provide an interface between a dedicated command buffer and components requesting command issuance. This component resolves the problems that can arise when the software processes command requests from other subsystems, and several requests are received at approximately the same time. Lost commands, incorrect commands, and erroneous indication that the software has completed issuance of a command are eliminated.

The command requests queue up at the new component — called a bus command processor. This component places the requests in the dedicated command buffer, waits for microcode to issue the commands, and returns a command-completed report to each of the requesting components. Requests are served on a first-in, first-out basis. Only one request is stored in the command buffer at a time.

This work was done by W. G. King, Jr., of IBM Corp. for **Kennedy Space Center.** *For further information, Circle 161 on the TSP Request Card.*
KSC-11226

Priority-Based Dispatching Algorithm

Tasks are assigned to different queues based on priority.

A proposed algorithm controls the execution of transient tasks of different priorities in real-time computation. Separate dispatching queues are set up, one for each priority level. As execution of a task is required, it is placed on the appropriate priority queue. The task-dispatcher-system module dispatches (allows the execution of) tasks on higher priority queues more often then those on lower queues. A dispatched task executes until it waits for a system resource or until its time slice expires. After dispatching each task on queue 1 once, a task on queue 2 is dispatched before again dispatching queue 1, and so on.

This work was done by G. Ouzts of IBM Corp. for **Kennedy Space Center.** *For further information, Circle 162 on the TSP Request Card.*
KSC-11277

More Efficient Structural Design by Optimality Criteria

An algorithm distinguishes between essential and nonessential constraints.

A computer algorithm aids in the selection of active constraints on structural design via the optimality-criterion method — a highly useful way of ensuring lightweight, low-cost structures. Computation time and cost that have been significantly greater for this type of analysis than for conventional structural analysis are now reduced.

Active constraints are those that are actively processed by the optimality-criterion program. Passive constraints are those that are assumed to be satisfied automatically. For computational simplicity and efficiency, the active set should be small and the passive set should be large.

The algorithm provides a key to successful design by indicating those constraints that should be considered active. The algorithm ensures that only the necessary constraints are included in the optimization.

This work was done by Roy Levy of Caltech for **NASA's Jet Propulsion Laboratory.** *For further information, Circle 163 on the TSP Request Card.*
NPO-15832 and NPO-15993

Adding Stale-Data Flag to an Error-Correcting Code

A suitable constant can be "exclusive-ORed" with the ECC to flag data without impairing detection of correctable errors.

Two theorems lead to a way of modifying the error-correction code (ECC) stored with each datum to encode a 1-byte flag that can be used to indicate stale (not currently valid) data. In the case considered, each datum comprises two 2-byte words, each containing 1 data byte and 1 ECC byte. Both ECC's are "exclusively-ORed" with hexadecimal 6F to flag a datum, yielding a datum that the original error-detection algorithm always interprets as having uncorrectable errors. A second algorithm remodifies the ECC's and retests for errors. Original uncorrectable data errors due to double hardware stuck-at faults will be misinterpreted as correct flagged data with a probability of 2.3×10^{-4}.

This work was done by N. J. Bell, Sr., J. E. Burkavage, and J. L. Wicks of IBM Corp. for **Kennedy Space Center.** *For further information, Circle 164 on the TSP Request Card.*
KSC-11134

Root-Locus Algorithms

Algorithms for solving root-locus problems are applicable to hand calculators.

Two algorithms for use on programable pocket calculators allow plotting of individual points on a root-locus diagram with or without time delay. The coordinates of the open-loop zeros and poles, the gain constant, and the time delay are the data inputs. One algorithm uses a Newton/Raphson iteration with 36 memory registers and 281 program steps. The second algorithm uses 41 memory registers and 351 program steps. Both algorithms enable the design of systems with up to 8 singularities a piece.

This work was done by Erwin R. Wechsler of Caltech for **NASA's Jet Propulsion Laboratory.** *For further information, Circle 165 on the TSP Request Card.*
NPO-16154

Algorithms for Finite-Element Equations

A collection of algorithms is evaluated for linear equilibrium problems.

Five direct and five iterative algorithms for finite-element equations in linear equilibrium problems are investigated for a number of parallel computer architectures, and their basic computation methods are compared. None of the algorithms considered here for the solution of these equations can be claimed to be superior to the others for all other computer architectures. Cyclic reduction appears to be best for reducing execution time when unlimited numbers of parallel processors are available. For a computer system with a limited number of parallel processors, both Gauss factorization and Jacobi-like iterative methods are found to rank favorably.

This work was done by Moktar A. Salama of Caltech and Robert Melosh and Senol Utku of Duke University for **NASA's Jet Propulsion Laboratory.** *For further information, Circle 166 on the TSP Request Card.*
NPO-16029

Software-Implementation Plan

Methodology for controlling software design uses hierarchical program structures.

A top-down implementation plan provides a methodology for solving problems in, or aiding, software engineering design. Specifically, the plan helps identify hierarchical relationships of individual software-design elements, aids the development of a sequence of functional steps, allocates subroutines, and helps objective-status reporting. The results are meaningful determination of milestones, improved managerial visibility, and better project control.

This work was done by Gerald Jacobson and Aaron Spinak of Caltech for **NASA's Jet Propulsion Laboratory.** *For further information, Circle 126 on the TSP Request Card.*
NPO-16123

Test Sequences for Reed-Solomon Encoders

Repeating input and output patterns verify operation.

The theory of Reed-Solomon codes yields sequences of input test symbols. Two specific sequences have been worked out for codes of 8 bits per symbol with 223 information symbols and 32 parity-check symbols per code word.

One input sequence is $(s_1s_2s_3)$ repeated 74 times, followed by s_1, where the s_i are any of the symbols. If the encoder is operating correctly, the output sequence will be $(s_1s_2s_3)$ repeated 85 times. The other test pattern is $(s_1s_2s_3s_4s_5)$ repeated 44 times, followed by $s_1s_2s_3$, for which the output should be $(s_1s_2s_3s_4s_5)$ repeated 51 times.

The test patterns can also be used for decoders. In addition, any combination of errors up to the maximum correctable number can be added to the pattern to test a decoder.

This work was done by Jun-Ji Lee of Caltech for **NASA's Jet Propulsion Laboratory.** *For further information, Circle 146 on the TSP Request Card.*
NPO-15542

SUBJECT INDEX

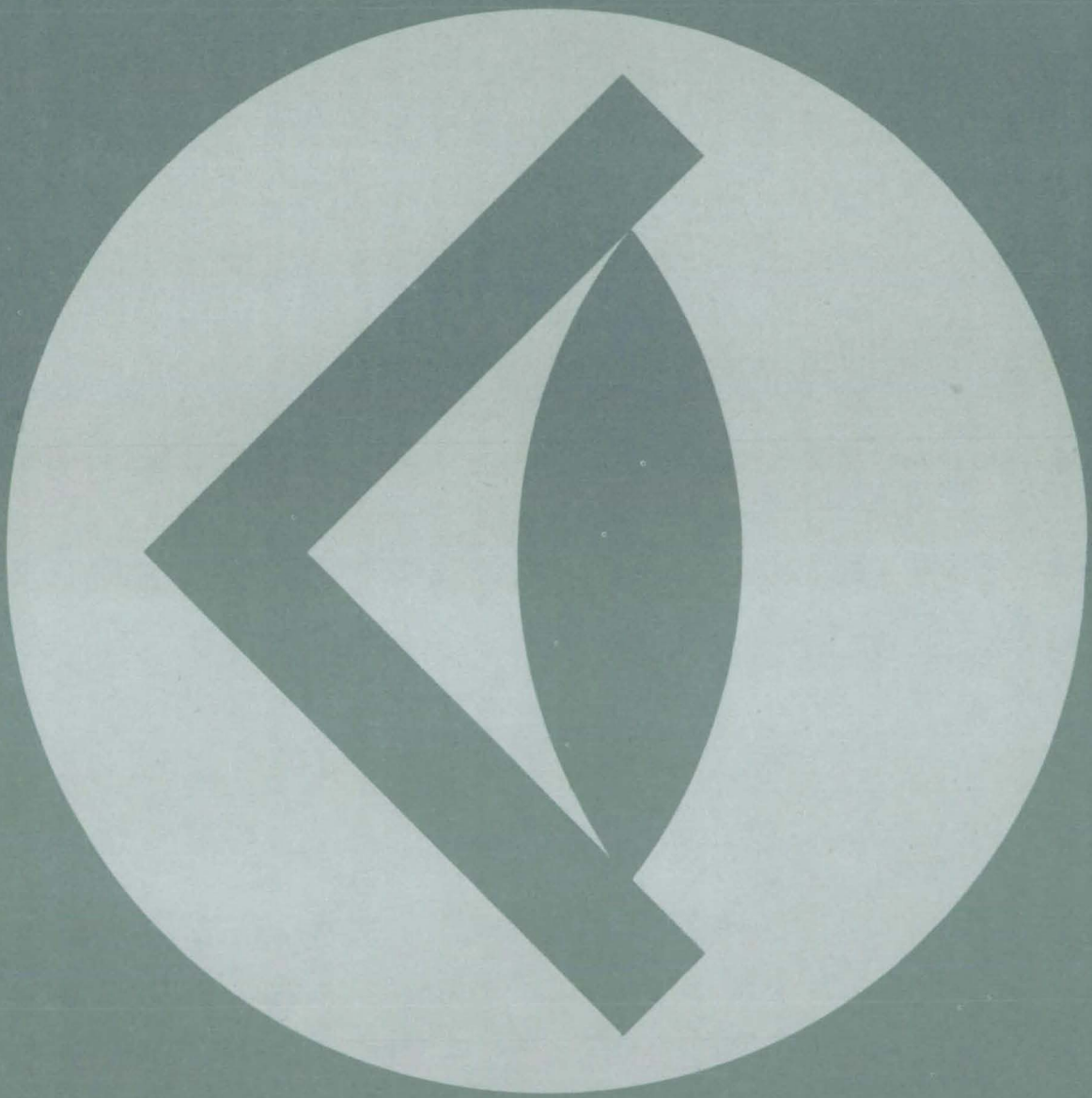

National Aeronautics and
Space Administration

Washington, D.C.
20546

THIRD-CLASS BULK

NASA

The computerized graphics station that produced this "metamorphosis" of a caterpillar into a butterfly evolved from technology originally developed for the Viking Mars missions. The equipment is now available commercially for such applications as CAD/CAM, film animation, and cartography. [*See the bottom of page A1.*]